

Materials with **N**ovel **E**lectronic **P**roperties

NATIONAL CENTRE of COMPETENCE in RESEARCH

# PROGRESS REPORT

## Year 6

April 1<sup>st</sup> 2006 - March 31<sup>st</sup> 2007



FONDS NATIONAL SUISSE  
SCHWEIZERISCHER NATIONALFONDS  
FONDO NAZIONALE SVIZZERO  
SWISS NATIONAL SCIENCE FOUNDATION

Die Nationalen Forschungsschwerpunkte (NFS) sind ein Förderinstrument des Schweizerischen Nationalfonds.  
Les Pôles de recherche nationaux (PRN) sont un instrument d'encouragement du Fonds national suisse.  
The National Centres of Competence in Research (NCCR) are a research instrument of the Swiss National Science Foundation.



## NCCR: 6<sup>th</sup> Progress Report - Cover Sheet

<b>Title of the NCCR</b>	<b>Materials with Novel Electronic Properties – <i>MaNEP</i></b>
<b>NCCR Director</b> Name, first name Institution address	<b>Professor Øystein FISCHER</b> UNIVERSITÉ DE GENÈVE, Faculté des Sciences Département de Physique de la Matière Condensée 24 quai Ernest-Ansermet, CH-1211 Genève 4
Office phone number	022-379.6270
E-mail	Oystein.fischer@physics.unige.ch

1. Executive summary [1]	5
2. Research	7
2.1. Structure of the NCCR and status of integration [2]	7
2.2. Results since the last progress report [3]	11
<i>Project 1 Strong interaction, low-dimensional and quantum fluctuations</i>	11
<i>Project 2 Superconductivity, unconventional mechanisms, novel materials</i>	35
<i>Project 3 Crystal growth</i>	57
<i>Project 4 Novel materials</i>	63
<i>Project 5 Thin films, artificial materials and novel devices</i>	79
<i>Project 6 Industrial applications and pre-application developments</i>	91
3. Knowledge and technology transfer [4]	111
4. Education/training and advancement of women [5]	117
5. Public relations [6]	123
6. Management	127
6.1. Activities [7]	127
6.2. Experiences, recommendations to the SNSF	129
7. Reaction to the recommendations of the review panel	131
8. Lists	133
8.1. Project list [8]	135
8.2. Personnel [9]	139
8.3. Cooperation with third parties [10]	161
8.4. PhD theses and prizes, awards etc. [11]	195
8.5. Publications [12]	241
8.6. Lectures at congresses etc. [13]	263
8.7. Services, patents, licences, start-up companies etc [14]	279
9. Statistical output data [15]	291
10. Finance	295
10.1. Target and actual comparison [16]	297
10.2. Financial overview [16]	300
10.3. Comments and equipment list [17]	307
Appendix A. Milestones of the MaNEP projects	321



## 1 Executive summary

MaNEP was established in 2001 in order to reinforce research in Switzerland in the field of Materials with Novel Electronic Properties. It brings together the main groups in Switzerland in this field with 30 senior members and about 260 researchers in total. At the beginning of the second phase (which started on July 1, 2005) the research structure was changed to six collaborative projects. During the second year of the second phase MaNEP has continued to implement this new research structure. The integration of efforts between the different MaNEP laboratories develops very well. In January 2007 six one-day meetings, each dedicated to one of the six projects, were held during which the results so far were discussed in detail among the members of the projects. This report contains an overview of these results for each project.

### Research

**Project one** is dedicated to the study of one of the key questions in condensed matter physics: the understanding of materials with strong spin and charge interactions. A wide range of strongly interacting electron materials and low-dimensional and quantum fluctuation systems has been investigated. The report reflects the richness of this field and covers the advance of experimental investigations and new theoretical concepts. Results are reported in the fields of magnetism, cold atoms in optical lattices, interfaces and heterostructures, spectroscopies on low dimensional metallic chalcogenides and 4f-electron systems, exotic phases and quantum phase transitions in itinerant electron systems, spectroscopy and transport in elemental bismuth and carbon-based systems as well as mesoscopic physics.

**Project two** addresses the fascinating field of superconductivity. Here the quest for a microscopic understanding of high temperature superconductivity (HTS) in the cuprates remains a key question and several important results contributing towards this goal are reported. The study of these materials has stimulated an exceptional development of experimental tools world wide, with the result that these materials have been studied to a detail that was never achieved on other materials before the HTS. In view of this development it becomes important to revisit other superconductors. In the same spirit many new and unusual superconductors have been found recently. Thus "project two" also continued during this year to evolve towards the study of such non-cuprate superconductors and several novel and surprising results are reported.

**Project three** reflects the importance of high quality crystal growth and MaNEP's dedicated effort to stimulate and to coordinate crystal growth among its members. During this year we can report new results on the crystal growth of several oxides and silicides. We also report

improved growth and control on different high temperature superconductors as well as vanadium chain compounds.

**Project four** represents a special effort to stimulate a search for new materials with strongly correlated behaviour and in particular new superconductors. This research was established at the beginning of phase II and this report gives the situation after 1 ½ years of research. Several different routes towards new materials are reported including high pressure synthesis, a combinatorial approach, thin film methods as well as nano structuration and morphology control.

**Project five** concerns the use of thin epitaxial films for basic and applied studies. The results in this project cover thin film ferroelectrics, with the study of size effects and screening lengths; polaronic transport in manganite thin films and the search for polaronic behaviour in thin strontium titanate films; as well as the use of thin superconducting films for single photon detectors.

**Project six** concerns applications resulting from basic research in MaNEP. Our approach here is to develop applied research projects of interest to industry based on materials and/or techniques present in MaNEP. Following this idea we have established collaborating efforts with 6 companies on specific questions of interest to these companies. This concerns 1) applications of superconductivity with research on improved wires for high field applications, thin film superconducting fault current limiters and a contribution to the development of a self screened high field magnet for neutron scattering studies; 2) sensors, with the search for a material for high precision ESR determination of weak magnetic fields and the development of novel gas sensors; 3) thin film preparation and applications including the development of superlattices for neutron supermirrors in neutron guides and the preparation and study of ferroelectric thin films for novel devices.

## Knowledge and Technology Transfer

Efforts to develop KTT were continued both inside MaNEP and towards industry. Promotion of inventions, disclosures and patenting were made within the MaNEP network. Two invention disclosures are under processing since last year, and a new one was added. In addition, two new patents were granted during Year-6. Collaborations with industrial corporations are progressing along the lines outlined in the proposal and discussed in the previous report. This includes collaborations with ABB, Bruker BioSpin, Swiss Neutronics, Metrolab, Phasis and Mecsens. We have also established several new industrial contacts which may lead to new collaborations.

## Education / training and advancement of women

**Education:** The second MaNEP summer school was organized in the week of 11-16 September, 2006 in Saas-Fee. The topic this year was “*Probing the Physics of Low Dimensional Systems*” and 68 PhD students enjoyed a series of high level lectures which resulted in lively discussion sessions. The courses were given by eight lecturers, of which half were external to MaNEP. We also organised in January 2007 a one-day training course on Superconductivity for Geneva high-schools physics teachers. This course was attended by 30 teachers. In order to implement our plans for a MaNEP doctoral school we have appointed a scientist part time to carry out this project.

**Advancement of women:** The MaNEP summer internship program for female students was carried out for the second time during the summer of 2006. This program was offered to students from all member institutions of MaNEP. Seven female students carried out interesting projects and expressed high degree of satisfaction. Following our proposal for phase II we have searched for and appointed a young female professor in the field of MaNEP at the University of Geneva.

## Public relations

We are continuing our outreach effort to motivate young people to enter into science. This year we have initiated a novel approach to interact with high-school students and teachers. This project which goes under the working title “*Physics Park*” is a joint effort between MaNEP and the Physics Department of Geneva University. “Physics Park” is a communication- and education-tool mainly dedicated to high-school students, but will also be useful in our communication with the public at large. Details of the concept, its financing and organization were worked out during MaNEP year 6, involving strong collaboration with the secondary schools. We have obtained important financial support from private foundations to carry out this project and the construction is to be completed by middle of Year 7. We have also prepared an open day event “Supra Fête” which shall take place in Geneva on June 8-10. We have furthermore explored the potential benefits of new web-based tools. Free broadcasting on *YouTube* and a *Google* exchange group, among others, were new actions of communication. The design of a new presentation booklet and the maintenance of the website are also emphasized.

## Management

To reinforce internal evaluation of performance within MaNEP – as suggested by the Review Panel – two new boards were established. We have replaced the former “advisory board” by an *Internal Evaluation Board*. This board is composed by the scientific committee and a limited number of senior members of MaNEP. We have also appointed an *Advisory Board* with a chair from Switzerland and six distinguished members from outside Switzerland. This board shall have its first meeting during the upcoming MaNEP meeting in Les Diablerets in the fall of 2007. This board will review the activities of MaNEP and give advice to the director on future activities.

## 2 Research

### 2.1 Structure of the NCCR and status of integration

#### 2.1.1 Structure of the NCCR

This section provides an up-to-date summary of the organization of MaNEP, the Swiss National Centre of Competence in Research (NCCR) on *Materials with Novel Electronic Properties*.

##### Academic institutions members of MaNEP

- University of Geneva (UNIGE), home institution
- University of Neuchâtel (UNINE)
- University of Fribourg (UNIFR)
- University of Berne (UNIBE)
- University of Zurich (UNIZH)
- Federal Institute of Technology, Lausanne (EPFL)
- Federal Institute of Technology, Zurich (ETHZ)
- Paul Scherrer Institute (PSI)
- Materials Science and Technology Research Institute (EMPA)

##### Industrial Partners

- ABB, Baden
- Bruker Biospin, Fällanden
- MecSens, Geneva
- Metrolab, Lausanne
- Phasis, Geneva
- Swiss Neutronics, Villigen

##### Scientific Committee

- Øystein Fischer, UNIGE, director
- László Forró, EPFL
- Jürg Hulliger, UNIBE
- Manfred Sigrist, ETHZ
- Jean-Marc Triscone, deputy director, UNIGE
- Dirk van der Marel, UNIGE

##### Research groups (MaNEP Forum)

###### From academic institutions:

- Philipp Aebi, UNINE
- Dionys Baeriswyl, UNIFR
- Christian Bernhard, UNIFR
- Gianni Blatter, ETHZ
- Markus Büttiker, UNIGE
- Leonardo Degiorgi, ETHZ
- Øystein Fischer, UNIGE
- René Flükiger, UNIGE
- László Forró, EPFL
- Thierry Giamarchi, UNIGE
- Marco Grioni, EPFL
- Martin Hasler, EPFL
- Jürg Hulliger, UNIBE
- Januz Karpinski, ETHZ
- Hugo Keller, PSI and UNIZH

- Giorgio Margaritondo, EPFL
- Dirk van der Marel, UNIGE
- Joel Mesot, PSI
- Frédéric Mila, EPFL
- Elvezio Morenzoni, PSI
- Reinhard Nesper, ETHZ
- Hans-Rudolf Ott, ETHZ
- Christophe Renner, UNIGE
- Maurice T. Rice, ETHZ
- Andreas Schilling, UNIZH
- Louis Schlapbach, EMPA
- Maria J.W. Seo, EPFL
- Manfred Sigrist, ETHZ
- Jean-Marc Triscone, UNIGE
- Matthias Troyer, ETHZ

###### From industrial partners:

- M. Abplanalp, ABB
- D. Eckert, Bruker BioSpin
- W. Hofer, MecSens
- P. Sommer, Metrolab
- J. Cors, Phasis
- P. Böni, Swiss Neutronics

##### Advisory Board

- Piero Martinoli, chair, Università della Svizzera Italiana,
- Dave Blank, University of Twente Netherlands
- Robert J. Cava, Princeton University USA,
- Antoine Georges, Ecole Normale Supérieure France,
- Denis Jérôme University Paris Sud, Orsay, France
- Andrew Millis Columbia University USA,
- George Sawatzky, University of British Columbia Canada.

##### Internal Evaluation Board

- Øystein Fischer, UNIGE, director
- René Flükiger, UNIGE
- László Forró, EPFL
- Jürg Hulliger, UNIBE
- Dirk van der Marel, UNIGE
- Hans-Rudolf Ott, ETHZ
- Maurice T. Rice, ETHZ
- Manfred Sigrist, ETHZ
- Jean-Marc Triscone, UNIGE, deputy director

## Management (UNIGE)

- Øystein Fischer, director
- Jean-Marc Triscone, deputy director
- Christophe Berthod, education
- Isabelle Bretton, administrative manager
- Renald Cartoni, technical organization
- Michel Decroux, scientific manager, education and training, advancement of women
- Stéphanie Grandjean, secretary,
- Matthias Kuhn, knowledge and technology transfer
- Ivan Maggio-Aprile, computer and internet resources
- Alfred A. Manuel, scientific manager, communication, education
- Anne Rougemont, communication,
- Heidi Segura, secretary.

## Collaborative projects

### 1. Strongly interacting electrons, low-dimensional and quantum fluctuation dominated systems.

*Project leader:*

- M. Sigrist (ETHZ).

*Members:*

- G. Blatter (ETHZ),
- M. Büttiker (UNIGE),
- L. Degiorgi (ETHZ),
- L. Forró (EPFL),
- T. Giamarchi (UNIGE),
- M. Grioni (EPFL),
- D. van der Marel (UNIGE),
- J. Mesot (PSI),
- F. Mila (EPF),
- H.R. Ott (ETHZ),
- T.M. Rice (ETHZ),
- L. Schlapbach (EMPA),
- M. Troyer (ETHZ).

*Contributions from:*

- Ph. Aebi (UNINE),
- D. Baeriswyl (UNIFR),
- Ø. Fischer (UNIGE).

### 2. Superconductivity, unconventional mechanisms and novel materials.

*Project leader:*

- D. van der Marel (UNIGE).

*Members:*

- D. Baeriswyl (UNIFR),
- C. Bernhard (UNIFR),
- G. Blatter (ETHZ),
- M. Büttiker (UNIGE),
- Ø. Fischer (UNIGE),
- T. Giamarchi (UNIGE),
- M. Grioni (EPFL),

- H. Keller (PSI),
- D. van der Marel (UNIGE),
- J. Mesot (PSI),
- E. Morenzoni (PSI),
- T.M. Rice (ETHZ),
- M. Sigrist (ETHZ).

*Contributions from:*

- H.R. Ott, ETHZ
- J.-M. Triscone (UNIGE).

### 3. Crystal growth.

*Project leader:*

- L. Forró (EPFL).

*Members:*

- J. Karpinski (ETHZ),
- D. van der Marel (UNIGE),
- J. Mesot (PSI),
- G. Margaritondo (EPFL).

### 4. Novel materials.

*Project leader:*

- J. Hulliger (UNIBE).

*Members:*

- J. Karpinski (ETHZ),
- R. Nesper (ETHZ),
- A. Schilling (UNIZH),
- L. Schlapbach (EMPA),
- J.W. Seo (EPFL).

### 5. Thin films, artificial materials and novel devices.

*Project leader:*

- J.-M. Triscone (UNIGE).

*Members:*

- P. Aebi (UNINE),
- G. Blatter (ETHZ),
- Ø. Fischer (UNIGE),
- T. Giamarchi (UNIGE),
- A. Schilling (UNIZH),
- D. van der Marel (UNIGE).

*Contribution from:*

- G. Margaritondo (EPFL),

### 6. Industrial applications and pre-application development.

*Project leader:*

- Ø. Fischer (UNIGE).

*Members:*

- M. Abplanalp (ABB),
- D. Eckert (BRUKER BIOSPIN),
- R. Flükiger (UNIGE),
- L. Forró (EPFL),
- M. Hasler (EPFL),
- J. Mesot (ETHZ-PSI),
- R. Nesper (ETHZ),
- J.-M. Triscone (UNIGE).



### 2.1.2 Status of integration

Since the beginning of the second phase MaNEP is organized around six collaborative projects. The members collaborate towards common goals and this furthers the synergies between the groups. This organisation by itself stimulates contacts between the groups and it fosters collaborations. This can be seen in that several smaller meetings have taken place between the members of the different projects. As an example we can mention that a closer collaboration between the crystal growth group in Geneva, the STM and the Optics group in Geneva as well as the ARPES groups at PSI, at EPFL and in Neuchâtel has been initiated. The goal of this collaboration is to compare and to analyse the different results obtained on the electronic properties of the HTS superconductor  $\text{Bi}_2\text{Sr}_2\text{Ca}_2\text{Cu}_3\text{O}_{10}$ .

As planned we have launched new calls for collaborative projects and 3 were started during this year. We have also appointed a new mobile post-doc who is now based at PSI and who will collaborate with groups at EPFL, UNIGE and UNINE.

As reported elsewhere we had a very well attended focused meeting on Novel Superconductors on September 27, 2006 and which was concluded by the Martin Peter Colloquium given by P. W. Anderson. Members from various institutions of MaNEP gathered to discuss the latest stand in this field. We also organised 6 internal workshops in January 2007 where the Forum Members of MaNEP contributing to the 6 different projects gathered and discussed in detail the results obtained.

Two years after the reorganization we observe a significant progress of the synergies within the MaNEP community. We believe that more can be done and we plan to continue along this path.

During the year we have continued our effort to integrate new young principal investigators into MaNEP:

- Prof. Christian Bernhard, a specialist in optical properties of solids and a new professor in at the University of Fribourg joined MaNEP starting July 1, 2006.
- Dr. Elvezio Morenzoni, a senior scientist at PSI and the builder of the unique slow muon beamline at that institution joined MaNEP at the same time.
- Prof. Christophe Renner, a specialist on local probes applied to the study of strongly correlated materials and a new professor at the University of Geneva, joined MaNEP from January 1, 2007.

The milestones (see appendix A) prove to be a valuable instrument of integration. Our milestones are revised and discussed among the members of the projects during the Internal Workshops. This discussion gives to the members of each Project an instrument to assess the progression of research and provides the group leaders with a global vision of the status of each project.

We also note that MaNEP is increasingly identified within the scientific community as well as by the authorities and the general public. MaNEP is also more and more considered as a partner in Swiss science. (Invitations to co-organise the Swiss Physical Society meeting, invitations to give our opinions on new projects etc.).

Integration within the home institution (UNIGE) is already considerable and this aspect was reinforced by launching our project "Physics Park", in collaboration with the Physics Department at the University. This project, a new instrument dedicated to knowledge transfer, has the full support of the University and its communication office as well as the Faculty of Sciences. This project will also help MaNEP integrate into the Canton of Geneva with the endorsement of the secondary schools as well as the financial support from private foundations in Geneva.



## 2.2 Results since the last progress report

This section reports on the research performed in the six MaNEP projects for the period from April 1<sup>st</sup> 2006 to March 31<sup>st</sup> 2007.

### **Project 1**                      **Strongly interacting electrons, low-dimensional and quantum fluctuation dominated systems**

**Project leader :** M. Sigrist (ETHZ)

**Participating members :** G. Blatter (ETHZ), M. Büttiker (UNIGE), L. Degiorgi (ETHZ), L. Forró (EPFL), T. Giamarchi (UNIGE), M. Gioni (EPFL), D. van der Marel (UNIGE), J. Mesot (PSI), F. Mila (EPF), H.R. Ott (ETHZ), T.M. Rice (ETHZ), L. Schlapbach (EMPA), M. Sigrist (ETHZ), M. Troyer (ETHZ). Contributions from Ph. Aebi (UNINE), D. Baeriswyl (UNIFR), Ø. Fischer (UNIGE).

**Summary:** This MaNEP project covers a wide range of subjects in the field of strongly correlated electron systems, encompassing the study of a variety of important material classes, the development and application of new experimental techniques and the advance of new theoretical concepts. The major interest strongly correlated electron systems receive lies in their wealth of exotic phases and properties, as well as their potential application, as is reflected in the research within this project.

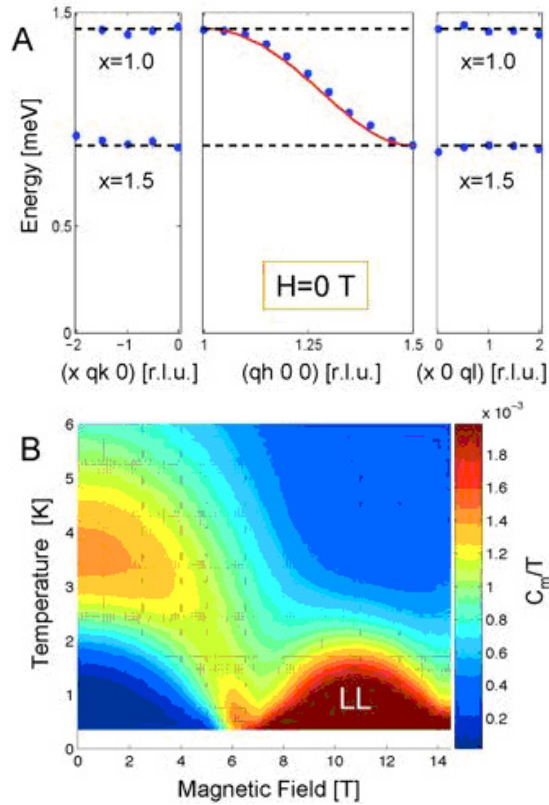
The importance of magnetism is underlined by a large number of studies on various types of quantum spin systems, whose connectivity involves spin-multimer units, frustration or low-dimensionality, thereby showing complex ordered phases or quantum liquid types of phases. Magnons behaving as hard-core bosons on a lattice for some systems yield in many respects very similar physics to that found in cold-atoms trapped in optical lattices: a superfluid-insulator transition, unusual collective modes, and aspects of the dimensional crossover. The possible existence of supersolid phases is another example where the quantum spin systems and bosonic liquids meet, as has been shown on the theoretical and computational studies. The study of correlation effects at interfaces (heterostructures) between different systems provides a further new pool of interesting physics and phenomena potentially relevant for applications. Several spectroscopic studies explore a variety of different materials. The puzzling magnetic properties of the 4f-electron (heavy Fermion) systems have been explored by NMR/NQR. Optical and photoemission spectroscopy have been employed to analyze the conditions for the realization of charge density waves in a series of chalcogenide compounds providing insight into the interplay of band structure and correlation effects. Quantum phase transitions are observed in many strongly correlated electron systems, as different ground states often depend in very subtle ways on external and internal system parameters. In this project field-induced transitions have been investigated in spin systems as well as in itinerant electron systems, such as those displaying metamagnetic transitions. In this context metal-insulator transitions in systems, such as manganites, FeSb<sub>2</sub>, and related compounds, are also explored by various techniques. Carbon systems in the form of graphite-related structures and carbon nanotubes have been investigated by spectroscopic methods and for their transport properties. In particular, the nano-carbon systems provide a clean way to study correlation physics in one-dimensional systems. The question of transport properties in nano-carbon systems is also connected with studies in mesoscopic physics. Finally a number of novel tools and techniques have been extended.

### **1. Magnetism**

Magnetism remains one of the dominant research topics in this project, which addresses the properties of systems with localized spin and orbital degrees of freedom, as well as f-electron systems belonging to the class of heavy Fermion compounds. The interest here lies particularly on the existence of exotic phases of various forms, such as quantum liquid states or systems with complex magnetic order or unusual dynamical properties.

#### **1.1 Spin multimer systems.**

**a) Phase diagram and spin dynamics in a novel organic spin ladder material:** During 2006 Mesot and coworkers investigated in detail the phase diagram and related spin dynamics of the novel organic material piperidinium copper bromide (C<sub>5</sub>H<sub>12</sub>N)<sub>2</sub>CuBr<sub>4</sub> which is a spin dimer system. The ratio of intra- ( $J_r=1.12$  meV) to inter-dimer ( $J_l=0.28$  meV) coupling and its very one-dimensional magnetic exchange (see Fig. 1:(a))<sub>2</sub> make this material one of the best quantum spin ladders known to date. The arrangement of the copper



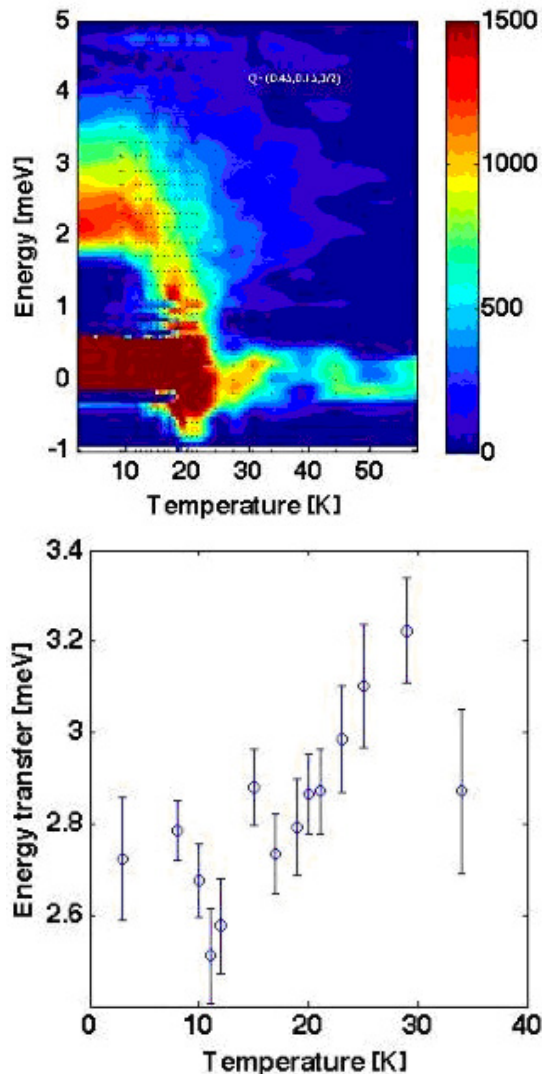
**Fig. 1. (A)** Dispersion of the triplet excitations in  $(C_5H_{12}N)_2CuBr_4$  measured at  $H=0T$  on TASP (SINQ). The absence of dispersion along the directions perpendicular to the ladder units, left and right panel, confirms the excellent low-dimensionality of the magnetic exchange in this material. **(B)** Magnetic part of the specific heat in  $(C_5H_{12}N)_2CuBr_4$  measured down to 300 mK and up to 14.5 T at HMI (Berlin, D) and down to 80 mK at NHMFL (Los Alamos, US, not shown). Notice the softening of the triplet energy gap below  $H_{c1}$  and the linear temperature-dependence of  $C_m$  between  $H_{c1}=6.7T$  and  $H_{c2}=14.5T$ , in the Luttinger-spin liquid (LL) phase.

ions was determined by neutron powder diffraction down to  $T=2K$ . The successful growth of fully deuterated single-crystal samples allowed for a systematic study of the spin dynamics across the whole phase diagram, which was also completely mapped by measurements of the specific heat, magnetization and magneto-caloric effect down to 80mK. A linear specific heat was found, characteristic for the field-induced Luttinger liquid (hard-core magnons) in an extended region between the quantum critical points  $H_{c1}=6.7 T$  and  $H_{c2}=14.5 T$  up to 1.5 K and no long-range magnetic order was detected by neutron scattering or specific heat measurements down to the lowest accessible temperatures. This is an additional confirmation of the excellent low-dimensionality of this spin system (see Fig. 1(b)). The magnetic excitations are gapped triplet modes for  $H < H_{c1}$ , and turn into a continuum with a field-dependent incommensurability between

$H_{c1}$  and  $H_{c2}$ , characteristic for the Luttinger liquid, and with a complete symmetry around the point of half magnetic saturation. Finally it reaches the ‘classical’ spectrum of a (field-aligned) ferromagnet above  $H_{c2}$ . This study benefited from the intensive collaboration with theorists (Giamarchi from Univ. Geneva, and Caux from Univ. Amsterdam) in order to explain these experimental findings on a quantitative level including the observed specific heat, field-dependence of the excitation spectrum, and details of the phase diagram.

**b) Excitations in the spin  $S=1/2$  tetrahedral system  $Cu_2Te_2O_5X_2$  ( $X=Cl, Br$ ):** The potential quadrumer systems  $Cu_2Te_2O_5X_2$  ( $X=Cl, Br$ ) with spin  $S=1/2$  coupled in tetrahedral subunits have already been characterized by Mesot and coworkers as system with a complex magnetic order in the last report. The excitation spectra show dominantly collective behavior, although the magnetic susceptibility can be fitted successfully by an isolated-tetrahedron model [1]. In a series of single-crystal experiments on triple-axis spectrometers at PSI and ILL Mesot *et al.* studied the magnetic excitations. Below flat magnon branches centered around 6 meV,  $Cu_2Te_2O_5Cl_2$  shows a very weak Goldstone mode and several dispersing modes gapped at 2 meV. These modes soften with increasing temperature and the gap closes around  $T_N$  ( $\approx 18 K$ ) (Fig. 2 up). In  $Cu_2Te_2O_5Br_2$  the gap is even larger ( $\approx 3 meV$ ), and magnetic modes persist almost without softening up to  $3 \times T_N$  with even a slight increase of the gap-energy at higher temperatures (Fig. 2 down). This behavior is consistent with the unusual thermodynamic properties observed for the Br-compound [2,3,4].

**c)  $Cu_4OCl_6$ (diallylcyanamide) $_4$ , a system of isolated tetrahedra:** Mesot and coworkers have observed puzzling properties in  $Cu_4OCl_6$ (diallylcyanamide) $_4$ . It turns out that the magnetic susceptibility, the magnetization and the specific heat cannot be explained by a simple Heisenberg quantum spin model. There is no drop of the susceptibility down to 1.8 K and the specific heat changes strongly with applied magnetic field at low temperatures, implying the presence of low-lying ferromagnetic spin states. On the other hand, the negative Curie-Weiss temperature points rather towards predominantly antiferromagnetic interactions. Moreover, the magnetization does not saturate even at 15 T reaching only  $0.3 \mu_B/Cu$ . A theoretical analysis and testing of models against the bulk measurements and inelastic neutron scattering



**Fig. 2.** *Top:* temperature dependence of the magnetic modes at 2 meV in  $\text{Cu}_2\text{Te}_2\text{O}_5\text{Cl}_2$ . *Bottom:* temperature dependence of the magnetic modes at around 3 meV in  $\text{Cu}_2\text{Te}_2\text{O}_5\text{Br}_2$  – some modes soften at  $T_N=11.4$  K, while some other do not up to at least 30 K.

data (FOCUS, SINQ) is in progress.

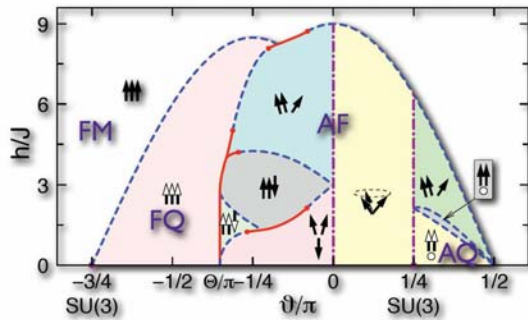
**d) Dzyaloshinskii-Moriya (DM) interactions in frustrated magnets:** Mila and coworkers have investigated the properties of the gapped spin-1/2 compound  $\text{Cu}_2(\text{C}_5\text{H}_{10}\text{N}_2\text{D}_2)_2\text{Cl}_4$  in collaboration with the experimental group of Claude Berthier (Grenoble, France). NMR measurements have revealed the presence of a magnetic field-induced transverse staggered magnetization (TSM) which persists well below and above the field-induced 3D long-range magnetically ordered (FIMO) phase. The symmetry of this TSM is different from that of the TSM induced by the order parameter of the FIMO phase. An extensive Density Matrix Renormalization Group investigation of a spin ladder with intra-dimer Dzyaloshinskii-Moriya

interactions has been performed, showing that the origin of the field dependence, and symmetry of the TSM, can be explained by this relatively simple model. This has also led to the prediction that the transition into the FIMO phase would not be in the BEC universality class [5].

**e) Quantum Dimer Models:** Mila's group has continued to study the quantum dimer model (QDM) on the triangular lattice. In order to better understand the transition between the RVB phase and the so-called plaquette phase, the Green function Quantum Monte Carlo approach has been extended to study the dynamical properties of the model [6]. It has been shown, in particular, that soft modes develop upon reducing the dimer-dimer repulsion, indicating the presence of a second-order phase transition into an ordered phase with broken translational symmetry. In addition, the nature of this ordered phase, for which a 12-site unit cell has been proposed, was studied with the surprising result that significant Bragg peaks are present only at two of the three high-symmetry points consistent with this unit cell. Mila *et al* attribute the absence of a detectable peak to strong quantum fluctuations of a local RVB type.

## 1.2 Exotic order in spin systems

**a) Quadrupolar order in a spin-1 Mott insulators:** A further spin system with geometric frustration is  $\text{NiGa}_2\text{S}_4$ , which caused Mila and coworkers to investigate a spin-1 model on a triangular lattice. When the  $SU(2)$  symmetry is broken in the low-temperature phase of Mott insulators, it is usually due to the development of some kind of magnetic long-range order. However, this is not the only possibility. If the order parameter is a tensor of higher order, breaking the  $SU(2)$  symmetry will not lead to magnetic order. One of the simplest possibilities is quadrupolar order, which can be realized in  $S > 1/2$  quantum magnets if the spins are locally in a state with a zero expectation value of the spin operators, as for instance the  $S_z=0$  state of a  $S=1$  spin. Motivated by the recent experiments on  $\text{NiGa}_2\text{S}_4$ , Mila's group has studied the bilinear-biquadratic spin-1 model on the triangular lattice. Using mean-field theory, exact diagonalizations, and  $SU(3)$  flavor theory, the phase diagram of this model in a magnetic field was mapped out precisely [7], with emphasis on the quadrupolar phases and their excitations. In particular, it was shown that ferroquadrupolar order can coexist with short-range helical magnetic order, and that the



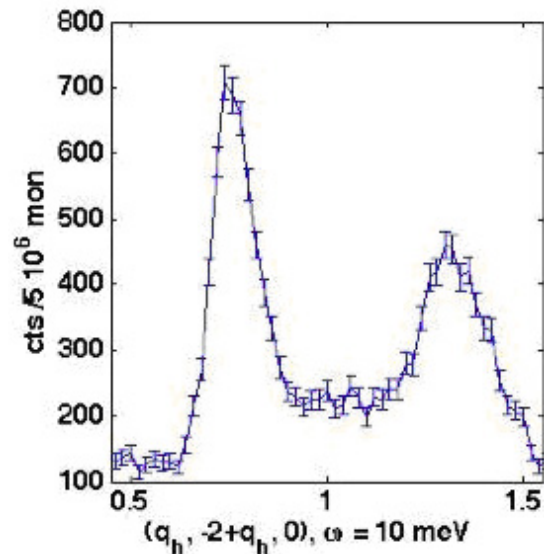
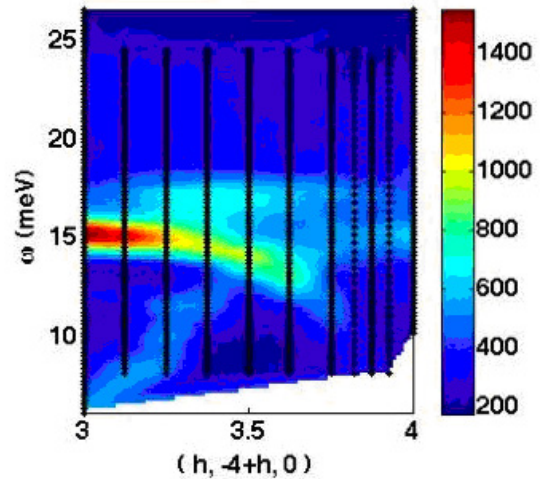
**Fig.3.** Zero-temperature phase diagram of the bilinear-biquadratic  $S=1$  model in a magnetic field on the triangular lattice.

antiferroquadrupolar phase is characterized by a remarkable  $2/3$  magnetization plateau, in which one site per triangle retains quadrupolar order while the other two are polarized along the field (Fig. 3). This has led to the conclusion that, in addition to the antiferroquadrupolar phase suggested previously, ferroquadrupolar order is a viable candidate to explain the properties of  $\text{NiGa}_2\text{S}_4$ .

**b) Topological quantum order in quantum spin systems:** Strongly correlated quantum systems can exhibit unusual quantum liquid phases with topological order. Such phases, if reliable, would pave the way towards stable, robust and decoherence-free quantum bits. Because the information is encoded in a non-local topological property no local source of noise can destroy the phase. Troyer and coworkers have shown by quantum Monte Carlo simulations that an abelian topological phase would be stable under imperfect realization with large corrections or noise terms, and is also stable under local dissipation [8]. A non-abelian topological phase with deconfined non-abelian anyonic excitations would be even more interesting, because their braiding would allow universal quantum computation. To investigate the interactions between such anyons Troyer and coworkers have developed an anyonic version of a quantum spin model, and have solved the one-dimensional chain of anyons, realizing a mapping of anyonic quantum chains to minimal models of conformal field theories [9].

### 1.3 Effective low-dimensionality

**a) The spin-web system  $\text{Cu}_3\text{TeO}_6$ :** The antiferromagnetic three-dimensional (3D) "spin-web" of  $\text{Cu}^{2+}$  ( $S=1/2$ ) ions [10] in insulating  $\text{Cu}_3\text{TeO}_6$  is a good candidate to search for quantum effects in the ordered regime of a 3D system. The spin-web is characterized by a



**Fig. 4.** *Top:* the high-energy spectrum of  $\text{Cu}_3\text{TeO}_6$  showing strong optical modes compared to the weak magnetic Goldstone mode. *Bottom:* the possible continuum in the spin-web – between the magnon branches scattering is clearly above the background level.

low connectivity – each spin has four neighbors and four next-nearest neighbors, similar to some two-dimensional (2D) cases. An inelastic neutron scattering study performed by Mesot's group on the triple-axis spectrometer PUMA (FRM2) reveals a complicated spectrum consisting of magnons and phonons [11]. The optical magnon branches show an intensity which is unusually strong for an antiferromagnetic material (Fig.4 up). From the dispersion of the acoustic magnon branches the estimated value of the antiferromagnetic exchange is  $13.5 \text{ meV}$ . Between the acoustic branches a finite spectral weight of currently unclear origin has been observed (Fig. 4 down). By analogy with 2D systems of the same connectivity, with similar reductions of the ordered moment (i.e. 2D  $S=1/2$  antiferromagnet on a square lattice)

this excess scattering might correspond to a strong two-magnon continuum and would be unusual for a 3D system. More experimental work is in progress to test for this possibility.

**b) Optical properties of  $KCuF_3$ :** Both localized spin and orbital degrees of freedom play an important role in  $KCuF_3$ . This perovskite compound is presumably one of the best realizations of an ideal 1D antiferromagnetic Heisenberg system. The low effective magnetic dimensionality is a direct consequence of orbital ordering in this compound, which leads to strong AF exchange  $J = 190K$ , within the chains (along the c-axis) and a weak ferromagnetic interchain coupling,  $J' = 0.01J$ , which is responsible for the 3D antiferromagnetic ordering at the Néel temperature  $T_N=39 K$ . Recent resonant x-ray scattering studies had shown a considerable change in the orbital ordering parameter at a temperature of 43 K, close to but well distinguishable from the antiferromagnetic ordering at the Néel temperature  $T_N=39 K$ .

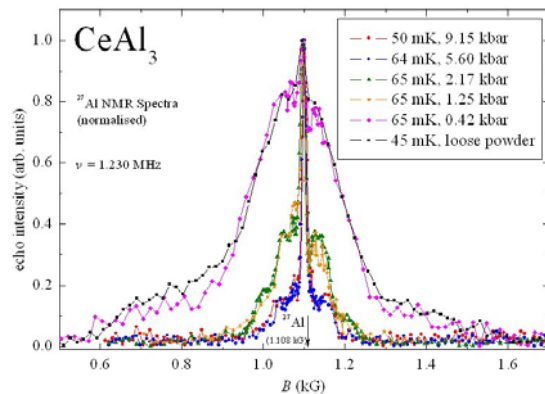
Using optical spectroscopy van der Marel's group could identify the local orbital excitations. These are observable due to their coupling to lattice vibrations which allow forbidden transitions to acquire a weak electric dipole contribution. The corresponding local  $d-d$  transitions represent a sensitive means to probe the change in the local symmetry and hence should reflect the reported changes in orbital ordering. Indeed, upon cooling below 43 K it was possible to observe the emergence of very sharp optical absorption features related to these local orbital excitations. The appearance of these transitions indicates a symmetry breaking at  $T = 43 K$ , which makes this excitation optically allowed. This structural change can be seen as a precursor for the antiferromagnetic ordering which locks in at 39 K and might be a generic feature of orbitally ordered antiferromagnetic systems as suggested by similar changes in the orbital order parameter in manganite system such as  $LaMnO_3$  or  $La_{0.5}Sr_{1.5}MnO_4$ .

**c) Spin-State Transition in  $LaCoO_3$ :** A gradual spin-state transition occurs in  $LaCoO_3$  around  $T \approx 80-120 K$ , whose detailed nature remains controversial. Mesot's group has studied this transition by means of inelastic neutron scattering [12] and found that with increasing temperature an excitation at 0.6 meV appears, whose intensity increases with temperature, following the bulk magnetization. Different origins for the observed excitation have been proposed. Within a model based crystal-field interactions and spin-orbit

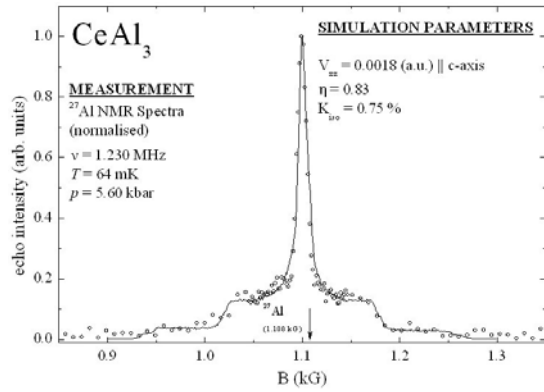
coupling, it was interpreted as the result of a transition between thermally excited states located around 120 K above the ground state. Alternatively, the nature of the magnetic excited states was discussed in terms of an intermediate-spin state ( $t_{2g}^5 e_g^1$ ,  $S=1$ ) versus a high-spin state ( $t_{2g}^4 e_g^2$ ,  $S=2$ ). Because the Landé  $g$ -factor deduced from the inelastic neutron scattering measurements is  $g \approx 3$ , the second interpretation is definitely favored.

### 1.4 Heavy Fermion systems

**a) Low-field NMR investigation of  $CeAl_3$  under hydrostatic pressure:**  $^{27}Al$  NMR spectra and spin-lattice relaxation rates were measured under pressure in the heavy-electron compound  $CeAl_3$  in the group of Ott. These challenging experiments with a powdered sample were performed in a rather low external magnetic field of approximately 0.1 T, under hydrostatic pressures up to 9 kbar and at temperatures between 60 mK and 2 K. Dramatic changes of the NMR spectra and of the spin-lattice relaxation rates  $T_1^{-1}$  were observed with increasing pressure. For  $p < 1.2 kbar$ , the  $^{27}Al$  spectra are rather broad and complicated, similar to those observed previously at ambient pressure [13]. The situation changes significantly at higher pressures (see Fig. 5). The spectra narrow rapidly and can be reproduced by simple simulations (see Fig.6). The spin-lattice relaxation rate drops by almost 2 orders of magnitude upon increasing the pressure up to 9 kbar, indicating a substantial decrease in the density of electronic states  $D(E_F)$  at the Fermi energy. Also the Knight shift  $K$  decreases upon enhancing the pressure. Earlier NMR experiments [13] on the same sample at zero external pressure revealed a broad signal, consisting of at least two contributions and



**Fig. 5.**  $^{27}Al$  NMR spectra of  $CeAl_3$  at very low temperatures under various external pressures. The solid lines are guides to the eye.

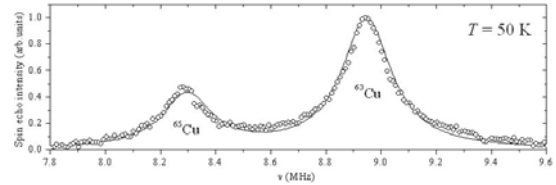


**Fig. 6.** Field sweep NMR powder-spectrum of  $CeAl_3$  at 5.60 kbar, 64 mK and for a frequency of 1.230 MHz. Symbols: experimental data; solid line: simulation. The essential numerical fit parameters, namely: the principal axis electric-field-gradient ( $V_{zz}$ ), the in-plane anisotropy ( $\eta$ ) and the isotropic Knight-shift ( $K_{iso}$ ), are displayed in the panel.

indicating a magnetically and electronically inhomogeneous ground state. The experiments by Ott *et al.* confirm this observation in the low-pressure regime, but their additional data at elevated pressures suggest that the ground state is that of a simple paramagnet at pressures exceeding 1.2 kbar. Rather unexpected is the considerable pressure-induced variation of the anisotropy parameter  $\eta$  of the electric-field gradients at the Al sites, which is revealed by the comparison of the measured spectra with corresponding simulations (see also section 9 below).

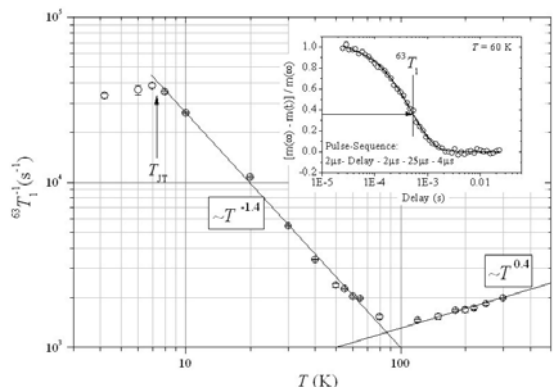
All these data indicate that rather moderate external pressures lead to a substantial alteration of the ambient-pressure ground state properties of  $CeAl_3$ . In particular, the considerable reduction of the anomalously enhanced effective mass of the conduction electrons agrees well with measurements of the specific heat under pressure [14]. Concomitantly, enhanced pressure seems to quench the electronic inhomogeneity reported in Ref.[13]. There is no doubt that the high-pressure low-temperature state of  $CeAl_3$  exhibits the properties of a simple paramagnetic metal and the data obtained indicate the absence of any magnetic order above 60 mK.

**b) Cu NQR measurements for  $PrCu_2$ :**  $PrCu_2$  is an intermetallic compound for which the  $Pr^{3+}$  4f-electron Hund's rule ground state is completely split into singlets. In such materials the onset of magnetic order is usually observed, if at all, only at low temperatures. Motivated by a recent report of a  $\mu$ SR study [15] on  $PrCu_2$  claiming the onset of magnetic order in this compound at  $T = 65$  K, Ott and



**Fig. 7.**  $^{63,65}Cu$  NQR spectrum of  $PrCu_2$ , representative for the entire covered temperature range. The open circles represent experimental data and the solid line is a simulation employing the code described in section 9.

coworkers attempted to confirm or refute this rather unexpected result by means of Cu-NMR experiments. The recorded  $^{63,65}Cu$ -NMR powder spectra, and the relaxation data were very difficult to analyze because of the large anisotropies of the Knight shift and of the electric-field gradient. More recently, attempts to observe the Copper nuclear quadrupole resonance (NQR) in  $PrCu_2$  in zero magnetic field were successful and a series of corresponding experiments in the temperature range between 4.2 K and room temperature were performed (see Fig.7). These data reveal no anomaly around 65 K, either in the temperature variation of the line width or - shape, or in the relaxation rates. By comparison with other similar data sets, Ott and coworkers conclude that their results do not reflect the onset of magnetic order in the claimed range of temperature. Nevertheless, the temperature dependence of the spin-lattice relaxation rate  $T_1^{-1}(T)$  exhibits anomalous features. Below 300 K, a power-law decrease of  $T_1^{-1}$  with decreasing temperature is intercepted by a different power-law increase below 100 K (see Fig.8). In view of the crystal-field-split 4f-electron levels and their decreasing occupancy with lowering temperature, this latter feature of  $T_1^{-1}(T)$  is rather unexpected and is not understood at



**Fig. 8.** Temperature dependence of the spin-lattice relaxation rate  $T_1^{-1}(T)$  of the  $^{63}Cu$  nuclei in  $PrCu_2$ . The inset represents the experimental magnetization recovery (open circles) and the appropriate fit function for extracting  $T_1$  (solid line).

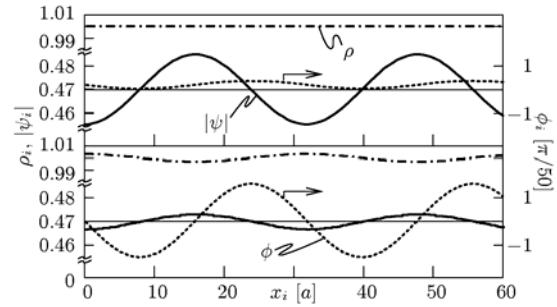


present. The cusp-like maximum in  $T_1^{-1}(T)$  at  $T = 7.5$  K reflects the previously reported phase transition [16,17] was identified by neutron scattering experiments as an induced Jahn-Teller structural phase transition [18,19].

## 2. Cold atoms in optical lattices

Some of the quantum spin-multimer systems reported in section 1 represent remarkable realizations of hard-core boson (spin triplet magnons) models, which are emulated also in systems of cold atoms in optical lattices. Indeed cold atoms provide a fascinating laboratory to study the physics of strongly correlated quantum systems, in large part because of the high degree of tunability achievable in systems such as optical lattices. It is possible to turn these generically weakly interacting dilute systems into strongly correlated ones by effectively quenching the kinetic energy of the atoms in the optical lattice. Within this project several theoretical groups have studied various aspects of cold atoms in optical lattices. Some aspects of these systems are also connected with project 2.

**a) Collective modes at superfluid-to-Mott-insulator transition:** Huber and Blatter have investigated the regime around the superfluid-to-Mott-insulator transition within the Bose-Hubbard model via approximate analytical methods allowing them to describe its dynamical properties. The method is optimized to study the Bose-Hubbard model within and in the close vicinity of the Mott-insulating phase, where number fluctuations are suppressed strongly due to the repulsive local interaction  $U$ . In this regime, a truncation to three local filling numbers (effectively rendering the problem to that of a  $S=1$  spin system) allows for the application of techniques used for interacting quantum spin systems. Within this approximation it is possible to obtain the (mean-field-based) ground state and its modifications due to fluctuations, as well as the spectra and eigenstates for the Mott phase (one particle- and one hole branch) and for the superfluid phase (one sound- and one gapped mode). The particle and the hole branches both exhibit a gap and a decreasing bandwidth with increasing interaction energy  $U$ . The phase boundary to the superfluid state is marked by the closing of either one of the two gaps, depending on the location of the chemical potential with respect to the lobe center. In the superfluid, the expected sound mode plays the role of the Goldstone mode



**Fig. 9.** Characterization of the Higgs and sound modes. Shown are the expectation values of the order parameter  $|\Psi|$  and  $\phi = \arg(\Psi)$  and the total density ( $\rho$ ) in an coherent state of a Higgs mode (upper panel) and a sound mode (lower panel). The Higgs mode is a periodic modulation of condensed and non-condensed fraction with constant density, while the sound mode is largely a modulation of the order parameter phase, accompanied by a modulation of the total density.

associated with the broken  $U(1)$  symmetry. The presence of the gapped (Higgs or amplitude) mode is not expected, *a priori*, as it is absent in  $^4\text{He}$ , as well as in weakly interacting theories for cold atoms.

One of the main achievements of this study is the characterization of this Higgs mode from two different points of view. First, from a microscopic point of view, the Higgs mode is just the remainder of the (particle or hole) mode of the Mott phase, which is not closing its gap. Second, a coherent states analysis of the sound and the gapped modes reveals its “classical” nature, see Fig.9. The sound mode is given by a periodic modulation of the phase of the order parameter, accompanied by a modulation of the total density. In contrast, the gapped mode involves a periodic modulation of the condensate fraction, effectively leading to a counterflow of condensate and non-condensate. This counterflow is known from the second sound mode in  $^4\text{He}$  where condensate- and thermally activated uncondensed fractions oscillate against one another, thus defining an entropy mode.

The two standard experimental techniques revealing directly the dynamics of ultracold atoms are known to be Bragg spectroscopy and a new modulation technique of the optical lattice introduced by Esslinger’s group at ETH [20]. While the first provides access to momentum-resolved quantities, the second technique is limited to zero momentum transfer but is relatively simple to apply in an optical lattice system. To compare with these experiments, Blatter and coworkers calculated two response functions, the dynamic structure factor and the hopping correlator (the response to a modulation of the hopping matrix element  $J$ ). The structure factor displays a gapped particle-hole continuum in the Mott phase and

single-mode peaks in the superfluid phase. However, it turns out that for sufficiently large hopping  $J$ , the single-particle energies in the Mott phase are visible as well [21]. The modulation of the lattice depth leads to excitations in the particle-hole continuum of the Mott phase, whereas in the superfluid phase a single-mode peak at the energy of the Higgs gap appears. As no momentum is transferred via the modulation of the lattice depth, no energy is pumped into the sound mode; this calculation then explains the puzzling finding of energy absorption at zero momentum transfer in this strongly correlated superfluid.

Recently Blatter *et al* developed a new method to investigate the fate of the Higgs mode when moving towards the weakly interacting regime. As this type of gapped mode is absent in the  $U = 0$  limit, the question arises of how this mode disappears with increasing ratio  $J/U$ . Within a family of Gaussian trial wave functions, whose validity extends over the whole parameter space of the interaction parameter  $U$ , the low-energy modes were analyzed within an equation-of-motion approach.

### **b) Coupled low-dimensional structures:**

Giamarchi's group has continued its research activities in this field, studying transitions in systems of coupled, one-dimensional tubes of cold atoms such as those realized in the group of Esslinger. In addition of obtaining the phase diagram, the various modes of such a system were analyzed, and it was shown that there is in addition to the conventional Goldstone mode a massive amplitude mode. Such a mode is not present in a standard isotropic superfluid obeying the Gross-Pitaevskii equation, because in that case such modes are overdamped [22].

Recently cold atomic systems have also provided a unique means of studying the Berezinsky-Kosterlitz-Thouless (BKT) transition in an interacting two-dimensional (2D) Bose gas. Such an experiment was performed in the ENS group by creating a system of two parallel, harmonically trapped 2D cold gases of Rb formed in the minima of a one-dimensional optical lattice (pancakes). Due to the large degree of flexibility of these atomic systems, it is possible experimentally to control the tunneling amplitude between the 2D gases formed in the optical lattice, and as shown by Giamarchi and coworkers [23], this allows the exploration of a much richer class of phenomena, which lies beyond the standard BKT physics. Indeed, the Josephson coupling between the 2D gases adds a new dimension to the phase diagram, which can be controlled more easily than the temperature. The

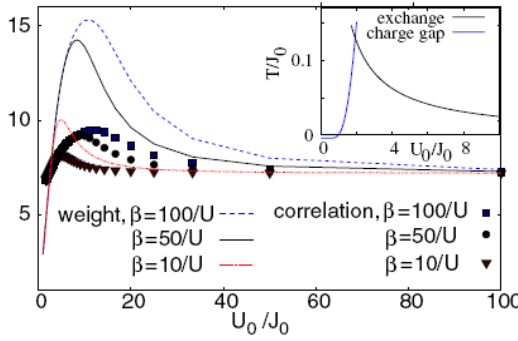
competition between the phase coherence established between neighboring pancakes when the tunneling is made large, and the thermally excited vortices in the planes, leads to a deconfinement transition similar to that analyzed for coupled chains. This study predicts two measurable effects: (i) the exponent which characterizes the scaling behavior of the interference contrast within the imaged area now experiences a jump of  $1/2$  instead of the  $1/4$  for the standard BKT transition in the absence of tunneling and (ii) the behavior of the pancakes in response to a slow rotation about the axis of the 1D lattice allows the measurement of the superfluid fraction, which experiences a jump at the crossover.

### **c) Probing cold atomic systems:**

Despite the high degree of tunability and control offered by cold quantum gases, they are difficult to probe. This makes the identification of exotic quantum phases extremely involved, and generates the demand for new detection techniques. Thus the studies in Giamarchi's group focused on two aspects of this question: (1) an in-depth analysis of one technique (shaking technique) which was used by Esslinger's group to probe the transition between a superfluid and a Mott insulator; (2) the proposal of a new technique, analogous to STM in condensed matter to create a local probe for cold atomic systems.

An experimental technique to probe the excitation spectrum in a gas of bosonic atoms relies on driving the system by periodic modulations of the optical lattice potential. As described in the report of the previous year, a linear-response analysis was performed for such a modulation. To go beyond this, as the experiment uses a very large modulation, and also to take into account additional effects such as the parabolic confinement potential, a numerical analysis was used. This problem is particularly difficult because it deals with a non-equilibrium situation where the system is driven. For this purpose a novel version of the DMRG technique was applied, taking into account time dependence (so called adaptive t-DMRG). The resulting full time evolution of the excited atomic gas gives the necessary information for the interpretation of the experimental observations [24]. It was shown that the presence of a peak at energy  $2U$  in the absorption spectrum, where  $U$  is the local interaction, is a direct measure of the degree of incommensurability present in the system.

The same analysis was applied to the problem of shaking a fermionic system [25]. Here it was shown that the absorption peaks give a remarkably accurate measure of the interaction



**Fig. 10.** Weight of the peak in the absorption spectrum for a fermionic system as a function of the interaction  $U$ , for various temperatures. There is a very good correlation between the weight and the nearest neighbor antiferromagnetic correlation. The shaking method can thus be used for fermionic systems to probe for the antiferromagnetism.

$U$ . Thus they can be used to determine the interaction experimentally. Indeed, contrary to the case of bosons, the direct calculation of this quantity from knowledge of the scattering length between two atoms is quite difficult. In addition, as shown in Fig.10, an excellent correlation was found between the weight of the peak in the absorption spectrum and the degree of antiferromagnetic correlations. Hence, for fermionic systems the shaking method can be used to probe directly the degree of antiferromagnetism, a quantity that is crucial to measure in connection with the possible realization of the Hubbard model.

These probes are designed essentially for a homogeneous atomic gas. Because cold atomic systems are inherently inhomogeneous due to the local trapping, it is crucial to realize a local probe. The trapping causes the coexistence of different spatially separated quantum phases and makes their observation very involved. Giamarchi and coworkers proposed [26] such a novel experimental procedure to probe cold atomic gases locally in an approach similar to, and as versatile as, the scanning tunneling microscope (STM) in condensed matter. This probe relies on the coherent coupling of a single particle to the atomic system. Depending on the measurement sequence either the local density, with a resolution on the nanometer scale, or the single-particle correlation function in real time, can be observed. The realization of such a probe would make possible the local investigation of the properties of exotic quantum phases. In this study it was shown how the possible phases for a two-dimensional Hubbard system of fermions in an optical lattice could be identified.

Finally Troyer's group has developed a further probing technique by using a Feshbach

resonance for the thermometry of fermionic gases [27].

**d) BCS-BEC crossover and mixed cold-atom systems:** Considering fermionic atomic systems Troyer and coworkers targeted another long-standing problem: the connection between the BCS theory of superconductivity with pairing in momentum space and the Bose-Einstein condensation (BEC) of bosonic "molecules" consisting of two fermions bound tightly in real space. At the BEC-BCS crossover there is no phase transition, but universal behavior is nevertheless present at the resonance point where the energy of a bound pair of two fermions is in resonance with the bottom of the band of unbound fermions. Using large-scale quantum Monte Carlo simulations, Troyer and coworkers could determine the value of the universal properties including the universal critical temperature at this point [28].

Besides models of relevance for electronic systems, such as the Hubbard model for two fermion flavors (spin up and down), cold gases allow for more exotic models to be realized, such as the Hubbard model for a mixture of a bosonic and a fermionic particle species, for which Troyer and coworkers have determined the phase diagram at double half-filling [29]. Moreover Troyer and coworkers compared the influence of quadratic and quartic traps on quantum phase transitions in such gases [30].

### 3. Interfaces and heterostructures

Interfaces between different states of matter are of great importance in many parts of condensed matter physics. Such interfaces also appear naturally in cold-atom systems due to the inhomogeneity induced by the shape of optical traps, and were one subject within this project. The properties of electrons at interfaces have also attracted much interest recently, as it has become possible to fabricate various heterostructures of correlated electron materials of extremely high quality, especially for transition metal oxides as realized, for example, in  $\text{LaTiO}_3 - \text{SrTiO}_3$  heterostructures [31].

While this subject also has a strong connection with project 5 (thin films, artificial materials and novel devices), here recent theoretical studies are reported, emphasizing in particular the high relevance of many-body physics and strong correlations present in these systems.

**a) Superfluid-Mott-insulator interface:** The local chemical potential approximation often

used in order to describe trapped systems leads naturally to an interface between a strongly correlated superfluid (largely depleted) and a Mott insulating region [32]. In this context, Blatter and coworkers have been addressing the question of how a phonon, the basic low energy excitation in the superfluid phase, traverses a Mott-insulating barrier. The similarity of this problem with that of Andreev reflection at a normal-metal–superconductor interface, inspired the use of methods known from the description of Andreev quantum dots. First milestones include the analysis of the scattering processes at a superfluid-to-Mott-insulator boundary and the description of phenomena known from the Klein paradox in relativistic quantum theories.

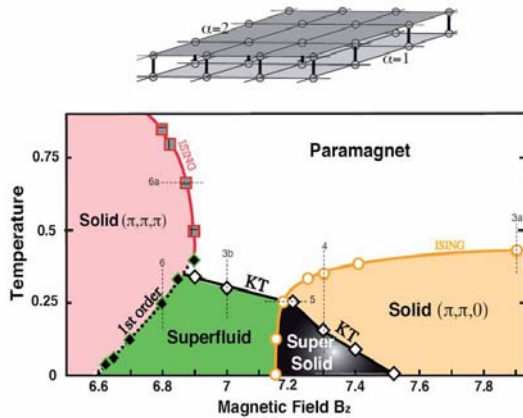
**b) Interfaces between band and Mott insulator:** Interesting novel electronic properties and phases can also occur in correlated electron systems with a spatial modulation. Ruegg, Pilgram and Sigrist have studied aspects of strong electron correlation for a model of a BI/MI/BI heterostructure where BI is a band insulator and MI can be tuned from the simple metallic to the Mott insulating regime by varying the on-site repulsion within an extended Hubbard model. The challenge here lies in the description of correlation effects in this inhomogeneous system. In prior works Okamoto and Millis have used DMFT to treat the correlation effects [33]. Ruegg et al. extended the Kotliar-Ruckenstein slave-boson mean-field scheme to the inhomogeneous situation and discussed the electronic properties for a wide range of on-site interaction strengths and of the width of the sandwich material MI [34]. There is a clear qualitative separation between the weakly (Hartree) and strongly correlated (Mott) regimes visible in various quantities such as the charge rearrangement and the optical conductivity, indicating a change in the charge fluctuations. It is also found that in the strongly interacting limit, coherent quasiparticles responsible for metallic behavior are confined to a relatively narrow region near the interfaces, where they form a strongly renormalized quasi-two-dimensional electron system. While this study has focused mainly on testing the applicability of the slave-boson theory, future efforts will aim to discuss more realistic models, and to calculate experimentally relevant quantities.

## 4. Supersolids

The supersolid state of matter, a phase that is at the same time solid and superfluid, has been elusive for many decades. It is one of the most intriguing phases of matter, as it combines two properties, which are seemingly mutually exclusive: liquid and solid. The studies within this project have examined the conditions for supersolid phases in  $^4\text{He}$ , and it has been shown also that it could be realized in certain quantum dimer spin systems related to section 1 of this project.

**a) Helium:** Following experimental evidence for the possible existence of a supersolid in  $^4\text{He}$  [35], Troyer and coworkers have performed *ab-initio* quantum Monte Carlo simulations of solid helium and found that a perfect helium crystal is insulating and not a supersolid [36]. Furthermore, they could show that the Andreev-Lifshitz-Chester vacancy mechanism for a supersolid is unstable in helium because vacancies attract each other and phase-separate instead of Bose-condensing. While the supersolid phase of matter is thus excluded in perfect helium crystals and the experiments most likely show superflow along grain boundaries, there is evidence for the existence of other types of supersolids: lattice supersolids can be realized using gases of ultra-cold polar molecules in optical lattices [37].

**b) Quantum antiferromagnets:** Bosonic models displaying supersolid phases can be realized in quantum antiferromagnets. A rather clean way is to consider weakly coupled dimers in a magnetic field, a system which has been studied extensively in the past within this project. Around the critical field where triplet and singlet dimer states start to mix, a hard-core boson description is very natural. In this mapping, an empty site represents a singlet, an occupied site a triplet, and the chemical potential describes the magnetic field. Regarding the possible low-temperature phases, an insulating solid phase signals a magnetization plateau, a Bose-Einstein condensation represents magnetic ordering of the transverse spin components, and a supersolid phase corresponds to the coexistence of both orders. In this context, Mila and coworkers have investigated the signature of such a supersolid phase in a quantum antiferromagnet, namely a spin-1/2 bilayer, with emphasis on a precise characterization of the quantum and thermal phase transitions out of the supersolid state [38]. The resulting magnetic field- temperature phase diagram is



**Fig. 11.** Phase diagram of a spin-1/2 bilayer quantum antiferromagnet with anisotropic in-plane couplings in a magnetic field.

depicted in Fig.11. This study shows that both  $T = 0$  quantum phase transitions (superfluid-supersolid and supersolid-solid) and the thermal transition display special features of direct experimental relevance. In particular, the melting of the supersolid is a two-step process in contrast to standard transitions usually observed in quantum antiferromagnets.

## 5. Optical and photoemission spectroscopy in low-dimensional metallic chalcogenide and 4-f-electron systems

Low-dimensional systems not only experience strong quantum and thermal fluctuations, but also admit ordering transitions or at least strong correlation effects, which are difficult to realize in three-dimensional materials. Well-known examples are spin and charge density waves in quasi-one-dimensional compounds due to strong nesting features. The competition between various trends and the possibility to tune certain system parameters allow us to influence the electronic properties in profound ways. In this project a number chalcogenide systems have been investigated by spectroscopic methods to search for the conditions for the formation of charge-density-wave (CDW) phases. Moreover, a hard x-ray photoemission spectroscopy (HAXPES) has been developed in order to gain access to bulk properties and has been tested successfully on several 4f-electron systems.

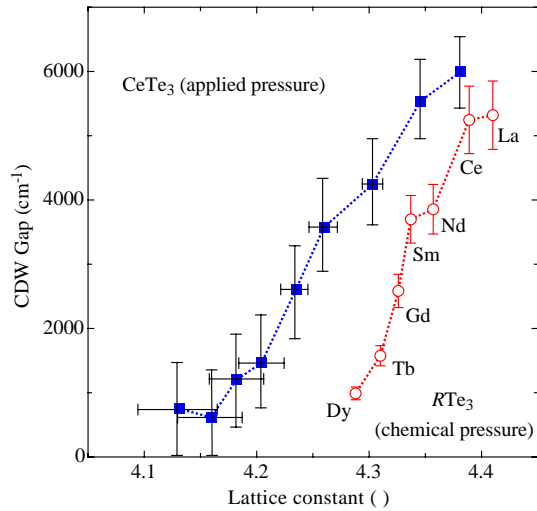
**a) Rare-earth tri-tellurides:** An interesting example of tunable low-dimensional systems is the series of the rare-earth tri-tellurides  $R\text{Te}_3$  ( $R = \text{La} - \text{Tm}$  with the exception of  $\text{Eu}$ ). They are quasi-2D systems forming an incommensurate CDW order. The average

crystal structure is layered and weakly orthorhombic, consisting of double layers of nominally square-planar Te sheets, separated by corrugated  $R\text{Te}$  slabs. The lattice constant decreases on going from  $R = \text{La}$  to  $R = \text{Tm}$ , i.e. by compressing the lattice chemically, as a consequence of the reduced ionic radius of the rare-earth atom. The physical properties in  $R\text{Te}_3$  can be then investigated as a function of the in-plane lattice constant  $a$ , which is related directly to the Te-Te distance in the Te-layers. Therefore,  $R\text{Te}_3$  provides a playground to study the effect of chemical pressure and externally applied pressure in influencing the conditions of these materials to undergo a CDW phase transition.

Degiorgi and coworkers have performed optical measurements of  $R\text{Te}_3$ . Their data, collected over an extremely broad spectral range, give access to both the Drude component and the single-particle peak, ascribed respectively to the contributions due to the free charge carriers and to the excitation across the CDW gap. On decreasing the lattice constant  $a$ , a reduction of the CDW gap together with an enhancement of the metallic (Drude) contribution were observed in the absorption spectrum.

Furthermore, the pressure dependence of the (infrared) optical reflectivity of  $\text{CeTe}_3$  at 300 K has been explored, i.e., below the CDW transition temperature, demonstrating that one can tune (in this case suppress gradually) the CDW gap by reducing the lattice constant using pressure. This control of the CDW gap is analogous to that caused by chemical means, when compressing the lattice by substituting large with small ionic radius rare-earth elements (i.e., by reducing  $a$ ). Therefore, this study establishes the equivalence of chemical and physical pressure in governing the onset of the CDW broken-symmetry ground state (see Fig.12). This is especially interesting because the present results emphasize that the suppression of the CDW gap is not a result of disorder, but arises most likely from internal changes of the effective dimensionality of the electronic structure. This strengthens the arguments regarding the link between CDW formations and nesting of the Fermi surface in these low-dimensional materials. Degiorgi and coworkers actually propose that the broadening of the bands upon lattice compression in the layered rare-earth tri-tellurides removes the perfect nesting condition of the Fermi surface and, therefore, diminishes the impact of the CDW transition on the electronic properties of  $R\text{Te}_3$ .

The formation of the CDW state in the  $R\text{Te}_3$  series was also found to be an indication for an



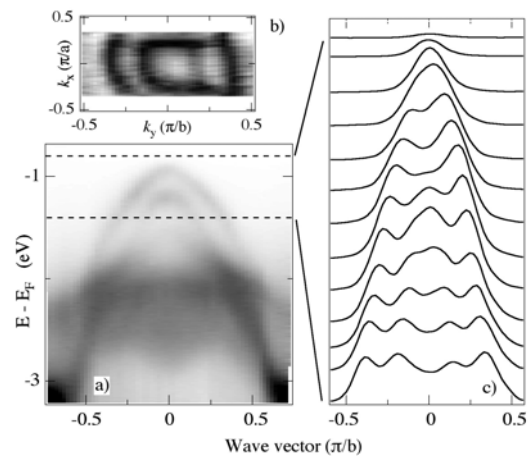
**Fig. 12.** CDW gap as a function of the lattice constant  $a$  for  $CeTe_3$  under applied pressures and for the  $RTe_3$  series. Dotted lines are guides to the eye.

effectively one-dimensional behavior (nesting) in these quasi-two-dimensional compounds. Measurements performed by Degiorgi *et al* at ambient pressure show the development of a characteristic power-law behavior in the high-frequency tail of the optical conductivity. The latter investigation of  $CeTe_3$  under applied external pressure, on the other hand, does not reveal the extent to which the applied pressure might influence the effect of electron-electron interactions and Umklapp processes, as suggested in the experiment at zero pressure over the rare-earth series, and the effect of the dimensionality crossover, in driving the CDW transition. Further experimental studies are still required, allowing the extension of the measured spectral range under pressure to higher as well as to lower energies than the energy window investigated so far. This could open new perspectives to a comprehensive study of the pressure dependence of the characteristic power law behavior seen in the absorption spectrum of the  $RTe_3$  series, and more generally of the influence of pressure in the formation of a Luttinger liquid state in quasi-one-dimensional systems.

**b) 1T-TaS<sub>2</sub>:** ARPES with high energy and momentum resolution provides a means to probe the band structure in order to obtain information on nesting properties. Aebi and coworkers studied the temperature dependence of the electronic structure of the quasi-two-dimensional compound 1T-TaS<sub>2</sub> in order to identify the origin of the CDW phase. Results of ARPES and density functional theory have been used to probe the importance of band nesting. While nesting appears to play a role in the high-temperature

phase, the ARPES line shapes reveal peculiar spectral properties inconsistent with the standard Peierls scenario for the formation of a CDW. The temperature dependence of these anomalous spectral features suggests an additional enhancement of electron-phonon interactions due to lattice-distortion at low temperatures [39].

**c) Transition-metal tri-chalcogenides:** Using ARPES, Griani and coworkers performed band-mapping measurements for  $ZrSe_3$ ,  $HfSe_3$ , and  $ZrS_3$ , three related 1D compounds which on the basis of lattice periodicity and electron counting are considered as band insulators. While these compounds do not show any lattice instabilities, they can serve as references for much-studied materials of the same family with more complex properties, like  $NbSe_3$  or  $ZrTe_3$ , which show CDW order and even superconductivity. Fig.13 shows ARPES data for  $HfSe_3$  [40]. The intensity map of Fig.13(a) displays the valence band dispersion along the infinite parallel chains of trigonal prismatic units, which characterize the structure of these quasi-1D compounds. The highest occupied band, with a maximum at the center of the Brillouin zone, is derived mainly from Se  $4p$ -states, with a minor admixture of metal  $d_{z^2}$  orbitals. It is separated by a hybridization gap from the lowest unoccupied band of similar orbital symmetry, while the 1D metal-derived band is still higher in energy. As a result of Se-Se inter-chain interactions, this band actually has a rather isotropic character, as suggested also by the rounded shape of a two-dimensional constant energy ARPES contour (Fig.13(b)). The overall band

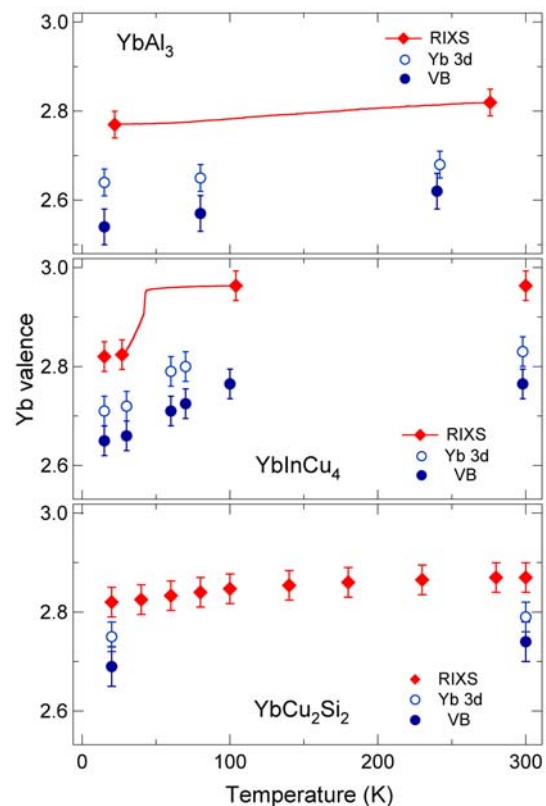


**Fig.13.** (a) ARPES intensity map of  $HfSe_3$ . (b) A two-dimensional constant energy slice near the center of the Brillouin zone, at  $E = -1.4$  eV. (c) Momentum distribution curves measured between  $-0.8$  and  $-1.4$  (horizontal dashed lines in (a)) with a step of  $0.05$  eV along the chains direction.

dispersion agrees well with the available (non-relativistic) band structure calculation, but the splitting into two nearly parallel sub-bands does not. The parallel dispersion of the two sub-bands is further illustrated by the constant-energy momentum distribution curves of Fig.13(c). A similar energy splitting is observed in  $ZrSe_3$ , and - reduced by a factor  $\sim 3$  - in  $ZrS_3$ . It is interpreted as the effect of spin-orbit interaction, by analogy with recent results in related di-chalcogenides [41]. This finding points to the need for relativistic calculations of the complex multi-sheet Fermi surface in the metallic sister compounds  $NbSe_3$  or  $ZrTe_3$ , because the description of their low-temperature CDW instabilities depends crucially on the accurate estimation of the nesting vectors. Degiorgi has demonstrated the 1D nature of the electronic properties of the insulating compounds by using complementary reflectivity measurements, which exhibit characteristic asymmetries for light polarized along or perpendicular to the chains. Moreover, the comparison of the ARPES and optical data leads to a precise determination of the energy gap [40].

**d) HAXPES on 4f-electron systems:** Ce- and Yb-based metallic materials are typical strongly correlated systems, where the partially localized nature of the 4f-orbitals leads to the intriguing Kondo and heavy Fermion phenomenology. In the past, Grioni and coworkers have studied these materials by high-resolution photoelectron spectroscopy (PES), which can probe the characteristic fine structure of the spectral function - the Kondo resonance and its spin-orbit and crystal-field satellites - in the vicinity of the Fermi surface. Those measurements suffer from the short probing depth of PES. Recent data have demonstrated that the surfaces of Ce and Yb compounds can often be regarded as distinct strongly correlated systems, with interaction parameters that do not necessarily represent the properties probed by conventional bulk measurements. The difficulty can be overcome by extending the depth of the spectroscopic probe, following two complementary strategies. In one approach, photon in - photon out experiments are performed, which are intrinsically much less surface-sensitive than PES. In another, Grioni's group participates in a widespread effort to extend PES to the hard x-ray domain, while still retaining a high energy resolution. These hard x-ray PES (HAXPES) measurements take advantage of the larger escape depth of photoelectrons at higher energy, albeit at the expense of a dramatic

reduction in the photo-ionization cross section. This kind of measurement requires special equipment, and high brilliance synchrotron radiation sources like the ESRF in Grenoble. Fig.14 shows a summary of high-resolution x-ray absorption (XAS), resonant inelastic x-ray scattering (RIXS), and HAXPES measurements (both of the valence band and of the Yb 3d core levels) performed at beamline ID16 of the ESRF on three typical Yb-based intermediate-valence materials. From each of the data sets the Yb valence was extracted and followed as a function of temperature [42]. The XAS/RIXS estimates are in very good agreement with thermodynamic and magnetic results. For a typical Kondo system such as  $YbAl_3$  one observes, as temperature is reduced, the smooth decrease of valence - with a variation of 0.05 between 300 K and 20 K - predicted by the Anderson impurity model. The temperature dependence could be traced by RIXS in a continuous way, with excellent statistics. A similar smooth dependence is observed for  $YbCu_2Si_2$ . By contrast, the RIXS data for  $YbInCu_4$  show a sharp step at 42 K, and a further decrease at lower temperature. The sharp step is the first unambiguous spectroscopic signature of a



**Fig. 14.** Yb valence values determined from Yb  $L_3$  XAS/RIXS as well as from Yb 3d and valence band HAXPES experiments. The solid lines refer to continuous temperature-dependent RIXS measurements.

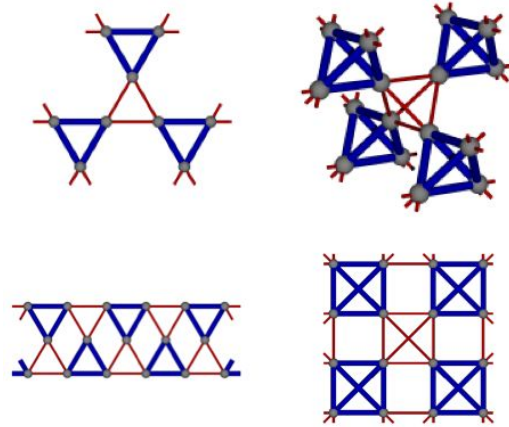
first-order valence transition already well characterized by other means, while the low-temperature evolution is probably due to a distribution of defects in a broad sub-surface region, with a thickness of several hundred Ångströms. The HAXPES data are much closer to the bulk values than conventional low-energy PES results, confirming the broader probing depth of hard x-rays, but do not coincide with them. The discrepancy is somewhat larger for the valence-band data, either because the spectral features at the Kondo scale are more sensitive to defects (samples were scraped), or for intrinsic but not yet understood reasons. Even if the photoemission results now exhibit the correct temperature and  $T_K$  trends - thus solving definitely some long-standing controversies - photoelectrons still remain too sensitive to surface conditions. Further experiments are planned to increase the bulk sensitivity by increasing the photon energy to 9 keV (from the 6 keV of the present data), and to reduce the thickness of the perturbed sub-surface layer in single-crystal samples prepared by in-situ cleaving.

## 6. Exotic phases and quantum phase transitions in itinerant electron systems

Strong correlation effects are responsible for a remarkable variety of ordered phases in itinerant electron systems, which depend subtly on system parameters such as lattice structure and electron concentrations. In this context quantum phase transitions between different phases tuned by external parameters, and the phenomena associated with them, are of major interest. Several studies, experimental and theoretical, have been devoted to these subjects during the past year. Naturally, the possibility of superconductivity in correlated electron systems has also been discussed, providing a connection to project 2.

### a) Valence-bond order in bisimplex lattices:

Frustrated lattice structures can give rise to unusual forms of order as shown in a study by Indergand and collaborators in the group of Sigrist. They have examined the class of highly frustrated bisimplex lattices, such as the kagome, the pyrochlore and the checkerboard lattice, for possible metal-insulator transitions at certain fractional carrier concentrations [43, 44]. This model study is based on a nearest-neighbor hopping model with electron correlation introduced through the Hubbard onsite repulsion  $U$  or on a  $t$ - $J$  model. For one sign of the hopping integral and the antiferromagnetic exchange in the  $t$ - $J$ -model, a



**Fig. 15.** Patterns of valence bond order in various bisimplex lattices with fractional filling [43].

generic symmetry-breaking instability towards a twofold degenerate ground state has been found for electron concentrations corresponding to two electrons per unit cell. By applying both analytical (plaquette perturbation theory and Gutzwiller renormalization mean field theory) and numerical (exact diagonalization, DMRG and CORE) methods a consistent picture was obtained that namely the ground state displays a pattern of modulated bond strengths (valence-bond order), which break only the lattice inversion symmetry. For example, on the kagome lattice this valence-bond ordered state has stronger correlations on one set of triangles (e.g. up triangles) and weaker on the others (down triangles), while analogous patterns are found for the other bisimplex lattices (Fig.15). Furthermore, a weak-coupling renormalization-group analysis was performed for the Hubbard model on the kagome strip and on the two-dimensional checkerboard lattice, using in the latter case an  $N$ -patch functional renormalization-group technique. At the some commensurate fillings a trend towards the valence-bond ordered phase emerges and dominates over other possible (magnetic) instabilities [43, 44]. The valence-bond ordered state is related to CDW phases, as discussed in the previous section. However, it is important to note that here the bond order is due entirely to correlation effects in this model, and the lattice electron-phonon coupling plays no role.

### b) Superconductivity in the two-dimensional repulsive Hubbard model:

A recent study by Baeriswyl's group led to important progress in the Gutzwiller-type variational treatments for the Hubbard model on a square lattice. The goal of this study was to settle the strongly debated issue in the context of high- $T_c$



superconductivity, of whether a superconducting ground state could be stable in the two-dimensional repulsive Hubbard model away from half filling. Improvements in numerical techniques allowed them to study larger systems than were previously accessible. The most recent results indicate that the variational wave function does exhibit (d-wave) superconductivity, in contrast to the standard Gutzwiller wave function. Both the gap parameter and the condensation energy agree surprisingly well with experimental data for the cuprates. The energy minimum for a finite gap parameter is due to a decrease in "kinetic energy" (the hopping term of the Hubbard Hamiltonian) and not due to a decrease in potential energy, as in BCS theory [45].

**c) General characterization of quantum phase transitions:** Recently a theory of "deconfined quantum criticality" [46] has been proposed for an unconventional quantum phase transition between two phases with different broken symmetries. According to Landau theory such a phase transition should be of first order, but it has been conjectured that in quantum systems a second-order quantum phase transition with deconfined fractionalized excitations could exist in bosonic or magnetic systems. By simulating the effective action of the proposed deconfined critical point, Troyer and coworkers could show that in the  $U(1) \times U(1)$ -symmetric case the transition is weakly first-order – in contrast to the proposed theory [47], but this study gives preliminary evidence for spin-1 quantum magnets that in a  $SU(2)$ -symmetric model such an unusual second order quantum critical point may exist [48].

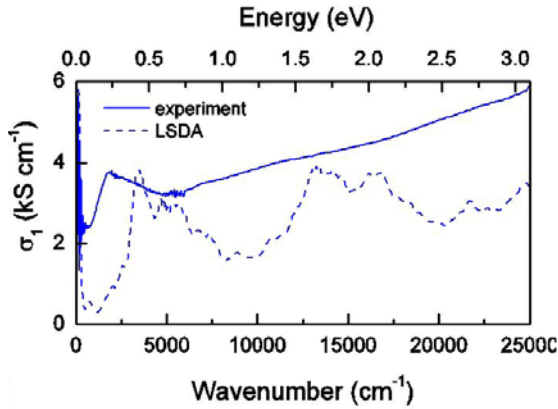
**d) Metamagnetism in the bilayer ruthenate  $Sr_3Ru_2O_7$ :** Metamagnetism at low temperatures can be discussed in terms of a quantum critical end point. At the metamagnetic transition of the metallic bilayer compound  $Sr_3Ru_2O_7$ , a peculiar low-temperature phase has been observed, whose nature is still a matter of debate [49, 50]. Binz, Braun, Rice and Sigrist have contributed to this discussion by investigating the possible occurrence of Condon domains around the metamagnetic transition [51]. At low temperatures the metamagnetic transition constitutes a first-order transition between two degenerate phases of different magnetization. In the coexistence region, domains of these two phases, Condon domains, can be formed as a result of long-range dipolar forces (demagnetization effects). Such domains,

appearing in various forms and in the simplest situation as bubbles or stripes, would cause a more complex structure of the magnetization process, as well as influence the electric transport properties, much as has been observed in experiment [49]. Nevertheless, the relevance to the experiments is unclear, as a strong dependence on the sample geometry is expected for this mechanism, which is apparently inconsistent with experimental findings. Nevertheless, this discussion serves as a prediction for a possibly strong modification of the metamagnetic transition, if the samples used in experiment are designed to have strong demagnetization effects.

**e) Nearly ferromagnetic narrow-gap semiconductor  $FeSb_2$ :** In a collaboration of Anisimov, Sigrist and Rice it was concluded based on band structure calculations that  $FeSb_2$  would be a nearly ferromagnetic narrow-gap semiconductor, and hence a direct analog of  $FeSi$  [52]. Despite different compositions and crystal structures, it was found by means of an augmented local density approximation (LDA+U) that magnetic and semiconducting solutions for  $U = 2.6$  eV are energetically degenerate. For both  $FeSb_2$  and  $FeSi$  (and the alloys  $FeSi_{1-x}Ge_x$ ) the underlying transition mechanism may allow one to switch from a narrow-gap semiconductor to a ferromagnetic metal with magnetic moment  $M = 1\mu_B$  per Fe ion by applying an external magnetic field. Interestingly this field-induced instability displays a number of features related with the metamagnetic transition discussed for  $Sr_3Ru_2O_7$ . However, due to the different starting point at zero fields the transition would constitute a metal-insulator transition, i.e. a very large magneto-resistance phenomenon.

**f) Optical evidence for heavy charge carriers in  $FeGe$ :** Cubic  $FeGe$  is a good metal at low temperatures with a low residual resistivity. It shows helimagnetic order for temperatures below  $T_C = 280$  K with a magnetic moment at the iron sites of  $1\mu_B$ . The non-centrosymmetric B20 crystal structure (cubic space group P213) is responsible for this helimagnetic order with a rather small Q-vector. The isoelectronic and isostructural compound  $FeSi$  has a large magnetic susceptibility at room temperature, which vanishes as  $T$  approaches zero due to a narrow (60 meV) semiconductor gap. A continuous series  $FeSi_{1-x}Ge_x$  can be formed, where a metal-insulator transition occurs for  $x=0.25$ .

Theoretical models, which have been proposed in the group of Van der Marel to



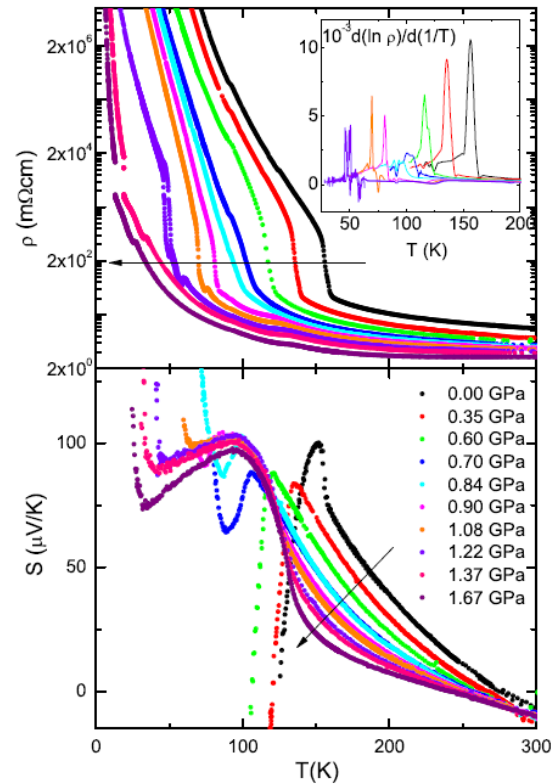
**Fig. 16.** The optical conductivity spectra of the helimagnetic state of FeGe. Solid and dashed lines denote the experimental and calculated optical spectra, respectively.

explain this behavior, invoke narrow bands and different ways of incorporating electron correlations [53]. The temperature dependent closing of the gap has been explained as a result of a correlation effects within a two-band Hubbard model. Excellent agreement with optical data was obtained. It was, however, argued that strong enough vibrational disorder also would close the gap. Anisimov, Rice and Sigrist have predicted a magnetic-field-driven metal-insulator transition for FeSi. They argue that the difference in electronic structure between FeSi and FeGe is in essence a correlation-driven transition between a narrow-gap semiconductor and a spin-polarized metal [54]. Following this model for FeGe, the optical spectra at low energies are expected to be the superposition of a Drude peak and an interband transition across an energy range corresponding to the afore-mentioned relative shift of the majority and minority bands (Fig.16). Experimentally, relatively little is known about the electronic structure of FeGe, so far no other optical data have been published.

**g) Pressure-induced phase transition in electrical transport properties of  $\beta$ - $\text{SrV}_6\text{O}_{15}$ :**

$\beta$ - $\text{Sr}_x\text{V}_6\text{O}_{15}$  is a quasi-1D compound which features a semiconductor-insulator transition strongly sensitive to the strontium stoichiometry [55]. The phase transition is only present for  $x=1$ , and disappears rapidly for  $x<1$ . Its mechanism has, despite many experimental efforts, remained poorly understood. It is considered to be either due to a charge ordering, where  $\text{V}^{4+}$  and  $\text{V}^{5+}$  sites localize onto different positions along the three crystallographic chains, or due to a CDW instability.

Forró's group continued their previous studies of the influence of disorder and pressure on



**Fig. 17.** ( $\text{SrV}_6\text{O}_{15}$ ) Resistivity (top) and thermoelectric power (bottom) are shown for various pressures. The inset depicts the logarithmic derivative of resistivity, which clearly shows an evolution from second to first order nature of the phase transition.

the transport properties for  $\beta$ - $\text{Sr}_x\text{V}_6\text{O}_{15}$ , for  $0.6 < x < 1$ . In recent experiments they investigated in detail how the phase transition evolves under pressure for the  $x=1$  compound. Both in the resistivity and in the Seebeck coefficient, a change was observed from a low-pressure ( $p < 0.7 \text{ GPa}$ ) 2<sup>nd</sup>-order to a high-pressure ( $p > 0.7 \text{ GPa}$ ) 1<sup>st</sup>-order phase transition (Fig.17) The high-temperature measurements at ambient pressure, showing non-metallic temperature dependence in both transport coefficients, indicate that it is unlikely that the phase transition is due to a CDW instability.

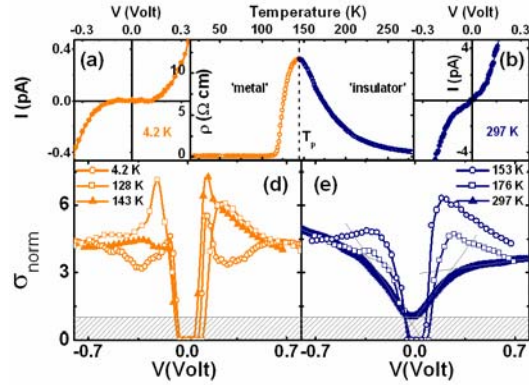
Additionally, Forró's group observed a current-induced resistance switching, and studied this effect for a range of pressures and temperatures. The resistive switching appears in the low-temperature, insulating phase, where a high current brings the system to a state of increased resistivity. The switching fields show neither pressure nor temperature dependence. This phenomenon may originate from inhomogeneous charge ordering, or from the existence of differently charge-ordered domains.

**h) Transport properties of BaVSe<sub>3</sub>:** BaVSe<sub>3</sub> is a quasi one-dimensional system, which undergoes a metal-insulator transition at 69K. This transition can be suppressed under a pressure of 2 GPa, leading to a non-Fermi-liquid ground state [56, 57]. Replacing the sulfur in BaVS<sub>3</sub> by isovalent but slightly larger selenium atoms brings a change in the overlap integrals between V 3d orbitals. BaVSe<sub>3</sub> has smaller direct overlap of V-ions along the c-axis than BaVS<sub>3</sub>, and increased ligand-mediated overlap between chains. The enhanced dimensionality of the system removes the metal-insulator transition. Instead, there is a metal-metal phase transition at 41K, accompanied by ferromagnetic order [58].

Using newly synthesized single crystals of BaVSe<sub>3</sub>, Forró's group has performed high-pressure measurements of resistivity and of the Seebeck coefficient. The crystals are of high quality with a residual resistivity ratio of 30-50. The temperature and pressure dependence of the thermopower are different from what had been observed previously by Forró's group on ceramic samples: the pressure has an important effect on the Seebeck coefficient, and there is a wide hump centered around 100K. In addition, comparative measurements of the thermal conductivity of BaVS<sub>3</sub> and BaVSe<sub>3</sub> were performed from 5 to 300K.

**i) Quasiparticle excitation spectrum in La<sub>0.77</sub>Ca<sub>0.23</sub>MnO<sub>3</sub> films:** The complex physics displayed by manganites stems from a subtle balance of competing interactions coupling spin, orbital, charge and lattice degrees of freedom. For certain compounds, a 'metal' to 'insulator' transition occurs on warming through  $T_p$  [59] (Fig 18c). Explaining the high-temperature transport properties of manganites requires the consideration of the electron-phonon coupling mechanism [60] in addition to double-exchange interactions. It is widely accepted that electrons are bound by a surrounding lattice distortion [60], forming polarons, which become the charge carriers in the 'insulating' phase [61]. However, the nature of the 'metallic' phase [62] and the relevance of nanoscale inhomogeneities to the metal-insulator transition [59] remain active subjects of debate. Insight into this problem can be gained from STM studies, which probe electronic properties at the atomic scale.

The quasiparticle excitation spectrum of a high-quality thin film of La<sub>1-x</sub>Ca<sub>x</sub>MnO<sub>3</sub> ( $x \sim 0.3$ ) was studied by Fischer's group as a function of temperature by scanning tunneling spectroscopy (STS) [63]. The film was fully strained and exhibited a metal-insulator

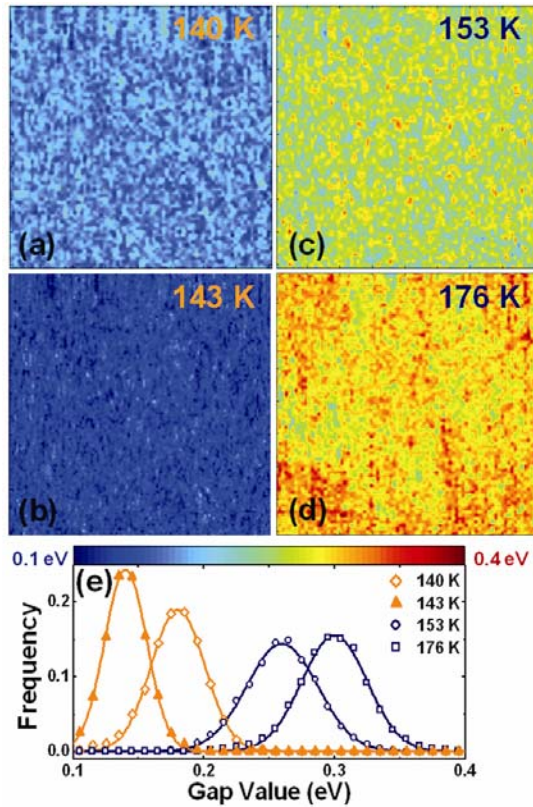


**Fig. 18:** Average tunneling  $I(V)$  curves for (a) 4.2K (2V/0.5 nA) and (b) 297 K (1V/1 nA).  $I(V)$  curves were measured with the tip grounded and a bias voltage applied to the sample. (c) The 'metal-insulator' transition temperature is detected in macroscopic resistivity measurements at  $T_p=147$ K (dotted line). (d) and (e) Selected normalized conductance curves at temperatures below and above  $T_p$ , respectively. When the measured average current was below the experimental noise ( $\sim 10$ -2 pA) was considered to be zero (hatched regions).

transition at  $T_p = 147$  K. The polaron binding energy,  $E_b$ , estimated from the fit of a small polaron model in the adiabatic limit to transport data above  $T_p$ , was found to be  $(0.22 \pm 0.02)$  eV.

Maps of tunnel current as a function of bias tension were recorded over a region of  $60 \times 60 \text{ nm}^2$  at different temperatures. Logarithmic or normalized conductance  $(dI/dV)/(I/V)$  was calculated from the data. This procedure has been proved to remove the barrier contribution from the tunneling spectrum [64] to obtain a quantity proportional to the density of states.

Spectra at all temperatures exhibited weak conductances at zero bias. In particular, above  $T_p$  and at temperatures up to at least 176 K, gapped spectra were observed over the whole field of view (Fig.18e). The measured gap amplitude, the order of 0.2-0.3 eV, is consistent with the polaron binding energy. Strikingly, below  $T_p$  in the macroscopic 'metallic' phase, the spectra remain gapped and band-edge peaks become more pronounced, even at temperatures as low as 4K (Figs.18a and d). Another surprising feature is the disappearance of the gap at room temperature, where a small but finite density of states at the Fermi level is observed over the whole field of view. This indicates that in the temperature range between 176 and 297 K the nature of polarons is changing (Figs.18b and e). Neutron scattering experiments [65] suggest that a freezing from a liquid to a glassy polaronic state with static correlations takes place at a temperature  $T > T_p$ . Thus, the 297 K normalized conductance might



**Fig. 19.** Mapping of local gap values at (a) 140, (b) 143, (c) 153 and (d) 176 K. All maps correspond to  $60 \times 60 \text{ nm}^2$  areas with a resolution of  $7.5 \text{ \AA}/\text{pixel}$ . (e) Distributions of gap values (symbols) obtained from the maps fitted with a Gaussian law (lines). The average noise of local  $I(V)$  curves in all maps is comparable, ranging from 0.2 to 0.4  $\mu\text{A}$ .

represent the quasiparticle spectrum of the polaron liquid. The results of the present study are consistent with previous STM measurements on LCMO/LAO at room and liquid-nitrogen temperatures [66]. In that work the gap measured at low voltages was identified with the polaron binding energy, where this quasiparticle represents an electron trapped in a Jahn-Teller lattice distortion.

The temperature evolution of the normalized conductance indicates that polarons in the ‘insulating’ and ‘metallic’ phase present different spectral features. In the latter case, the sharpness of band-edge peaks, signature of a well-defined binding energy, suggests that polarons order in a coherent state. The temperature dependence of the gap is consistent with polaron binding energies obtained from macroscopic optical reflectivity data [67]. The gradual broadening of the peaks on increasing temperature in the ‘insulating’ phase indicates that polarons start to lose coherence above  $T_p$  and eventually melt at  $T^*$  [65]. These findings suggest a similarity between spectroscopic properties of manganites and high-temperature

superconductors that should be considered in explaining the physics of the transition-metal-oxide family.

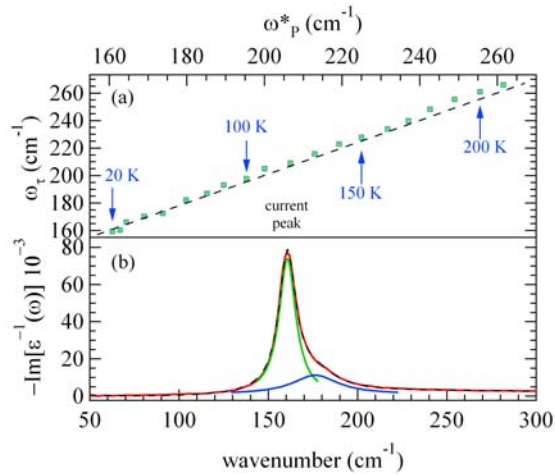
Thin films are ideal systems to investigate electronic phase separation in the absence of chemical and crystalline inhomogeneities. Fig.19 shows maps of local gap values for temperatures close to the metal-insulator transition, where phase separation would be most likely. Within the experimental resolution (ca.  $0.03 \text{ eV}$ ), a gap is detected everywhere, indicating that a phase separation between ‘metallic’ (ohmic) and ‘insulating’ domains does not occur at length scales greater than  $10 \text{ \AA}$  (Figs.19a to d). The gap-value distributions are Gaussian, with a dispersion of up to 20%, which does not change significantly with temperature, varying only 2.5% from 176 to 140K (Fig.19e). Furthermore, no bimodal distribution of  $\Delta$  is detected within  $0.03 \text{ eV}$ , suggesting that a ‘soft’ phase separation in domains with different gaps is not likely. These results imply that ‘intrinsic’ nanoscopic electronic disorder is not relevant to the physics of homogeneous optimally doped  $\text{La}_{1-x}\text{Ca}_x\text{MnO}_3$  films.

## 7. Spectroscopy and transport properties in elemental bismuth and carbon-based systems

Elemental systems with peculiar band structures have attracted much interest in recent years especially in the context of carbon-based systems such as graphite (graphene) and carbon nanotubes. However, other materials such as the semi metal bismuth also show intriguing features.

**a) Bismuth:** Elemental semi metals, such as graphite and bismuth, are materials of much long-term interest due to their exceptional properties. Although some of the basic aspects of these (only apparently) simple materials are already known, many effects observed in experiments remain unexplained. Despite the strong similarities with graphite, which is now a very active field because of its monatomic layered derivative *graphene*, the optical and infrared properties of bismuth have seen little investigation.

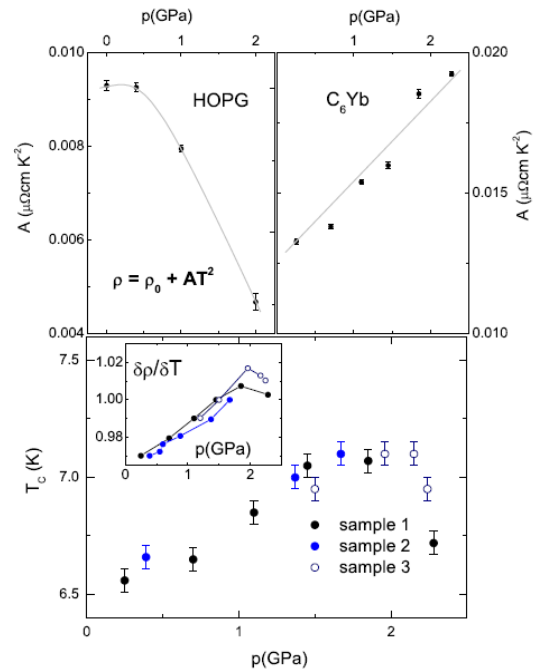
In the group of van der Marel a study of the frequency and temperature dependence of the optical properties of single-crystal bismuth was carried out using Fourier-transform spectroscopy in the infrared and visible spectral range [68]. The analysis of the optical data revealed an absorption anomaly in an energy range not compatible with any direct



**Fig. 20.** (a) A parametric plot  $\omega_p^*$  vs.  $\omega_p$  shows a slope of 1 supporting the hypothesis of an electron-plasmon interaction. (b) The 20K electron energy loss (EEL) function (red) presents the main plasmon peak and a plasmaron peak appearing as a shoulder of the main one.

inter-band transitions. Such an effect appears as a pronounced absorption peak in the mid-infrared region, preceded by a tiny pre-peak structure. The temperature dependence of this anomaly, as shown in Fig. 20, seems to follow the progressive reduction of the screened plasma frequency  $\omega_p^*$  with decreasing  $T$ . In particular the onset of the pre-peak absorption is found to be always above  $\omega_p^*$  indicating a clear relation between the two effects. The extended Drude analysis revealed that the position of the absorption feature corresponds to an abrupt increase of the scattering rate, very similar to that predicted in the case of electron-boson interaction. The electron-energy-loss function extracted from the experimental data showed together with the expected plasmon peak a second feature centered at the same frequency of the pre-peak. This observation proves unambiguously a coupling between the electron system and a longitudinal bosonic electronic collective mode. Such an interaction has been called *plasmaron*. To the best of our knowledge this represents the first optical observation of such an interaction [68].

**b)  $C_6Yb$  and graphite:** Studies of graphite intercalated with various metals have generated renewed interest since the discovery of surprisingly high superconducting transition temperatures in  $C_6Ca$  and  $C_6Yb$  [69]. In order to understand the superconducting state of  $C_6Yb$ , Forró's group has investigated the influence of high pressure on two transport parameters, the electrical resistivity and the Seebeck coefficient. To be able to separate what is intrinsic to the superconducting



**Fig. 21.** Resistivity of HOP graphite (top) and  $C_6Yb$  (bottom), under different pressures. The inset shows the blow-up of the low temperature resistivity in  $C_6Yb$ .

compound, they have also studied the response of the pristine, non-intercalated material to pressure.

The resistivity and Seebeck coefficient of  $C_6Yb$  are both markedly different from those of the starting material, HOP graphite. The resistivity shows typically metallic behavior, with a quadratic term at low temperatures, characteristic of electron-electron correlations. The coefficient  $A$ , which describes the  $T^2$  dependence, increases with pressure (Fig. 21). However, the strongest pressure dependence is observed for the residual resistivity. Forró and coworkers explain this increase by the warping of the graphene sheets. The Seebeck coefficient or thermoelectric power shows clearly metallic temperature dependence. This suggests a single-band description, as opposed to graphite where a two-carrier description is needed due to the semi metallic character of the electronic structure.

**c) Defects in carbon nanotubes:** Carbon nanotubes, with their great potential as electronically active materials in electronic devices such as field effect transistors (FET) or single electron transistors (SET) have also been a topic of this project. Gröning and coworkers at EMPA investigate the effect of defects in single-walled carbon nanotubes (SWNT) with the aim that in future single defects may be introduced in a controlled way with well-defined effects on the transport

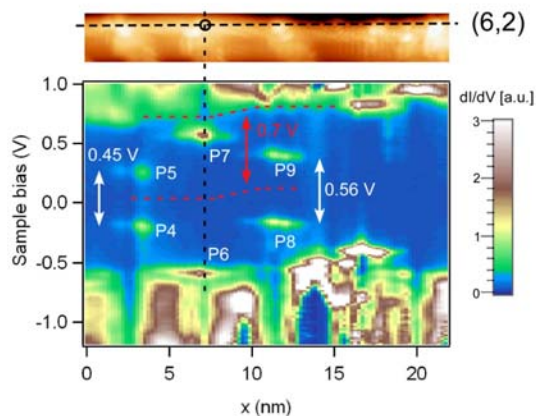
properties. They have shown that exposure of graphite surfaces to a hydrogen electron cyclotron resonance (ECR) plasma is very effective in creating single defects of C-H chemisorption and C-vacancy type [70,71]. Both kinds of defects act as strong electron scatterers [72].

In the previous period the group reported that defects on metallic SWNT showed a characteristic  $\sqrt{3} \times \sqrt{3} R30^\circ$  superstructure in the STM topography which is well-known for defects in graphite. Due to the 1D character of the SWNT the superstructures can be observed at quite large distances from the defect, up to 6-10 nm. More surprising is the observation of the superstructure on semiconducting tubes, as there is no point-like Fermi-surface. However, the band onsets are still close to the  $K$ -points in the underlying 1<sup>st</sup> Brillouin zone of graphene, and the structure exists with a shorter range and amplitude as compared to the metallic ones [73].

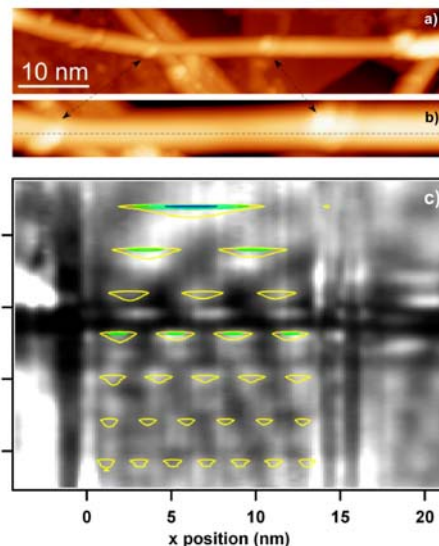
Interesting correlation effects have been observed in some high-resolution line scans. Close to defects on metallic SWNT, beating patterns were observed in the LDOS, similar to those reported STM/STS investigations near the ends of nanotubes [74]. The observed patterns could be identified as electronic standing waves of two different wavelengths caused by separate spin and charge bosonic excitations, which constitute a characteristic signature of a Luttinger liquid (theoretical basis in [75]). Further investigations are needed to confirm the nature of the observed patterns.

For the metallic tubes Gröning and coworkers could observe a strong increase of the local density of states (LDOS) at defect positions, showing a pronounced peak close to the Fermi

energy [76]. Density functional theory (DFT) calculations reproduce several features of the spectra very well, assuming that the defects are of vacancy type. The appearance of sharp, spatially localized peaks in the LDOS is also characteristic for the hydrogen ECR plasma-induced defects on semiconducting SWNT. Single peaks can be observed at the Fermi energy as for the metallic tubes, but also at other energetic positions in the gap, conduction or valence bands. However, two sharp peaks were observed in the LDOS, more often than were single peaks. These peaks are separated in energy, but not spatially. Fig. 22 shows a STS line-scan map at 5 K on a (6,2) SWNT with several defect sites. The two peaks of such structures are symmetric around the gap centre. DFT calculations of different vacancy configurations on semiconducting tubes could not reproduce this characteristic double-peak feature in the LDOS. All these configurations yield a single, weakly dispersing band, as a single peak in the LDOS. DFT simulations of H-chemisorption-type defects show, however, that nearby chemisorbed H adatoms give rise to two split, weakly dispersive bands, which would generate the sharp double peaks in the LDOS. The double-peak structure can be understood by analogy with the bonding – antibonding orbital splitting of the H molecule. However, in the present case the interaction between the two H atoms is mediated by the lattice of the SWNT [77]. One of the goals of this project is the creation of quantum dots (QD) on metallic SWNT using



**Fig. 22.** *Top:* STM topographic image of a semiconducting (6,2) tube with a number of H-ion induced defects. *Bottom:* tunneling spectroscopy map (5 K) along the line indicated in the topographic image. The symmetric gap state visible at the defect positions are labelled from P4 to P9.



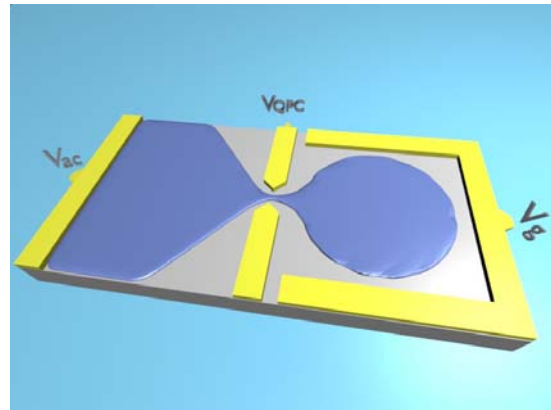
**Fig. 23.** *a) and b)* topographic STM images of a metallic SWNT with two  $Ar^+$ -ion ( $E_{kin}=400$  eV) induced defects in the middle section. *c)* Tunneling spectroscopy mapping (5 K) along the line indicated in image *b)* showing quantum dots states in the region between the two defects.

defects. In the case of the hydrogen ECR plasma-induced defects, so far no QD behavior could be observed. However, using  $\text{Ar}^+$  ions of 400 eV kinetic energy defects acting as tunneling barriers on metallic SWNT, and leading to discrete QD states between them, could be produced. Fig. 23 shows the LT-STM/STS signature of a defect-induced QD. Figs. 23a) and b) display the topographic STM images of a metallic SWNT with the  $\text{Ar}^+$  ion-induced defects. Fig. 23c) depicts the spectra recorded at 5 K along the line indicated in Fig. 23b). Discrete states with an energy splitting of 120 meV can be observed. The color contour plot in Fig. 23c) is a simulation using a Fabry-Pérot interferometer model to calculate the QD states. These data are still of preliminary nature, and future studies will aim to calculate the transparencies of the barriers and the coupling between adjacent QD's.

**d) Perfectly conducting channel in disordered graphene ribbons:** Besides nanotubes 1D graphene systems with boundaries, such as ribbons, are also of interest, as boundaries influence the properties in a crucial way. This has become obvious in graphene ribbons with zigzag edges, where edge states dominate the transport properties [78]. The band structure of such graphene ribbons possess two valleys well separated in momentum space, related to the two Dirac points of the graphene spectrum. Wakabayashi, Takane and Sigrist have shown that the propagating modes in each valley contain a single chiral mode originating from a partially flat band at the band center [79]. This feature gives rise to a perfectly conducting channel in the disordered system, if the impurity scattering does not connect the two valleys, i.e. for long-range impurity potentials. Ribbons with short-range impurity potentials, however, display ordinary localization behavior due to inter-valley scattering. The two regimes belong to different universality classes: unitary for long-range and orthogonal for short-range impurity potentials. Experiments in graphene have shown that inter-valley scattering is weak. Thus, it should in principle be feasible experimentally to realize graphene ribbons in the unitary class with a perfectly conducting channel.

## 8. Mesoscopic physics: Quantized charge relaxation resistance

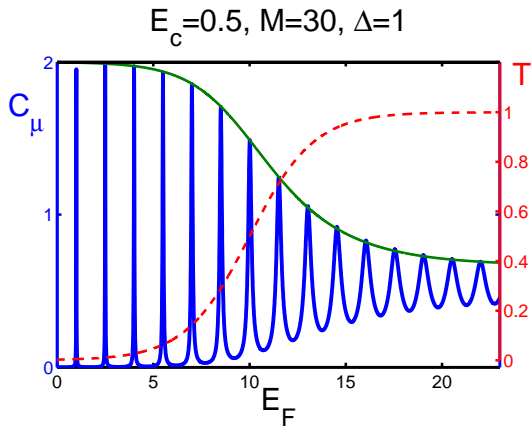
As shown in the previous section, quantum dots created in nano-carbon systems open the door to mesoscopic aspects of electron



**Fig. 24.** Mesoscopic capacitor: With the help of side gates (yellow) a two dimensional electron gas (blue) is patterned into a cavity connected via a narrow channel (controlled by  $V_{QPC}$ ) to a metallic contact (at potential  $V_{ac}$ ). The cavity is capacitively coupled to a gate at potential  $V_G$ . Of interest is the RC-time and in particular the resistance  $R$ . After Ref. [83].

transport. Hence it is also important to explore transport conditions for interacting electrons in mesoscopic devices within this project. In the past year the group of Büttiker studied various aspects of the quantization of charge relaxation resistance. Unlike other quantized resistances, the charge relaxation resistance determines not a dc resistance but describes a dynamic phenomenon. In contrast to the quantization of resistances in quantum point contacts or in the integer quantized Hall effect, the quantization of the charge relaxation resistance rests on the fact that the ratio of the mean square dwell time of reflected particles is equal to the square of the average dwell time [80]. This is true only for a single quantum channel, but remarkably it is true independent of any degree of elastic scattering. However, it is true only if the reflection is quantum coherent.

A recent experiment by the group of Glattli in Paris measured the charge relaxation resistance of a quantum coherent mesoscopic capacitor [81]. The experimental arrangement is shown in Fig. 24. The capacitor is patterned in a 2D electron gas (shown in blue) with the help of top gates. A narrow channel whose width can be controlled with a gate voltage  $V_{QPC}$  connects a cavity to a large region of the 2D electron gas, which is connected in turn to a metallic contact. The cavity is coupled capacitively to a side gate at voltage  $V_G$ . This structure supports no dc current. An ac current can be induced by an oscillating voltage difference  $V_{ac} - V_G$ . The experiment determines the capacitance  $C_\mu$  of the structure and the relaxation resistance  $R_q$ , and confirms a theoretical prediction by Büttiker et al. [80], according to which this resistance is quantized at half a resistance quantum independent of



**Fig. 25.** Capacitance: As a function of Fermi level the number of electrons in the cavity increases one by one. At the same time the transmission probability (red broken line) through the narrow channel increases. The theory uses a single particle scattering matrix for a cavity with  $M=30$  levels and achieves quantized filling (Coulomb blockade) of the cavity through an approach which excludes self-interaction.  $E_c$  is the Coulomb energy. Energies are measured in units of the level spacing  $\Delta$  in the cavity. After Ref. [83].

the transmission probability of the channel connecting the capacitor plate to a metallic contact.

If the quantum point contact in Fig. 24 is almost closed, moving an electron onto the cavity must overcome the Coulomb blockade. In a recent study Büttiker and coworkers investigated the effect of interaction, treating it on the level of the Hartree-Fock approximation. They demonstrate that as long as the connection of the island to the contact is through a single channel, interactions do not affect quantization. Interestingly, the key effect, which separates Hartree from Hartree-Fock, the exclusion of self-interaction, can be incorporated directly into a single-particle scattering matrix [82]. Fig. 25 shows a theoretical result for the capacitance of this structure as a function of the Fermi energy. For a nearly closed channel, strong Coulomb peaks are observed. With increasing energy the transmission probability through the channel increases, and at the same time the Coulomb peaks become smaller in height and broaden. In contrast to  $R_q$  the capacitance  $C_\mu$  is strongly sample-specific.

Because quantum coherence is essential for the quantization of the charge relaxation resistance, it is also important to investigate effects, which destroy or mask quantum coherence. Büttiker and coworkers have investigated the effects of phase breaking (using a fictitious voltage probe) on the charge relaxation resistance [83, 84]. For a perfectly transmitting channel, a one-channel dephasing probe leaves  $R_q$  invariant and quantized at half

a resistance quantum. The same result is obtained in the high-temperature limit due to thermal averaging. In contrast, a multi-channel dephasing probe yields (for perfect transmission) a charge relaxation resistance of a full resistance quantum. Thus only in the multi-channel limit does the cavity act like a thermal equilibrium electron reservoir.

## 9. New algorithms and new instruments

New techniques developed within this MaNEP project have already been reported in parts above, in their physical context as direct applications. Here we report on advances on the computational physics side and the development of packages useful for the analysis of experimental data in NMR/NQR.

**a) ALPS:** Troyer's group continues to work on the development of new algorithms for the simulation of strongly correlated quantum systems. Recently this group developed an algorithm to optimize temperature sets for parallel-tempering simulations [85]. A new and very efficient quantum Monte Carlo solver for the dynamical mean field theory developed last year has been published [86]. In addition, release 1.3 of the open-source ALPS software for the simulation of quantum systems has been released.

**b) NMR/NQR spectrum simulation package:** NMR and NQR spectra of solids are often characterized by very complex structures containing several peaks and broad features, which are in most cases difficult to identify and to assign *a priori*. The possibility of simulating the NMR/NQR spectra starting from the microscopic parameters characterizing the nuclear-spin Hamiltonian is thus extremely useful in this context. Despite this, to the best of our knowledge, such a tool, developed specifically for solid-state NMR/NQR, seems not to be available. Application of current general-purpose NMR codes for this task is far from straightforward. For this reason, Ott and coworkers developed a simple but powerful *fortran77* code, designed especially for the simulation of solid-state NMR/NQR spectra. The program starts from the microscopic parameters describing the hyperfine field (in the form of the Knight-shift parameters) and the quadrupolar components (in the form of the electric-field-gradient parameters) of the nuclear-spin Hamiltonian and performs a numerical diagonalization. The spectrum is then reconstructed according to the energy eigenvalues and to the corresponding



transition probabilities obtained from the eigenvectors. Also the possibility of considering different isotopes and/or different lattice sites for the nucleus under consideration were implemented, as was the calculation of both single-crystal and powder spectra. The simulation can be run equally well for a fixed magnetic field as a function of the frequency or for a fixed frequency while sweeping the magnetic field.

In Fig. 6 the experimental  $^{27}\text{Al}$  NMR field-sweep powder spectrum obtained in the high-pressure phase of the heavy-electron compound  $\text{CeAl}_3$  is compared with the corresponding simulation. The surprisingly good agreement between the experimental and simulated curves allows us to conclude that the high-pressure phase of  $\text{CeAl}_3$  is characterized by an anomalously large anisotropy ( $\eta$  parameter) of the electric-field gradients at the Al sites.

This code is currently being applied successfully for the interpretation of experimental NMR/NQR spectra of several other compounds studied in the framework of this project (section 1).

## References

- [1] M. Johnsson, *Chem.Mater* **12**, 2853 (2000).
- [2] P. Lemmens *et al.* PRL **87**, 227201 (2001).
- [3] Z. Jaglicic *et al.* PRB **73**, 214408 (2006).
- [4] K. Prša *et al.*, in preparation.
- [5] M. Clémancey *et al.*, Phys. Rev. Lett. **97**, 167204 (2006).
- [6] A. Ralko, M. Ferrero, F. Becca, D. Ivanov, F. Mila, Phys. Rev. B **74**, 134301 (2006).
- [7] A. Läuchli, K. Penc, F. Mila, Phys. Rev. Lett. **97**, 087205 (2006).
- [8] S. Trebst *et al.*, Phys. Rev. Lett. (2007) in press
- [9] A. Feiguin *et al.*, Phys. Rev. Lett. (2007) in press
- [10] M. Herak *et al.*, J. Phys: Cond. Mat. **17**, 7667-7679 (2005).
- [11] K. Prša *et al.*, in preparation.
- [12] A. Podlesnyak *et al.*, PRL **97**, 247208 (2006).
- [13] J.L. Gavilano, J. Hunziker, and H.R. Ott, Phys. Rev. B **52** R13106 (1995).
- [14] G.E. Brodale *et al.*, PRL **56**, 390 (1986).
- [15] A. Schenck, F. N. Gyax, and Y. Onuki, Phys. Rev. B **68** 104422 (2003).
- [16] K. Andres, E. Bucher, J. P. Maita, and A. S. Cooper, Phys. Rev. Lett. **28** 1652 (1972).
- [17] M. Wun and N.E. Phillips, Phys. Lett. **50A**, 195 (1974).
- [18] H. R. Ott, J.K. Kjems and K. Andres, Proc. of the Conf. on Rare Earth and Actinides, Durham 1977, IOP Conference Series **37**, 149.
- [19] J.K. Kjems, H.R. Ott, S.M. Shapiro and K. Andres, J. Phys.(Paris), Colloq. **39**, C6 (1978).
- [20] T. Stöferle *et al.*, Phys. Rev. Lett. **92**, 130403 (2004).
- [21] S. Huber *et al.*, cond-mat/0610773 (2006).
- [22] M. A. Cazalilla, A. F. Ho and T. Giamarchi, New. J. Phys. **8** 158 (2006).
- [23] M. A. Cazalilla, A. Iucci and T. Giamarchi, cond-mat/0701761.
- [24] C. Kollath, A. Iucci, T. Giamarchi, W. Hofstetter and U. Schollwock, Phys. Rev. Lett. **97** 050402 (2006).
- [25] C. Kollath, A. Iucci, I. P. McCulloch and T. Giamarchi, Phys. Rev. A **74** 041604(R) (2006).
- [26] C. Kollath, M. Köhl and T. Giamarchi, preprint (2007).
- [27] H.G. Katzgraber, *et al.*, Phys. Rev. A **74**, 043602 (2006).
- [28] E. Burovski *et al.*, Phys. Rev. Lett. **96**, 160402 (2006); New J. Phys. **8**, 153 (2006).
- [29] L. Pollet *et al.*, Phys. Rev. Lett. **96**, 190402 (2006).
- [30] O. Gygi *et al.*, Phys. Rev. A **73**, 063606 (2006).
- [31] A. Ohtomo *et al.*, Nature **419**, 378 (2002).
- [32] S. Fölling *et al.*, Phys. Rev. Lett. **97**, 060403 (2006).
- [33] S. Okamoto and A.J. Millis, Nature **428**, 630 (2004).
- [34] A. Rüegg, S. Pilgram and M. Sigrist, cond-mat/0701642.
- [35] E. Kim and M.H.W. Chan, Science **305**, 1941 (2004).
- [36] M. Boninsegni *et al.*, Phys. Rev. Lett. **97**, 080401 (2006).
- [37] S. Wessel and M. Troyer, Phys. Rev. Lett. **95**, 127205 (2005).
- [38] N. Laflorencie and F. Mila, preprint.
- [39] F. Clerc, C. Battaglia, M. Bovet, L. Despont, C. Monney, H. Cercellier, M. G. Garnier, P. Aebi, H. Berger, and L. Forró, Phys. Rev. B **74**, 155114 (2006).
- [40] D. Pacilé *et al.*, Phys. Rev. B, submitted.
- [41] F. Clerc *et al.*, J. Phys.: Condens. Matter, **16**, 3271 (2004).
- [42] L. Moreschini *et al.*, Phys. Rev. B **75**, 035113 (2004).
- [43] M. Indergand, A. Läuchli, S. Caponi and M. Sigrist, Phys. Rev. B **74**, 064429 (2006).
- [44] M. Indergand, C. Honerkamp, A. Läuchli, D. Poilblanc and M. Sigrist, Phys. Rev. B **75**, 045105 (2007).
- [45] D. Baeriswyl, D. Eichenberger and B. Gut, cond-mat/0612690, to appear in phys. stat. sol. (b).
- [46] T. Senthil, A. Vishwanath, L. Balents, S. Sachdev, M.P.A. Fisher, Science **303**, 1490 (2004).
- [47] A. Kuklov *et al.*, Ann. of Phys. **321**, 1602 (2006).
- [48] K. Harada *et al.*, J. Phys. Soc. Jpn. **76**, 013703 (2007).
- [49] S.A. Grigera *et al.*, Science **306**, 1154 (2004).
- [50] R.A. Borzi *et al.*, Science **315**, 214 (2007).
- [51] B. Binz, H.B. Braun, T.M. Rice and M. Sigrist, Phys. Rev. Lett. **96**, 196406 (2006).
- [52] A.V. Lukoyanov, V.V. Mazurenko, V.I. Anisimov, M. Sigrist and T.M. Rice, Eur. Phys. J **B53**, 205 (2006).
- [53] V. Guritanu, D. van der Marel, J. Teyssier, T. Jarlborg, H. Wilhelm, M. Schmidt and F. Steglich, cond-mat/0702341.
- [54] V.I. Anisimov *et al.*, Phys. Rev. Lett. **76**, 1735 (1996); Phys. Rev. Lett. **89**, 257203 (2002).
- [55] Y. Ueda, M. Isobe, T. Yamauchi, J. Phys. Chem. Solids **63** 951–955 (2002).
- [56] G. Mihaly *et al.*, Phys. Rev. B **61**, R7831 (2000).
- [57] L. Forró *et al.*, Phys. Rev. Lett. **85**, 1938 (2000).
- [58] M. Shiga and H. Nakamura, RIKEN Rev. **27**, 48 (2000).
- [59] E. Dagotto, *Nanoscale Phase Separation and Colossal Magnetoresistance*, Springer-Verlag, Berlin (2003).
- [60] A. J. Millis *et al.* Phys. Rev. Lett. **74**, 5144 (1995); A. J. Millis *et al.*, Phys. Rev. Lett. **77**, 175 (1996).
- [61] D. C. Worledge *et al.*, Phys. Rev. B **57**, 15267 (1998), V. Drozd *et al.*, Acta Phys. Polon. A **106**, 751 (2004), M. Jaime *et al.*, Phys. Rev. Lett. **78**, 951 (1997),
- [62] N. Mannella *et al.*, Nature **438**, 474 (2005).
- [63] S. Seiro *et al.*, submitted to Phys. Rev. Lett.
- [64] R. M. Feenstra *et al.*, Surface Science **299/300**, 965 (1994),
- [65] J. M. De Teresa *et al.*, Nature **386**, 256 (1997); D. N. Argyriou *et al.*, Phys. Rev. Lett. **89**, 036401 (2002).
- [66] J. Y.T. Wei *et al.*, Phys. Rev. Lett. **79**, 5150 (1997),
- [67] C. Hartinger, *et al.*, Phys. Rev. B **69**, 100403 (2004).
- [68] Riccardo Tediosi, N. P. Armitage, E. Giannini, D. van der Marel, cond-mat/0701447.
- [69] T.E. Weller *et al.*, Nature Physics **1**, 39 (2005).

- [70] P. Ruffieux, O. Gröning, M. Biemann, P. Mauron, P. Gröning, and L. Schlapbach, *Physical Review B* **66(24)**, 245416-1/7 (2002).
- [71] P. Ruffieux, O. Gröning, M. Biemann, and P. Gröning, *Applied Physics A* **78**, 975 (2004).
- [72] P. Ruffieux, M. Melle-Franco, F. Zerbetto, O. Gröning, M. Biemann, and P. Gröning, *Phys. Rev. B.* **71**, 153403 (2005).
- [73] G. Buchs, P. Ruffieux, P. Groening and O. Groening, *Appl. Phys. Lett.*, **90**, 013104 (2007).
- [74] J. Lee *et al.*, *Phys. Rev. Lett.*, **93**, 166403 (2004).
- [75] S. Eggert, *Phys. Rev. Lett.*, **84**, 4413 (2000).
- [76] G. Buchs, P. Ruffieux, P. Groening and O. Groening, *Journal of Physics : Conference Series*, in press
- [77] G. Buchs, A. Krasheninnikov, P. Ruffieux, P. Groening, A. S. Foster, R. M. Nieminen and O. Groening, in preparation for *Nature Materials*.
- [78] K. Wakabayashi and M. Sigrist, *Phys. Rev. Lett.* **84**, 3390 (2000).
- [79] K. Wakabayashi, Y. Takane and M. Sigrist, *cond-mat/0702230*.
- [80] M. Buttiker, H. Thomas and A. Prêtre, *Phys. Lett. A* **180**, 364 (1993).
- [81] J. Gabelli, *et al.* *Science* **313**, 499 (2006).
- [82] Simon E. Nigg, Rosa Lopez, and Markus Buttiker, *Phys. Rev. Lett.* **97**, 206804 (2006).
- [83] Markus Buttiker and Simon Nigg, *Nanotechnology* **18**, 044029 (2007).
- [84] Simon Nigg and Markus Buttiker, (unpublished).
- [85] H.G. Katzgraber *et al.*, *J. Stat. Mech.* P03018 (2006).
- [86] P. Werner *et al.*, *Phys. Rev. Lett.* **97**, 076405 (2006).

## Project 2 Superconductivity, unconventional mechanisms and novel materials

**Project leader :** D. van der Marel (UNIGE)

**Participating members :** D. Baeriswyl (UNIFR), C. Bernhard (UniFR), G. Blatter (ETHZ), Ø. Fischer (UNIGE), T. Giamarchi (UNIGE), M. Grioni (EPFL), H. Keller (PSI), D. van der Marel (UNIGE), J. Mesot (PSI), E. Morenzoni (PSI), T.M. Rice (ETHZ), M. Sigrist (ETHZ). Contributions from H.R. Ott and J.-M. Triscone (UNIGE).

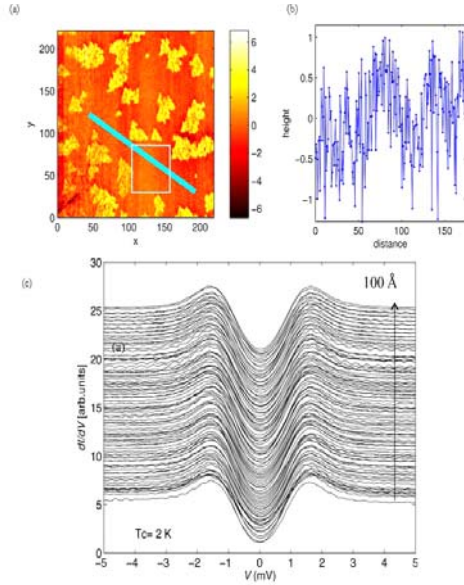
**Summary:** The activities in this project concern superconducting materials with novel and unusual properties, the macroscopic properties of the superconducting state, and the microscopic properties and theory of high temperature superconductors. During the past year research of novel superconducting materials has been concentrated on the pyrochlore compound  $\text{KOs}_2\text{O}_6$ , the non-centrosymmetric superconductor  $\text{CePt}_3\text{Si}$ , the boride superconductors  $\text{Mg}(\text{B}_{1-x}\text{C}_x)_2$ ,  $\text{Mg}_{1-y}\text{Al}_y\text{B}_2$  and  $\text{ZrB}_{12}$ , and the magnetically fluctuating superconductor  $\text{YbNi}_2\text{Ge}_2$ . The behaviour of dynamically asymmetric dc-SQUID was modeled theoretically. The magnetic field profile was studied in  $\text{Y123/SrRuO}_3$  and  $\text{YBCO/PBCO}$  multilayers using muon-SR, showing the existence of surprisingly long penetration of magnetic order into the superconducting regions. A roughly hexagonal vortex lattice was found in the Chevrel phase  $\text{PbMo}_6\text{S}_8$  using STM. In the high  $T_c$  cuprates the STM-work has been concentrated on detailed modeling and comparison of  $\text{Bi2223}$  and  $\text{Y148}$  data with experimental STM data. The effect of isotope substitution on STM tunneling matrix elements has been studied theoretically. Optical data and specific heat on  $\text{Hg1201}$  single crystals have been measured and analyzed, and the relation between Drude spectral weight and condensation energy was studied. A novel refined variational wave function was found to exhibit d-wave superconductivity for the repulsive U Hubbard model, with gap parameter and the condensation energy in accordance with experimental data for the cuprates, due to a "kinetic energy" decrease as opposed to the potential energy as in BCS theory. LSCO was investigated with neutrons, ARPES and muons. The spin gap decreases faster than  $T_c$  as a function of underdoping, in contrast to the doping dependence reported for most electronic energy scales. ARPES reveals a high-energy anomaly in both the electronic dispersion and life-time of the excitations having a strong momentum dependence. The temperature and the magnetic field dependences of the superfluid density indicate multi-band superconductivity with mixed s-d wave symmetry. In underdoped high  $T_c$  films of  $\text{NdBa}_2\text{Cu}_3\text{O}_{7-x}$ , it is found that  $T_c$  is proportional to the carrier density and the inverse square penetration depth suggesting a quantum superconductor-insulator transition in 2D and confirming the Uemura relation. In doped  $\text{SrTiO}_3$ , local ferroelectric field effect has been demonstrated and it is shown that the artificially induced array of normal state dots in a superconducting background favors phase slip lines. In a theoretical study it was shown that a very weak interlayer coupling can lead to a superconducting temperature that are widely different from the two dimensional ones and remove the apparent universality of the Beresinsky-Kosterlitz-Thouless physics. In a theoretical study single-molecule spectroscopy was shown to provide an appropriate tool to detect the electric charge associated with a vortex line.

### 1. Novel superconductors

#### a) Gap symmetry and vortices in pyrochlore $\text{KOs}_2\text{O}_6$

Geometrically-frustrated spin systems is currently attracting great interest. The question of the origin of superconductivity in this class of materials has been addressed by the Fischer group. The research has focused on the pyrochlore compound  $\text{KOs}_2\text{O}_6$ , a recently discovered superconductor which presents many striking unusual characteristics. The temperature dependence of the upper critical field is linear down to sub-Kelvin temperatures and its amplitude is far greater than the Clogston limit. In addition, the absence of inversion symmetry in the crystal structure raises the question of its Cooper pair symmetry as regards spin-singlet and spin-triplet state mixing.

The surface topography of as-grown samples (shown in Fig. 1a) reveals atomically flat regions speckled with small corrugated non-superconducting islands. The large flat regions display highly spatially homogeneous superconducting spectra (see Fig. 1c), which were perfectly reproducible over the timescale of the experiments (4 months). The lack of inversion symmetry in this compound, together with several experimental findings raises the question of the symmetry of the gap function. In order to clarify this point, the STM data were fitted [1] to several symmetry models, i.e. an isotropic s-wave, a d-wave ( $\Delta\cos\phi$ ) and an "anisotropic" s-wave ( $\Delta_0 + \Delta\cos\phi$ ). The results are presented in Fig. 2. Distinguishing between the models is difficult using the tunneling conductance (Fig. 2c), but the fact that the zero bias conductance (ZBC) is larger in the d-wave model than in experiment, rules out this



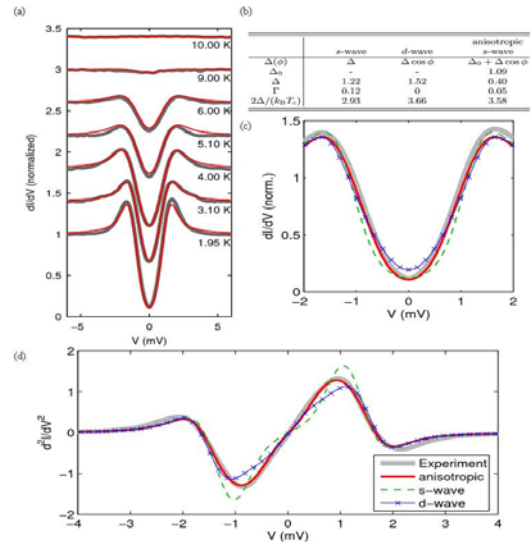
**Fig. 1:** (a) Large-scale topography of  $\text{KOs}_2\text{O}_6$  at  $T=2$  K, ( $R_i= 60$  M $\Omega$ ). (b) Profile of a 1750 Å trace along the surface (blue line in (a)). (c) Spectroscopic trace along a 100 Å path taken on an atomically flat region with one spectrum every 1 Å. The spectra are raw but offset for clarity ( $T=2$  K,  $R_i= 20$  M $\Omega$ ).

symmetry. The differences appear much more clearly in the derivative of the STM spectrum ( $d^2I/dV^2$  plot in Fig. 2d) which emphasizes the symmetry dependence in the low-energy region. The best fit is given by the "anisotropic" s-wave model with an anisotropy of around 30%. The authors point out that the anisotropic gap found is compatible with the p-wave singlet-triplet mixed state which has been suggested [2], although no evidence is found in the data of a second coherence peak arising from a spin-orbit splitting. The absence of this second peak seems to rule out the possibility of two different gap amplitudes in the two FS sheets.

To investigate the evolution of the quasiparticle DOS, tunneling conductance spectra were acquired at different temperatures between 1.95K and 10K (Fig. 2a). The closure of the gap at the bulk  $T_c$  shows that the bulk properties of  $\text{KOs}_2\text{O}_6$  is probed. This is further confirmed by similar spectra obtained on cleaved surfaces. The uniform flat conductance spectra at higher temperature show no support for a pseudogap in the DOS above  $T_c$  implying that the steep decrease in the  $1/T_1T$  curve around 16 K in NMR data [2] must have a different origin. The BCS coupling ratio inferred from the measured anisotropic s-wave gap and critical temperature,  $2\Delta/k_B T_c = 3.6$ , is slightly smaller than the value reported from specific heat measurements [3].

## b) Superconductivity in non-centrosymmetric materials

Superconductivity in metals without inversion center has recently emerged as a new, largely unexplored topics in unconventional superconductivity [4]. The largest bulk of experimental results showing unusual behavior has been accumulated for the heavy Fermion system  $\text{CePt}_3\text{Si}$  whose recent discovery had initiated this research field. In non-centrosymmetric materials spin-orbit coupling leads to a spin-splitting of the Fermi surfaces, influencing in this way strongly the properties of the superconducting phase. The previous works in Sigrist's group investigating the gap structure in  $\text{CePt}_3\text{Si}$  found a consistent qualitative explanation of many experimental data in terms of the most symmetric superconducting phase, which is a superposition of pairing states with "s-" and a "p-wave" character, a so-called mixed parity phase. This phase has different gap structures on the spin-split Fermi surface sheets [5], and allows to explain the Hebel-Slichter peak at  $T_c$  in the the NMR-data as well as the low-temperature power-laws behavior indicating the presence of line nodes in the quasiparticle gap [6, 7]. More recent studies of this group have been concerned with possible tests of the pairing symmetry [4] and aspects of the coexistence of antiferromagnetism and superconductivity in  $\text{CePt}_3\text{Si}$  [5].



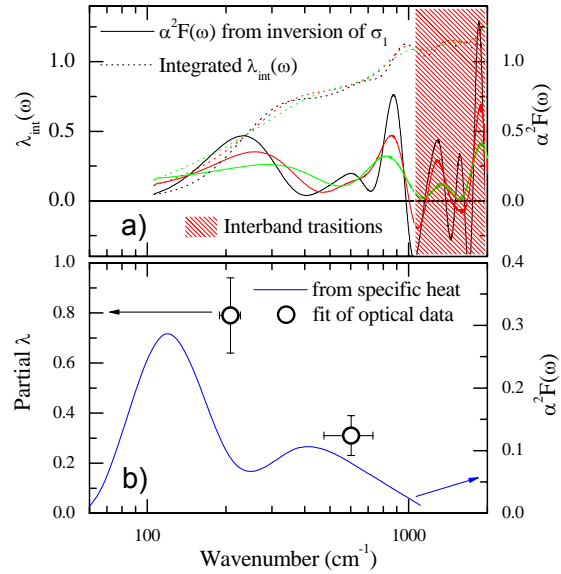
**Fig. 2:** Experimental and theoretical tunneling spectra of  $\text{KOs}_2\text{O}_6$ . (a)  $dI/dV$  spectra at different temperatures from 1.95 to 10 K (each spectrum is offset by 0.4 with respect to the previous one for clarity). (b) Parameters for the different theoretical models. (c) Detailed low-energy comparison between the experimental spectrum at low temperature (1.95 K) and the different theoretical models. (d) Comparison between the derivative of the low-temperature spectrum ( $d^2I/dV^2$ ) from experiment and the models. The curves are explained in (d).

(1) It is well known that a non-trivial phase structure can lead to Andreev bounds at the surface of an unconventional superconductor. This is also the case for the mixed parity  $s$ -/ $p$ -wave state in the presence of line nodes. For the surfaces normal to the inplane direction of the tetragonal crystal lattice of  $\text{CePt}_3\text{Si}$  subgap surface bound states are expected. Such bound states may be detected by resonant quasiparticle tunneling and reveal themselves through zero-bias anomalies in the  $I$ - $V$ -characteristics [7]. The presence of such features in the tunneling spectra could provide information on the relative magnitude of the  $s$ - versus  $p$ -wave component in the mixed-parity state. Moreover, as the zero-bias anomaly should only appear for specific orientations of the tunneling contact, it would provide a strong evidence for the  $s$ -/ $p$ -wave state.

(2)  $\text{CePt}_3\text{Si}$  has an antiferromagnetic transition at  $T_N=2.2\text{K}$  not much above the onset of superconductivity at  $T_c=0.75\text{K}$ . The behavior of the two transition temperatures under pressure suggests that the superconductivity is associated with the antiferromagnetic quantum critical point, analogous to other Ce-based heavy Fermion superconductors. The antiferromagnetism influences the superconducting phase in special way. In previous studies ignoring the antiferromagnetic order it was shown that the spin susceptibility has a very specific anisotropy in the superconducting state [8]. Experimental results contradict this theoretical prediction. In the present study it was shown that the antiferromagnetic phase could be responsible for this discrepancy [9]. The antiferromagnetic order may also play an essential role for the low-energy physics, in particular, for the structure of line nodes in the gap. Taking the spin fluctuations responsible for the  $A$ -type antiferromagnetic order into account two pairing states are possible: an in-plane  $p$ -wave dominated phase and a inter-plane  $d$ -wave dominated phase [9]. The former is consistent with the phase which was identified as the most likely one explaining an important set of experiments in  $\text{CePt}_3\text{Si}$ . Predictions have been made for the behavior of the superconducting state as a function of pressure. Recent experimental studies on the related systems  $\text{CeRhSi}_3$  show that some of these predictions are possibly verified for that material.

### c) Electron-phonon coupling function in $\text{ZrB}_{12}$

In this study [10], the optical conductivity of high quality  $\text{ZrB}_{12}$  single crystals was



**Fig. 3.** a) Eliashberg function (solid lines) and integrated coupling constant (dotted lines) obtained from direct inversion of optical conductivity. The different colors represent different smoothing of experimental data. b) 2 modes in the  $\alpha^2 F(\omega)$  function resulting of the fit of optical data (symbols). The Eliashberg function measured from specific heat is also displayed (blue line).

measured from (6 meV-4 eV) by a combination of reflectivity and ellipsometry. The transport Eliashberg function  $\alpha^2 F(\omega)$  has been extracted from optical spectra using two different methods: a direct inversion of optical conductivity (Fig. 3a) and a fit with a Drude model including frequency dependence of the scattering rate due to electron-boson interaction (Fig. 3b). The two extraction procedures lead to consistent  $\alpha^2 F(\omega)$  functions that both present two peaks at 200 and 700  $\text{cm}^{-1}$  (25 and 85 meV) with partial coupling constants of 0.8 and 0.3 respectively (Fig. 3). The low energy peak corresponds to the vibration mode of Zr weakly bonded to the surrounding  $\text{B}_{24}$  cages, while the second one involves the rigid boron network. In addition to the usual narrowing of the Drude peak with cooling down, an unexpected removal of about 10 % of the Drude spectral weight was observed which is partially transferred to the region of the lowest-energy interband transition ( $\approx 1$  eV). This effect may be caused by a delocalization of the metal ion from the centre of the  $\text{B}_{24}$  cage.

### d) Thermal transport experiments in the mixed state of $\text{Mg}(\text{B}_{1-x}\text{C}_x)_2$ and $\text{Mg}_{1-y}\text{Al}_y\text{B}_2$

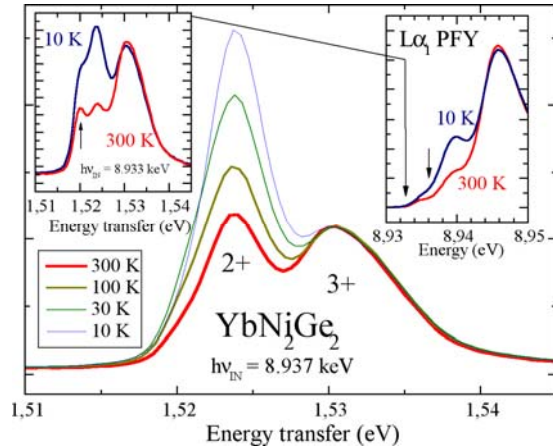
From results of measurements of the thermal conductivity and its magnetic-field induced variation  $\kappa(H)$  in the mixed state of single-crystalline superconducting  $\text{MgB}_2$ ,  $\text{Mg}(\text{B}_{1-x}\text{C}_x)_2$  and  $\text{Mg}_{1-y}\text{Al}_y\text{B}_2$  ( $x, y < 0.1$ ), H.R. Ott and

collaborators have identified the individual contributions of the  $\sigma$  and the  $\pi$  band to the electronic transport of heat in this 2-band superconductor at low temperatures [11]. While in pure  $\text{MgB}_2$ , the electronic heat transport is almost equally divided between the electrons occupying states in the  $\sigma$  and the  $\pi$  band, respectively, a small concentration of C atoms replacing B at the few at% level reduces the  $\sigma$  band contribution by two orders of magnitude, leaving the  $\pi$  band electrons as the dominant contributors. More recent experiments, again probing  $\kappa(H)$  in the basal plane of the hexagonal crystal lattice with two different field orientations, revealed that substituting small amounts of Mg by Al enhances the *intra*band scattering of both the  $\sigma$  and the  $\pi$  band in approximately the same way. For both types of defects, our data indicates that the *inter*band scattering is not much affected by the introduction of the quoted substitutions on either the B or the Mg sublattice and therefore, the gap anisotropy between the  $\sigma$  and the  $\pi$  bands is preserved.

## e) Electronic structure of $\text{YbNi}_2\text{Ge}_2$

Strong electron-electron interactions are traditionally considered antithetical to superconductivity. While this is true for most materials, at least in a conventional scenario, a growing number of examples of superconductivity in strongly correlated materials like the organic conductors, the heavy fermions, and the cuprates not only provide important exceptions to the general rule, but also point to possible new mechanisms of pairing. Namely, in magnetic heavy fermions compounds like e.g.  $\text{CePd}_2\text{Si}_2$ , spin or valence fluctuations associated with the strongly correlated 4f states, could replace the phonons as the glue that binds electrons in Cooper pairs. In these compounds, superconductivity is found in narrow regions around a quantum critical point (QCP), where the system can be driven by hydrostatic pressure from a magnetic to the SC phase [12, 13]. One important element of the puzzle is the 4f population near the QCP, and its dependence on temperature and pressure. This information can be directly obtained, at least in principle, from resonant x-ray absorption (XAS) and x-ray scattering experiments (RIXS) [14].

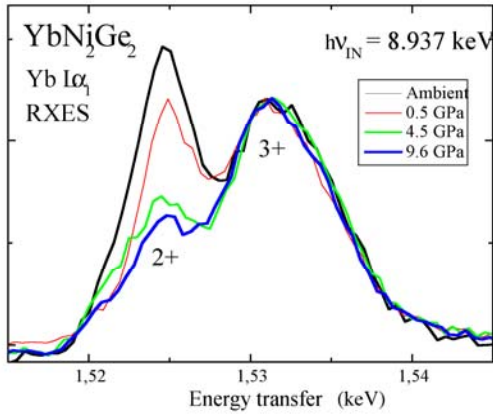
The Gironi-group has studied the pressure dependence of the 4f configuration in metallic ytterbium [15], to set a reference for further analysis, and also because it represents a very interesting problem in itself. Unlike many of its



**Fig. 4.** Right inset: high resolution Yb  $L_3$  XAS spectra of  $\text{YbNi}_2\text{Ge}_2$  at 300 K and 10 K. Main panel: RIXS spectra between 300 K and 10 K, measured in correspondence of the  $\text{Yb}^{2+}$  resonance (short arrow on the XAS spectra). Left inset: RIXS spectra measured at an incident energy below threshold (long arrow on the XAS spectra).

metallic compounds, bulk Yb is divalent at ambient pressure, i.e. it retains the atomic  $4f^{14}$  configuration. Under hydrostatic pressure, the energy of the smaller  $\text{Yb}^{3+}$  ion decreases with respect to the  $\text{Yb}^{2+}$  ground state configuration, and the system is driven to intermediate valence. This evolution is well captured by Yb  $L_3$  XAS and RIXS data, and they could follow a continuous increase of Yb valence, up to 2.55 at 20 GPa. These spectroscopic data on a paradigmatic 4f material were also used in a comparison with state-of-the-art first-principle calculations of the absorption spectra from the Uppsala group, which take into account dynamical screening effects in the presence of the core hole. They found that only including such effects is it possible to reproduce at all pressures the spectral line shape.

The temperature- and pressure-dependence has been measured of high-resolution XAS and RIXS on the representative heavy fermion compound  $\text{YbNi}_2\text{Ge}_2$ . Here, the physical properties are determined by a competition between Kondo and RKKY interactions, which are of the same order magnitude. High pressure resistivity measurements have shown that this system can be continuously tuned from an intermediate valent state at low pressure to a magnetically ordered Kondo lattice at high pressure, with an Yb valence close to 3. A QCP is expected at around 5 GPa. Spectroscopic data of Gironi's group show a clear evolution of valence with temperature and pressure [16]. Figure 4 (right inset) shows two high resolution Yb  $L_3$  XAS spectra measured at 300 K and 10 K at ambient pressure, and normalized to the main



**Fig. 5.** Pressure dependence of the Yb  $L_3$  RIXS, measured in correspondence of the  $Yb^{2+}$  resonance, showing the pressure-induced reduction of the  $Yb^{2+}$  weight.

peak, representative of the  $Yb^{3+}$  ( $4f^{13}$ ) ground state configuration. The larger pre-edge feature in the 10 K spectrum is indicative of a larger  $Yb^{2+}$  weight in the hybrid ground state at the lower temperature. The valence change is further enhanced in the RIXS spectra (main panel, and left inset) measured at two different incident photon energies: well below threshold (left inset) and at in correspondence of the resonance of the  $Yb^{2+}$  configuration. The pressure dependence is illustrated in Figure 5. The RIXS spectra were measured at 300 K and increasing pressure, at the  $Yb^{2+}$  resonance. Pressure induces a very strong, although not complete, reduction of the  $Yb^{2+}$  configuration. A further set of data was collected in a subsequent and more challenging experiment while varying both temperature and pressure. These data are now being analyzed.

**f) Superconducting gap symmetry in the Chevrel phase  $PbMo_6S_8$**

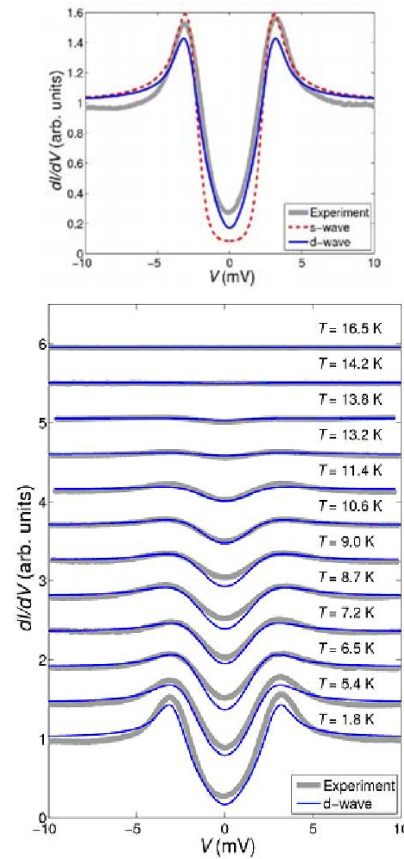
Spectroscopic results of Fischer’s group for the short coherence length superconductor  $PbMo_6S_8$  and their characteristics reminiscent of what is observed in the high- $T_c$  compounds led us to consider the existence of unconventional superconductivity in this material. The Fischer group has made an advance in the analysis and modeling of the spectra by considering the 3D character of  $PbMo_6S_8$  [17]. Describing the density of states (DOS) with the BCS Green’s function and including lifetime effects ( $\Gamma$ ) due to impurity scattering, Fits were performed to the experimental spectra using the superconducting gap representations compatible with the rhombohedral symmetry of the crystal (see Table I). Since representations  $R_2$ ,  $R_3$  and  $R_4$  give identical DOS once

	Pairing symmetry	$k$ -dependence of the gap, $\psi(\mathbf{k})$	Relation to point-group symmetry
$R_1$	$s$	1	Preserving (isotropic)
$R_2$	$d$	$(k_x \pm ik_y)^2$	Breaking
$R_3$	$d$	$k_z(k_x \pm ik_y)$	
$R_4$	$d$	$(k_x^2 + k_y^2)$	Preserving
$R_5$	$d$	$\frac{1}{2}(3k_z^2 - 1)$	

**Table I.** Lowest-order representations compatible with rhombohedral symmetry for the gap  $\Delta k = \Delta 0 \Psi(k)$ .  $z$  is chosen along the 3-fold axis.

integrated over the Fermi surface; they group them under the collective label “d-wave”. In contrast, the typical DOS from  $R_5$  shows greatly reduced peaks (similar to higher-order g-wave cases not shown in Table I) which are totally incompatible with the observed spectra.

The average experimental spectrum at 1.8 K is shown in Fig. 6 (top) together with the fits [17]



**Fig. 6. Top:** experimental  $dI/dV$  spectrum spectra of the Chevrel phase  $PbMo_6S_8$ , at 1.8 K (thick line) compared to the  $s$ -wave and  $d$ -wave fits described in the text (dashed and solid lines respectively). **Bottom:**  $dI/dV$  spectra obtained at various temperatures (thick lines) and  $d$ -wave fits (thin lines). Each experimental spectrum is normalized so as to ensure state conservation within the measurement energy range and offset by 0.45 with respect to the previous one for clarity.

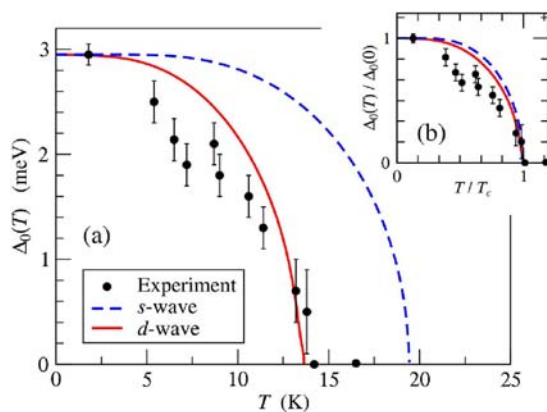
defined to optimally reproduce the peak energy positions and widths. The isotropic s-wave case systematically fails to describe the spectrum between the coherence peaks. In direct contrast, the d-wave cases for  $\Delta_0=2.95$  meV and  $\Gamma=0$  meV provide a much better fit in the low-energy region which is the most sensitive to changes in the gap symmetry. Fischer and collaborators emphasize that within the d-wave scenario, the measured ZBC is a natural consequence of the low-lying excitations and thermal smearing. As shown in Fig. 6 (bottom) spectra taken at different temperatures are well fitted by the d-wave models, in contrast to the s-wave which consistently fails to reproduce the spectral shape at low energy. The gap amplitudes  $\Delta_0(T)$  from the fits to their experimental spectra are plotted as a function of temperature in Fig. 7a, together with the solutions of the BCS gap equation for both the s-wave and d-wave symmetries. These were calculated by selecting the simplest separable coupling interaction preserving the gap symmetry, i.e.  $V_{k,k'}=V_0\psi(k)\psi^*(k')$ , and determining  $V_0$  so as to fix the zero-temperature gap at their experimental value (2.95 meV). The s-wave solution gives a  $T_c$  of 19.4 K, as expected from the well-known  $2\Delta_0/k_B T_c$  ratio of 3.52 but clearly at variance with their experiment. On the other hand, the  $T_c$  from the 3D d-wave model is 13.6 K, giving a ratio of 5.0 in agreement with their experimental value of  $4.9 \pm 0.3$ . These results are also shown renormalized by their respective  $T_c$  values in the inset of Fig. 7, highlighting the facts that the presence of nodes affects the shape of the curve (and not only the  $2\Delta_0/k_B T_c$  ratio) and the experimental gap closes faster with increasing

temperature than the theoretical curves. This very small coherence length and the large coupling ratio of 4.9 further confirm the similarity with the high- $T_c$  materials. Such d-wave superconductivity in  $\text{PbMo}_6\text{S}_8$  could result from the very short coherence length which would favour the appearance of a repulsive component in the coupling interaction.

## 2. Quantum matter

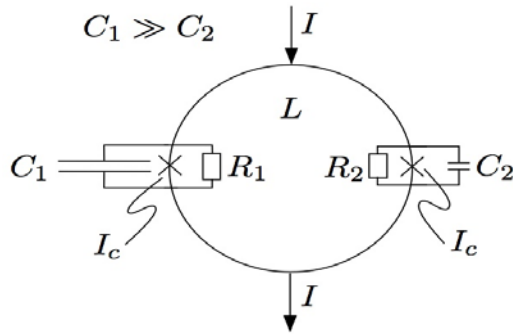
### a) Quantum instability in a dynamically asymmetric SQUID

Most theoretical discussions and experiments on the Josephson effect and on Josephson devices focus on the classical limit characterized by large capacitance junctions. Technological advances allowing to fabricate submicron and nano scale junctions with small capacitances push the behavior of these devices into the quantum regime, opening up new applications in solid state implementations of quantum information processors. Central features of the quantum operation of such devices are the phenomena of macroscopic quantum tunneling and macroscopic quantum coherence. Here, Blatter and collaborators are interested in the dynamical behavior of the phase difference  $\varphi$  across a superconducting junction, a macroscopic quantum variable which can tunnel out of a metastable minimum and induce a dynamical (dissipative) behavior of the device. They are interested in the behavior of a dc-SQUID device combining two junctions in a current-biased superconducting ring which couples the two phase-differences  $\varphi_1$  and  $\varphi_2$  across the junctions through the loop inductance. The symmetric setup involving identical junctions with equal parameters  $I_c$  (critical current), capacitance (C) and normal resistance (R) has been discussed in Ref. [18]: the quantum decay out of a symmetric minimum ( $\varphi_1 = \varphi_2$ ) occurs either via a diagonal instanton, where both phases decay simultaneously ( $\varphi_1 = \varphi_2$ ), or via two symmetric off-diagonal instantons with equal contributions, with the two regimes separated by a 'dynamical phase transition'. In the present case, Blatter and collaborators are interested in the situation where the dynamic properties of the two junctions, i.e. the capacitance and the normal resistance, are largely different, with one of the junctions (say junction 1) residing in the classical limit with no tunneling present, whereas junction 2 behaves fully quantum-mechanical; the question they address is under which conditions the quantum



**Fig. 7.** (a) Temperature dependence of the superconducting gap spectra of the Chevrel phase  $\text{PbMo}_6\text{S}_8$  from the spectra in Fig. 6b (circles) compared to the s and d-wave cases from solving the BCS gap equation for  $\Delta_0(0)=2.95$  meV (dashed and solid curves respectively). (b) Same data with gaps rescaled by  $\Delta_0(0)$  and temperatures rescaled by the respective  $T_c$  values.



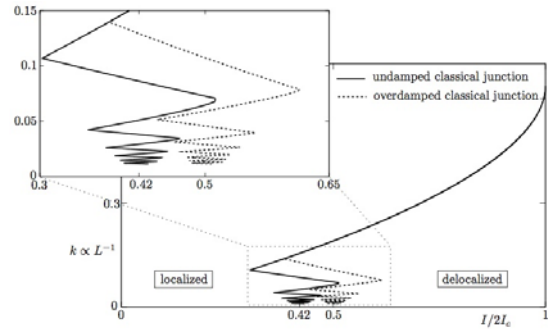


**Fig. 8.** Schematics of the dynamically asymmetric SQUID. Two Josephson junctions with equal critical currents  $I_c$  are inserted in a symmetric superconducting ring with inductance  $L$ . Junction 1 is held in the classical limit by a large shunt-capacitance  $C_1$ , whereas junction 2 is behaving quantum-mechanically/quasi-classically.

tunneling of the small junction entails finite motion of the large junction as well, leading to a quantum induced instability of the entire SQUID.

The Blatter group has studied such a dynamically asymmetric dc-SQUID using the RCSJ-model (Resistively and Capacitively Shunted Junction model, cf. Fig. 8) with a symmetric drive  $I$  and an inductive coupling  $L$  between the two junctions. Shunting one of the junctions with a large (infinite) capacitance and/or a small (zero) normal resistance, the junction behaves classically; any tunneling of the small junction then happens along directions of constant phase  $\varphi_1$  of the large junction, with the phase slip dynamics limited to the phase  $\varphi_2$  of the small junction. The quantum motion of the small junction describes the entry of flux into the SQUID loop which redirects part of the transport current across the heavy junction. The enhanced current drives the large junction out of its metastable state; the associated classical motion of  $\varphi_1$  describes the subsequent relaxation of the SQUID loop as (part of the) flux leaves the ring. The amount of flux entering the SQUID loop and the magnitude of the induced screening current depend on the bias current  $I$  and on the inductance  $L$  of the ring; the behavior of the system then is conveniently described by a current  $I$  - inductance  $L$  diagram, cf. Fig. 9.

As a first step the case of strong dissipation for the quantum junction was tackled, as obtained by a small shunt resistance. The symmetrically prepared SQUID (a metastable state at  $\varphi_1 = \varphi_2$ ) decays via tunneling of the quantum-



**Fig. 9.** Phase diagram of the dynamically asymmetric SQUID for a quantum-junction with strong dissipation. The classical junction is localized for small bias current  $I$  and small inductance  $L$ . The critical line develops a zig-zag like shape, which has its origin in the amount of magnetic flux necessary to enter the SQUID in order to delocalize the classical junction. The undamped classical junction (full line) uses the energy of an initial oscillation to overcome a remaining small potential barrier and thus the critical line is at lower currents than for the overdamped junction (dotted line), where the barrier has to fully disappear in order to lead to a delocalized state.

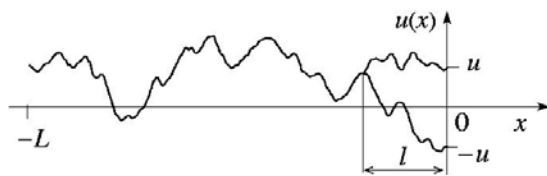
variable  $\varphi_2$  and subsequent relaxation to the global minimum of its effective potential. This process has two effects on the classical junction: Firstly, the local minimum in the effective potential of the classical junction is shifted, inducing (plasma) oscillations of the classical junction. Secondly, the potential barrier preventing the decay of the classical junction is lowered; the combination of these effects then induce a classical decay of the metastable state of the large junction. Fig. 9 shows the resulting 'dynamical phase diagram' of the SQUID describing the dependence of the decay of the classical junction on the transport current  $I$  and the coupling strength  $k \propto L^{-1}$  as obtained by combining approximate analytical and numerical methods. Blatter and collaborators find that the delocalization of the classical junction is only possible for sufficiently large inductances. The critical line exhibits a peculiar zig-zag like shape, originating in the (approximately) quantized jumps of increasing magnetic flux leading to the decay of the classical junction with increasing inductance. If the classical junction is shunted by a large capacitance only (the case of negligible damping), the energy of the initial oscillation can be used to overcome a remaining small potential barrier. If the classical junction is overdamped, the energy of the oscillation is dissipated and the potential barrier needs to vanish in order for the classical junction to be delocalized; in this case, the critical line is located at larger bias current, cf. Fig. 9.

The case of small dissipation for the light junction has been analyzed numerically, assuming a classical motion of the phase  $\varphi_2$  after tunneling. Within an adiabatic approximation, the effective force on the classical junction is generated by the time-averaged value of  $\varphi_2$ . As a result, they find a smoothing of the critical line in both cases of no damping and of overdamping of the heavy junction.

Ongoing investigations include studies of different critical currents of the two junctions, of asymmetric geometrical construction of the SQUID loop (which can be interpreted as an asymmetric inductance), and the application of additional external magnetic flux threading the ring, as well as a more elaborate quasi-classical study of the low-dissipation case.

## b) Joint free energy distribution in the random directed polymer problem

Directed polymers subject to a random disorder potential exhibit a non-trivial behavior deriving from the interplay between elasticity and disorder; numerous physical systems can be mapped onto this model and the topic has been the subject of intense investigations [19]. Despite its undisputable importance, the knowledge on this generic problem is, according to Blatter and collaborators, still quite limited. Traditionally, the main focus is on the free energy distribution function, for which two types of analytical solutions are known for the (1+1)-dimensional case, a polymer confined to a plane, see Fig. 10: one class [20, 21] addresses the 'longitudinal' problem and determines the distribution function  $P_L(E)$  for the free energy  $F$  at fixed displacement  $u$ , while the other [22] concentrates on the 'transverse' problem aiming at the distribution function  $P_u(F')$  involving the free energy difference  $F'$ , assuming no dependence on  $E$  in the limit of large  $L$ . Both approaches have been helpful in finding the wandering exponent



**Fig. 10.** Illustration of thermally averaged trajectories  $\langle u(x) \rangle_{th}$  of a random directed polymer in a fixed disorder potential  $V(x, u)$ . Blatter and collaborators let the polymer start in an arbitrary position at  $x = -L$  and fix the displacement  $u$  at  $x = 0$ . Forcing the polymer to end in  $-u$  produces an alternative average trajectory on a distance  $l$ .

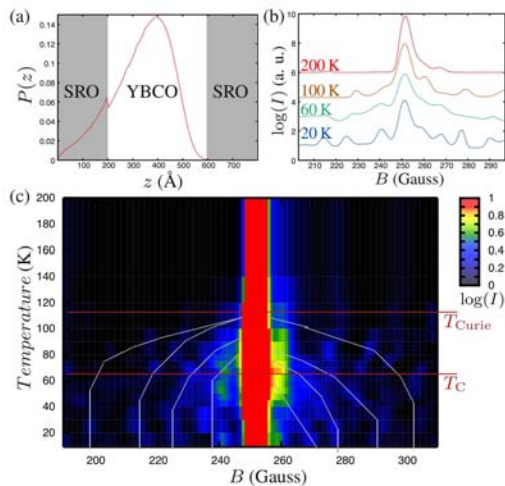
$\xi$  of transverse fluctuations  $\delta u(L) \sim L^\xi$  of the polymer. On the other hand, questions how the result for  $P_u(F')$  is approached from finite  $L$  and how the transverse and longitudinal problems are interrelated have remained unclear; in their work with have attempted to shed light upon this question.

In order to do so, two configurations were studied of the string ending in two points separated by  $2u$ , and treat both the mean free energy  $\underline{E} = [F(L, u) + F(L, -u)]/2$  and the free energy difference  $F' = F(L, u) - F(L, -u)$  as relevant variables. Using the replica approach, they determine the joint distribution function  $P_{L, u}(E, F')$ . The particular structure of their solution allows us to prove (for a  $\delta$  correlated disorder potential) the separation  $P_{L, u}(F, F') = P_{L, u}(E) P_u(F')$  in the limit of large  $L$  and for large negative values of the mean free energy  $\underline{E}$ . Furthermore, they are able to determine the functional dependencies of the two resulting factors  $P_{L, u}(E)$  and  $P_u(F')$ : on the one hand, they recover the left tail of the distribution function  $P_{L, u=0}(E)$  in the form of Zhang's tail [21] for  $P_L(F)$ . On the other hand, to their surprise, they find that the transverse part  $P_u(F')$  exactly coincides with the stationary distribution function of the Burgers problem [22], although the solution is associated with rare events in the far-left tail, while the result of Ref. [22] describes an equilibrium situation reached in the limit of infinite  $L$ .

## c) Competition between high $T_c$ superconductivity and ferromagnetism in artificial oxide multilayers

The group of C. Bernhard performed low-energy muon-spin-rotation (LE- $\mu$ SR) measurements on multilayers that consist of alternating layers of perovskite ferromagnets like  $\text{SrRuO}_3$  and  $\text{La}_{2/3}\text{Ca}_{1/3}\text{MnO}_3$  and the high- $T_c$  superconductor  $\text{YBa}_2\text{Cu}_3\text{O}_7$ . Their data provide evidence for the formation of a spin density wave in the  $\text{YBa}_2\text{Cu}_3\text{O}_7$  layers that is induced by the proximity to the ferromagnet.

Here LE- $\mu$ SR measurements are reported on a thin film multilayer sample with alternating 400Å thick  $\text{YBa}_2\text{Cu}_3\text{O}_7$  (YBCO) layers and 200Å thick ferromagnetic  $\text{SrRuO}_3$  (SRO) layers. The sample has a Curie Temperature of  $T^{\text{Curie}} = 120\text{K}$  and a superconducting critical temperature of  $T_{sc} = 65\text{K}$ . The LE- $\mu$ SR technique is an ideal tool to explore the depth profile of the local magnetic field on the true nanometer length scale [23]. In particular, it allows us to obtain on a layer by layer scale the magnetic field distribution of the artificially

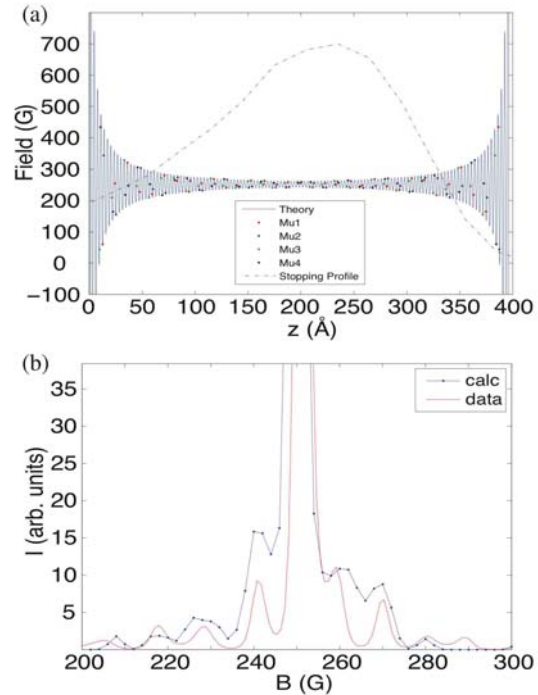


**Fig. 11.** (a) Depth of the muon implantation with 8keV muon energy. (b) Magnetic field distribution as seen by the muons at different temperatures. (c) Temperature dependent magnetic field distribution as seen by the muons.

grown multilayers. This unique technique has been pioneered by the group of PD Dr. Elvezio Morenzoni at PSI.

Figure 11 shows the temperature dependence of the magnetic field distribution within a buried 400Å thick YBCO layer (as sketched in Figure 11a). Above  $T^{Curie}$  the lineshape of the local magnetic field distribution in YBCO as probed by the muons is fairly narrow and centered around the applied field of  $B_{ext} = 252$  Oe. Below  $T^{Curie}$  well defined sidebands occur on both the high- and the low-field side of the main line. These sidebands exhibit a characteristic evolution with temperature: With decreasing temperature they move further away from the central peak and new bands appear as indicated by the gray lines in Figure 11c. This suggests that the FM phase transition in the SRO layers gives rise to induced magnetic moments within the YBCO layer that have a fairly well defined spatial order. If these bands would arise from dipolar stray fields due to imperfections of the SC/FM interface, the corresponding field distribution would not exhibit well defined peaks but instead would be broad and featureless.

The observed behavior is reminiscent of the one in classical Fe/Ag/Fe and Fe/Pb/Fe multilayers. There, a spin density wave (SDW) state is known to be induced in the classical metal and the SC layers [24, 25]. The data presented here hence provide evidence that a spin density wave is induced in the YBCO layers (Figure 12): It is indeed possible to model the measured magnetic field distribution

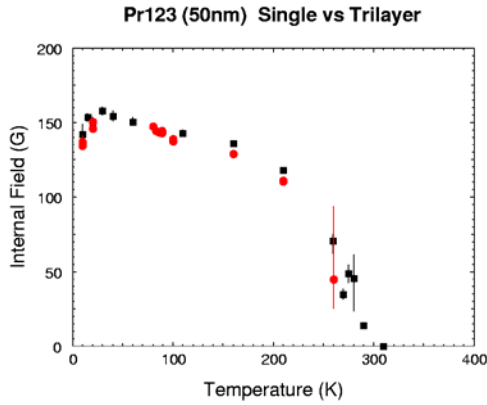


**Fig. 12.** Model of a spin density wave in a YBCO layer as proposed in [25]. (a) The model with the muon stopping sites. (b) Calculation compared to the measured data.

by modeling a SDW as proposed in [26]. While it is unlikely that the SDW in YBCO can be described in terms of a classical RKKY model its origin may be linked with the recent observation of the formation of a magnetic field induced SDW state in strongly underdoped bulk high- $T_C$  superconductors [27]. Clearly further measurements are required on samples with even thicker YBCO layers and for different stopping depth distribution of the low-energy muons.

#### d) Superconductivity and magnetism in $YBa_2Cu_3O_7/PrBa_2Cu_3O_7/YBa_2Cu_3O_7$ trilayers

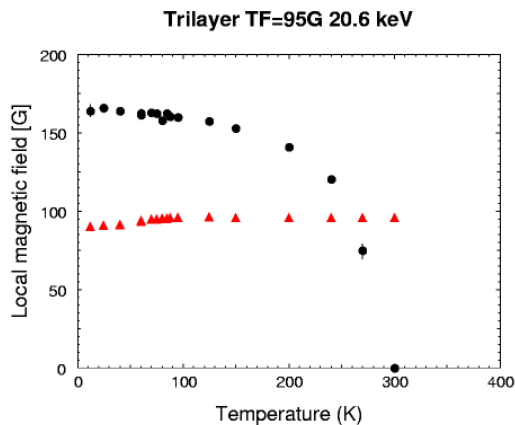
Proximity effects in magnetic superconducting multilayers have been subject of intense research in recent years by Keller, Morenzoni and collaborators at PSI due to the variety of phenomena resulting from the interplay (competition and coexistence) between the two orderings in heterostructures. For instance in superlattices consisting of one unit cell thick of  $YBa_2Cu_3O_7$  (YBCO) layer separated by  $PrBa_2Cu_3O_7$  (PBCO) layers of variable thickness the critical temperature of the heterostructure has been found to continuously decrease as the PBCO thickness is increased indicating that some sort of coupling persists over distances of  $\sim 10$  nm [23].



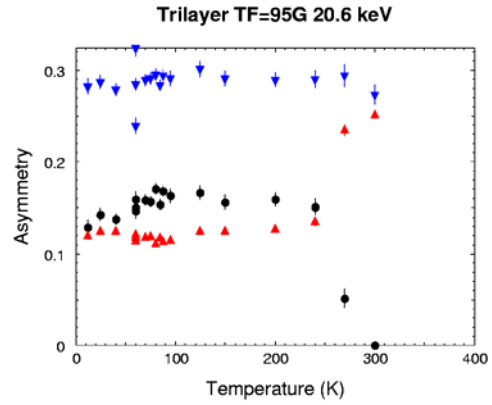
**Fig. 13.** Spontaneous internal fields in PBCO (black squares: single layer 50 nm, red circles: trilayer) as a function of temperature.

Polarized low energy muons were implanted in a  $\text{YBa}_2\text{Cu}_3\text{O}_7$  (75nm) /  $\text{PrBa}_2\text{Cu}_3\text{O}_7$  (50nm) /  $\text{YBa}_2\text{Cu}_3\text{O}_7$  (75nm) trilayer to investigate the local superconducting and magnetic properties of this structure. Low energy SR offers the unique possibility to study the magnetic properties selectively in the different layers and as a function of depth on a nm scale. Particularly, the spatial distribution of the magnetization throughout the layers and at the interfaces can be obtained, a quantity about which very little is known. For comparison single layer films of the constituents were also investigated.

Figure 13 shows the internal field measured by Zero Field- $\mu\text{SR}$  in the PBCO layer as single film (50nm) or embedded in the two YBCO layers in a YBCO/PBCO/YBCO (75/50/75 nm) structure. In both cases the energy of the muons has been chosen so that they stop in the center of PBCO. The evolution of the internal field and of the relaxation (not shown)



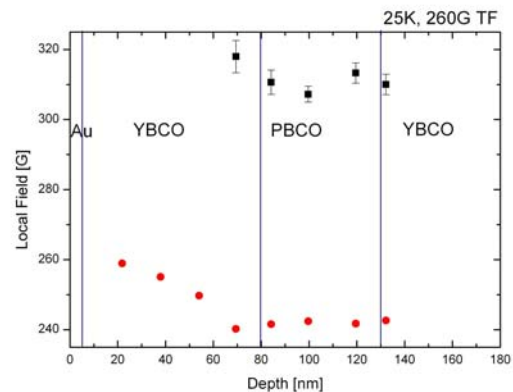
**Fig. 14.** Measured fields in the center of the PBCO layer as a function of temperature. (Red points diamagnetic component (below 90K), black points magnetic component). A field of 95 G is applied.



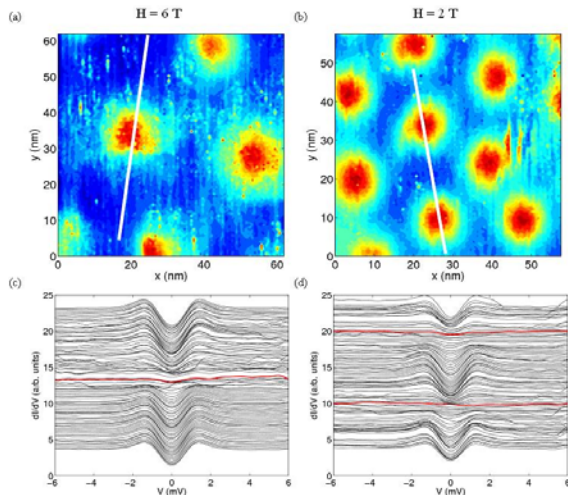
**Fig. 15.** Relative fraction of the field components of Fig. 14 measured in the center of the PBCO layer of the YBCO/PBCO/YBCO trilayer as a function of temperature.  $TF=95$  G. Blue points represent the total fraction.

with temperature clearly show the ordering of the copper moments ( $T_N \sim 285\text{K}$ ) and of the Pr moments ( $T_N=17\text{K}$ ).

If an external magnetic is applied parallel to the surface (and perpendicular to the c-axis), the microscopic field measurements show two components (Fig. 14) with relative amplitude of about 60% and 40%, respectively (see Fig. 15), developing below  $T_N$ . The first component reflects the magnetic order and appears at fields corresponding to the superposition of the internal field of the ordered Cu moments and of the external field. The second component is found at the value of the external field for  $T > 90\text{K}$ . However, below the critical temperature of YBCO ( $T_c=87\text{K}$ ,  $\lambda_{ab}=187(2)$  nm) this fraction displays a sizeable diamagnetic shift. The depth profile of the diamagnetically shifted component shows that the value decays monotonously in the YBCO layer and reaches the maximum shift in the PBCO layer (Fig. 16). The preliminary analysis indicates that a sizable fraction of the 50 nm PBCO layer



**Fig. 16.** Depth profile of the field components in the trilayer (red points; diamagnetic field, black squares: field arising from the AF ordering of the Cu moments).



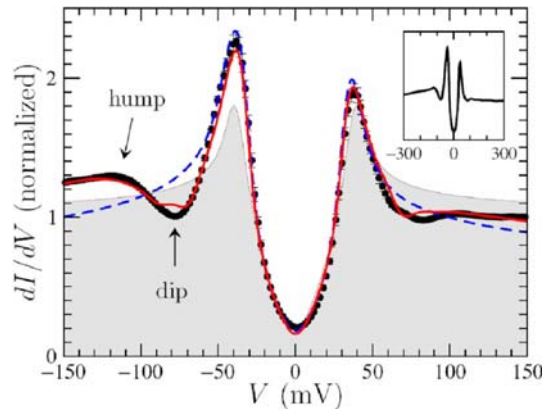
**Fig. 17:** Experimental ZBC maps spectra of  $\text{KOs}_2\text{O}_6$  ( $T = 2 \text{ K}$ ) normalized to the background conductance at  $2 \text{ T}$  (a) and  $6 \text{ T}$  (b). Spectroscopic traces through the centers of vortices at respectively (c)  $2$  and (d)  $6 \text{ T}$  at  $2 \text{ K}$ . In both figures the spectra at the vortex centers have been highlighted in red for clarity.

becomes superconducting below  $\sim 87 \text{ K}$ . This couples the two adjacent YBCO layers but appears to be spatially separated from the coexisting intrinsic magnetism which is only weakly affected by the onset of superconductivity. The result presents the signatures of a large proximity effect not expected in this material on the base of conventional proximity models.

### e) Vortex imaging study of the pyrochlore compound $\text{KOs}_2\text{O}_6$

A vortex imaging study was carried out by Fischer and collaborators at  $2 \text{ K}$  for two fields,  $2 \text{ T}$  and  $6 \text{ T}$ , over an especially flat region of about  $60 \times 60 \text{ nm}^2$  shown in Fig. 17a. The vortex maps (ZBC normalized to the high-energy conductance) (see Fig. 17a) show a roughly hexagonal vortex lattice with vortex spacing of  $d = 216 \pm 21 \text{ \AA}$  and  $d = 352 \pm 17 \text{ \AA}$  at  $2 \text{ T}$  and  $6 \text{ T}$  respectively, in line with the spacing expected from the reported critical field [28]  $H_{c2} = 32 \text{ T}$  i.e.  $199 \text{ \AA}$  and  $345 \text{ \AA}$  respectively. They ascribe the irregular core shapes and the deviation from a perfectly hexagonal vortex lattice in their maps to vortex pinning.

Fig. 17b displays the spectra taken along traces passing through vortex cores for each of the two fields considered. The spectra at the center of the vortices are flat at both fields, with no excess spectral weight at or close to zero bias. This absence of localized states, normally understood to be a signature of the dirty limit, is striking since the mean free path in  $\text{KOs}_2\text{O}_6$  has been estimated to be  $l \cong 200 \text{ nm} \gg \xi$  [29].



**Fig. 18.** Typical spectrum of  $\text{Bi2223}$  compared with three theoretical models.

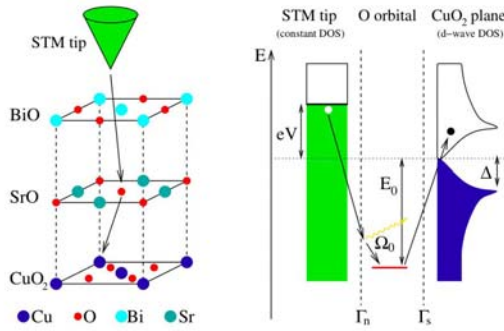
The Fischer group is currently modeling the ZBC spatial dependence to independently estimate the superconducting coherence length  $\xi$ .

### 3. Microscopic properties of the cuprates

#### a) Signatures of the van Hove singularity in the tunneling spectra of superconducting cuprates:

The tunneling spectra of  $\text{Bi-2212}$  and  $\text{Bi-2223}$  have a very unusual and asymmetric shape. The goal of this sub project was to get a quantitative understanding of these spectra. During the past year the Fischer group has performed an extensive analysis of the STM tunneling spectra of the tri-layer compound  $\text{Bi}_2\text{Sr}_2\text{Ca}_2\text{Cu}_3\text{O}_{10+\delta}$  ( $\text{Bi2223}$ ). For slightly overdoped samples, these spectra presents a d-wave like gap structure with strong coherence peaks plus an asymmetric dip-hump feature at higher energy (see Fig. 18). It was already shown in Fischer's group [30] that similar spectra of  $\text{Bi2212}$  can be understood in terms of the electronic band structure where BCS d-wave superconductivity settles and couples to a bosonic mode, at least for overdoped samples. Within this model, the asymmetries of the spectra are a consequence of the existence of a van Hove singularity below the Fermi level.

In an attempt to extract the properties of this collective mode directly from the tunneling data, a computer program was developed which allows determining all model parameters (i.e. the band-structure, superconducting, and collective mode parameters) from a least-square fit of the spectra. The result is shown by the red curve, to be compared with a conventional free-electron BCS d-wave model



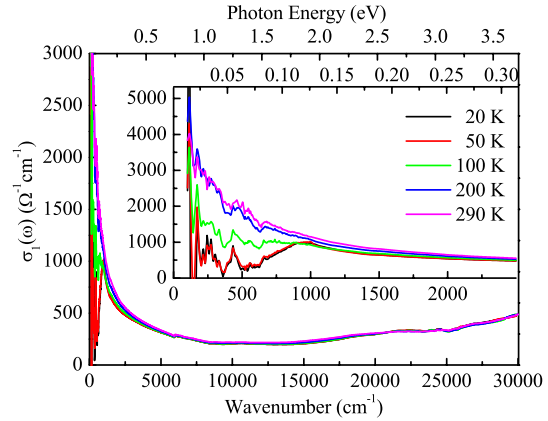
**Fig. 19.** Left panel: geometry relevant for the STM experiment; the superconducting  $\text{CuO}_2$  plane lies below the BiO and SrO layers. Right panel: suggested inelastic co-tunneling process via the apical oxygen atom leading to phonon satellites in the current-voltage characteristics in electron-energy scheme.

(shaded curve). The latter reproduces the experimental data well at low energy ( $\Delta_p/2$ ), but fails to account for the various features present at higher energy, in particular the asymmetry of the coherence peak height. A much better description of the coherence peak height, width, and asymmetry can be achieved by incorporating the actual band structure. The resulting theoretical curve (dashed line) is very similar to the free-electron model at subgap energies, but performs much better up to an energy slightly above the coherence peaks. Finally, when the coupling to the bosonic mode is taken into account, the model follows the data to a high level of accuracy.

Fischer and collaborators are currently investigating the doping dependence of the parameters determined from these fits, which will hopefully provide useful hints on the origin of the bosonic mode.

**b) Isotope shift in the STM tunneling in high- $T_c$  superconductors:**

Recent experiments by Davis' group show a pronounced isotope shifts in spectral features above the quasiparticle gap in scanning tunneling microscope (STM) measurements [31]. The question arises which phonons influence the tunneling process. Pilgram, Rice and Sigrist have considered the tunneling path between the  $\text{CuO}_2$  layers in the cuprate superconductor and a STM tip passes through a barrier made from other oxide layers, e.g. BiO (Fig. 19) [32]. This opens up the possibility that inelastic processes in the barrier contribute to the tunneling spectra. Such processes cause one or possibly more peaks in the second derivative current-voltage spectra displaced by phonon energies from the density of states singularity associated with



**Fig. 20.** The ab-plane optical conductivity of Hg1201.

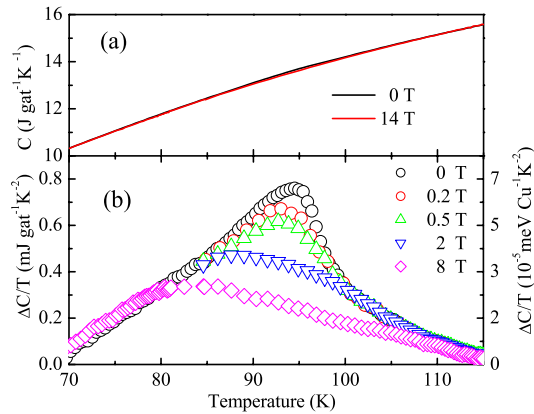
superconductivity. Calculations of inelastic processes generated by apical O phonons show good qualitative agreement with the experiments. Further tests to discriminate between these inelastic processes and coupling to planar phonons have been proposed.

**c) Rotational Symmetry Breaking in the Ground State of Sodium-Doped Cuprate Superconductors**

The spatial pattern of the STM spectra generated by a hole bound to a  $\text{Na}^+$  acceptor doped into  $\text{Ca}_2\text{CuO}_2\text{Cl}_2$  was calculated by Chan, Rice and Zhang using an extended t-J model to describe the electronic properties on the  $\text{CuO}_2$ -plane [33]. The Na-acceptor replaces a Ca-ion and sits in the centre of a  $(\text{CuO})_4$ -square. Exact diagonalization of a small cluster with an attractive potential on the central square shows that the groundstate of the hole is doubly degenerate corresponding to even(odd) reflection symmetry around the x(y)-axes. The conductance pattern of the broken symmetry groundstate is anisotropic as the tip of the STM scans above the Cu-O-Cu bonds along the x(y)-axes although the Na-acceptor sits in asymmetric position. This anisotropy is pronounced at low voltages but reduced at higher voltages. These features are prominent in the recent STM spectra of this cuprate [34].

**d) Optical and thermodynamic properties of the high-temperature superconductor  $\text{HgBa}_2\text{CuO}_{4+\delta}$**

Measurements of the optical spectra (Fig. 20) and the specific heat (Fig. 21) for the single layer cuprate superconductor  $\text{HgBa}_2\text{CuO}_{4+\delta}$  (Hg-1201) single crystals provided by M. Greven (Stanford) at optimal doping ( $T_c = 97$



**Fig. 21.** Difference of the specific heat data for a number of magnetic fields  $B$  and the 14 T data  $\Delta C/T = (C(B, T) - C(B_0, T))/T$  showing the anomaly at the superconducting transition, where the reference field  $B_0$  is 14 Tesla.

K) have been measured by van der Marel and collaborators in collaboration with C. Homes (Brookhaven). The optical data on the ab-plane were measured at the University of Geneva, c-axis infrared reflectivity was measured at Brookhaven National Light source. The ab-plane superfluid plasma frequency is found to be  $\omega_{ps} = 9600 \text{ cm}^{-1}$ . The low frequency spectral weight increases in the superconducting state, following the same trend found in underdoped and optimally doped multi-layer  $\text{Bi}_2\text{Sr}_2\text{CaCu}_2\text{O}_{8+\delta}$  (Bi-2212) and  $\text{Bi}_2\text{Sr}_2\text{Ca}_2\text{Cu}_3\text{O}_{10+\delta}$  (Bi-2223). The specific heat anomaly at  $T_c$  is relatively weak compared to  $\text{YBa}_2\text{Cu}_3\text{O}_{6+y}$  (YBCO) or Bi-2212. The shape of the anomaly is similar to the one observed in YBCO showing that the superconducting transition is governed by thermal fluctuations.

The specific-heat measured in magnetic fields up to 14 T (see Fig. 21) shows an anomaly at the phase-transition which is only 0.4 % of the total specific heat and thus particularly small as compared to other cuprate superconductors.

**e) Kinetic energy and spectral weight transfer in cuprate superconductors**

Regardless of the microscopic mechanism driving the superconductivity in the high- $T_c$  cuprates, the superconducting transition occurs due to the more advantageous internal energy of the superconducting phase as compared to the one in the normal state. In the Bardeen-Cooper-Schrieffer (BCS) theory the decrease of the potential, or interaction, energy slightly overweighs the increase of the electronic kinetic energy. However, there is no reason to exclude a priori an opposite scenario when the kinetic energy is lowering in the superconducting state. This would only be

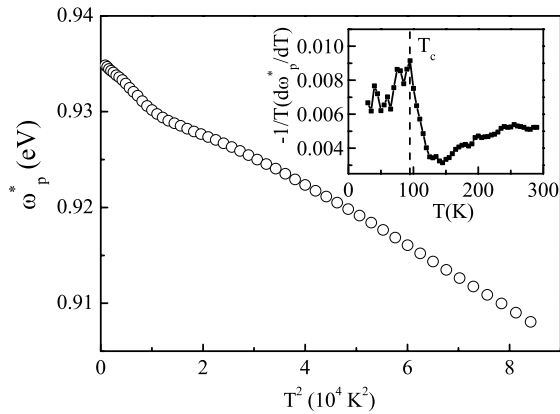
possible, of course, if the normal state is not Fermi-liquid like. The latter assumption is supported by some experiments (ARPES, specific heat, STM) in the underdoped and optimally doped cuprates.

Optical measurements allow one, in principle, to monitor specifically the electronic kinetic energy, and therefore to distinguish between these two scenarios. The change of the integrated optical spectral weight of the Drude peak is defined as

$$W(T) = \int_0^{\Omega_c} \sigma_1(\omega) d\omega$$

In a nearest neighbor tight binding model the relation between  $W(T)$  is proportional to the negative of the change of the kinetic energy. The calculation of Marsiglio et al.[35] in the group of van der Marel for a realistic band structure consistent with ARPES data has shown that this relation is qualitatively fulfilled in the range of the hole doping below about 0.28 holes/Cu although at higher doping concentrations the presence of the van Hove singularity makes it much more complicated. In the previous study of the optimally and underdoped Bi2212 [36] the spectral weight was found to increase in the superconducting implying the lowering of the kinetic energy below  $T_c$ , opposite to the expectation from the BCS model. According to BCS theory the kinetic energy increases when the system is driven into the superconducting state but it was proposed theoretically and found experimentally that in cuprates the kinetic energy decreases over a large doping range. Recently, in studies of the doping dependence of Bi-2212 it was found that on the overdoped side of the phase diagram the kinetic energy follows the BCS prediction. Experimentally,  $W(\Omega_c, T)$  gives a handle on the superconductivity induced change in kinetic energy. A qualitative indication of the superconductivity induced changes of low frequency spectral weight can be obtained from the dielectric function measured directly with ellipsometry. This can be done by monitoring the shift of the screened plasma frequency  $\omega_p^*$ , i.e the frequency for which  $\text{Re}\epsilon(\omega)=0$ , with temperature. Although it gives a first indication it does not give a definite answer since  $\omega_p^*$  can be influenced by other factors, for instance the temperature dependence of the interband transitions. In figure 22,  $\omega_p^*$  is plotted versus  $T^2$ .

The screened plasma frequency shows an extra blueshift below  $T_c$ , suggesting an increase of the low frequency spectral weight.



**Fig. 22.** Screened plasma frequency  $\omega_p^*$  versus  $T^2$ . The inset shows the derivative.

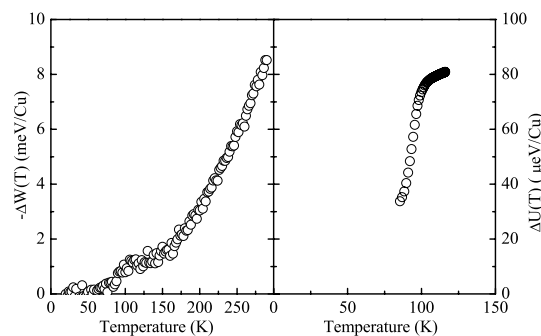
By extrapolating the normal state trend to  $T=0$ , the superconductivity induced increase of spectral weight is estimated to be  $\Delta W=0.5$  meV/Cu, which is about 0.5 % of the total spectral weight. This increase is sufficient to explain the condensation energy extracted from the specific heat measurements.

From the specific heat the change in internal energy was estimated by integrating

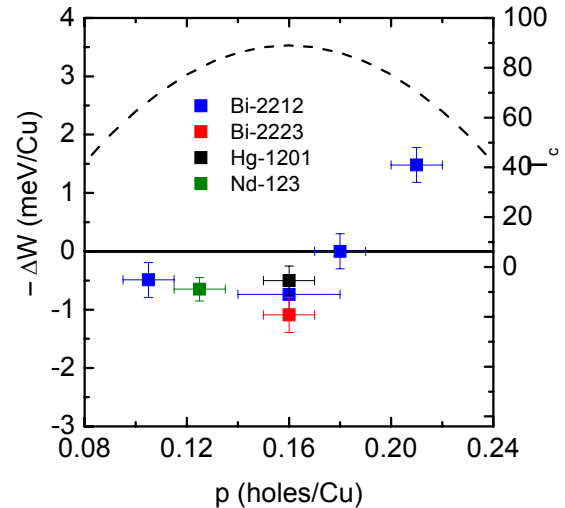
$$\Delta U(T) = \int_0^T [C(0, T') - C(B, T')] dT'$$

where  $B = 8$  Tesla. Fig. 23 shows a comparison between the internal energy and the change in kinetic energy defined as  $-\Delta W(T)=W(\Omega_c, T)-W(\Omega_c, T=20K)$ . The change in kinetic energy is about 10 times larger than the change in internal energy, so in principle the change in kinetic energy is large enough to account for the condensation energy.

The van der Marel group has determined the spectral weight difference  $\Delta W=W_{SC}-W_N$  for a number of superconducting cuprates (single-layer Hg1201 [37], double-layer Bi2212 [38],



**Fig. 23.** Comparison between internal energy  $\Delta U(T)$  and the change in kinetic energy  $-\Delta W(T)$ .



**Fig. 24** The doping dependence of the superconductivity induced change of free carrier optical spectral weight,  $-\Delta W$ , which is approximately proportional to the change of the electronic kinetic energy. The critical temperature is indicated for Bi2212.

tri-layer Bi2223 [39]) in order to establish its dependence on doping, the number of the  $\text{CuO}_2$  planes and the chemical composition. Since the energetic changes are rather small they used spectroscopic ellipsometry in combination with reflectivity measurements in order to improve the accuracy of  $\Delta W$ . The results of these studies are summarized in Fig. 24.

The cuprates from the studied cuprate families appear to follow the same trend, although the doping dependence was examined only for Bi2212. A surprising result is that  $\Delta W=-E_{\text{kin}}$  is negative (unconventional) at low doping levels but crosses over to the positive, i.e. BCS-consistent, values for the overdoped regime. Intuitively this can be associated with the fact that the electron-hole quasiparticles in the normal state are much more coherent, or Fermi-liquid like, for the overdoped samples than for the underdoped ones, which make the energetics more conventional. This result is also in agreement with the cluster Dynamical Mean-Field Theory calculations [38].

#### f) Superconductivity in the two-dimensional repulsive Hubbard model

The emergence of a superconducting ground state of the two-dimensional repulsive Hubbard model away from half filling remains a heavily debated issue among the various theories of high- $T_c$  cuprates. Perturbation theory yields a Kohn-Luttinger type instability for small  $U$ , due to strong correlation effects [40], without however giving quantitative results for the gap



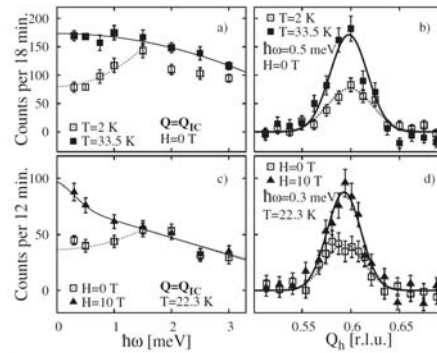
parameter or the condensation energy. Moreover, the Hubbard parameter  $U$  is clearly not small in the cuprates. Variational studies have therefore been undertaken very soon after the discovery of high- $T_c$  superconductors. In the opinion of Baeriswyl and collaborators the early attempts were not convincing [41], either because the ansatz used was too simple or because the limit considered (that of the t-J model) may have strongly overestimated the pair formation.

Focusing on the overdoped regime, Baeriswyl and collaborators proposed a variational wave function that takes into account both the kinetic exchange and the delocalization of holes. In their work [42], two different approaches have been chosen. For the “canonical ensemble”, the number of electrons in the system is fixed by projecting the wave function onto a subspace with a fixed number of particles. For the “grand canonical ensemble”, the wave function contains contributions with various numbers of electrons, but the average density is fixed by the “chemical potential”. Although completely equivalent in the thermodynamic limit, these approaches lead to conflicting results for a small system size (8x8). A finite gap is found for the canonical approach, but not for the grand canonical ensemble [42]. This calls for finite size scaling and thus for improvements in the numerical simulation.

A study of a 10x10 lattice has already been realized, using the grand canonical version. In contrast to the 8x8 lattice, Baeriswyl and collaborators did find an energy minimum for a finite gap parameter. In this context, it is very interesting to make contact with rather recent work on the reduced BCS Hamiltonian [43], where one finds a critical system size above which superconductivity is found for the grand canonical ensemble, while pairing occurs for all system sizes for the canonical version. This agreement with their findings for the repulsive Hubbard model is very encouraging and should help us to reach some clear conclusions in the near future, i.e. as soon as the trend observed for the 10x10 lattice is confirmed by simulations on a 12x12 lattice, which are on the way.

**g) Spin fluctuations in underdoped LSCO**

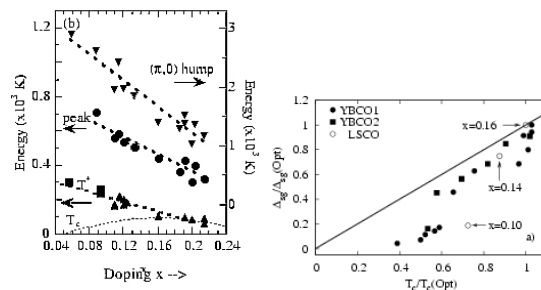
For underdoped  $\text{La}_{2-x}\text{Sr}_x\text{CuO}_4$  ( $x=0.1$ ) Mesot and collaborators report a strong field-induced enhancement of the inelastic neutron scattering response at low energy transfers and in a restricted temperature range (see Figure 25). The field dependence suggests



**Fig. 25.** Energy and Q dependence of magnetic scattering from Underdoped LSCO ( $x=0.105$ ).

- Energy scans are taken at the incommensurate wavevector  $Q_{IC}$ : a) comparison of the response in the SC phase with that of the normal state in zero field. c) Effect of a 10T field at 22.3K.
- Q-scans through  $Q_{IC}$ : b) comparison of the response in the SC phase with that of the normal state at energy transfer 0.5meV. d) The effect of a 10T field at 22.3K, energy transfer 0.3meV.

that the approach developed by Demler et al. [44] to explain the previously observed field-induced static magnetic order [45] may also be applicable to the dynamics. The field-induced excitations may be more difficult to capture within a phenomenological Fermi-liquid approach. Furthermore, a spin gap (SG) energy  $\Delta_{SG}=1.5$  meV could be identified in this underdoped LSCO ( $T_c=29$  K) sample, which is much reduced when compared to  $\Delta_{SG}=6$  meV obtained for optimally doped ( $T_c=40$ K) samples. The strong renormalization of the SG as a function of underdoping appears to be a generic feature of HTSC (see Figure 26, left) and indicates a profound modification of the underlying electronic excitations as the system approaches its Mott insulating phase. Notice that this behavior contrasts with the doping dependence of most electronic energy scales [46]. This apparent conflicting behavior can be understood in terms of different doping dependence of the SC-gap at the nodal and anti-nodal points [47, 48].



**Fig. 26.** Left panel: doping dependence of various electronic energy scales as measured by ARPES. Right panel: Doping dependence of the spin-gap energy  $\Delta_{SG}$  normalized to that of the optimally doped compound (filled (VBCO) vs empty (LSCO) symbols [49]).

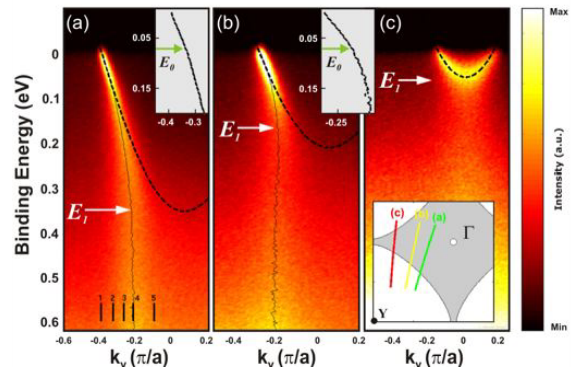
## h) Theory of inelastic neutron scattering in orthorhombic high- $T_c$ superconductors

Schnyder, Manske, Mudry and Sigrist have investigated the effect of orthorhombic deformation of the crystal lattice on the spin spectra observed in the inelastic neutron scattering [50]. Using a Fermi-liquid-based theory they calculated the in-plane anisotropy of the spin susceptibility  $\chi(q,\omega)$  for hole-doped high- $T_c$  cuprates. Within the two-dimensional one-band Hubbard model and a generalized RPA-based theory anisotropic hopping matrix elements and a mixing of d- and s-wave symmetry of the superconducting order parameter were considered in order to parametrize the orthorhombic superconductor. The results of this calculations have been compared with available inelastic neutron scattering data on untwinned  $\text{YBa}_2\text{Cu}_3\text{O}_{6+x}$  and good agreement was found. Furthermore, a strongly anisotropic in-plane dispersion of the resonance peak has been predicted based on this study.

## i) ARPES measurements on optimally doped LSCO

It is now well established, by angle resolved photoemission spectroscopy (ARPES), that in the under- to optimally-doped regime of Bi-based high-temperature superconductors (HTSC) no well defined quasiparticles (QP) exist in the normal state. This fact is in itself remarkable and is a signature of unusually strong electron correlations. Even more remarkable is the observation, in the superconducting-state, of sharp QP. One common feature of both the normal and superconducting states is that the energy width of the excitations (or inverse lifetime) is strongly anisotropic: sharpest along the nodal direction (of the superconducting gap and broadest at the antinodal points (close to  $(\pi,0)$ ).

It is the belief of Mesot and collaborators that the process by which these QP emerge upon entering the superconducting state is a key element to understand the mechanism of HTSC. Their most recent findings provide completely new information related to this important issue [51]. While a vast majority of ARPES papers concentrate on the low-energy ( $< 0.1$  eV) part of the spectral function, several groups have started to investigate the high-energy end (0.1-1.5 eV) of the spectrum. Recent papers on the cond-mat [52-55] report on the existence of a high-energy anomaly

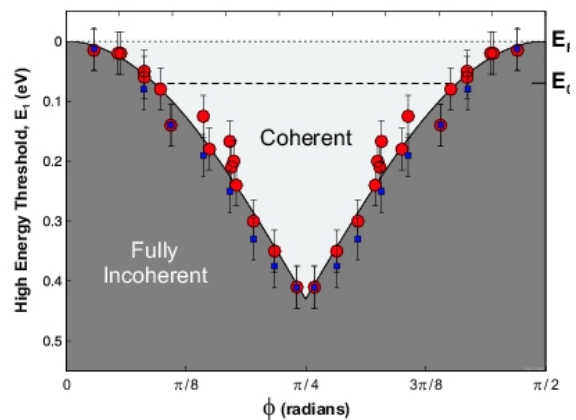


**Fig. 27.** (a-c) Plots of ARPES intensity as a function of binding energy and momentum taken along the 3 cuts a, b, and c shown in the bottom-right inset. The thin black line represents the MDC peak positions. Zooms of the brightest part of the dispersion are shown in the top insets. The dashed black line represents a tight-binding model dispersion along each of the cuts in the Brillouin zone.

around 0.4 eV. As a consequence, the spectra can be divided into two parts : a low energy part where quasiparticles are well defined and a high energy part composed of a broad incoherent background (see Figure 27).

In the current work [51], the optimally doped LSCO compound has been studied carefully, allowing to establish the following points:

- that this the high-energy feature is dispersing (see Figure 28).
- They further find that the momentum points for which the high-energy anomaly is closest to the Fermi energy, corresponds to the points where the QP's lifetime is shortest.
- Finally, by mapping the Brillouin zone as a function of increasing energy up to 0.6 eV Mesot and collaborators show that the region where QPs exist continuously shrinks from a line (the Fermi surface at



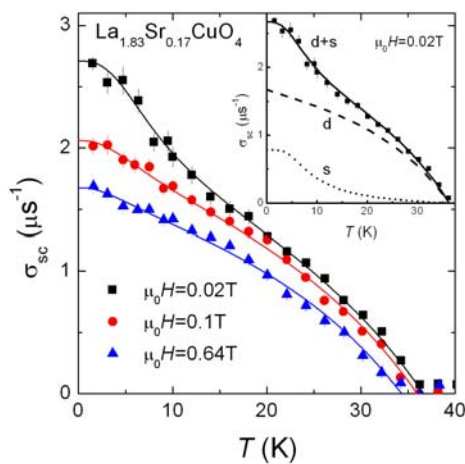
**Fig. 28.** Dispersion of  $E_1$  as a function of the FS angle. [51].

low energy), to a single point along the  $(\pi,\pi)$  direction at high energy. This behavior resembles very much that of the so-called Fermi-arcs as a function of temperature [56].

**j) Two-gap superconductivity in the cuprate superconductor  $\text{La}_{1.83}\text{Sr}_{0.17}\text{CuO}_4$**

It is mostly believed that the order parameter in cuprate high-temperature superconductors (HTS) has purely d-wave symmetry, as indicated by e.g. tricrystal experiments [57]. There are, however, a wide variety of experimental data that support s or even more complicated types of symmetries (d+s, d+is etc.) [58]. In order to solve this controversy Müller suggested the presence of two superconducting condensates with different symmetries (s- and d-wave) in HTS [59]. This idea was generated partly because two gaps were observed in n-type  $\text{SrTiO}_3$  [60], the first oxide in which superconductivity was detected. In addition, it is known that a two-order parameter scenario leads to a substantial enhancement of the superconducting transition temperature in comparison to a single-band model [61].

Important information on the symmetry of the order parameter can be obtained from magnetic field penetration depth  $\lambda$  measurements. Recently, Keller, Morenzoni and collaborators performed a study of the in-plane magnetic penetration depth ( $\lambda_{ab}$ ) in slightly overdoped single-crystal  $\text{La}_{1.83}\text{Sr}_{0.17}\text{CuO}_4$  by means of the muon-spin-rotation ( $\mu\text{SR}$ ) technique [62]. At low magnetic fields ( $\mu_0 H < 0.3$  T),  $\lambda_{ab}^{-2}(T)$  exhibits an inflection



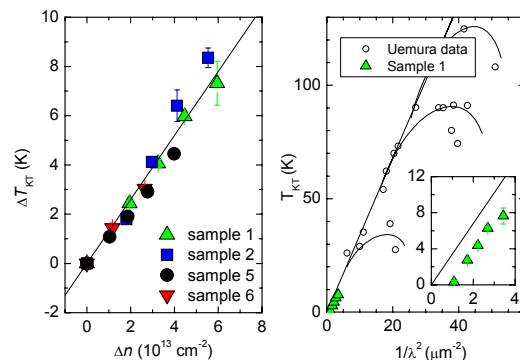
**Fig. 29.** Temperature dependence of the  $\mu\text{SR}$  depolarization rate  $\sigma_{sc} \propto \lambda_{ab}^{-2}$  of single-crystal  $\text{La}_{1.83}\text{Sr}_{0.17}\text{CuO}_4$  measured at 0.02T, 0.1T, and 0.64T (field-cooled). Lines in the main figure and in the inset represent the fit with the two gap model [63]. In the inset the contributions from the large d-wave gap and the small s-wave gap are shown separately.

point at  $T \sim 10\text{-}15\text{K}$  (see Fig. 29). These authors interpret this feature as a consequence of the presence of two superconducting gaps, analogous to double-gap  $\text{MgB}_2$  [58]. It is suggested that the large gap ( $\Delta_1^d(0) = 8.2(2)\text{meV}$ ) has d- and the small gap ( $\Delta_2^s(0) = 1.57(8)\text{meV}$ ) s-wave symmetry. With increasing magnetic field the contribution of  $\Delta_2^s$  decreases substantially, in contrast to an almost constant contribution of  $\Delta_1^d$ . Both the temperature and the field dependences of  $\lambda_{ab}^{-2}$  were found to be similar to what was observed in double-gap  $\text{MgB}_2$  [63, 64].

**k) Electrostatic field effect probing of the phase diagram of  $\text{NdBa}_2\text{Cu}_3\text{O}_{6+x}$  thin films**

Triscone and collaborators completed the study on the very underdoped part of the high  $T_c$  temperature-doping phase diagram ( $T_c$  vs.  $n$ ) of the  $\text{NdBa}_2\text{Cu}_3\text{O}_{6+x}$  high- $T_c$  compound. Using electric field effect on very thin films - only three to four unit cells thick - they obtained  $T_c$  shift of unprecedented amplitudes. Consistency with a Kosterlitz-Thouless (KT) transition has been checked and used to determine  $T_{KT} = T_c$ . This, combined with their method to precisely determine the amount of charge brought to the films, allowed us to draw  $\Delta T_{KT}$  as a function of the change in areal charge density  $\Delta n$ . The measured linear relation between  $\Delta T_{KT}$  and  $\Delta n$  is a signature of a quantum superconductor to insulator phase transition occurring in 2D (2D-QSI).

Penetration depth ( $\lambda$ ) values were also extracted from transport measurements. Triscone and collaborators demonstrated that  $T_c$  is proportional to  $1/\lambda^2$ , thus following the ‘‘Uemura relation’’ as can be seen on Figure 30 (right) and consistent with a 2D-QSI. Finally, this result also implies that  $T_c$ ,  $n$  and  $1/\lambda^2$  are



**Fig. 30** Left: change in the Kosterlitz-Thouless temperature as a function of the induced 2-D carrier density. Right: the Uemura plot and data by Triscone et al (green), notice that the slope is in agreement with the Uemura relation.

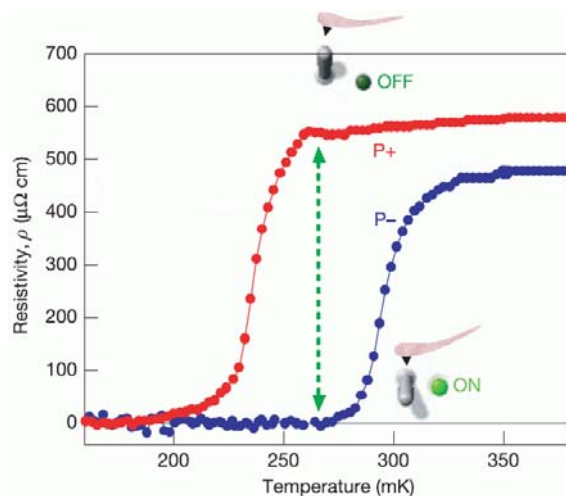
correlated in the very underdoped region of the phase diagram.

## l) Local electrostatic modulation of the electronic properties of Nb-doped SrTiO<sub>3</sub> superconducting films

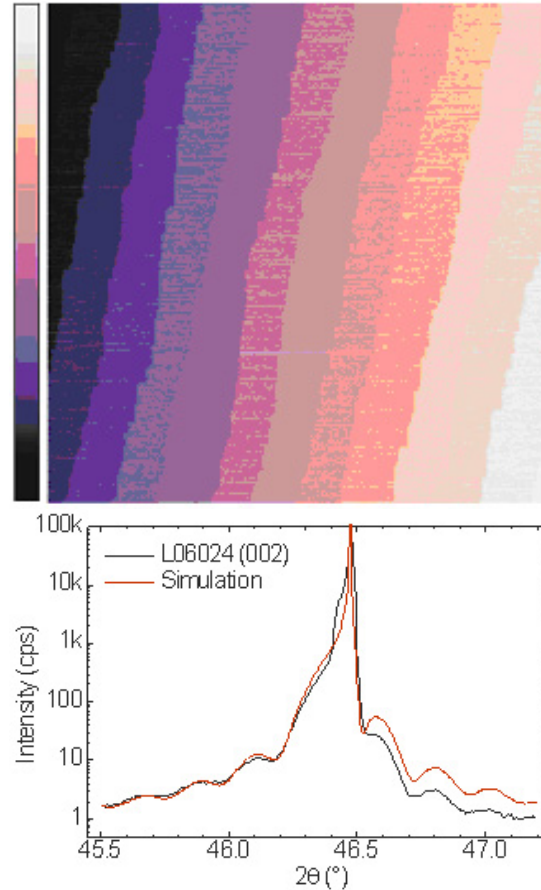
The Triscone group has previously shown that heterostructures composed of ferroelectric PbZr<sub>0.2</sub>Ti<sub>0.8</sub>O<sub>3</sub> (PZT) and metallic Nb-doped SrTiO<sub>3</sub> (Nb-STO) can be used as a model system for realizing ferroelectric field effect experiments.

Switching the polarization of the PZT layer with an atomic force microscope allows us to change the carrier concentration of the Nb-STO film underneath at the nanoscale. Figure 31 shows the shift in  $T_c$  obtained in such a structure while switching the ferroelectric polarization. As shown by the green arrow, in a temperature range around 0.27 K, switching of the ferroelectric polarization induces a remarkable transition from the normal metallic state ( $P^+$  state) to the superconducting zero resistance state ( $P^-$  state). In this experiment, the Nb-STO films were typically 250Å thick. For most of the planned experiments, a larger effect is desirable. Ideally one would like to obtain superconductivity for the  $P^-$  state and normal state down to the lowest temperatures in the  $P^+$  state. Triscone and collaborators thus decided to try realizing thinner Nb-STO films which are both metallic and superconducting. They also studied the transport properties of such films as a function of the film thickness.

The 1wt-% Nb-doped SrTiO<sub>3</sub> films are prepared using pulsed laser deposition (PLD) at very high deposition temperatures (1200-1300°C) on insulating (001) SrTiO<sub>3</sub> (STO)



**Fig. 31** Demonstration of the shift in superconducting transition curves of a heterostructure of Nb-STO/PZT, depending on the PZT polarization.

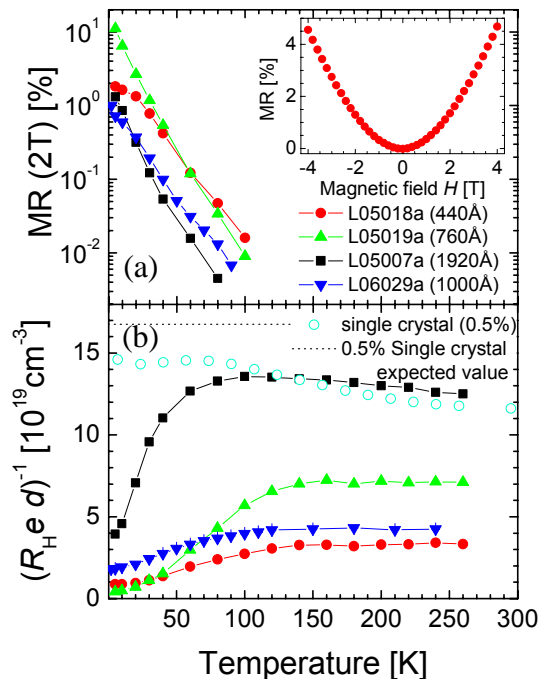


**Fig. 32.** Top: a typical surface of thin Nb-STO films. The height of each step corresponds to one unit cell (vertical scale: 6nm, horizontal 1.3μm). Bottom: standard  $\theta$ -2  $\theta$  diffraction pattern for a 453Å film.

substrates. The temperature is high enough to obtain a step flow growth mode. Hence the surface qualities are as good as the ones of the substrates (which are etched to obtain a TiO<sub>2</sub> termination and which display atomically flat terraces). As can be seen on Figure 32 (left) where a film surface topography is shown, the atomic terraces of the substrates are indeed reproduced.

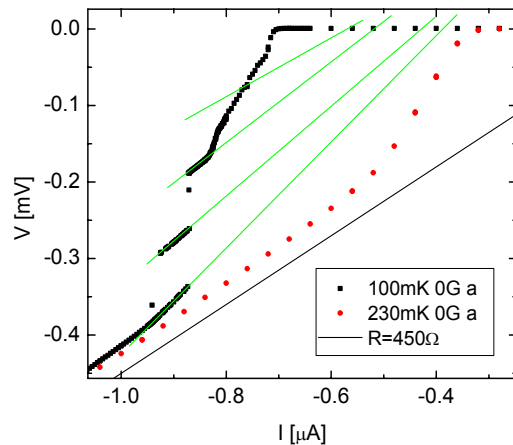
The same group recently succeeded preparing metallic Nb-STO films with thicknesses between 140 and 160Å. This is very promising for obtaining large ferroelectric field effects and the devices will be measured soon.

Using these thin films, Triscone and collaborators also investigated the normal state transport properties which are found to be different from the bulk. The carrier concentration in thin films, deduced from the room temperature Hall constant, is typically three times smaller than expected in a naïve model, where each dopant gives one electron to the system, while this simple assumption works well for bulk. Several models have been proposed to explain this reduced carrier



**Fig. 33.** Magnetoresistance and carrier concentration of films (1wt-% Nb doped) of different thicknesses. For comparison, data from a single crystal with half the Nb content (open circles, 0.5wt-%) are plotted. The inset shows the magnetoresistance as a function of the magnetic field at 20K.

density. One model considers an interface dead layer which reduces the effective thickness of the film: this could explain why their films thinner than 10nm are often found to be insulating. Another difference between bulk and films is the temperature dependence of the Hall constant. In bulk, it is found to be temperature independent as they confirmed by measuring several single crystals with dopings ranging from 0.05wt-% to 1wt-% (see Figure 33). In thin films however the Hall constant shows a large increase below 100K, temperature at which an antiferrodistortive structural phase transition occurs. The increase of the Hall constant below 100K can be explained by the presence of two bands with different carrier effective masses. These two bands have been calculated and measured in bulk systems. They are degenerated at high temperatures, above the structural phase transition; the structural transition lifts the degeneracy, splitting the two bands roughly 30meV apart. In a two band scenario, the Hall coefficient is then a function of the mobilities and concentrations of each band. Another signature of two band conduction can be found in the magneto-resistance. As can be observed in Fig. 33, a large magneto-resistance indeed appears below 100K. These transport data might thus suggest that, in thin films, a signature of two



**Fig. 34** I-V curves exhibiting steps structure.

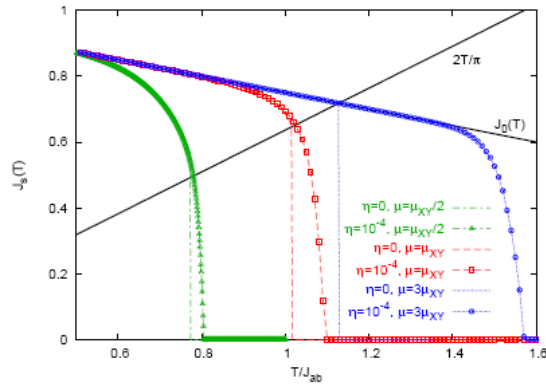
band conduction can be found, possibly because of a small level of strain.

As a first step in the direction of local ferroelectric field effect, an array of normal state “dots” was created in a high  $T_c$  background (switching locally the ferroelectric polarization using the AFM). As can be seen on Figure 34, such structures show a step like behavior in the I-V curves that Triscone and collaborators ascribe to phase slip lines which are more easily generated in inhomogeneous 2-D superconductors. They are currently investigating novel structures with different dot densities to confirm that phase slip processes are at the origin of the steps observed in the I-V curves.

For more details, see Ref. 66.

#### m) Phase fluctuations in quasi 2D superfluid systems:

Much attention has been devoted to the effect of phase fluctuations in quasi 2D superfluid systems. Thin films are natural candidates for the observation of the “universal” (i.e. sample-independent) behavior characteristic of the Beresinsky-Kosterlitz-Thouless (BKT) physics, as the universal jump of the superfluid density, measured in 4He superfluid films, or the non-linear I-V characteristic, observed in thin films of conventional superconductors. Signatures of BKT physics can be expected also in layered superconductors with weak interplane coupling. A remarkable example of systems belonging to this class are underdoped samples of high- $T_c$  superconductors. Recently, various experimental data ranging from finite-frequency conductivity, Nernst signal and non-linear magnetization have been interpreted as signatures of BKT phase fluctuations. Nonetheless, several experiments failed to observe any effect reminiscent of the universal



**Fig. 35.** Temperature dependence of the superfluid stiffness  $J_s(T)$  in the 2D case (lines) and in the layered 3D case (symbols). The  $T_{BKT}$  is identified by the intersection between  $J_s(T)$  and the straight line  $2T/\pi$ . The results for  $\mu \leq \mu_{XY}$  show a rapid downturn of  $J_s(T)$  at  $T_d \approx T_{BKT}$ . As  $\mu$  increases  $T_d$  increases as well, so that at  $T_{BKT}$  no signature is observed in  $J_s(T)$  of the jump present in the 2D case.

jump of the superfluid density at the critical temperature, which would be the most direct probe of BKT physics in these systems.

Until now, the 2D-3D crossover in anisotropic layered superconductors has been discussed mainly within the theoretical framework of the anisotropic 3D XY model. Within this model a finite interlayer coupling  $J_c$  stabilizes the superconducting phase, by cutting the vortex potential. However the superfluid phase has a critical temperature  $T_c$  at most a few percents above  $T_{BKT}$ . This would be inconsistent with several recent measurements of the superfluid density in strongly underdoped  $YBa_2Cu_3O_{6+x}$  (YBCO) samples.

Giamarchi and collaborators have thus re-analyzed [67] the role played by the interlayer coupling and the vortex-core energy at the crossover from 2D KT to 3D superconducting behavior in layered superconductors. In particular, this group focuses on the behavior of the superfluid density below  $T_c$  and of the phase fluctuations correlation length above  $T_c$ . To perform this analysis they use the renormalization group techniques that were developed and used in the context of the metal-insulator transition in the quantum 1D sine-Gordon model for the cold atomic gases described in MaNEP project 1. In these systems the interchain tunneling amplitude plays the same role of the Josephson coupling in layered superconductors. This group shows that in the presence of a finite interlayer coupling the superfluid density loses its universal character. The jump in  $\rho_s(T)$  at  $T_{BKT}$  observed in the pure 2D system is replaced by

a downturn curvature at a temperature  $T_d$  which is determined by the vortex-core energy  $\mu$  (see Fig. 35). While in XY models, where  $\mu$  is fixed by the in-plane coupling  $J_{ab}$ ,  $T_d \approx T_{BKT}$ , in the general case the ratio  $T_d/T_{BKT}$  increases as  $\mu/J_{ab}$  increases. Analogously, by approaching the transition from above, the increasing of the phase-fluctuation correlation length is controlled by the scale  $T_d$  instead of the  $T_{BKT}$  of the pure 2D system. Based on these results, they argue that the various experimental data in cuprates concerning BKT behavior can be reconciled by assuming a vortex-core energy larger than the typical XY value.

### n) Single-molecule spectroscopy as a possible tool to study the electric field in superconductors

The trapping of a flux quantum by a vortex in a type II superconductor is a basic characteristic of this topological excitation. Less widely known is the fact that vortices trap electric charge as well, a consequence of particle-hole asymmetry generating an energy dependent density of states. The magnitude of this charge is small. At the surface of the superconductor it generates a dipolar electric field corresponding to roughly one Debye (corresponding to a unit charge dipole of size of order one Bohr radius). Various techniques have been suggested or used to observe this charge, e.g., atomic force microscopy and nuclear quadrupole resonance, where an experiment has been carried out on cuprate superconductors. Buzdin et al. have worked out a method to exploit spectral shifts in single-molecule spectroscopy, thus providing an efficient way to observe both the vortex charge dipole in type II superconductors as well as charge dipoles associated with the intermediate state domain formation in type I material.

### References

- [1] C. Dubois et al., to be submitted to Physical Review Letters 2007
- [2] N. Hayashi et al., Physica C **437-438**, 96 (2006).
- [3] K. Arai et al., Physica B **359-361**, 488 (2005)
- [4] E. Bauer et al., AIP Conference Proceedings **850**, 695 (2006).
- [5] P.A. Frigeri, D.F. Agterberg, I. Milat and M. Sigrist, Eur. Phys. J. B **1434**, 6028 (2007).
- [6] N. Hayashi, K. Wakabayashi, P.A. Frigeri and M. Sigrist, Phys. Rev. B **73**, 092508 (2006).
- [7] C. Iniotakis, N. Hayashi, Y. Sawa, T. Yokoyama, U. May, Y. Tanaka, and M. Sigrist, cond-mat/0701643.
- [8] P.A. Frigeri, D.F. Agterberg and M. Sigrist, New J. Phys. **6**, 115 (2004).
- [9] Y. Yanase and M. Sigrist, preprint.
- [10] J. Teyssier, A. B. Kuzmenko, D. van der Marel, F. Marsiglio, V. Filippov, N. Shitsevalova, Phys Rev B, in press (2007)
- [11] A.V. Sologubenko et al., Phys. Rev. B **74**, 184523 (2006).

- [12] F.M. Grosche et al., *J. Phys.: Condens. Matt.* **13**, 2845 (2001).
- [13] J. Flouquet et al., *cond-mat/0505713*, (2005).
- [14] C. Dallera and M. Grioni, *Structural Chemistry* **14**, 57 (2002).
- [15] C. Dallera et al., *Phys. Rev. B* **74**, 081101(R) (2006).
- [16] C. Dallera, E. Annese, G. Knebel, A. Barla, J.-P. Sanchez, M. D'Astuto, and M. Grioni, to be published
- [17] C. Dubois et al., to be published in *Physial Review B*.
- [18] C. Morais Smith, B Ivlev, and G. Blatter, *Phys. Rev. B* **49**, 4033 (1994)
- [19] T. Halpin-Healy and Y.-C. Zhang, *Phys. Rep.* **254**, 215 (1995).
- [20] M. Kardar, *Nucl. Phys. B* **290**, 582 (1987).
- [21] Y.-C. Zhang, *Europhys. Lett.* **9**, 113 (1989).
- [22] D.A. Huse, C.L. Henley, and D.S. Fisher, *Phys. Rev. Lett.* **55**, 2924 (1985).
- [23] E. Morenzoni et al., *J. Phys.: Cond. Matt.* **16**, S4583-S4601 (2004).
- [24] H. Lütken et al., *Phys. Rev. Lett.* **91** (2003), 017204
- [25] A. Drew et al., *Phys. Rev. Lett.* **95** (2005), 197201
- [26] P. Bruno and C. Chappert, *Phys. Rev. B* **46** (1992), 261
- [27] B. Lake et al., *Nature*, **415** (2002) 299
- [28] M. Brühwiler et al., *Phys. Rev. B* **73**, 094518 (2006)
- [29] T. Shibauchi et al., *Phys. Rev. B* **74**, 220506(R) (2006)
- [30] B.W. Hoogenbom et al., *Phys. Rev. B* **67**, 224502 (2003).
- [31] J. Lee et al., *Nature* **442**, 546 (2006)
- [32] S. Pilgram, T.M. Rice and M. Sigrist, *Phys. Rev. Lett.* **97**, 117003 (2006).
- [33] Y. Chan, T.M. Rice and F.C. Zhang, *Phys. Rev. Lett.* **97**, 237004 (2006).
- [34] Kohsaka et al., *Science*, in press.
- [35] F. Marsiglio et al., *Phys. Rev. B* **74**, 174516 (2006).
- [36] H. Molegraaf et al., *Science* **295**, 2239 (2002).
- [37] E. van Heumen et al., *Phys. Rev. B* (2007), in press.
- [38] F. Carbone et al. *Phys. Rev. B* **74**, 064510 (2006).
- [39] F. Carbone et al. *Phys. Rev. B* **74**, 024502 (2006).
- [40] See for instance B. Binz, D. Baeriswyl and B. Douçot, *Ann. Phys. (Leipzig)* **12**, 704 (2003).
- [41] D. Eichenberger and D. Baeriswyl, *cond-mat/0608210*, to be published in *Physica C*.
- [42] D. Baeriswyl, D. Eichenberger and B. Gut, *cond-mat/0612690*, to appear in *Phys. Stat. Sol. (b)*.
- [43] For a review see J. van Delft, *Ann. Phys. (Leipzig)* **10**, 219 (2001).
- [44] E. Demler et al., *Phys. Rev. Lett.* **87**, 067202 (2001).
- [45] B. Lake et al., *Science* **291**, 1759 (2001).
- [46] J. C. campuzano et al., *Phys. Rev. Lett.* **83**, 3709 (1999).
- [47] J. Mesot et al., *Phys. Rev. Lett.* **83**, 840 (1999).
- [48] M. Le Tacon et al., *Nature Physics* **2**, 537 (2006).
- [49] J. Chang et al., *Phys. Rev. Lett.* **98**, 77004 (2007).
- [50] A.P. Schnyder, D. Manske, C. Mudry and M. Sigrist, *Phys. Rev. B* **73**, 224523 (2006).
- [51] J. Chang et al., *cond-mat/0610880*, submitted.
- [52] J. Graf et al., *cond-mat/ 0607319*
- [53] B.P.Xie et al., *cond-mat/ 0607450*,
- [54] X.-H.Pan et al., *cond-mat/0610442*
- [55] T. Valla et al., *cond-mat/0610249*.
- [56] M. R. Norman et al., *Nature* **392**, 157 (1998 ).
- [57] C.C. Tsuei et al., *Phys.Rev.Lett.* **73**, 593 (1994).
- [58] G. Deutscher, *Rev.Mod.Phys.* **77**, 109 (2005).
- [59] K.A. Müller, *Nature (London)* **377**, 133 (1995).
- [60] G. Binnig et al., *Phys.Rev.Lett.* **45**, 1352 (1980).
- [61] A. Bussmann-Holder et al., *Eur. Phys. J. B* **37**, 1434 (2004).
- [62] R. Khasanov et al., *Phys.Rev.Lett* **98**, 057007 (2007).
- [63] A. Carrington and F.Manzano, *PhysicaC* **385**, 205 (2003).
- [64] S. Serventi et al., *Phys. Rev. Lett.* **93**, 217003 (2004).
- [65] D. Matthey, N. Reyren, T. Schneider, and J.-M. Triscone, *Phys. Rev. Lett.* **98**, 57002 (2007).
- [66] K. Takahashi, D. Jaccard, M. Gabay, K. Shibusya, T. Ohnishi, M. Lippmaa, J.-M. Triscone, *Nature* **441**, 195 (2006).
- [67] L. Benfatto, C. Castellani and T. Giamarchi, *cond-mat/0609287*, to be published in *PRL*.





## Project 3 Crystal growth

**Project leader** : L. Forró (EPFL).

**Participating members** : J. Karpinski (ETHZ), D. van der Marel (UNIGE), J. Mesot (PSI), G. Margaritondo (EPFL)

**Summary** : The objective of this MaNEP project is the synthesis of two-dimensional superconductors, geometrically frustrated conductors and magnetic materials in single crystalline form. In the last year the highlights were on the synthesis of a wide variety of magnetic materials. These include large  $\text{cm}^3$  size single crystals of:  $\text{CaVO}_3$ ,  $\text{SmBaMn}_2\text{O}_6$ ,  $\text{Nd}_{0.33}\text{Sr}_{0.66}\text{FeO}_3$ ,  $\text{La}_{1-x}\text{Sr}_x\text{CoO}_3$  ( $x=0.002, 0.005$ ),  $\text{SrCu}_2(\text{}^{11}\text{B}\text{O}_3)_2$ ,  $\text{LuFe}_2\text{O}_4$ ,  $\text{La}_{0.7}\text{Sr}_{0.3}\text{MnO}_3$ , and layered cobaltites  $\text{Tb}_{0.9}\text{Dy}_{0.1}\text{BaCo}_2\text{O}_{6-\delta}$ ,  $\text{NdBaCo}_2\text{O}_{6-\delta}$ ,  $\text{LiCu}_2\text{O}_2$  helimagnet,  $\text{Cu}_2\text{Te}_2\text{O}_5\text{X}_2$  ( $\text{X} = \text{Cl, Br}$ ),  $\text{Ni}_5(\text{TeO}_3)_4\text{Cl}_2$ ,  $\text{Fe}_{1-x}\text{Co}_x\text{Si}$ ,  $\text{Sr}_2\text{VO}_4$  and more. Besides these materials a progress has been done in the synthesis of cuprate and magnesium-boride superconductors and vanadium-chain conductors.

### Facilities for single crystal preparation

Crystal growth is present at four sites: at ETHZ (Head of the laboratory: J. Karpinski), at PSI (the scientist in charge: K. Conder), at EPFL (the scientist in charge H.Berger) and at DPMC, Uni Geneva (the scientist in charge: E. Giannini). The major change in the crystal growing infrastructure has happened at University of Geneva. During the past year the laboratories for metallurgy, materials processing and crystal growth have moved to a renewed place. The move was made necessary by the need of a more efficient management of all the facilities of the DPMC. The new Laboratory for Crystal Growth can host several scientists, and makes it possible to process and grow simultaneously various materials at the same time.

### 1. Synthesis of magnetic materials and related compounds

In the last period the major progress was achieved in the synthesis of magnetic materials. This includes the preparation of new systems and the improvement of size and quality of crystals synthesized previously. In this report besides the names of the compounds, the major experiments performed or to be performed on them are mentioned.

The following materials have been grown:

**$\text{CaVO}_3$**  (in collaboration with Prof. Bruce Patterson, SLS, PSI). The compound is a member of the "3d<sup>1</sup>" perovskite series ( $\text{SrVO}_3$ ,  $\text{CaVO}_3$ ,  $\text{LaTiO}_3$ ,  $\text{YTiO}_3$ ), with one d-electron per unit cell. Simple band-theory predicts that all of these materials are metallic. As one moves along the series, a rotation of the  $\text{VO}_6$  or  $\text{TiO}_6$  octahedra becomes stronger, reducing the electron hopping probability and hence the electronic bandwidth causing a metal to

insulator transition. It is believed that this occurs close to  $\text{CaVO}_3$ . The material near the surface can be structurally and electronically different from the bulk, and surface-sensitive techniques, such as X-ray photoelectron spectroscopy will be applied in order to study the effect of the surface on electron correlation effects. Additionally, it is important to accurately know the true surface structure (e.g., how are the octahedra at the surface rotated) and how the distortion depends on the depth into the sample. We hope to study it with surface X-ray diffraction experiments. Large crystals of a good quality ( $\varnothing 6$  mm, 20mm length) were grown in Ar atmosphere (2bar) with a rate of 1mm/h.

**$\text{SmBaMn}_2\text{O}_6$**  (in collaboration with Dr. Urs Staub, SLS PSI). The compound is showing a charge (CO) and orbital ordering (OO) transition, however, an orbital reorientation is proposed to occur at the antiferromagnetic transition temperatures, indicative of strong correlations between the magnetic and orbital degrees of freedom. Resonant soft X-ray diffraction at the SLS will be applied to study the orbital ordering and its order parameters in a direct way. In combination with resonant hard x-ray diffraction, it will allow to dis-entangle the different effects between orbitals, Jahn-Teller distortion, structure and magnetism in this material, and test recent predictions on the forces driving these phase transitions. Good quality crystals of several  $\text{mm}^3$  could be selected from a rod grown in Ar+20%  $\text{O}_2$  atmosphere (2bar) with a rate of 2mm/h.

**$\text{Ln}_{0.33}\text{Sr}_{0.66}\text{FeO}_3$**  (project proposal Dr. Joel Mesot, LNS, ETHZ and PSI). In  $\text{Ln}_{0.33}\text{Sr}_{0.66}\text{FeO}_3$  ( $\text{Ln}=\text{rare earth}$ ) charge disproportionation:  $2\text{Fe}^{4+} \leftrightarrow \text{Fe}^{3+} + \text{Fe}^{5+}$ , is observed below 200K. Pressure-induced (above 20 GPa) transition from a charge-disproportionated antiferromagnetic to a charge-uniform ferromagnetic phase was

identified in  $\text{La}_{0.33}\text{Sr}_{0.66}\text{FeO}_3$ . Large crystals of a very good quality ( $\varnothing 7$  mm, 40mm length) were grown in  $\text{O}_2$  atmosphere (5bar) with a rate of 1mm/h.

**$\text{La}_{1-x}\text{Sr}_x\text{CoO}_3$  ( $x=0.002, 0.005$ )** (in collaboration with Dr. Andrei Podlesnyak, Hahn-Meitner-Institut, Berlin). For  $\text{LaCoO}_3$  it was found by inelastic neutron scattering that with increasing temperature an excitation at  $\sim 0.6\text{meV}$  appears [1]. For slightly Sr-doped materials already at 1.5K an additional magnetic excitation ( $\approx 0.75$  meV) is observed. This could be explained within a scenario involving the existence of magnetic polarons [2]. Large ( $\varnothing 7$  mm, 60mm length) high quality single crystals have been obtained by applying a growth rate of 7mm/h in  $\text{O}_2$  atmosphere (5bar).

**$\text{SrCu}_2(^{11}\text{BO}_3)_2$**  (in collaboration with Prof. H.M. Ronnow, EPFL) and Dr. Ch. Rüegg, UCL, UK). The structure of this compound is a physical realization of the Shastry-Sutherland model. It is a quasi-two dimensional spin system with a singlet dimer ground state. With a hydrostatic pressure and chemical substitution (doping) the magnetic phase diagram of the system has been investigated. Large ( $\varnothing 6$  mm, 60mm length) high quality single crystals have been obtained applying a very small growth rate of 0.25 mm/h in  $\text{Ar}+20\%$   $\text{O}_2$  atmosphere (5bar).

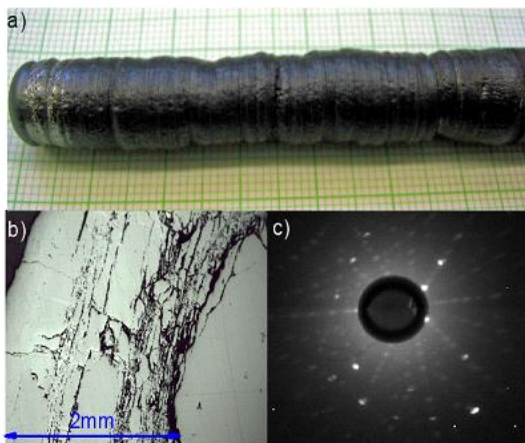
**$\text{LuFe}_2\text{O}_4$**  (in collaboration with Prof. Michel Kenzelmann, ETHZ & LNS PSI). The ferroelectricity of this multiferroic material appears to result from ordering of  $\text{Fe}^{2+}$  and  $\text{Fe}^{3+}$  ions. In order to understand the field dependence of the magnetic order and to

determine the magnetic structure, neutron diffraction experiments have been performed using the triple-axis spectrometer RITA-2 at SINQ. Different field and temperature dependent behavior of two magnetic peaks have been observed. This fact allows concluding that two magnetic order parameters exist in the system  $\text{LuFe}_2\text{O}_4$ . Large crystals of good quality were grown in 2 bars pressure of  $\text{CO} + \text{CO}_2$  (5:2) with a rate of 1mm/h.

**$\text{La}_{0.7}\text{Sr}_{0.3}\text{MnO}_3$**  (in collaboration with Dr. Luc Patthey and Juraj Krempasky, SLS, PSI). First ARPES results on the band structure have been obtained on cleaved crystal. Large ( $\varnothing 6$  mm, 60mm length) high quality single crystals have been obtained applying growth rate of 2 mm/h and  $\text{Ar}+10\%$   $\text{O}_2$  atmosphere (5bar).

**$\text{Tb}_{0.9}\text{Dy}_{0.1}\text{BaCo}_2\text{O}_{5+x}$ ,  $\text{NdBaCo}_2\text{O}_{5+x}$** . (PhD work of Marian Stingaciu). Layered cobalt oxide compounds  $\text{LnBaCo}_2\text{O}_{5+x}$  have a perovskite-derived structure similar to those of high temperature superconductors. Despite not being superconducting, these compounds have interesting physical properties (magnetoresistance, metal-insulator transition, ionic conductivity). Further experiments have been performed in order to optimise the growth conditions. Increasing the diameter of the grown crystal and optimising the growth rate (0.5 mm/h), we managed to obtain crystal rods with high quality cores (see Fig. 1).

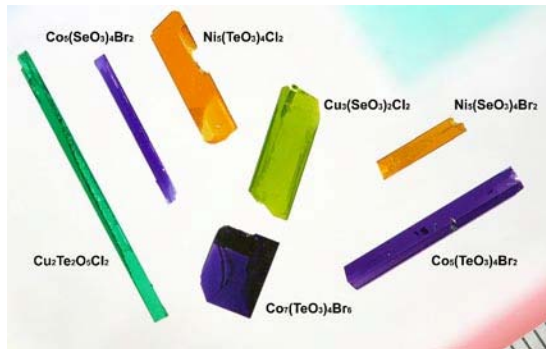
**$\text{LiCu}_2\text{O}_2$**  is a quasi-one-dimensional  $S=1/2$  antiferromagnetic spin-chain compound. Angle-resolved photoemission (ARPES) and optical measurements were performed on single crystals. The ARPES spectra show several dispersive branches associated with hybrid copper-oxygen states. The occurrence of the valence band maximum halfway between the center and the edge of the Brillouin zone, and the complex spectral line shapes are not reproduced by the existing calculations of the electronic structure. They can be interpreted within a one-dimensional scenario of strongly correlated antiferromagnetic insulators. The combination of ARPES and optics allows us to estimate the magnitude of the charge-transfer gap to be 1.95 eV. Moreover, the temperature-dependent optical conductivity bears signatures of the three different magnetic phases of this material. The field dependence of the electron spin resonance of a helimagnet  $\text{LiCu}_2\text{O}_2$  was also investigated for the first time [3, 4].



**Fig. 1.** **a)** Single crystal of  $\text{Tb}_{0.9}\text{Dy}_{0.1}\text{BaCo}_2\text{O}_{5+x}$  obtained with a growing rate 0.5 mm/h in an atmosphere of 2%  $\text{O}_2$  in argon (1 bar); **b)** Cross section of the grown crystal showing a high quality core; **c)** Laue diffractogram of the core crystal.

**Cu<sub>2</sub>Te<sub>2</sub>O<sub>5</sub>X<sub>2</sub> (X = Cl, Br).** The work has successfully continued on oxohalides with determination of crystal structure and magnetic properties of Cu<sub>2</sub>Te<sub>2</sub>O<sub>5</sub>X<sub>2</sub> (X = Cl, Br) [5], as well as the effect of externally applied pressure on the magnetic behavior of Cu<sub>2</sub>Te<sub>2</sub>O<sub>5</sub>(Br<sub>x</sub>Cl<sub>1-x</sub>)<sub>2</sub>. The size and the purity of these crystals (Fig. 2) have been considerably improved within the last year.

**Ni<sub>5</sub>(TeO<sub>3</sub>)<sub>4</sub>Cl<sub>2</sub>** Large single crystals of the transition metal tellurium oxychloride (Fig. 2) has been investigated by high-field electron-spin resonance for frequencies up to 3 THz, at temperatures well below the magnetic ordering at 23 K [6]. At zero external field several resonance modes have been identified. When the applied magnetic field is perpendicular to both the **a** and **b** crystallographic directions, one of the magnetic-resonance modes softens, and a spin-flop transition occurs around 10 T. The results are discussed in terms of the crystal structure, and compared to other magnetically ordered materials with multiple magnetic sublattices, including orthoferrites and triangular antiferromagnets.



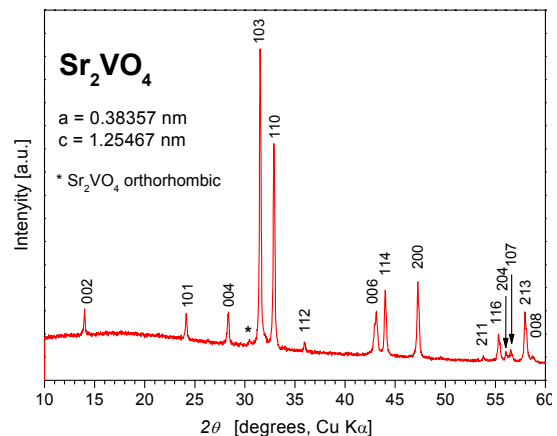
**Fig. 2.** A representative set of single crystals of magnetic materials grown by chemical vapor transport method.

## 2. Processing and crystal growth of layered perovskites with the K<sub>2</sub>NiF<sub>4</sub> structure: Sr<sub>2</sub>TiO<sub>4</sub> and Sr<sub>2</sub>VO<sub>4</sub>

Transition metal oxides with the crystal structure of the layered perovskite K<sub>2</sub>NiF<sub>4</sub> have been intensively studied due to the extent of their exciting properties, like high-T<sub>c</sub> superconductivity, ferroelectricity, spin and/or charge ordering, CMR, and multiferroics. Two Cu-free compounds have aroused our interest, Sr<sub>2</sub>TiO<sub>4</sub> and Sr<sub>2</sub>VO<sub>4</sub>, as they can strongly help us to unravel the mechanism of high-T<sub>c</sub> superconductivity in cuprates and discover new high-T<sub>c</sub> superconducting materials. No crystals of both of these compounds have been grown so far and the experimental

studies on this topic have been hindered by the difficulties in processing these materials.

**Sr<sub>2</sub>VO<sub>4</sub>.** In view of the insulating behavior with a small Mott gap, the S=1/2 configuration and the AF ordering at low temperature, Sr<sub>2</sub>VO<sub>4</sub> is considered as being the electronic counterpart of the high-T<sub>c</sub> superconductor La<sub>2</sub>CuO<sub>4</sub>. Theoretical works have predicted doping- as well as pressure- induced superconductivity to occur in Sr<sub>2</sub>VO<sub>4</sub> [7]. However, this material revealed to be very difficult to synthesize, mainly because of the difficulty in favoring and stabilizing the V<sup>+</sup> valence state of V ions. Reduction and/or oxidations reactions should be carefully controlled for the formation of Sr<sub>2</sub>VO<sub>4</sub> when starting from V<sub>2</sub>O<sub>5</sub> or V<sub>2</sub>O<sub>3</sub> precursors, respectively. We have recently succeeded in processing single-phase ceramic samples of Sr<sub>2</sub>VO<sub>4</sub> following a two-step reaction-reduction processing route. The intermediate Sr<sub>4</sub>VO<sub>9</sub> oxide was obtained first from SrCO<sub>3</sub> and V<sub>2</sub>O<sub>5</sub>, then it was treated at T=950°C in an evacuated sealed tube together with metallic Zr, and reduced by the Zr oxidation. The formation of other vanadium oxides must be carefully avoided at any step of preparation, as this can easily follow from reactions with solvents, crucibles, and atmosphere. The XRD spectrum of Sr<sub>2</sub>VO<sub>4</sub> is shown in Fig. 3. The only impurity peak is the very weak reflection from the orthorhombic modification of Sr<sub>2</sub>VO<sub>4</sub>. In order to synthesize large amounts of both pure and doped Sr<sub>2-x</sub>A<sub>x</sub>V<sub>1-y</sub>M<sub>2y</sub>O<sub>4±δ</sub> (A = alkaline or lanthanide, M = transition metal), a strong effort is still needed. For this purpose, a collaboration with Prof. J. Hülleriger (University of Bern, MaNEP project 4) has started. New routes have to be found in order to improve the precursor preparation and grow crystals of this material.



**Fig. 3.** X-Ray Diffraction pattern of Sr<sub>2</sub>VO<sub>4</sub> powder. Inset: magnetic susceptibility as a function of T at m<sub>0</sub>H=0.2T.

Magnetic ordering is expected to occur at low  $T$  in  $\text{Sr}_2\text{VO}_4$ . Several magnetic states have been reported so far (spin-glass, AF) depending on doping. The magnetic susceptibility  $\chi(T)$  of ceramic  $\text{Sr}_2\text{VO}_4$  is plotted as a function of  $T$  in the inset of Fig.3. Two magnetic transitions occur at  $\sim 10\text{K}$  and  $\sim 30\text{K}$ .

$\text{Sr}_2\text{TiO}_4$  is a band gap insulator, with an empty  $d$  orbital ( $d^0$  for  $\text{Ti}^{4+}$ ) and no spin ( $S=0$ ). It can be seen as the non-magnetic reference for the study of the isostructural series  $\text{Sr}_2\text{MO}_4$  ( $M$ =transition metal). We have successfully synthesized highly pure  $\text{Sr}_2\text{TiO}_4$  from  $\text{SrCO}_3$  and  $\text{TiO}_2$  by solid-state reaction in air. No secondary Ruddlesden-Popper phases are found in the final product. Crystal growth experiments are in progress by using the Traveling Solvent Floating Zone method

### 3. Processing and crystal growth of Transition Metal Monosilicides: $\text{Fe}_{1-x}\text{Co}_x\text{Si}$ and $\text{CrSi}$ .

Transition metal monosilicides  $\text{TMSi}$  ( $\text{TM}=\text{Cr}, \text{Mn}, \text{Fe}, \text{Co}, \text{Ni}$ ) exhibit a large assortment of intriguing physical properties and have been object of outstanding reports during the last few years [8, 9]. After the success in growing high-quality  $\text{CoSi}$  crystals (see previous reports) and the wide investigation carried out on  $\text{MnSi}$  [10], we are now facing the problem of growing and studying crystals of  $\text{Fe}_{1-x}\text{Co}_x\text{Si}$  and  $\text{CrSi}$ .

**$\text{Fe}_{1-x}\text{Co}_x\text{Si}$ .** The solid solution  $\text{Fe}_{1-x}\text{Co}_x\text{Si}$  offers the opportunity of tuning the magnetic ordering by increasing the amount of  $\text{Co}$  between the two non-magnetic end compounds  $\text{FeSi}$  and  $\text{CoSi}$ . Transport properties are strongly affected by the doping-induced magnetic ordering and spin-controlled charge localization can occur at a given  $\text{Co}$  content, thus opening interesting perspective for spintronics applications [11, 12].

Single crystals of  $\text{Fe}_{1-x}\text{Co}_x\text{Si}$  are grown by crucible-free techniques in order to prevent any contamination. Both the Czochralski pulling from levitating melt and the Travelling Solvent Floating Zone (TFSZ) methods are successfully employed for growing  $\text{Fe}_{1-x}\text{Co}_x\text{Si}$  crystals under inert atmosphere. Precursor rods for TFSZ are made in an arc furnace and vacuum cast *in-situ* (as-cast feed rod is shown in Fig.4, together with the XRD spectrum). This material melts congruently at  $\sim 1450^\circ\text{C}$ . In order to understand the nature of magnetic ordering and the effect of the disorder induced by doping on the local spin, the growth of large

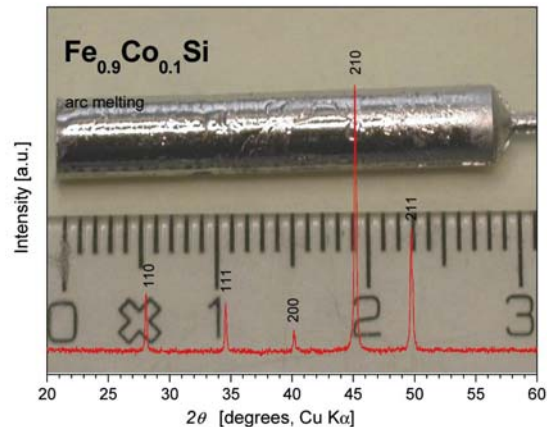


Fig. 4. X-Ray diffraction pattern of  $\text{Fe}_{0.9}\text{Co}_{0.1}\text{Si}$ . In the background, a typical size of the as-cast rod is shown.

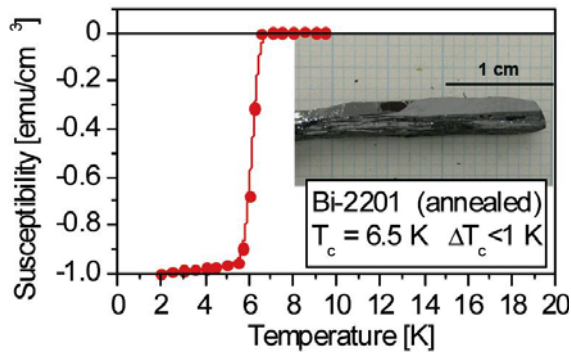
crystals of  $\text{Fe}_{0.9}\text{Co}_{0.1}\text{Si}$ ,  $\text{Fe}_{0.5}\text{Co}_{0.5}\text{Si}$  and  $\text{Fe}_{0.3}\text{Co}_{0.7}\text{Si}$  has started.

**$\text{CrSi}$ .** Among the  $\text{TMSi}$  series,  $\text{CrSi}$  is the only compound not melting in a congruent way and exhibiting a complex phase diagram. The formation of both the secondary phases  $\text{Cr}_5\text{Si}_3$  and  $\text{CrSi}_2$  always hinders the processing and single crystal growth of  $\text{CrSi}$ . For this reason, a poor literature exists on experimental studies of  $\text{CrSi}$ . We have recently started to deal with this not trivial materials issue. Either arc melting, or HF melting in an induction furnace have been used for the precursor reaction. Only 85% pure  $\text{CrSi}$  phase has been obtained so far.

### 4. Crystal growth of Bi-based high- $T_c$ superconducting cuprates.

A very productive crystal growth activity concerns the superconducting family of compounds  $\text{Bi}_2\text{Sr}_2\text{Ca}_{n-1}\text{Cu}_n\text{O}_{4+2n}$  ( $n=1,2,3$ ). Crystals of  $\text{Bi}_2\text{Sr}_2\text{Ca}_2\text{Cu}_3\text{O}_{10}$  ( $T_c \sim 110\text{K}$ ) of unique size and quality have been grown in the recent past at the DPMC in Geneva. This has led to outstanding experiments on this material, in optics as well as in local spectroscopy and structural investigations [11, 13, and 14]. This activity is still going on with the aim of exploring both the underdoped and the overdoped regime of the superconducting phase diagram of  $\text{Bi}_2\text{Sr}_2\text{Ca}_2\text{Cu}_3\text{O}_{10}$ . Numerous collaborations, either internal within the NCCR-MaNEP or external, are working ahead on these crystals.

On the other hand, the  $n=1$  compound  $\text{Bi}_2\text{Sr}_2\text{CuO}_6$  ( $T_c \sim 10\text{K}$ ) has also aroused our interest, and has been the object of crystal

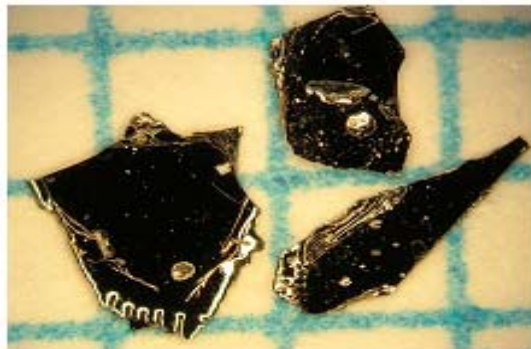


**Fig. 5.** Magnetic transition of a  $\text{Bi}_2\text{Sr}_2\text{CuO}_6$  crystal as measured with a SQUID magnetometer after post-annealing in 7% $\text{O}_2$ -93%Ar. A large as-grown crystal is shown in the picture.

growth experiments during the last year (Fig. 5). Thanks to its low  $T_c$  and  $H_{c2}$ , pure  $\text{Bi}_2\text{Sr}_2\text{CuO}_6$  allows us to gain access into the normal state even at low temperatures. Despite of the stronger effort done by several authors in growing La and/or Pb doped  $\text{Bi}_2\text{Sr}_2\text{CuO}_6$  ( $T_c$  up to 41 K), experiments on pure  $\text{Bi}_2\text{Sr}_2\text{CuO}_6$  have been a little disregarded so far, also due to the higher difficulty in growing the pure compound.  $\text{Bi}_2\text{Sr}_2\text{CuO}_6$  crystals of a large size ( $> 20$  mm in the growth direction) have been grown at the DPMC by the TSFZ method in a two-mirror furnace. Crystals grow at a rate of 0.2-1 mm/h under an oxygen overpressure of 2-3 bar. Critical temperatures as high as 6.5 K have been obtained in large samples. The work is in progress with the aim of better controlling the oxygen content both during the growth and post-annealing.

## 5. Crystal growth of superconductors and related compounds

**MgB<sub>2</sub>.** Critical temperature and other superconducting properties of a two-band superconductor depend on the doping level and therefore, they can be modified by chemical substitutions. Substitutions change the electronic structure, the gap values, the defect structure, inter- and intra-band scattering, and thus superconducting properties such as  $T_c$ , upper critical field,  $H_{c2}$ , and its anisotropy [15]. With this in mind, we have synthesized crystals with a wide range of substitutions in the parent compound  $\text{MgB}_2$ . Single crystals of  $\text{Mg}_{1-x}\text{Li}_x(\text{B}_{1-y}\text{C}_y)_2$  were grown under pressure of 30 kbar at temperature 1850-2000°C using the cubic anvil press (see Fig 6). Studies of the phase diagram of Mg-B and Mg-B-N systems have been performed at

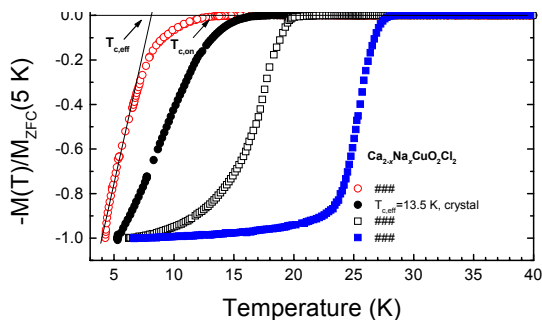
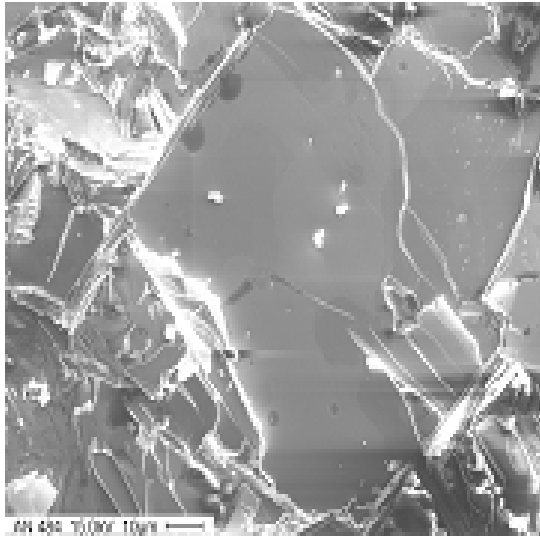


**Fig. 6.**  $\text{MgB}_2$  crystals grown in BN crucible: view from the top and crystals after separation.

pressures 10-30 kbar at temperature up to 2200°C.

The effect of Li substitution for Mg and Li-C co-doping on the superconducting properties and crystallographic structure of  $\text{MgB}_2$  single crystals has been investigated. Hole doping with Li decreases the superconducting transition temperature  $T_c$ , but in much slower rate than electron doping with C or Al. For  $\text{MgB}_2$  crystals with simultaneously substituted Li for Mg and C for B,  $T_c$  decreases more than in the case where C is substituted alone. The  $T_c$  reduction in co-doped crystals is a sum of  $T_c$  reductions observed for separate C and Li substitutions. This means that holes introduced with Li cannot counterbalance the effect of electrons coming from C. The possible reason of it can be that holes coming from Li occupy the  $\pi$  band while electrons coming from C fill the  $\sigma$  band. The detailed investigation of the physical properties of these substituted crystals is in progress in different MaNEP groups.

**$\text{Ca}_{2-x}\text{Na}_x\text{CuO}_2\text{Cl}_2$ .** It is a structural analogue to the  $\text{La}_{2-x}\text{Sr}_x\text{CuO}_4$  superconductor. By substituting  $\text{Na}^+$  for  $\text{Ca}^{2+}$  mobile holes are introduced into the  $\text{CuO}_2$  planes. Synthesis of the  $\text{Ca}_{2-x}\text{Na}_x\text{CuO}_2\text{Cl}_2$  compounds is only possible under high pressure of several tens of kbar. High-pressure experiments have been



**Fig. 7.**  $\text{Ca}_{2-x}\text{Na}_x\text{CuO}_2\text{Cl}_2$  crystals grown under high-pressure and the normalized diamagnetic signal for a series of samples with various Na contents.

performed in a cubic anvil and opposed anvil-type high-pressure devices at 35-55 kbar and 1250-1700°C. As a result solidified blocks with crystallites of sizes up to  $1 \times 1 \text{ mm}^2$  have been obtained (Fig. 7). A series of experiments at 45 kbar shows that the Na content depends not only on the pressure of the synthesis, as it was established before [16,17], but also on the reaction temperature and time. The lower part of Fig. 7 shows the normalized diamagnetic signal for a series of  $\text{Ca}_{2-x}\text{Na}_x\text{CuO}_2\text{Cl}_2$  samples with various Na content.  $T_c$  varies systematically with the Na content. Introducing holes by Na substitution is accompanied by an expansion of the unit cell along the c, and a contraction along the a axis. Applying higher synthesis pressure (55 kbar) and temperature (up to 1700°C) results in samples with highest  $T_{c,on} = 28.0 \text{ K}$  at  $x=0.20$ .

## 6. Vanadium-chain compounds

**BaVS<sub>3</sub>.** This material is especially interesting because the metal-insulator transition (MIT) at 69 K is due to a weakly coupled two electronic bands. The effort in the last year was devoted to the synthesis of large, oxygen impurity free crystals for performing NMR and optical conductivity measurements. Polarized infrared data obtained on a mosaic of 10 oriented single crystals allowed to deconvolute the contribution of the two bands [18].

Its sister compound **BaVSe<sub>3</sub>** which shows a paramagnetic metal to ferromagnetic metal transition existed only in a polycrystalline form. Its synthesis in a single crystalline form represents one of the breakthroughs of the last year in this project. Its in-depth investigation is in progress.

## Summary

The high output of the single crystal growing activity in the second year of the second phase of MaNEP strongly enhances the collaborations between various groups of the Pool and helps to establish numerous international collaborations, as well.

## References

- [1] A. Podlesnyak et al., Phys. Rev. Lett. **97**, 247208 (2006)
- [2] A. Podlesnyak et al., to be published in JMMM
- [3] L. Mihaly et al., Phys. Rev. Lett, **97**, 067206 (2006).
- [4] M. Papagno et al., Phys. Rev. B **73**, 115120 (2006)
- [5] O. Zaharko, et al., Phys. Rev. B **73**, 064422 (2006).
- [6] L. Mihaly et al., Phys. Rev. B **74**, 174403 (2006).
- [7] R.Arita et al., cond-mat/ 0611698 v1 (2006)
- [8] C.Pfleiderer et al., Nature **427**, 227 (2004)
- [9] Y.Onose et al., Phys. Rev. B **72**, 224431 (2005)
- [10] F.Carbone, PhD Thesis, University of Geneva (2007)
- [11] NCCR - MaNEP, 5<sup>th</sup> Progress Report, (2006)
- [12] P.Mena, Phys. Rev. B **73**, 85205 (2006)
- [13] F.Carbone, Phys. Rev. B **74**, 024502, (2006)
- [14] M.Kugler et al., J. Phys. Chem. Solids **67**, 353, (2006).
- [15] Bernardini and S. Massidda, Phys. Rev. B **74**, 014513 (2006).
- [16] Z. Hiroi, N. Kobayashi, M. Takano, Nature (London) **371** (1994) 139.
- [17] A. Azuma, et al., J. Low Temp. Phys. **131** (2003) 671.
- [18] I. Kezsmarki, Phys. Rev. Lett. **96**, 186402 (2006).

## Project 4 Novel materials

**Project leader** : J. Hulliger (UNIBE)

**Participating members** : J. Hulliger (UNIBE), J. Karpinski (ETHZ), R. Nesper (ETHZ), A. Schilling (UNIZH), L. Schlapbach (EMPA), J.W. Seo (EPFL)

**Summary** The search for new materials featuring physical properties of interest to MaNEP was continued by a variety of synthetic approaches applied to different classes of materials. N-doped perovskite type titanates and molybdates with diverse composition were prepared in powder form, thin films and single crystals. A semiconductor or metallic behaviour of the conductivity depends on composition (O,N). LaBaNiO<sub>4-δ</sub> and LaSrNiO<sub>4</sub> were investigated for the possibility of superconductivity in nickel based perovskites. Oxygen deficient LaBaNiO<sub>4-δ</sub> transforms into LaBaNiO<sub>4</sub> when treated under high oxygen pressure showing a variable range hopping type electrical conductivity and an insulator state for T=0. Cation substitution in metallic LaSrNiO<sub>4</sub> resulted in a new series of compounds. The combinatorial approach to new superconductors was extended to a random neck synthesis using larger starting grains. In magnetic separation, a sensitivity of 1 ppm was demonstrated for extracting superconducting grains. Application of AC magnetic fields turned out to be the key method for effective separation. New efforts in producing homogeneously doped ZnO by paramagnetic ions and application of the pyrolysis to nitrates has led to low temperature ferromagnetism in Zn<sub>1-x</sub>Mn<sub>x</sub>O. Thin film deposition of Zr doped LaTiO<sub>3</sub> resulted in a metallic or semiconductor material. Extended series of novel pyrochlore and non-pyrochlore materials were obtained by high pressure syntheses or low temperature ionic exchange. Physical measurements revealed a temperature independent paramagnetism, metallic conductivity but no superconductivity so far. Nanostructured tungsten bronze rods were produced by hydrothermal and microwave assisted techniques up to the gram scale. Morphology control over three levels was achieved. A new collaborative project on the possibility of superconductivity in d<sup>1</sup> vanadium oxides is started.

### 1. Synthesis of new bulk materials at ambient and high pressure

**Anionic substitutions in perovskites:** Perovskite type materials have attracted great interest due to their abundance and varieties of their properties and applications. The most common way to tune the material properties is substitution of different elements in the perovskite crystal structure. While most research efforts on oxide compounds have been focused on modifications of the cationic composition, a less explored approach was to investigate modifications of the *anionic* composition. The group of L. Schlapbach and A. Weidenkaff (EMPA) could show in the first stage of their MaNEP project that the substitution of oxygen by nitrogen to form perovskite type *oxynitrides* is changing the properties in a profound way. The new materials exhibit promising electrical and optical properties, which can be tuned by continuous substitution of O by N. The oxynitride perovskites were prepared by 2 different approaches: 1) A 2-step process, which implies the preparation of the corresponding oxide precursors and subsequent thermal or plasma ammonolysis. 2) A direct deposition of oxynitride films by pulsed laser deposition (PLD). Strontium and calcium titanates were chosen as a model

system to investigate the influence of different ammonolysis parameters on the crystal structure, chemical composition and properties.

**Surface plasma ammonolysis of large single crystals:** Perovskite type SrTiO<sub>3</sub> is a non conducting material (band insulator) with a gap of 3.2 eV. Low level doping with electrons (10<sup>18</sup>-10<sup>19</sup> cm<sup>-3</sup>) makes non-conducting SrTiO<sub>3</sub> metallic and even superconducting below 1 K. Surface reduction by different preparation methods has been studied intensively and shows formation of chemical heterogeneities [1-4] in the top most layers which leads to different transport properties depending on methods of preparation. In this work the group at EMPA partially substituted oxygen by nitrogen in a microwave induced quasi neutrally glow discharge plasma of reactive ammonia (NH<sub>3</sub>). SrTiO<sub>3</sub> single crystals with (111) orientation cut were used as starting material since the exposed surface is assumed to be more reactive than the non-polar (100) surface.

The studies on chemical compositions and structure of the products were performed by X-ray diffraction (XRD), in-depth profile X-Ray Photoelectron Spectroscopy (XPS) of core level binding energies and Elastic Recoil Detection Analysis (ERDA) confirms a

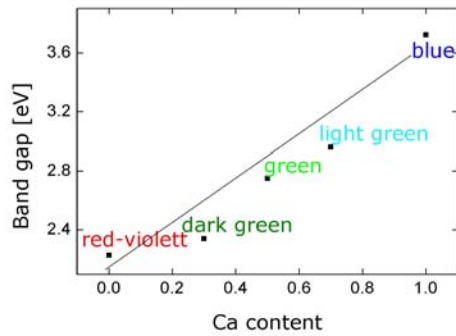


Fig. 1. Variation of the optical band gap of  $La_{1-x}Ca_xTiO_{2+x}N_{1-x}$  with composition.

perovskite type structure with a nitrogen content of up to 8%. The materials show different transport properties, e.g. the so called “giant Seebeck effect” as recently described by Koumoto and co-workers for similar compounds [5].

Oxynitrides with the general formula  $La_{1-x}Ca_xTiO_{2+x}N_{1-x}$  ( $x = 0, 0.3, 0.5, 0.7, 1.0$ ) were synthesized by thermal ammonolysis of oxide precursors produced by a soft chemistry method. The crystallographic structure, optical properties and the thermal stability of the compounds were studied with X-ray and neutron diffraction, UV VIS and Raman spectroscopy as well as thermal analysis. All materials crystallize in a perovskite type pseudo cubic unit cell. The lattice parameters decrease with increasing Ca content, while the optical band gap width increases with increasing  $x$ . The nitrogen content of the material was precisely controlled by the amount of calcium in the lattice. Consequently, they were able to obtain a linear dependence between the optical band gap and the amount of incorporated nitrogen (Fig. 1). Neutron diffraction studies revealed a distorted perovskite structure (Pnma) with a disordered O/N arrangement for all the synthesized materials. Thermal analysis showed that the obtained oxynitrides are stable in air up to  $T = 523$  K.

**Cation and anion substitutions in  $LaSrNiO_4$  and  $LaBaNiO_{4-\delta}$ :**

The essential idea of the project of A. Schilling (UNIZ) is to find a nickel based perovskite with a  $3d^7$  low spin  $S = 1/2$  configuration of  $Ni^{3+}$  that orders antiferromagnetically and is an insulator, in analogy to the “parent compound”  $La_2CuO_4$  of cuprate superconductors which becomes metallic and eventually superconducting upon doping with charge carriers. First, they were focusing on  $LaBaNiO_{4-\delta}$  because this compound has indeed been reported to be a poor electrical conductor, in contrast to metallic  $LaSrNiO_4$ .

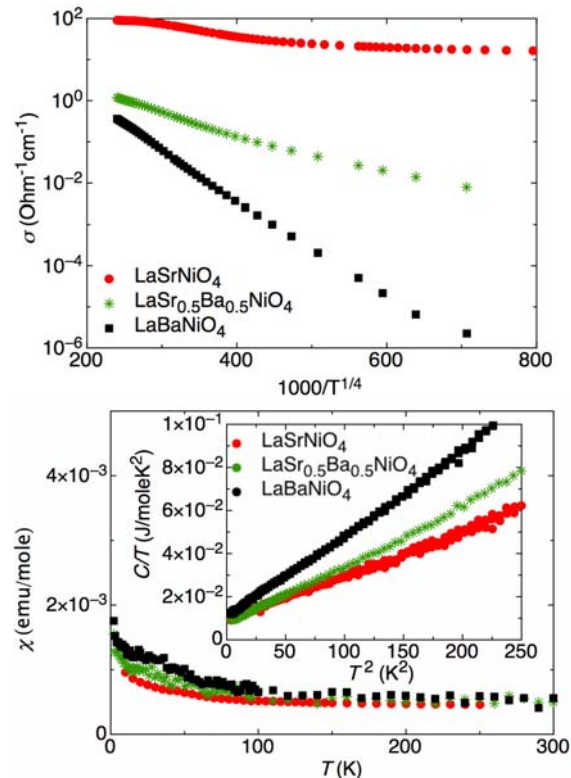


Fig. 2 (a): Electrical conductivity of  $LaSrNiO_4$ ,  $LaSr_{0.5}Ba_{0.5}NiO_4$  and  $LaBaNiO_4$  after high oxygen pressure annealing.  $LaBaNiO_4$  exhibits an almost perfect variable range hopping type conductivity. (b): Magnetic susceptibilities and specific heats of  $LaSrNiO_4$ ,  $LaSr_{0.5}Ba_{0.5}NiO_4$  and  $LaBaNiO_4$ . In all samples the magnetic susceptibility is almost  $T$  independent and the specific heat shows a linear behaviour at low temperatures, as it is expected for ordinary metals.

Last year the group in Zürich had reported that polycrystalline  $LaBaNiO_{4-\delta}$  (as prepared by standard wet chemical procedures) is oxygen deficient with  $\delta \approx 0.15$ . The magnetic susceptibility exhibits a weak temperature dependence with a small Curie constant (corresponding to localized magnetic moments  $\mu \approx 0.1 \mu_B$  per formula unit) and a fairly large constant contribution of  $\chi_0$ . The specific heat shows a large linear term at low temperatures that is comparable to what they had measured in *metallic*  $LaSrNiO_4$ . In contrast to this seemingly metallic like behaviour, the electrical conductivity is very low and is best described by a variable range hopping type (VRH) temperature dependence.

Schilling and co-workers have hypothesized that fully oxygenated  $LaBaNiO_{4-\delta}$  might behave in a very different way as  $\delta = 0$  is achieved. To verify this hypothesis they have prepared single phased  $LaBaNiO_4$  and  $LaSr_{0.5}Ba_{0.5}NiO_4$ , annealed at  $400^\circ C$  at an  $O_2$  pressure of 880 bar (higher annealing temperatures resulted in a partial decomposition of the samples).



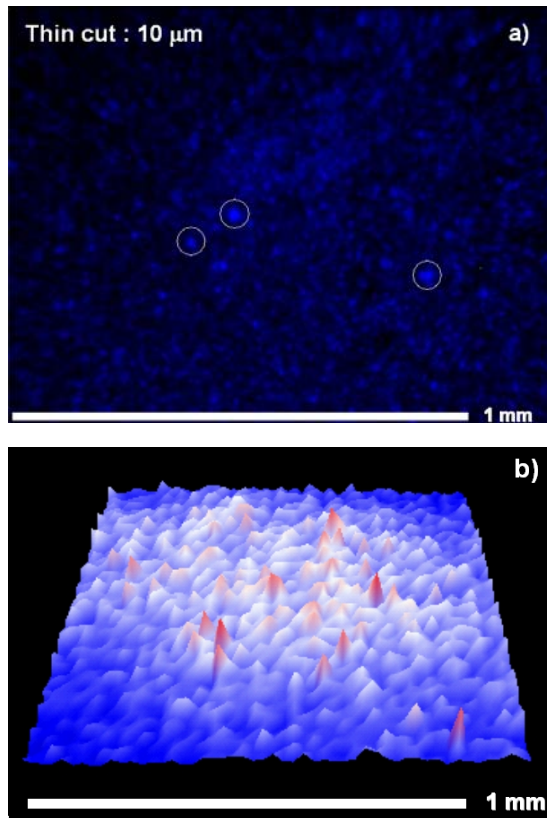
Chemical analysis (K. Pomjakushina, LNS, Villigen) revealed an oxygen content of 4.03(1) confirming the desired oxygen stoichiometry. In Fig. 2 they show the corresponding electrical conductivity, the magnetic susceptibility and the specific heat, in comparison with corresponding data from metallic LaSrNiO<sub>4</sub>. While the magnetic susceptibilities of all stoichiometric samples are now almost temperature independent, the electrical conductivity of LaBaNiO<sub>4</sub> still shows a pronounced variable range hopping type temperature dependence over a wide range of temperatures. Therefore, it is clear that the electrical transport in LaBaNiO<sub>4</sub> is indeed different from LaSrNiO<sub>4</sub>, while other electronic properties are almost identical. A similar situation as in LaBaNiO<sub>4</sub> is also met in a so called Fermi glass [6], where the density of states at the Fermi level is finite but these states are localized. This typically leads to VRH transport properties as they have observed here in LaBaNiO<sub>4</sub>, but to a Pauli like paramagnetism as in a metal. Neutron-diffraction experiments on fully oxygenated LaBaNiO<sub>4</sub> (M. Medarde, LNS, Villigen) did not show any sign of magnetic ordering of the Ni magnetic moments down to  $T = 1.5$  K. From all these facts they conclude that LaBaNiO<sub>4</sub>, although an insulator at  $T = 0$ , does not represent the sought analogue to La<sub>2</sub>CuO<sub>4</sub>. Their doping experiments on LaBaNiO<sub>4</sub> (La by Ca, La by Ba, both hole and electron doping) indeed did not result in metallic transport properties of the substituted samples (note that attempts to substitute La by Sr lead to a substitution of Ba by Sr).

By a different approach to find a nickel based analogue to La<sub>2</sub>CuO<sub>4</sub> Schilling's group used the hypothesis that a modification of the physical properties of LaSrNiO<sub>4</sub> might be achieved by the substitution of La or Sr with elements of smaller ionic radii, i.e. by the application of "chemical pressure". This might distort the crystal structure in a way that a transition to an insulating state can be achieved. This argument is based on the observation that in some perovskite oxides an increasing distortion of the oxygen octahedra around the transition metal atoms is indeed accompanied by such a transition [7]. To achieve this, Schilling's group has made a number of experiments, substituting La in LaSrNiO<sub>4</sub> by rare earth elements and Sr by Ca. Up to now, only the stoichiometric compounds LaSrNiO<sub>4</sub>, NdSrNiO<sub>4</sub>, SmSrNiO<sub>4</sub>, EuSrNiO<sub>4</sub>, and GdSrNiO<sub>4</sub> have been reported to exist (all metallic) [8], while partial substitution has been achieved for Dy<sub>1.5</sub>Sr<sub>0.5</sub>NiO<sub>4</sub> [9], and Nd<sub>1.4</sub>Ca<sub>0.6</sub>NiO<sub>4</sub> [10]. Their conventional

synthesis procedure (1100 °C at ambient pressure in air) always produced multiphase samples, but the preparation under elevated oxygen pressure (1 kbar at 1000 °C, J. Karpinski, ETHZ) resulted in the formation of the new compounds: DySrNiO<sub>4</sub>, HoSrNiO<sub>4</sub>, NdCaNiO<sub>4</sub> and SmCaNiO<sub>4</sub>. Preliminary resistivity measurements on DySrNiO<sub>4</sub> and NdCaNiO<sub>4</sub> indicate a high room temperature resistivity (of the order of 500 mΩcm, as compared to 10 mΩcm measured in LaSrNiO<sub>4</sub>), that increases with decreasing temperature.

Finally, a number of attempts were made to change the electronic structure of LaSrNiO<sub>4</sub> by replacing the apical oxygen in the oxygen octahedra by halogen atoms. This substitution has been reported to be possible in transition metal perovskites with the K<sub>2</sub>NiF<sub>4</sub> structure for the case of Cu (full or partial substitution with F, Cl or Br [11, 12]), Fe (partial substitution with Cl or Br [13]), Co (full substitution with Cl or Br [14]), and Mn (partial substitution with Cl [15]). In analogy to these structures one might expect the existence of compounds such as Sr<sub>2</sub>NiO<sub>3</sub>X or Ca<sub>2</sub>NiO<sub>3</sub>X with X = F, Cl or Br. Among the several possible preparation techniques described in the literature they chose to fluorinate with NH<sub>4</sub>F and to try a direct solid state reaction using NiCl<sub>2</sub>. In none of these experiments compounds with the K<sub>2</sub>NiF<sub>4</sub> structure, containing halogen atoms were formed.

**Random neck syntheses for superconductors:** By preliminary SSC syntheses, particle sizes in the order of micrometers were typically obtained. At that size, experimental characterization of product grains by some physical methods may, however, be difficult. Therefore, the group of J. Hulliger (UNIBE) has performed syntheses using optical materials, for which light responses could be detected also below optical image resolution. For this the luminescence of Eu<sup>3+</sup> and the second harmonic generation response of Ti<sup>4+</sup> and Nb<sup>5+</sup> containing oxides were used. Both types of experiments (Fig. 3) clearly showed hot spot formation in agreement with local product formation and property generation in SSC ceramic samples upon 0.5 to 1 micrometer sized precursor materials [16]. Following up all of what the group at Berne had developed during the 5<sup>th</sup> year, they were now able to give estimates for lower possible concentrations of any kind of a stoichiometry of cuprates (superconducting or not) which may be formed in SSC samples. These statistical calculations based on random densely packed



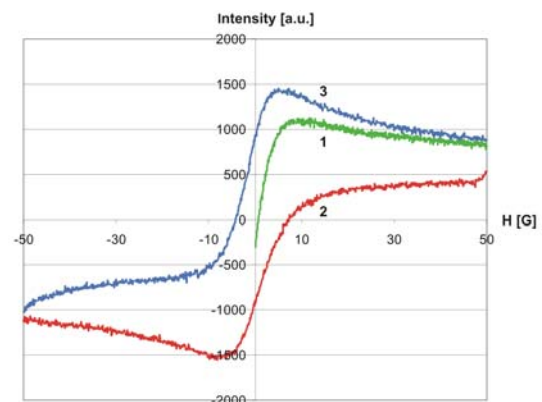
**Fig. 3.** Optical confirmation of local formation of products showing optical responses: **a).** 16 oxides including Eu. UV excitation for a 10 μm cut through a SCC pellet. Circles: hot spots of property formation. **b).** Second harmonic response from 30 oxides containing Nb and Ti oxide. Fundamental wave: 1063 nm. Peaks represent spotwise materials with high second harmonic response.

spheres providing a realistic log volume size distribution revealed that typical stoichiometries can attain a concentration of some 10 to 100 ppm (particles per million). Furthermore, calculations showed that solid solutions are reasonably well represented. Susceptibility measurements made earlier on SSC samples allowed to conclude that the total amount of superconductive matter in the Meissner state at 10 K is about 2 vol. % (collaboration with Dr. K. Kremer, MPI Stuttgart). Summing up a number of possibly found superconductors in SSC samples yields the proper order of magnitude of what can be expected. Although the concentrations attained are large enough to achieve separation (see below), SSC samples using starting grain sizes in the order of micrometers will produce something of the same size. These particles are considered as being too small for realistic separation experiments and phase separation including elemental analysis and structural characterization.

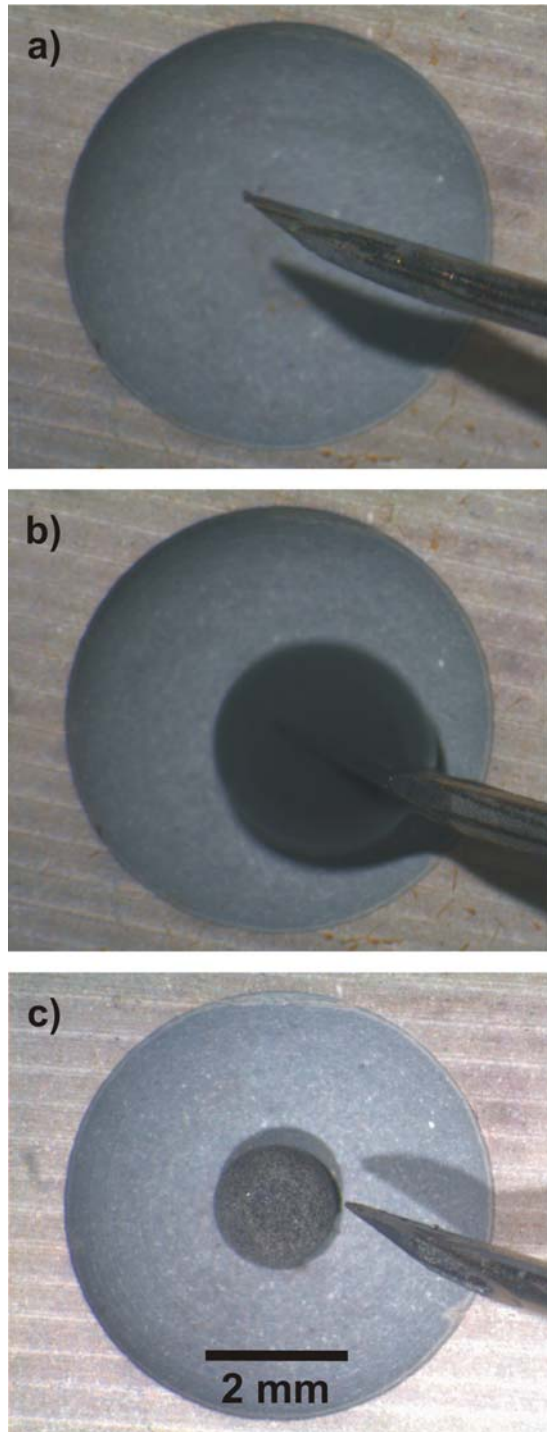
Based on these results and conclusions, the group in Berne decided to modify their concept for exploring superconductors. The basic idea

was maintained, however, the initial particle size was increased and instead of single metal oxides binary mixtures are now being used to obtain ternary and quaternary products upon such kind of an input.

Statistically, high temperature superconductors emerge most frequently from a combination of the following elements: Cu; Ca, Sr, Ba, Y, La, Hg, Tl, Pb, Bi. Consequently, a reasonable upper limit for potentially existing cuprates (made at 1 bar total pressure) of less than 1000 phases was estimated. Given a relatively small phase space, one may increase the particle size of starting materials to take advantage of a better control over locality of reactions and larger product particles. Using starting grains of an average size of 80 - 100 μm (instead of 0.5 to 1 μm as before), there are still more than  $10^6$  binary contact reaction zones per  $\text{cm}^3$  of sample. In view of obtaining products by binary contacts, binary initial oxide particles (ij) are used to induce formation of (ijk) and (ijkl) product particles. This means that every phase diagram of the order  $q = 3, 4$  out of 330 in total constituted by i, j, k and i, j, k, l components will be explored by more than 3000 local attempts per  $\text{cm}^3$ . This new modification of the SSC, the *random neck synthesis* (RNS), was tested by at first producing BaY, BaCu and YCu oxide particles, sieved to an average size of 80 - 100 μm. These (ij) particles were then pressed into pellets to promote reactions in contact zones. Susceptibility measurements revealed a  $T_c$  of 92 K and a volume fraction of 20 % of superconductive matter (mostly YBCO) in the Meissner state. Further confirmation was obtained by low frequency microwave absorption (EPR) showing a hysteresis around zero field (Fig. 4) and its disappearance above about 94 K.



**Fig. 4.** Microwave absorption in low magnetic field showing a hysteresis typical of a type II superconductor formed by the random neck synthesis of  $\text{YBa}_2\text{Cu}_3\text{O}_x$ . 1: Virgin curve after ZFC to 91 K. 2: descending field, 3: rising field.

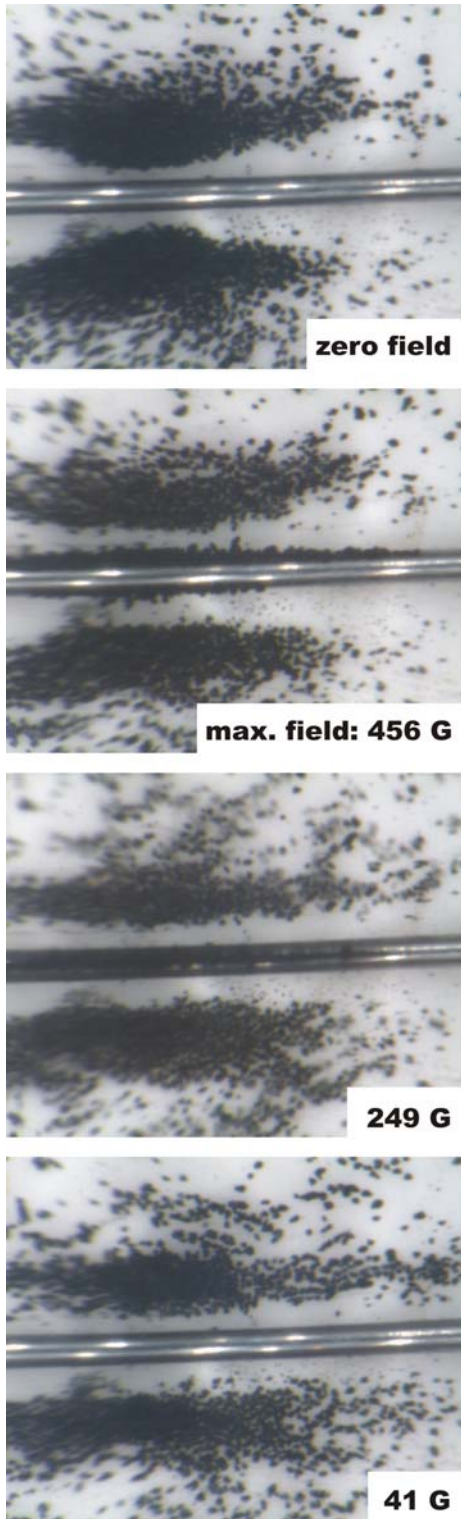


**Fig. 5.** Spherical particle synthesis starting from a suspension of metal oxides in 2-butanone. The particles were synthesized on a  $ZrO_2$  / boron nitride template at 200 °C. **a).** Empty template, **b).** liquid drop with suspension, **c).** final sphere after evaporation of solvent.

Similarly, the RNS was applied to the Bi-family by preparing at first CaBi, CaCu, CaSr, SrBi, SrCu oxide particles of an average size of 80 – 100  $\mu\text{m}$ . Pressed into pellets, these samples were left to react for 3 weeks at temperatures around 850 °C.

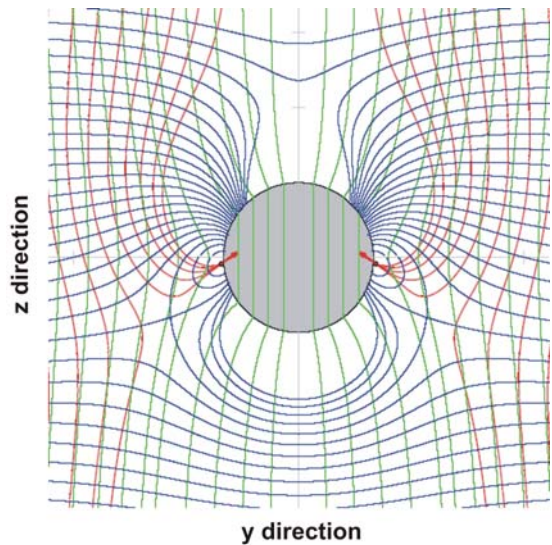
Attempting most localized products representing a volume as large as possible, the group in Berne developed a new procedure to make spherical oxide particles (ij) or made of any other combination i, j, k ... for RNS. For this a slurry of i, j components dropped into a hemispherical  $ZrO_2$  / BN template heated to 200 °C was used (Fig. 5). Predried spheres were then sintered at appropriate temperatures. Sizes in the range of 100 to 1000  $\mu\text{m}$  were easily accessible. Long term reactions using such spherical particles showed formation of necks to be analyzed for their properties. RNS samples made from spheres of a similar size are particularly suited for analytical measurements such as scanning electron microscopy, micro probe analysis (elemental analysis), magneto optical imaging (spatial distribution of superconductive phases; collaboration with Dr. J. Albrecht, MPI Stuttgart) and others. Extension to the TI-family is in preparation.

**Magnetic separation of superconductors:** In magnetic separation, the group of J. Hulliger (UNIBE) has achieved a real breakthrough [17]: Attractive mode separation was demonstrated for polycrystalline YBCO both in DC (Fig. 6) and AC fields. Under AC operation, superconductive grains undergo random oscillatory motions, which help to separate them from normal state matter – see the video on [www.manep.ch/restricted/](http://www.manep.ch/restricted/) (username: manep password: year6). As compared to preliminary attempts, experiments were performed in liquid oxygen cooled down to 77 K. At that temperature no disturbing effect of boiling in the liquid phase was observed during documentation (photographs and films). At low fields of several hundreds of Gauss the magneto-archimedian effect of the paramagnetic medium had non significant influence on magnetic forces of superconductive particles. This is different for fields in the order of  $10^4$  G or more. Under such conditions most diamagnetic matter is attracted by a wire or shows levitation above a ring magnet. Theoretical calculations of the separation behaviour using the Bean model are in qualitative agreement with experimental observations. Trajectories for particles moving in the gravitational and magnetic potential were calculated (Fig. 7). From these theoretical studies we can conclude that a rather large diameter of 500  $\mu\text{m}$  is suited for effectively capturing many particles in the vicinity of a wire, whereas a very small wire of 10  $\mu\text{m}$  would provide the strongest force exerted on particles. However, the capturing radius in this case is as small as the wire diameter. Most of



**Fig. 6.** Attractive mode separation for polycrystalline  $YBa_2Cu_3O_x$  in a DC field after ZFC to 77 K and liquid  $O_2$  for a medium. Magnetic field perpendicular to the image plane. Wire (Fe) diameter: 500  $\mu m$ .

the present experiments were performed using a 500  $\mu m$  wire made of pure iron. Particularly, field change induced movements of particles was found a clear feature for having a superconductor captured by the



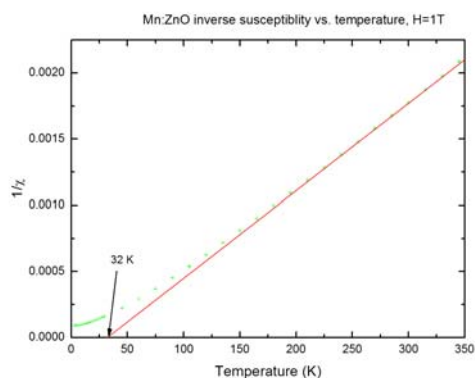
**Fig. 7.** Trajectories of sedimenting particles with  $\chi = -0.1$  (SI system, dimensionless) approaching a wire from both sides in the  $(y, z)$  plan. In red the trajectories of the moving particles (lines representing the gradient of the total potential energy). The red arrows represent the force acting on particles, when arrived at the surface of the wire. In blue is given the potential energy. Green: the resultant magnetic field  $H$ .

ferromagnetic wire: Rising the field from zero to  $H$  Gauss, particles were held sidewise to the wire (position where theory predicts that diamagnetic matter is being attracted). Lowering the field from  $H$  to  $H - \Delta H$ , particles where moving to the zone where  $\chi > 0$  matter is attracted (on top and below the wire). Raising again the field from  $H - \Delta H$  to  $H$  particles moved back to the original side position. Switching off the field caused a repulsion of grains from the wire. All this is a clear sign for a magnetization  $M(H)$  showing a hysteresis typical for a superconductor in the vortex state. Separation was improved for taking out individual grains from SSC or RNS samples. Here, a new set up providing room for two sample chambers (capturing, depositing) was constructed.

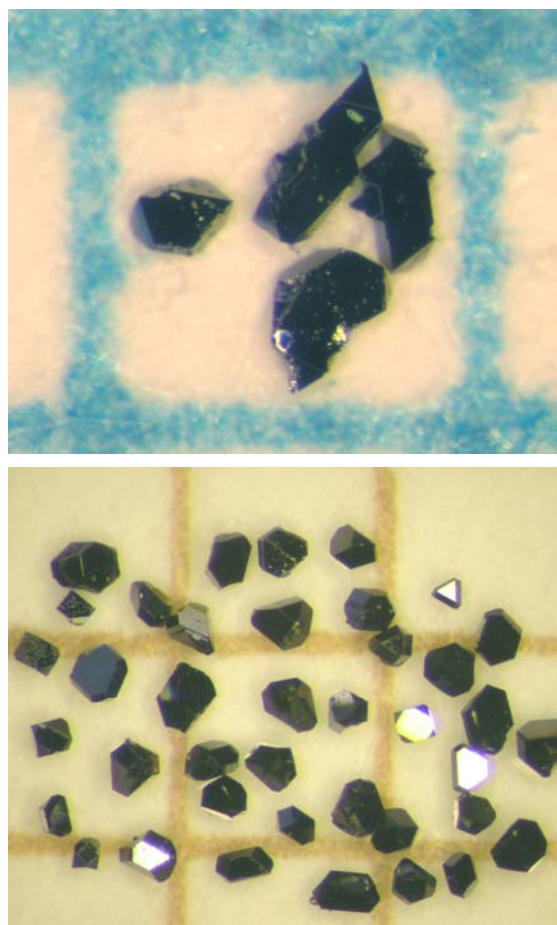
**$d^1$  vanadium oxides: an alternative approach to superconductors ?** The possible occurrence of high  $T_c$  superconductivity in cooper free oxides is an issue arousing shortly after the discovery of cuprates. In particular,  $Sr_2VO_4$  is an insulator with a small Mott gap showing antiferromagnetic ordering below 50 K. Because of the oxidation state IV of vanadium ( $d^1$ ),  $Sr_2VO_4$  can be viewed as a charge conjugate of  $La_2CuO_4$ . Therefore, hole or electron doping is of interest. First attempts to produce phase pure  $Sr_2VO_4$  at in the groups of D. van der Marel (UNIGE) and J. Hulliger

(UNIBE) were started by an approved collaborative project.

**ZnO doped with Mn, Co and Cu:** Here, the group of J.W. Seo (EPFL) investigated the solubility of different transition metal ions in ZnO. However, the difficulty with doped ZnO is that controversial results have been published in the recent years [18-21], showing that properties can vary greatly for samples of the same nominal composition prepared by different methods or different groups. Therefore, at first they had to find a reliable method to produce homogeneously doped ZnO with a well defined doping concentration. Nitrates were used as precursors for the synthesis. Appropriate mixtures of salts were heated above melting temperature followed by quenching samples in liquid nitrogen. Subsequently the solidified matter was annealed at temperatures between 600 to 800°C. Compared to other methods reported so far, this procedure seems to produce a homogeneous distribution of dopants. The solubility for transition metal ions in ZnO was, however, limited by the formation of  $\text{ZnMnO}_3$  or  $\text{ZnCo}_2\text{O}_4$ , respectively. In particular for Co and Mn, the secondary phase was formed because of the oxidation power of nitrates. Consequently, the annealing was performed in reducing atmosphere (Ar and  $\text{H}_2$ ). For Mn and Co doping, they have obtained a solubility limit of about  $x = 0.1$ . For Cu the solubility limit was about  $x = 0.35$ . Exceeding this limit has led to the formation of  $\text{CuO}_2$  precipitates. The  $\text{Zn}_{1-x}\text{Cu}_x\text{O}$  system seems to be the most favorable in order to introduce a significant level of spin carriers. This is in particular of interest when considering the recent theoretical prediction of DMS in Cu-doped ZnO based on first principle calculations [22].



**Fig. 8.** Inverse susceptibility versus temperature measured by SQUID at  $H = 10$  kOe for ZnO with 10% Mn doping. At high temperature a ferromagnetic Curie-Weiss plot is obtained with  $T_c$  of 32 K.



**Fig. 9.** Single crystals of superconducting  $\beta$ -pyrochlore  $\text{RbOs}_2\text{O}_6$ .

For  $x = 0.10$  Mn-doped ZnO sample, the temperature dependence of the inverse susceptibility (Fig. 8) followed a ferromagnetic Curie-Weiss behaviour at high temperature, yielding a  $T_c$  of about 32 K. Electron spin resonance has confirmed the presence of a  $\text{Mn}^{2+}$  state also indicating that the Mn ions are on Zn sites and not forming clusters. The present approach seems to be promising in view of investigating the effect of DMS in ZnO as a possibly *intrinsic* effect.

**Novel pyrochlore materials:** The investigations on the growth of single crystals of superconducting osmates  $\text{AOs}_2\text{O}_6$  ( $A = \text{K}, \text{Rb}$ ) with the  $\beta$ -pyrochlore structure were continued by the group of J. Karpinski (ETHZ). The process of crystal growth of  $\text{RbOs}_2\text{O}_6$  has been optimized by using a temperature gradient. Single crystals of superconducting  $\beta$ -pyrochlore  $\text{RbOs}_2\text{O}_6$  with sizes up to 0.4 mm have been grown (Fig. 9). Single crystal X-ray diffraction studies have shown that both  $\text{KOs}_2\text{O}_6$  and  $\text{RbOs}_2\text{O}_6$  crystallize in the non-centrosymmetric space group  $F-43m$  [23,24]. Electrical resistivity measurements of the

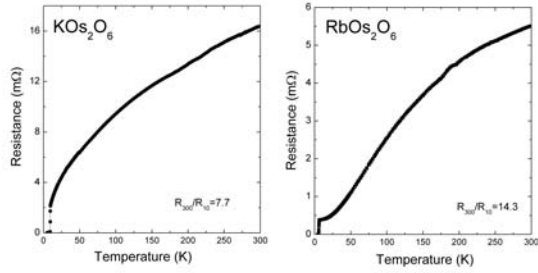


Fig. 10. Temperature dependence of resistance for single crystals of the  $\beta$ -pyrochlore  $\text{KOs}_2\text{O}_6$  and  $\text{RbOs}_2\text{O}_6$ .

$\text{KOs}_2\text{O}_6$  and  $\text{RbOs}_2\text{O}_6$  single crystals have been performed at low temperatures and in high magnetic fields (Figs. 10, 11). The high values of the resistance ratio  $R_{300}/R_{10} = 7.7$  for  $\text{KOs}_2\text{O}_6$  and  $R_{300}/R_{10} = 14.3$  for  $\text{RbOs}_2\text{O}_6$  suggest good quality of the obtained crystals. The temperature dependences of the upper critical field  $H_{c2}$  for  $\text{KOs}_2\text{O}_6$  and  $\text{RbOs}_2\text{O}_6$  were determined from the resistivity data and are shown in Fig. 12.

It has been demonstrated that high pressure synthesis is highly effective in preparation of many pyrochlore type compounds [25]. This motivated us to use high pressure and high temperature techniques in a search for other pyrochlore compounds in related systems. The syntheses were carried out in a cubic anvil device at 30 kbar in the temperature range of 800 - 1100°C using AgO as an oxidizer. The results are summarized in Table 1.

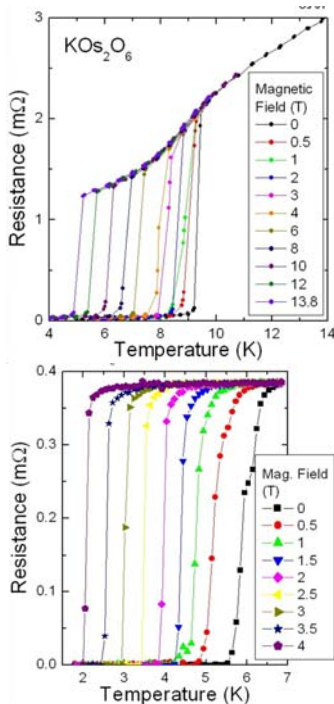


Fig. 11. Temperature dependences of the resistance for single crystals of the  $\beta$ -pyrochlore  $\text{KOs}_2\text{O}_6$  and  $\text{RbOs}_2\text{O}_6$ , measured in applied magnetic fields.

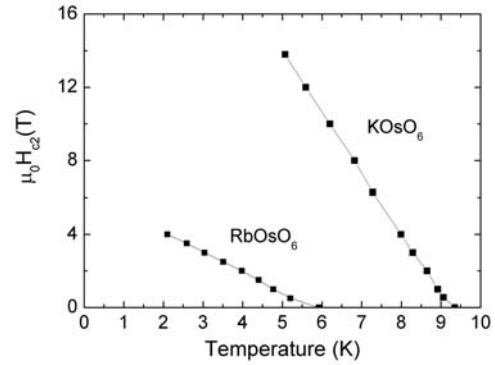
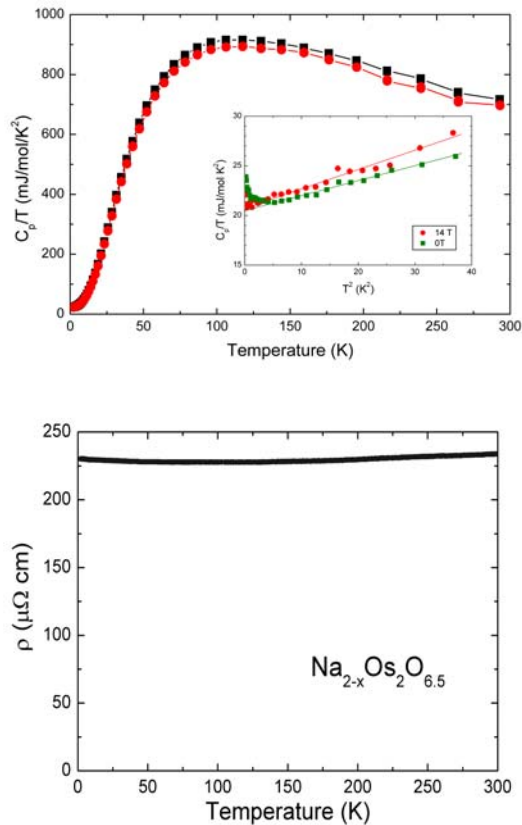


Fig. 12. The upper critical fields vs. temperature for the  $\beta$ -pyrochlore  $\text{KOs}_2\text{O}_6$  and  $\text{RbOs}_2\text{O}_6$ .

The synthesis of sodium osmate under high pressure resulted in octahedral single crystals. From the single crystal X-ray diffraction data we have found that this compound crystallizes in the  $\alpha$ -pyrochlore structure (Fd-3m) and exhibits high Na deficiency which leads to the composition of  $\text{Na}_{1.6}\text{Os}_2\text{O}_{6.6}$ . Heat capacity measurements (Fig. 13a) show slightly enhanced value of the Sommerfeld coefficient  $\gamma = 21 \text{ mJ/mol K}^2$  what is roughly a half of that value observed for superconducting  $\beta$ -pyrochlore  $\text{RbOs}_2\text{O}_6$  [26]. The absolute value of the electrical resistivity is relatively low but in contrast to typical metals, it is almost

Nominal composition	A-ionic radius rVIII (Å)	Lattice parameter (Å)	Obtained compound
$\text{LiOs}_2\text{O}_6$	0.92	no pyrochlore	$\text{LiOsO}_3$
$\text{Cd}_2\text{Os}_2\text{O}_7$	1.10	10.170(1)	$\alpha\text{-Cd}_2\text{Os}_2\text{O}_7$
$\text{Ca}_2\text{Os}_2\text{O}_7$	1.12	10.211(1)	$\alpha\text{-Ca}_{1.5}\text{Os}_2\text{O}_{6.5}$
$(\text{Na}_{1.5}\text{Cd}_{0.5})\text{Os}_2\text{O}_7$	1.16	10.220(1)	$\alpha\text{-Na}_{1.7}\text{Cd}_{0.3}\text{Os}_2\text{O}_{6.5}$
$\text{NaOs}_2\text{O}_6$	1.18	10.170(1)	$\alpha\text{-Na}_{1.6}\text{Os}_2\text{O}_{6.6}$
$\text{Sr}_2\text{Os}_2\text{O}_7$	1.26	no pyrochlore	$\text{Sr}_3\text{Os}_4\text{O}_{14}$
$\text{KOs}_2\text{O}_6$	1.51	no pyrochlore	
$\text{RbOs}_2\text{O}_6$	1.61	10.1137(1)	$\beta\text{-RbOs}_2\text{O}_6$
$\text{Zn}_2\text{Re}_2\text{O}_7$	0.90	no pyrochlore	
$\text{Ca}_2\text{Re}_2\text{O}_7$	1.10	10.285(1)	$\alpha\text{-Ca}_{1.62}\text{Re}_2\text{O}_{6.82}$
$\text{Ca}_2\text{Ru}_2\text{O}_7$	1.12	10.197(1)	$\alpha\text{-Ca}_2\text{Ru}_2\text{O}_7$
$\text{Ca}_{1.7}\text{Na}_{0.3}\text{Ru}_2\text{O}_7$	1.13	no pyrochlore	new compound (cubic)
$\text{Hg}_2\text{Re}_2\text{O}_7$	1.14	no pyrochlore	$\text{HgReO}_4$
$\text{Na}_2\text{Re}_2\text{O}_7$	1.18	no pyrochlore	$\text{NaReO}_4$

Table 1. High pressure syntheses of pyrochlore compounds.



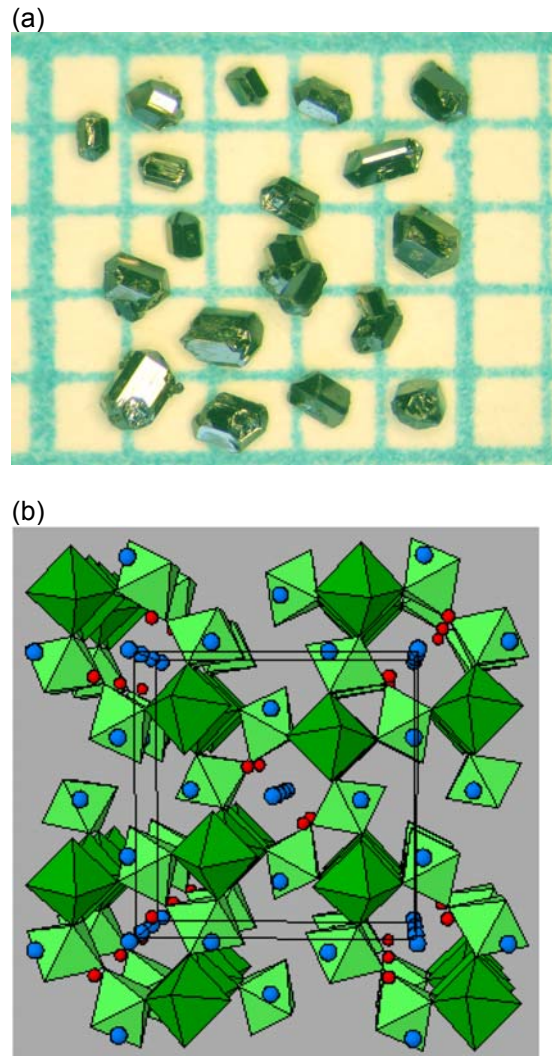
**Fig. 13.** Heat capacity (a) and resistivity (b) vs. temperature for an  $\alpha$ -pyrochlore  $\text{Na}_{1.6}\text{Os}_2\text{O}_{6.6}$  single crystal.

temperature independent (Fig. 13b). The magnetic susceptibility of this compound is also temperature independent suggesting a Pauli paramagnetism. Superconductivity has not been detected down to 0.5 K.

Using high pressure methods they were able to synthesize  $\alpha$ -pyrochlore  $\text{Ca}_{1.66}\text{Os}_2\text{O}_7$  and  $\text{Ca}_{1.62}\text{Re}_2\text{O}_{6.82}$ . Their physical properties have not been reported systematically. These compounds have in common a substantial Ca deficiency. Karpinski's preliminary measurements suggest for both compounds metallic behavior and temperature independent paramagnetism down to 4 K.

They have also prepared  $\alpha$ -pyrochlore  $\text{Cd}_2\text{Os}_2\text{O}_7$  which is reported to show metal to insulator transition at 225 K [27]. Using high pressure synthesis it was possible to prepare solid solutions of  $\text{Cd}_{2-x}\text{Na}_x\text{Os}_2\text{O}_{7-d}$  which may be interesting objects for further studies. They have obtained the  $\alpha$ -pyrochlore ruthenate  $\text{Ca}_2\text{Ru}_2\text{O}_7$  showing properties being similar to that found for  $\text{Ca}_2\text{Ru}_2\text{O}_7$  prepared hydrothermally [28].

Their attempt to prepare strontium osmate under high pressure resulted in a novel compound  $\text{Sr}_3\text{Os}_4\text{O}_{14}$ . A collection of single crystals of this compound is shown in Fig. 14a.



**Fig. 14.** (a) Single crystals of  $\text{Sr}_3\text{Os}_4\text{O}_{14}$  grown under high pressure. (b) Crystal structure of  $\text{Sr}_3\text{Os}_4\text{O}_{14}$  along [001] direction (green octahedra –  $\text{OsO}_6$ , blue spheres – Sr, red spheres – O).

The crystal structure is tetragonal and isostructural to  $\text{Pb}_3\text{Nb}_4\text{O}_{12}\text{F}_2$  [29] (lattice parameters  $a = 12.2909(8)$  and  $c = 7.2478(5)$ ). The analysis of collected data suggests  $\text{P4}_2\text{nm}$  or  $\text{P4}_2/\text{mnm}$  as a possible space group. The crystal structure viewed along [001] direction is shown in Fig. 14b. In general, the structure may be regarded as the pyrochlore type. Here, zigzag chains of  $\text{BO}_6$  octahedra linked to each other in the same manner are directed along face diagonals of the cubic unit cell, forming a symmetrical framework. In the studied structure such chains retained only in one dimension. In a and b directions the chains are "broken" and only fragments of two octahedra remain connecting chains into a three-dimensional framework. The arrangement of such structural fragment creates another type of channels, running in the same direction, namely, along the c axis. The presence of

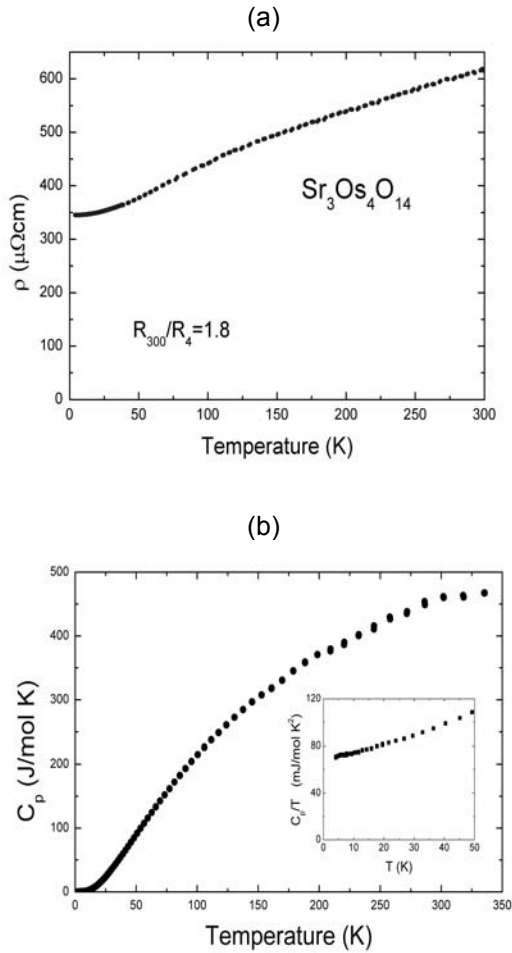


Fig. 15. Temperature dependence of resistance (a) and heat capacity (b) for  $Sr_3Os_4O_{14}$  single crystals.

terminal oxygen atoms from  $Os(2)O_6$  octahedra and the size of the channels allow to suggest that small cations may be intercalated into them. This compound is metallic as evidenced from resistivity measurements (Fig. 15a) and exhibits temperature independent paramagnetism. Superconductivity has not been observed down to 2 K. The heat capacity is shown as well (Fig. 15b).

An attempt to prepare lithium osmate resulted in novel compounds  $LiOsO_3$ . This phase crystallizes in a rhombohedral system and presumably is isostructural with  $LiReO_3$ . Its properties are not known yet. In an attempt to substitute Ca by Na in  $Ca_2Ru_2O_7$  a novel cubic  $Ca_{1-x}Na_xRuO_3$  has been synthesized under high pressure.

The pyrochlore structure contains tunnels surrounded by six  $BO_6$  octahedra. These tunnels intersect in a three dimensional manner. The ionic mobilities of ions in the tunnels are expected to be strongly dependent on the size of both the ion and the tunnel. The sodium or potassium ions in the pyrochlore

Starting composition	Exchanged ions	Final composition	Lattice parameter of the pyrochlore phase (Å)
$\beta-KOs_2O_6$	$K^+ / Na^+$	$\alpha-Na_{2-x}Os_2O_{6+d}$	10.160
$\beta-KOs_2O_6$	$K^+ / Ag^+$	$\alpha-Ag_xOs_2O_{6+d}$	10.152
$\alpha-Na_{1.6}Os_2O_{6.6}$	$Na^+ / K^+$	$\beta-KOs_2O_6$	10.092
$\alpha-Na_{1.6}Os_2O_{6.6}$	$Na^+ / Ag^+$	$\alpha-Ag_xOs_2O_{6+d}$	10.166
$\alpha-Na_{1.6}Os_2O_{6.6}$	$Na^+ / Sr^{2+}$	$\alpha-Sr_xOs_2O_{6+d}$	10.232
$\alpha-Na_{1.6}Os_2O_{6.6}$	$Na^+ / H^+$	$\alpha-NaOs_2O_6$	10.199

Table 2. Results of ionic exchange experiments.

structure are readily exchanged by most other monovalent cations. This low temperature ion exchange allows for the formation of novel, often metastable, compounds that cannot be synthesized by conventional high temperature solid state reactions.

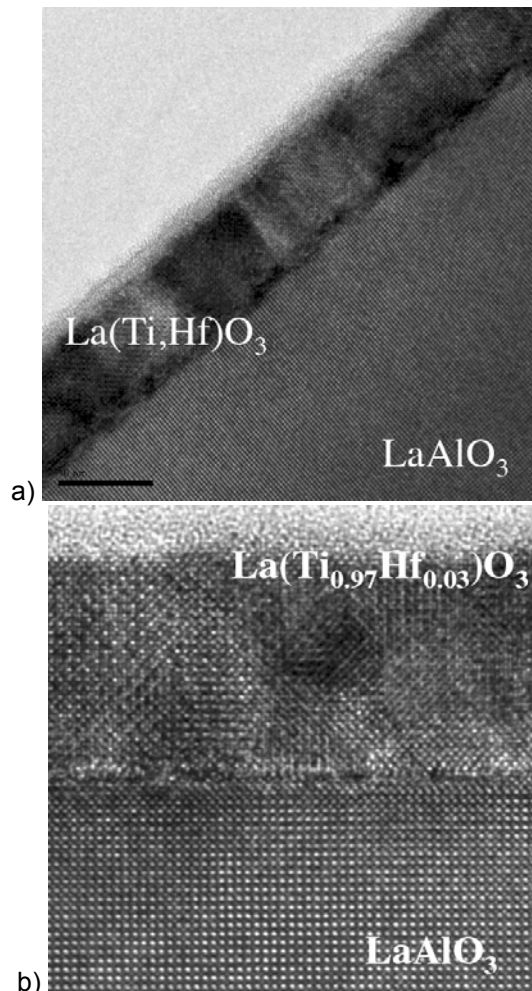
The ionic exchange experiments were carried out in reaction of the pyrochlore powder with an excess of metal nitrates in air at 175 – 300°C (1M  $HNO_3$  at 80°C). The results are summarized in Table 2. It was observed by them that  $Na^+$  ions in  $\alpha$ -pyrochlore  $Na_{1.6}Os_2O_{6.6}$  can be easily exchanged for  $K^+$ ,  $Ag^+$  or  $H^+$ . Similarly,  $K^+$  in  $\beta$ -pyrochlore  $KOs_2O_6$  can be exchanged for  $Na^+$ , and  $Ag^+$ . It is interesting to note that when  $Na^+$  ions are replaced for  $K^+$  in  $Na_{1.6}Os_2O_{6.6}$  the  $\alpha$ -pyrochlore structure transforms into the  $\beta$ -pyrochlore one and the product become superconducting and vice versa, when  $K^+$  ions in superconducting  $\beta$ -pyrochlore  $KOs_2O_6$  are exchanged for  $Na^+$ , not superconducting  $\alpha$ -pyrochlore is formed. The exchange of  $Na^+$  or  $K^+$  ions for  $Ag^+$  results in formation of the  $\alpha$ -pyrochlore  $Ag_xOs_2O_{6+d}$  (non-superconducting). Since the ionic radius of  $Ag^+$  is larger than that of  $Na^+$ , but smaller than that of  $K^+$ , we may conclude that for osmates  $K^+$  is the smallest cation which can occupy 8b sites in the  $\beta$ -pyrochlore structure. All smaller cations occupy 16d sites and the  $\alpha$ -pyrochlore structure is formed.

They have found that  $Na^+$  ions can be also exchanged for divalent Sr cations but this process is very slow and requires long lasting experiments (3 weeks). Their attempts to ion exchange of  $Rb^+$ ,  $Ca^{2+}$ ,  $Pb^{2+}$  for  $Na^+$ ,  $K^+$ ,  $Ag^+$  or  $H^+$  as well as exchange of  $Na^+$  for  $Ba^{2+}$  in the pyrochlore compounds were unsuccessful which means that ion exchange is practically limited to the small monovalent ions.



**2. Materials preparation by thin films methods**

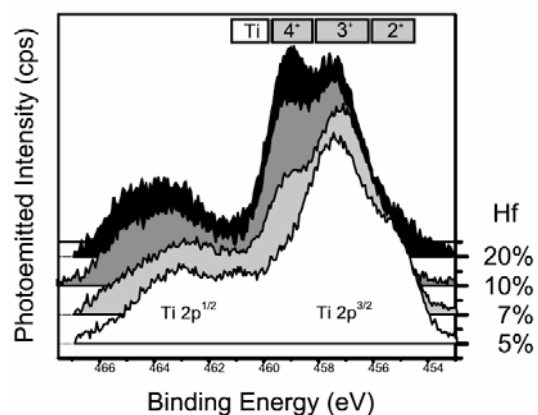
**LaTiO<sub>3</sub> doped with Hf:** LaTiO<sub>3</sub> is an antiferromagnetic insulator (3d<sup>1</sup> state) with a small energy gap of 0.2 eV. The electronic property of this compound is strongly related to the titanium oxidation state, and therefore sensitive to slight deviations in stoichiometry (cation substitutions, oxygen content). The electronic structure evolves from a Mott insulator (Ti<sup>3+</sup>) via a metallic phase up to a band insulator (Ti<sup>4+</sup>) upon oxidizing LaTiO<sub>3</sub> [30]. The dopant Hafnium features a stable Hf<sup>4+</sup> state. LaHfO<sub>3.5</sub> shows pyrochlore structure, Hf occurring in tetrahedral coordination. Thus, doping may on the one hand affect the Ti oxidation state or neutralize oxygen defects and/or stabilize Ti<sup>3+</sup> (even a lower Ti oxidation state may occur). On the other hand, the doping may induce a structural change.



**Fig. 16.** Cross sectional TEM micrograph of LaTiO<sub>3</sub> doped with 3% of Hf grown on LaAlO<sub>3</sub>; a): low; b): high magnification, respectively. The film was crystalline without precipitates but showed a columnar growth. The contrast variation in the high resolution image indicates that domains with slightly different structure exist. The scale bar in the left image corresponds to 10 nm.

The group of J.W. Seo (EPFL) has grown LaTiO<sub>3</sub> thin films up to x = 0.2 Hf doping on single crystalline LaAlO<sub>3</sub> substrates. Crystallinity was monitored by in-situ RHEED giving rise to sharp diffraction patterns. Planarity and low roughness was confirmed by XRD analysis yielding well defined finite size effects up to the 10th order around the diffraction peak. No indications of Hf segregation or Hf rich secondary phases have been observed as also confirmed by TEM (Fig. 16). However, the film showed highly columnar growth. In high resolution (Fig. 16b) it can be seen that domains of the size of 10 - 20 nm exist showing a slightly different phase contrast which might originate from a different structure.

By means of XPS the group of Seo has studied the valence state of Ti (Ti 2p<sup>3/2</sup> peak) as a function of the Hf doping. Upon Hf doping (Fig. 17), the Ti<sup>2+</sup> state appeared which vanished as the doping level was exceeding x = 0.05. At higher Hf contents, Ti converted into Ti<sup>3+</sup> and Ti<sup>4+</sup>. These results suggest that there is a transition at a Hf concentration of about x = 0.05. As confirmed by XPS, Hf remains as Hf<sup>4+</sup> for all concentrations. Therefore, the origin of the transition is not connected to a change of the Hf oxidation state. Seo and co-workers assume a structural transition: At a low doping level, Hf<sup>4+</sup> replaces Ti<sup>3+</sup> within oxygen octahedral. As the doping level increases, Hf in the perovskite unit cell is energetically not anymore favorable and may form a pyrochlore like structure with tetrahedral coordination. Indeed, such structural inhomogeneities have been observed by TEM. Based on the XPS data, they could estimate the oxygen content in the case of x = 0.2 Hf doping to La(Hf<sub>0.2</sub>Ti<sub>0.8</sub>)O<sub>3.3</sub>. Such a composition can

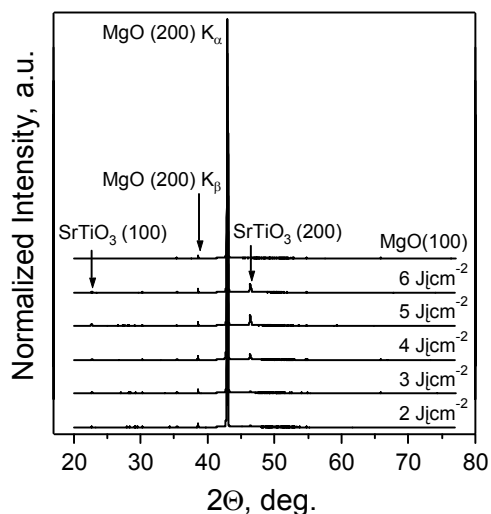


**Fig. 17.** Evolution of the Ti oxidation state in LaTiO<sub>3</sub> for different Hf doping as derived from XPS measurements. Below 5% Hf doping, the Ti oxidation state decreases (Ti<sup>2+</sup> contribution), whereas between 7% and 20% the Ti oxidation state increases (Ti<sup>4+</sup> contribution) corresponding to a more oxidized environment.

theoretically be obtained by assuming that the direct neighboring Ti occupies a tetrahedral site. The excess of oxygen might be explained by a higher oxygen migration in disordered systems as they have recently demonstrated in the case of the  $\text{LaZrO}_{3.5}$  system [31].

For samples of Hf lower than  $x = 0.1$ , the resistivity of  $\text{La}(\text{Hf},\text{Ti})\text{O}_{3+\delta}$  was metallic, whereas higher doping lead to a semiconducting behaviour. This trend is in agreement with the phase diagram of the  $\text{LaTiO}_{3+\delta}$  compound.

**Thin films of  $\text{SrTiO}_3$  by pulsed laser deposition:** Nitrogen doped strontium titanate thin films were deposited by pulsed reactive crossed beam laser ablation (PRCLA, L. Schlapbach, A. Weidenkaff, EMPA). A KrF excimer laser ( $\lambda = 248 \text{ nm}$ ) was used at a repetition rate of 10 Hz. All studied films were deposited on  $\text{MgO}(100)$  substrates. To investigate the influence of different PLD parameters several sample series were prepared. Most of the studied  $\text{SrTiO}_3:\text{N}$  films revealed epitaxial growth along the (100) plane direction even despite the relatively high lattice mismatch with  $\text{MgO}(100)$  substrate of +7.8 %. As an example, Fig. 18 shows the X-ray diffraction patterns of the films deposited at different laser fluence. All of them exhibit only the (h00) peak series of  $\text{SrTiO}_3$  confirming epitaxial film growth. The phase purity of the studied samples was also confirmed by grazing incidence XRD. However, films deposited at the lowest substrate temperature of  $600^\circ\text{C}$ , shortest target to substrate distance of 3.0 cm, as well as films prepared using any source of oxygen (either as the background or for the gas pulse) revealed non-oriented



**Fig. 18.** XRD patterns of the films deposited at different laser fluences. The diffraction results reveal just a (h00) peak series of  $\text{SrTiO}_3$  suggesting epitaxial film growth.

growth. The lattice constant of any  $\text{SrTiO}_3:\text{N}$  films is higher than for bulk strontium titanate due to a positive lattice mismatch with the  $\text{MgO}$  substrates, which is compensated by a tensile strain in the film, and substitution of the smaller oxygen anions with the larger nitrogen. The substrate tensile influence is higher for thinner films, which results in a larger deviation of the lattice parameter from the bulk value at low film thicknesses.

The chemical composition of films was determined in two steps. First, Rutherford backscattering spectroscopy (RBS) measurements were performed to obtain the Sr:Ti:O stoichiometry. The sensitivity of RBS for light elements is relatively poor. However, the RBS analysis revealed stoichiometric transport of cations from the target to the growing film. Therefore, elastic recoil detection analysis (ERDA) was used to determine the N concentration. The difference between the Sr and Ti content in the films is small and lies within the limit of experimental uncertainty. The probability for N species arriving at the heated substrate to incorporate in the film depends mainly on their chemical reactivity and the substrate temperature (although other parameters such as the presence of oxygen species can have an influence). Higher laser fluences resulted in higher ablation rates, kinetic energies, and plasma ionization degree, which provide a higher reactivity of the nitrogen species. This can lead to an increase of the relative N concentration in the films with increasing laser fluence.

The conductivity of selected samples was measured as a function of temperature and revealed a semiconductor like behaviour. The activation energy ( $E_A$ ), calculated using the standard Arrhenius model, increases with temperature and reaches  $\sim 10 \text{ kJmol}^{-1}$  at room temperature. Assuming that the oxygen and nitrogen content do not change with temperature within the studied temperature range, the observed increase of the conductivity is associated with the thermally activated mobility and might be an indication of the small polaron conduction mechanism.

### 3. Preparation and modification of fiber materials

**Alkali Tungstate fibers:** The family of tungsten bronzes ( $\text{M}_x\text{WO}_3$ ) and tungstates ( $\text{M}_x\text{WO}_{3+x/2}$ ) with open structures represents an interesting and versatile target of modern materials chemistry. Their unique chemical, electrochemical and structural properties have attracted considerable research interest. They readily incorporate cations, and the

modification of the host tungstate framework opens up new options for tailoring novel materials [32]. This renders tungstates promising materials for the application as active electrodes. These materials can enhance the performance of electrochromic devices, catalysts or large-scale static displays.

Among the  $M_xWO_3$  /  $M_xWO_{3+x/2}$  frameworks, three main structural types have been described: a cubic form, the pyrochlore type tungstates (P) and the hexagonal tungstate framework (HTB). Both the P and the HTB phases contain tunnels: in the HTB phase, they run along the *c* axis. These tunnel systems are frequently stabilized by alkali and ammonium cations. Whereas HTB and P alkali tungstates have been accessed through soft chemistry routes, little is known about their targeted transformation upon the nanoscale [33]. The specific capacities and  $Li^+$  cycling behavior of Li-HTB tungstates, for example, have proven superior to other tungstates, and the HTB tungstate framework can be employed to remove cations from radioactive waste. Such processes can considerably benefit from the controlled synthesis of HTB tungstate nanoparticles as a major step forward to their industrial application.

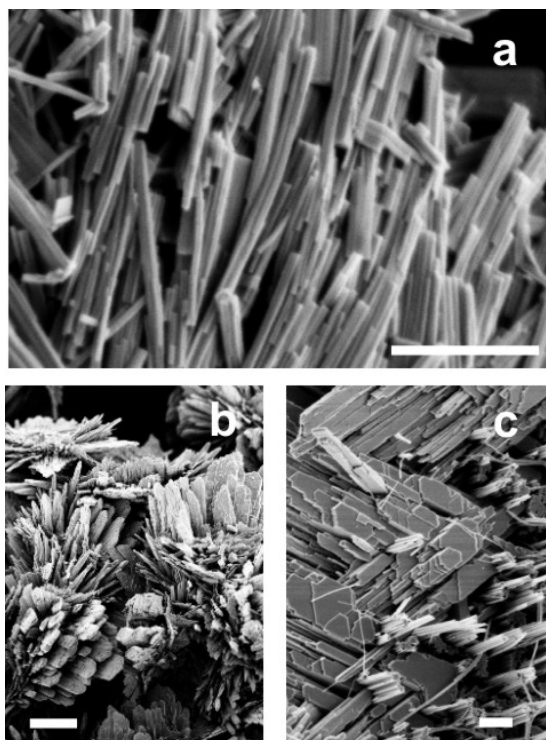
In the course of our previous investigations [34], the group of R. Nesper and G. Patzke (ETHZ) established a preparative pathway to nanoscale ammonium pyrochlore tungstates based on ammonium metatungstate (AMT,  $(NH_4)_6[H_2W_{12}O_{40}] \cdot 2H_2O$ ) [35]. Starting from these results, they have systematically studied the morphochemistry and kinetics of the hydrothermal formation of nanostructured alkali tungstates in MCl/AMT systems ( $M = Li - Cs$ ). A comprehensive morphological study of the alkali tungstates has never been undertaken before. In addition, they have employed microwave hydrothermal techniques to compare the morphological behavior of selected MCl/AMT systems under the influence of microwave irradiation to conventional hydrothermal conditions. In the next step, they have evaluated the kinetics of nanostructured alkali HTB tungstate formation through in situ EXAFS and EDXRD methods. These investigations are part of a comprehensive study on the formation mechanisms of Mo/W-oxide materials. In the following, new preparative pathways are presented that permit the production of alkali HTB tungstates in gram scale amounts. Furthermore, key kinetic data of their hydrothermal formation are presented that are essential to design further technical scale up processes.

**(i) Hydrothermal synthesis of nanoscale alkali HTBs: role of the alkali cations], synthesis and characterization:** The hydrothermal preparation of nanoscale alkali HTB tungstates is quite straightforward: AMT and the according alkali chloride are reacted in 25 vol.% acetic acid in a Teflon-lined stainless steel autoclave. After 2 days of hydrothermal treatment at 180 °C, the quantitative formation of nanostructured products is completed under standard conditions. The microwave-hydrothermal experiments were conducted using a MARS5 microwave digestion system (cooperation with Prof. Dr. S. Komarneni, Pennsylvania State University). For further details on the EXAFS and EDXRD measurements, see Ref. [33] (co-operations with Prof. A. Baiker/PD J.-D. Grunwaldt, ETH Zürich and Prof. W. Bensch, University of Kiel). The Li- and Na-HTB tungstates readily incorporate ammonium cations from the AMT precursor, whereas the K-, Rb- and Cs-HTBs are practically ammonium free. This has been analyzed in terms of IR spectroscopy and LA-ICP-MS analyses (cooperation with Prof. D. Günther, Laboratory of Inorganic Chemistry, ETH Zürich). The alkali cations exert a distinct structure-directing influence on the phase and the morphology of the products. Although the formation of HTB tungstates is domineering throughout, the use of LiCl may lead to the formation of side products with an orthorhombic structure. Similarly, RbCl and CsCl tend to favor the formation of pyrochlore tungstates under hydrothermal conditions. Thus, they have conducted extensive optimization work to establish clear cut preparative approaches to phase pure HTB tungstates that can be directly used for the production of larger quantities.

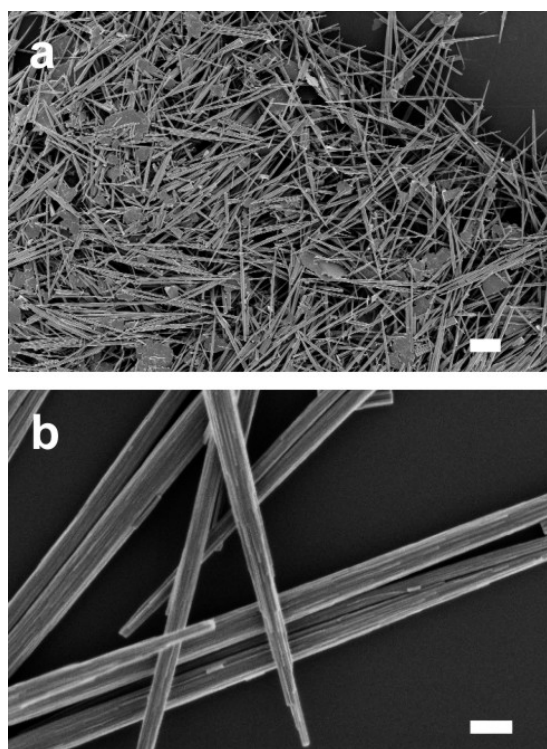
**(ii) Morphology Control:** The aspect ratio of Li-HTB nanorods can be adjusted through the initial concentration of the AMT precursor (Fig. 19). Further dilution of the starting materials induces the growth of flower like microscale orthorhombic lithium tungstate with HTB nanorods emerging from the “flower leaves” (Fig. 19 b – c).

Similarly, the shape of Na-HTB tungstate nanorods can be controlled via dilution techniques. The emerging particles range from small rods with lengths around 100 nm and diameters in the 50 nm range to fibers with microscale lengths and diameters around 100 nm (Fig. 20).

Whereas the morphology of K-HTB tungstate nanorods is similar to the Na-HTB tungstate nanorods, the XRD patterns of the obtained rods reveal their almost amorphous structure.



**Fig. 19.** Representative SEM images of lithium tungstates synthesized (a) under standard conditions (scale bar = 300 nm), (b, c) from highly diluted AMT solutions ( $c(W) = 0.007\text{ M}$ ; scale bar =  $3\ \mu\text{m}$  and 300 nm, respectively).



**Fig. 20.** Representative SEM images of Na-HTB tungstate rods synthesized from highly diluted AMT solutions ( $c(W) = 0.007\text{ M}$  in  $\text{H}_2\text{O}$ ) (a, b; scale bar =  $3\ \mu\text{m}$  and 300 nm, respectively).

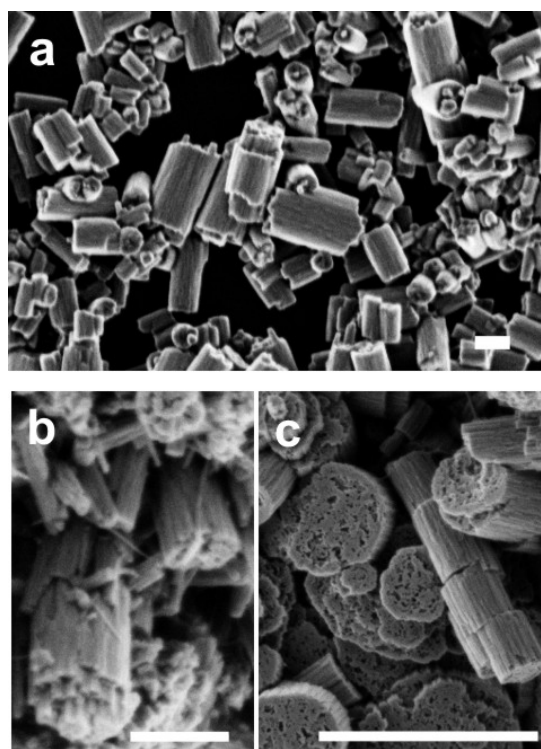
tungstate hydrothermal systems compared to their Na-based analogues.

When the hydrothermal reaction of AMT is performed in the presence of RbCl, a significant morphological change is induced: the resulting Rb-HTB tungstate nanorods are very small (Fig. 21 a – b), and they show a strong tendency towards the self assembly into cylindrical arrangements.

This effect is even more pronounced in the preparation of nanostructured Cs-HTB tungstates: they exhibit a hierarchical structure on three levels, because the above mentioned cylindrical arrangements (Fig. 21 c) tend to form microspheres.

**(iii) Microwave hydrothermal experiments:**

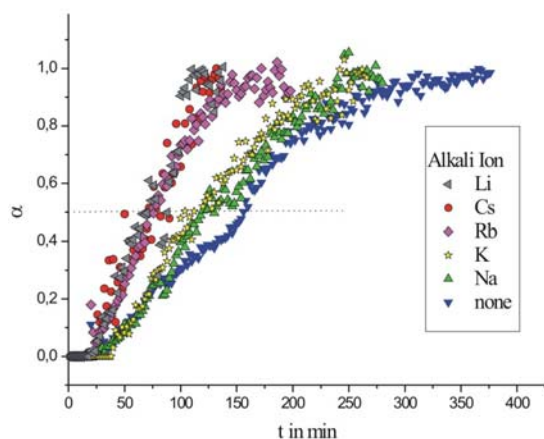
The use of microwave irradiation can dramatically speed up hydrothermal reactions, and the full potential of this combined preparative approach for nanomaterials synthesis still remains to be tapped. The group at ETH has studied the effect of microwave hydrothermal treatment on the formation of Li- and Cs-HTB tungstates. Careful adjustment of the initial Li:W ratio opens up a preparative pathway to orthorhombic tungstates with a flower like morphology and a very low uptake of lithium. The influence of microwave treatment is even more pronounced in the



**Fig. 21.** Representative SEM images of nanostructured Rb-HTB tungstate rods synthesized under standard conditions (a, b; scale bar = 200 nm) and of Cs-HTB tungstates (c; scale bar = 800 nm).

CsCl-AMT hydrothermal system: low Cs:W ratios favor the formation of a microcrystalline cesium tungstate with a hitherto unidentified structural motif. When an excess of CsCl is employed, phase-pure nanostructured Cs-HTB tungstates are formed: This direct preparation method saves a considerable amount of optimization work that is required for suppressing the formation of the concurring pyrochlore tungstate formation under conventional hydrothermal conditions.

**(iv) Time dependent conversion of AMT into nanostructured tungstates:** Whereas the hydrothermal formation of MoO<sub>3</sub> nanorods is completed in less than 10 minutes [36], ex situ experiments pointed to a slow, hour scale conversion process of the MCl/AMT (M = Li – Cs) systems into nanoscale alkali tungstates. This process was studied with in situ EDXRD experiments, and Fig. 22 displays the extent of reaction  $\alpha$  vs. time for the different alkali cations. The presence of Li<sup>+</sup>, Rb<sup>+</sup>, or Cs<sup>+</sup> reduces both the induction time ( $t_{ind} = 9-12$  min.) and the half-life time ( $t_{0.5} = 67-71$  min.) of nanoscale tungstate formation significantly with respect to the reference system in the absence of alkali cations ( $t_{ind} = 14$  min.,  $t_{0.5} = 134$  min.). Kinetic analyses were performed by fitting the experimental data to a theoretical expression relating the extent of reaction  $\alpha$  vs.



**Fig. 22.** Extent of reaction  $\alpha$  versus time for the (101/200) reflections for different alkali ions.

time (Fig. 22). While the induction times and half life times depend on the presence of the alkali cation, no influence onto the reaction mechanism is observed. For all reactions, the experimental data fit with nucleation control. This is in line with the anisotropic dimensionality displayed by all products in the initial phase of the reaction.

## References

- [1] K. Szot et al., *Nature Mater.* **5**, 312 (2006).
- [2] D. W. Reagor et al., *Nature Mater.* **4**, 593 (2005).
- [3] D. S. Kan et al., *Nature Mater.* **4**, 816 (2005).
- [4] K. S. Takahashi et al., *Nature* **441**, 195 (2006).
- [5] H. Ohta et al., *Nature Mater.* **6**, 129 (2007).
- [6] P. W. Anderson, *Com. Solid State Phys.* **2**, 193 (1970).
- [7] J. B. Torrance et al., *Phys. Rev.* **B 45**, 8209 (1992).
- [8] G. Demazeau et al., *J. Solid State Chem.* **18**, 159 (1976). M. James et al., *J. Mater. Chem.* **6**, 57 (1996).
- [9] G. L. Lu et al., *Pao* **54**, 667 (1996).
- [10] Y. Takeda et al., *J. Solid State Chem.* **96**, 72 (1992).
- [11] M. Al-Mamouri et al., *Nature* **369**, 382 (1994).
- [12] B. Grande et al., *Z. Anorgan. Allg. Chem.* **429**, 88 (1977).
- [13] J. A. Ackerman, *J. Solid State Chem.* **92**, 496 (1991).
- [14] C. S. Knee et al., *J. Solid State Chem.* **168**, 1 (2004).
- [15] C. S. Knee et al., *Chem. Commun.* **3**, 256 (2002).
- [16] G. Couderc et al., *Mater. Res. Bull.* (2007), in press.
- [17] L. Dessauges et al., *Supercond. Sci. Technol.* **19**, 748 (2006).
- [18] S. A. Chambers et al., *Mater. Today* **9**, 28 (2006).
- [19] R. Seshadri, *Curr. Op. Sol. St. Mat. Sci.* **9**, 1 (2005).
- [20] C. Liu et al., *J. Mat. Sci: Mat. Elect.* **16**, 555 (2005).
- [21] J. M. D. Coey et al., *Nature Mater.* **4**, 173 (2005).
- [22] L. M. Huang et al., *Phys. Rev.* **B 74**, 75206 (2006).
- [23] G. Schuck et al., *Phys. Rev.* **B 73**, 144506 (2006).
- [24] G. Schuck et al., *Proc. 8<sup>th</sup> International Conference on Materials and Mechanism of Superconductivity and High Temperature Superconductors, M<sup>2</sup>S-HTSC VIII, 2006, Dresden, Germany, p. 251.*
- [25] M. A. Subramanian, *Prog. Solid State Chem.* **15**, 55 (1983).
- [26] M. Brühwiler et al., *Phys. Rev.* **B 73**, 094518 (2006).
- [27] A. W. Sleight et al., *Solid State Commun.* **14**, 357 (1974).
- [28] T. Munenaka et al., *condmat/0608593* (2006).
- [29] Ö. Sävborg et al., *J. Solid State Chem.* **57**, 135 (1985).
- [30] F. Lichtenberg et al., *Z. Phys. B: Condens. Matter* **82**, 211 (1991).
- [31] J. W. Seo et al., *Appl. Phys. Lett.* **83**, 5211 (2003).
- [32] K. P. Reis et al., *Chem. Mater.* **2**, 219 (1990).
- [33] A. Coucou et al., *Solid State Ionics* **28-30**, 1762 (1988).
- [34] A. Michailovski et al., *Chem. Mater.* **19**, 185 (2007).
- [35] A. Michailovski et al., *Mater. Res. Bull.* **39**, 887 (2004).
- [36] A. Michailovski et al., *Angew. Chem. Int. Ed.* **44**, 5643 (2005).



## Project 5 Thin films, artificial materials, and novel devices

**Project leader:** J.-M. Triscone (UNIGE)

**Participating members:** P. Aebi (UNINE), G. Blatter (ETHZ), Ø. Fischer (UNIGE), T. Giamarchi (UNIGE), G. Margaritondo (EPFL), D. Pavuna (EPFL), A. Schilling (UNIZH), J.-M. Triscone (UNIGE), D. van der Marel (UNIGE).

Our year 6 efforts are summarized below. The report is organized in sections describing our efforts in: 1. "Epitaxial ferroelectric films and artificial insulating superlattices for basic studies and future applications"; 2. "Oxide thin films and heterostructures as model systems for spectroscopic, field effect and transport studies"; 3. "Novel single photon detectors using low and high  $T_c$  superconducting nanostructures".

It has to be noticed that Piero Martinoli has retired and that, for a better consistency, all the efforts on field effect tuning of superconductivity will be reported in project 2. Also former part 4, "Giant electroresistive effect in correlated oxide thin films" has not been started, most of the efforts having been put in the realization of artificial ferroelectric systems, a very promising area which is developing rapidly.

### PROJECT SUMMARY

In this project, thin films, heterostructures, and superlattices of correlated oxides are realized and studied. One of the goals is to realize high quality materials in thin film form which are essential for some applications and may be particularly useful for specific studies and novel devices. Another goal is to use advanced deposition techniques to fabricate heterostructures and novel oxide superlattices that will be used to create new materials with designed properties and to address well defined issues.

#### Summary of the results by sub-projects:

**Sub-project 1. (Aebi-Triscone)** Superlattices based on ferroelectric  $\text{PbTiO}_3$  and paraelectric  $\text{SrTiO}_3$  have been realized. In this system, the key ferroelectric properties can be tailored by changing the volume ratio between  $\text{PbTiO}_3$  and  $\text{SrTiO}_3$ . Also, at short wavelengths, an improper ferroelectricity is observed due to a coupling between an antiferrodistortive transition and a polar mode.

On the question of size effect in ferroelectrics, the role of the electrodes was investigated and it has been shown that, depending on the electrode, the system "switches" to a polydomain structure allowing a more efficient screening of the polarization. Also, a key parameter for understanding ferroelectricity in thin films, the effective screening length, has been determined by means of photoemission in  $\text{PbTiO}_3$  epitaxial thin films deposited onto  $\text{Nb-SrTiO}_3$  substrates. The advantage of this approach is that it allows the measurement of the effective screening length in the absence of a top electrode and it probes the screening capacity of the film's surface layer and surface adsorbates.

**Sub-project 2. (Aebi, Margaritondo, Pavuna, Fischer, van der Marel)** A new promising cleaning procedure has been developed for thin films allowing surface sensitive photoemission experiments on air-transferred thin film samples to be performed. Successful application to  $\text{PbTiO}_3$  and  $\text{Bi}_2\text{Te}_3$  has been demonstrated. In manganites, the transport properties have been shown to be strongly

influenced by the strain state of the film (homogeneous or inhomogeneous) and the role of the strain on polaronic transport and the polaronic activation energies has been studied. Electron phonon coupling has been probed in doped  $\text{SrTiO}_3$  and reveals a modest mass-enhancement ( $m^*/m_b = 2$ , where  $m^*$  is the effective mass and  $m_b$  is the unrenormalized band-mass) at the lowest carrier concentration. Upon increasing the charge carrier density the mass-renormalization is found to be essentially independent of the doping concentration. Finally, ARPES experiments have been performed on the 214 high  $T_c$  compound under tensile strain and reveal anomalous features compatible with c-axis dispersion.

**Sub-project 3. (Blatter, Schilling, Fischer)** In the current report period, alternative materials to  $\text{NbN}$  have been investigated, in particular alternative transition metal nitrides and high  $T_c$  compounds with efforts on the production and structuring of very thin films. Also, a full and flexible electro-optical test set-up for SSPDs has been developed. This set-up allows electrical characterization of the devices or films. In the framework of the European project Sinphonia, a two channels SSPD system fabricated in Moscow has been characterized in detail. Finally, we have made substantial progress in our nanostructuring technology and a lift-off process that enables us to generate structures with a minimum feature size down to 10 nm has been developed.

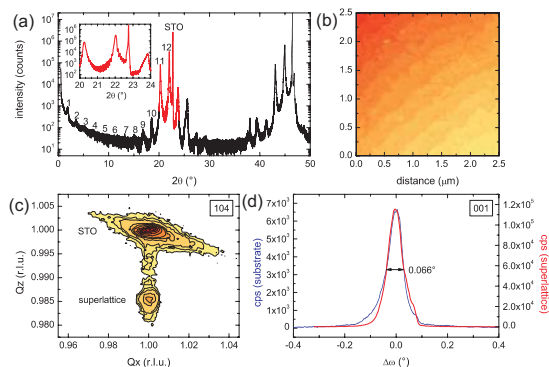
**1. Epitaxial ferroelectric films and artificial insulating superlattices for basic studies and future applications**

In this sub-project, the properties of ultrathin films and superlattices of ferroelectric materials have been studied. The problem of ferroelectricity in very thin films has been addressed using different types of electrodes using x-ray photoelectron diffraction and artificial ferroelectric materials with tailored properties have been realized.

**1.1 Tailoring the properties of artificially layered ferroelectric superlattices.**  
(Triscone)

A key attraction of artificial ferroelectric superlattices is the potential to be able to tailor the properties of the material to a particular application. Experimentally we have developed the ability to produce superlattice structures of the highest quality as shown on Figure 1 where x-ray diffraction and atomic force microscopy analyses are shown for a typical superlattice.

We have demonstrated that the key ferroelectric parameters, polarization and critical temperature, can be tuned over a very large range in PbTiO<sub>3</sub>/SrTiO<sub>3</sub> superlattices. Polarization can be tuned from 0-60 μC/cm<sup>2</sup> and the transition temperature from room temperature to 700°C while maintaining a perfect crystal structure and low leakage currents in these heterostructures. We developed a simple model based on Landau theory that would guide straightforward production of samples with ferroelectric properties designed for particular applications.



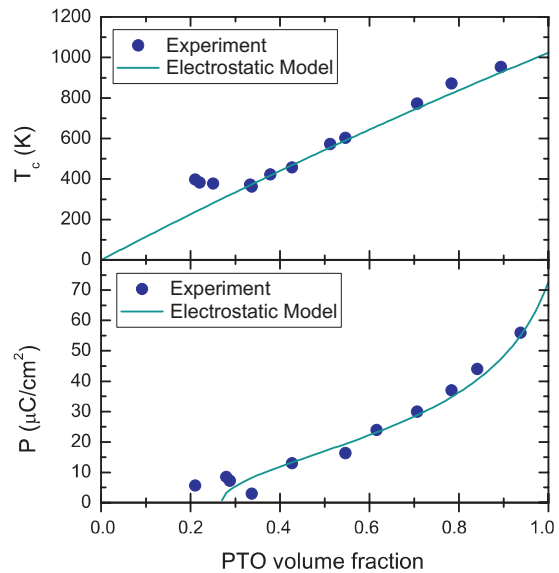
**Fig. 1** (a)  $\theta$ - $2\theta$  x-ray diffractogram for a 20 bilayer PbTiO<sub>3</sub>/SrTiO<sub>3</sub> 9/3 superlattice, (b) AFM topography image of typical superlattice surface showing unit cell steps, (c) x-ray diffraction q-space map for a PbTiO<sub>3</sub>/SrTiO<sub>3</sub> 2/5 superlattice around the 104 reflection showing coherent growth of superlattice, (d) rocking curve of substrate and superlattice.

As electrostatic considerations force the two materials in the superlattice to have near identical polarizations, the PbTiO<sub>3</sub> volume fraction,  $x = \frac{l_p}{l_p + l_s}$ , where  $l_p$  and  $l_s$  are the

thicknesses of the PbTiO<sub>3</sub> and SrTiO<sub>3</sub> layers respectively in the superlattice, is the key parameter in controlling the properties of the system, as demonstrated in Fig. 2 where the dependencies of T<sub>c</sub> and polarization on x are shown.

We also reported [1] on an anomalous recovery of ferroelectricity for x<0.4. We now believe that this recovery is the signature of an improper ferroelectricity (the polarization is not the main order parameter) driven by a special antiferrodistortive transition in the system, most probably at the interfaces. If this is confirmed, this would be a new type of induced ferroelectricity with record high values of polarization. This point is investigated in detail at the moment in collaboration with Ph. Ghosez (Univ. of Liège).

Two other material properties are keys for a number of applications, the dielectric constant and the piezoelectric coefficients which quantify the strain induced in the material for a



**Fig. 2.** Demonstration of the tunability of the transition temperature and remnant polarization in PbTiO<sub>3</sub>/SrTiO<sub>3</sub> superlattices. It can be seen that by varying the PTO volume fraction of the superlattices, the transition temperatures and polarization values can be tuned over a very large range, at the same time maintaining outstanding sample quality for all samples regardless of composition. The departure of the experimental points from the theoretical curves at low volume fractions is the unusual recovery of polarization that we initially discovered from x-ray diffraction studies [1].



given applied electric field. Extremely large values can be engineered in our artificial structures but in practice are limited by the electrode interfaces. Detailed work on measuring the piezoresponse in superlattices using an atomic force microscopy technique and a scanning tunneling microscopy technique is in progress.

**For more details and further reading,** [1] M. Dawber, C. Lichtensteiger, M. Cantoni, M. Veithen, P. Ghosez, K. Johnston, K.M. Rabe, and J.-M. Triscone, *Phys. Rev. Lett.* **95**, 177601 (2005).

## 1.2 Finite size effects in thin ferroelectric $\text{PbTiO}_3$ thin films: a study of ferroelectricity and tetragonality in ultrathin $\text{PbTiO}_3$ films.

(Aebi, Triscone)

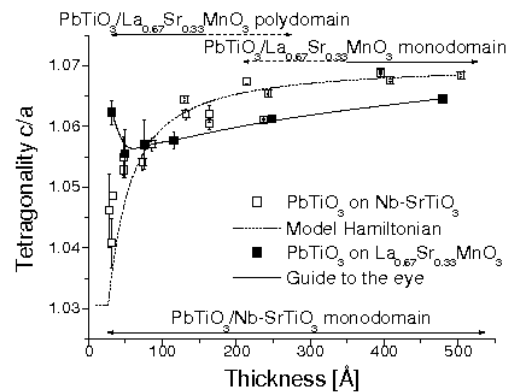
This part contains the results of the active (Neuchâtel - Geneva, Aebi - Triscone) collaboration on the study of thin ferroelectric  $\text{PbTiO}_3$  films.

### 1.2.1 Monodomain to polydomain transition in ferroelectric $\text{PbTiO}_3$ thin films with $\text{La}_{0.67}\text{Sr}_{0.33}\text{MnO}_3$ electrodes films.

Ferroelectricity is typically regarded as a collective phenomenon, and is consequently expected to be strongly influenced by surface and finite-size effects [1]. In particular, it has been shown from first principles that for ultrathin films in the case of perfect screening of the depolarization field perovskite slabs can sustain a polarization perpendicular to the surface at least down to a thickness of 3 unit cells [2]. However, the ferroelectric properties can be drastically modified by an incomplete screening of the depolarization field resulting from a non-zero screening length of the metal electrode [3-6]. The majority of these studies illustrate the predominant role of electrostatic boundary conditions, i.e., of the electrodes, making the knowledge of their screening capacity (expressed by an effective screening length  $\lambda_{\text{eff}}$ ) crucial in order to control/stabilize the ferroelectric polarization in ultrathin films.

In this study, finite size effects in ferroelectric thin films have been probed in a series of epitaxial perovskite c-axis oriented  $\text{PbTiO}_3$  (PTO) films grown on thin  $\text{La}_{0.67}\text{Sr}_{0.33}\text{MnO}_3$  (LSMO) epitaxial electrodes (typically 200-300 Å thick) deposited onto (001) insulating  $\text{SrTiO}_3$  (STO) substrates. The film thickness ranges from 480 down to 28 Å (7 unit cells).

The evolution of the film tetragonality  $c/a$  was studied using high resolution x-ray diffraction measurements, and compared to what was



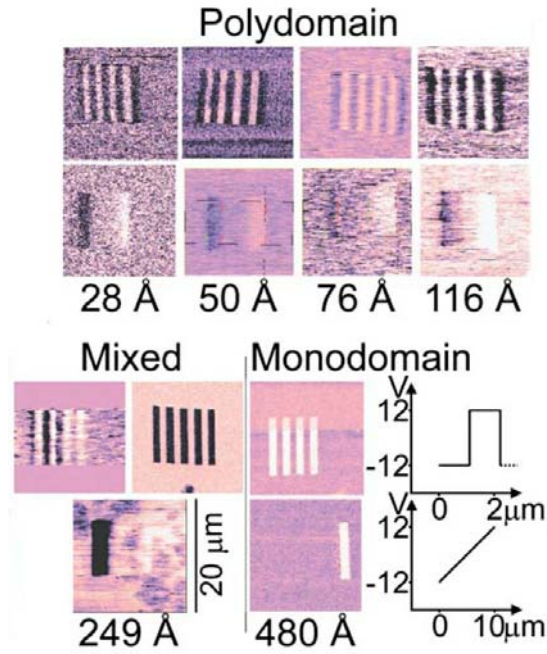
**Fig. 3.** Tetragonality as a function of film thickness for PTO films grown on LSMO (black squares), compared to what was obtained in the case of PTO films grown on Nb-STO (open squares).

obtained for PTO thin films prepared on metallic Nb-doped STO substrates. All the samples being epitaxially strained to the substrates, the main difference between the two PTO series is the change of the bottom electrical boundary conditions. In uniformly polarized (monodomain) thin PTO epitaxial films prepared on Nb-doped STO substrates, it was experimentally shown that the increase of the depolarization field as the film thickness decreases leads to a reduction of the polarization accompanied by a continuous reduction of the film tetragonality  $c/a$ . It is found that the behavior of the tetragonality for the series on LSMO is dramatically different, with an increase of  $c/a$  observed for the thinnest film studied (see Fig.3).

We have shown that this behavior is related to a change in the ferroelectric domain structure, from a monodomain to a polydomain configuration of the polarization with  $180^\circ$  alternating polarization, as directly demonstrated by piezoresponse atomic force microscopy measurements (see Fig. 4).

The results presented here demonstrate the key role of the electrical boundary conditions on ferroelectricity and on the ferroelectric domain structure of very thin PTO films, and reveal in thin films the direct relationship between the tetragonality value and the domain configuration.

**For more details and further reading,** see C. Lichtensteiger, M. Dawber, N. Stucki, J.-M. Triscone, J. Hoffman, J.-B. Yau, C. H. Ahn, L. Despont and P. Aebi, *Appl. Phys. Lett.* **90**, 052907 (2007).

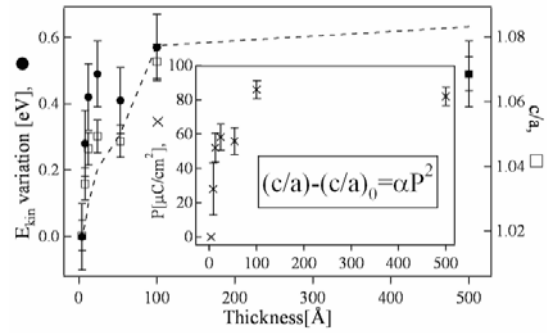


**Fig. 4.** *Top* - Piezoresponse signals obtained after alternate -12V and +12V voltages were applied between the metallic tip and the conducting LSMO layer to polarize nine stripes over a  $10 \times 10 \text{ mm}^2$  area. *Bottom* - Piezoresponse signal obtained after application over a  $10 \times 10 \text{ mm}^2$  square of a voltage gradually ramped from -12V up to +12V. These data also demonstrate ferroelectric switching of the polarization in PTO films as thin as 28 Å.

**1.2.2 Finite size effects in thin ferroelectric  $\text{PbTiO}_3$  thin films: a study of the effective screening length.**

Here, we demonstrate that, using photoemission based x-ray photoelectron spectroscopy (XPS), measuring the potential drop across the ferroelectric film, and x-ray photoelectron diffraction (XPD), probing the tetragonality (and therefore the polarization via polarization-strain coupling), one can extract the effective screening length of ferroelectric thin films with the substrate as a bottom electrode and the exposed-to-air surface as the top electrode. We find that we can experimentally modify the effective surface screening length provided by surface adsorbates, recently highlighted as effective screeners by first principles calculations [7], by a controlled modification of the surface using O-plasma.

In a ferroelectric thin film the polarization can only be stabilized if charges are provided that compensate the ferroelectric polarization. In the case of real electrodes, the compensation charges are not located “exactly” at the location of the ferroelectric polarization



**Fig. 5.**  $\text{Pb } 4f_{7/2}$  emission line position shifts (black circles) measured by XPS and tetragonality  $c/a$  (open squares) obtained by XPD measurements (and re-calibrated to be representative for the bulk of the film) as a function of film thickness. Potential variation (dashed line) calculated separately for each thickness using the electrostatic model. The inset shows the polarization calculated using the measured tetragonality. The  $c/a$  is the ratio of the out-of-plane and in-plane lattice constants of the PTO films.

charges, they are distributed over a finite length scale. One way of mathematically dealing with the problem is the so called air-gap approach in which one considers a sheet of charge separated by a finite distance, the effective screening length  $\lambda_{\text{eff}}$ , from the physical ferroelectric-electrode interface. As a consequence, an effective potential drop appears across the film, resulting in a measurable shift of core level photoemission lines as displayed in Fig. 5 as a function of film thickness. In Fig. 5 are superimposed the  $E_{\text{kin}}$  and the tetragonality ( $c/a$ ) decrease, with  $c/a$  the ratio of the out-of-plane and in-plane lattice constants. The similarity of these two curves suggests a correlation between both results, which can be obtained thanks to the electrostatic model shortly described above, linking the polarization, correlated to the tetragonality via the polarization-strain coupling, to a surface potential drop that affects the photoelectron kinetic energy  $E_{\text{kin}}$ . The polarization in Fig. 5 (inset) is calculated using  $(c/a)-(c/a)_0 = \alpha P^2$ . The  $(c/a)_0 = 1.03$  value corresponds to the paraelectric phase [8] and  $\alpha=0.0574 \text{ m}^4/\text{C}^2$  is the polarization-strain coupling parameter. In order to consider the polarization of the bulk of the films, the  $c/a$  values obtained by the XPD measurements, therefore sensitive to the surface, have been rescaled according to the bulk sensitive XRD values as described in detail in Ref. [9].

Combining both, XPS, which allows the measurement of the potential drop, and XPD, which leads to an estimate of the polarization, it is possible to access the surface  $\lambda_{\text{eff}}$ . In fact, the maximum potential drop at the surface of

the film can be expressed in terms of the surface  $\lambda_{\text{eff}}$  and the polarization  $P$ . Therefore, with a fixed surface  $\lambda_{\text{eff}}$  and  $P$  extracted from  $c/a$  (see above) for every thickness  $d$  (inset of Fig. 5), the potential drop can be computed and compared to the measured variation of  $E_{\text{kin}}$ . The procedure can be repeated for different surface  $\lambda_{\text{eff}}$  in order to optimize agreement as shown in Fig. 5 for a surface  $\lambda_{\text{eff}} = 0.07\text{\AA}$ , comparable to the value reported in Ref. [8].

It is clear that the value obtained for the surface  $\lambda_{\text{eff}}$  heavily depends on the parameters used in the model. However, in comparison to the determination of the screening length from XRD alone [8], this method has an advantage in that one level of modeling is removed from the process. Although it is still necessary to infer the polarization from structural information through the use of the strain-polarization coupling, we now measure directly the potential drop that results from the depolarization field, whereas previously a model Hamiltonian was used to fit the data and from which the screening length could then be estimated.

The position of the photoelectron  $E_{\text{kin}}$  in ferroelectrics is thus directly correlated to the ferroelectric polarization of the film and to the capacity of its electrodes to compensate the ferroelectric polarization charges. An interesting application of this observation would be the possibility to directly measure the polarization by a simple photoemission measurement (XPS) when working with ferroelectric films whose electrodes have well known screening properties.

**For more details and further reading,** see C. Lichtensteiger, J.-M. Triscone, J. Junquera, and P. Ghosez, *Phys. Rev. Lett.* **94**, 047603 (2005), L. Despont, C. Lichtensteiger, C. Koitzsch, F. Clerc, M. G. Garnier, F. J. Garcia de Abajo, E. Bousquet, P. Ghosez, J.-M. Triscone, and P. Aebi, *Phys. Rev.* **B 73**, 094110 (2006).

#### References:

- [1] M. E. Lines and A. M. Glass, *Principles and applications of ferroelectrics and related materials* (Oxford University Press, Oxford, (1977).
- [2] P. Ghosez and K. M. Rabe, *Appl. Phys. Lett.* **76**, 2767 (2000).
- [3] I. P. Batra and B. D. Silverman. *Solid. Stat. Comm.*, **11** 291 (1972).
- [4] I. P. Batra, P. Wurfel, and B. D. Silverman, *J. Vac. Sci. Technol.* **10**, 687 (1973).
- [5] R. R. Mehta, B. D. Silverman, and J. T. Jacobs., *J. Appl. Phys.*, **44** 3379 (1973).
- [6] M. Dawber, P. Chandra, P.B. Littlewood and J.F. Scott, *J. Phys.: Condens. Matt.* **15** L393 (2003).
- [7] D.D. Fong et al., *Phys. Rev. Lett.* **96** 127601 (2006).
- [8] C. Lichtensteiger, J.-M. Triscone, J. Junquera, and P. Ghosez, *Phys. Rev. Lett.* **94**, 047603 (2005).

[9] L. Despont, C. Lichtensteiger, C. Koitzsch, F. Clerc, M. G. Garnier, F. J. Garcia de Abajo, E. Bousquet, P. Ghosez, J.-M. Triscone, and P. Aebi, *Phys. Rev. B* **73**, 094110 (2006).

## 2. Oxide thin films and heterostructures as model systems for spectroscopic, field effect and transport studies

In this sub-project, correlated oxide films are used to address open questions on the nature of the transport in complex oxides such as doped SrTiO<sub>3</sub> and manganites and thin films will be realized specifically for scanning tunneling, angular resolved photoemission and optical spectroscopy experiments. The part describing the efforts on trying to better understand the nature of high  $T_c$  superconductivity and on the electronic writing of superconducting nanostructures in doped-SrTiO<sub>3</sub> will appear in project 2 for consistency.

### 2.1 Thin films for STS / ARPES studies and surface cleaning procedures. (Aebi, Fischer)

We have continued to elaborate surface cleaning procedures in order to perform surface sensitive photoemission experiments on air-transferred thin film samples. On ferroelectric PbTiO<sub>3</sub> (PTO) thin films, this has allowed us to modify the effective surface screening length using a soft oxygen plasma cleaning procedure together with a sample annealing. In this process, the sample temperature is first increased up to  $\sim 500^\circ\text{C}$  in vacuum during several hours. No modification of the PTO compound stoichiometry could be observed after this annealing. Following this, an O plasma (0.05 mbar of O<sub>2</sub>) is produced near the surface for few minutes. After the plasma treatment, the sample is kept at high temperatures for a few minutes.

The effect of this procedure, applied to the different films, is clearly seen on the XPS spectra as a shift of the Ti and Pb emission lines (indicating the modified effective screening, see above). The C emission and the O emission lines of the surface contamination layer are drastically reduced and a low energy electron diffraction pattern can be obtained, indicating a good surface cleaning but also long range order.

Finally, a combined O plasma and heating procedure was successful in obtaining a low electron diffraction pattern on air-cleaved Bi2212 single crystal.

## 2.2 Thin films of manganites

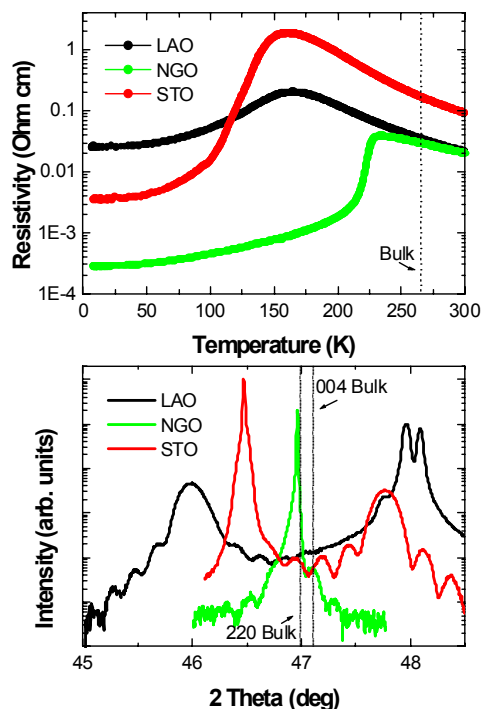
The growth of colossal magnetoresistive manganites in the form of thin films is not only fundamental for the fabrication of devices but also provides a versatile path to control physical properties by means of substrate-induced biaxial strain [1]. Therefore, the choice of an appropriate substrate becomes crucial. Suitable candidates include SrTiO<sub>3</sub> (STO), LaAlO<sub>3</sub> (LAO), and (110)-oriented NdGaO<sub>3</sub>. When compared to the paradigmatic manganite La<sub>0.67</sub>Ca<sub>0.33</sub>MnO<sub>3</sub> (LCMO), LAO and STO exhibit the largest mismatch (~2% and ~1% respectively) and are expected to produce an important variation of properties. NGO presents a much smaller mismatch (~0.03%) and seems almost ideal to grow films with bulk-like properties. NGO is however strongly paramagnetic, and the effect on the film of substrate magnetization in a magnetic field may not be negligible.

We have grown LCMO films by off-axis RF sputtering at a substrate temperature of 675°C and a pressure of 0.2 Torr of O<sub>2</sub>+Ar. The films were slowly cooled down to room temperature

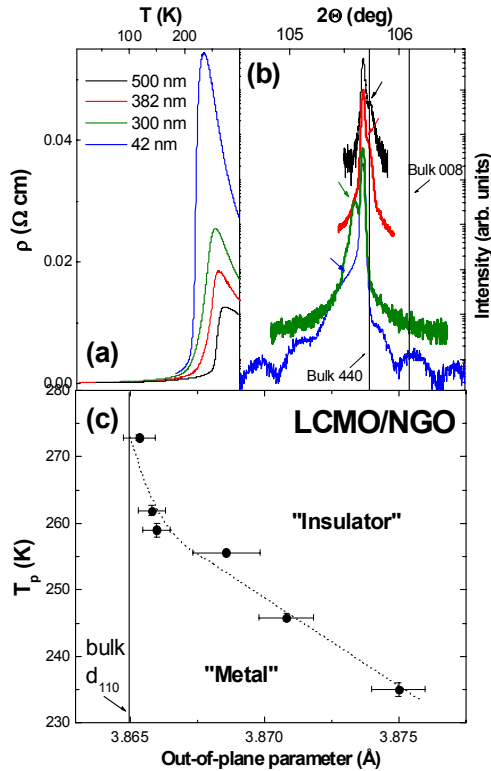
in the gas flow. The properties of the films were characterized by x-ray diffraction, resistivity and magnetization measurements.

In Fig 6 we show transport and structural properties for 50nm-thick films grown on LAO, STO and NGO. The metal-insulator transition temperature,  $T_p$ , is lower than in bulk LCMO, and decreases on increasing mismatch with the substrate. This is due to an increased tetragonality of the structure, which favors the formation of polarons, electrons coupled to their surrounding lattice distortion that are responsible for transport at  $T > T_p$ . The resistivity of the film grown on LAO is anomalously high at low temperatures due to the presence of grain boundaries induced by the transition of LAO from cubic to rhombohedral at 544°C, which is accompanied by substantial twinning. The out-of-plane lattice parameter is larger than in bulk LCMO for films grown on LAO and NGO, a signature of compressive in-plane strain, while for the film grown on STO, strain is tensile and the out-of-plane parameter is smaller than in the bulk. On increasing thickness, for films grown on STO and LAO, multiple diffraction peaks appear corresponding to different out-of-plane parameters, signature of an inhomogeneous strain relaxation. This observation is crucial, since the question of whether an intrinsic electronic phase separation plays a major role in determining the transport properties of manganites has been matter of extensive debate [2]. Since charge, lattice and spin are intimately coupled in these materials, substrate-mismatch-induced (and therefore extrinsic) structural inhomogeneities can give rise to inhomogeneous electronic properties. Evidence for both homogeneous and inhomogeneous local electronic properties measured by STM has been reported [3-4].

In the case of NGO, lattice parameters are very close to those of LCMO. This complicates the determination of the film structural properties by x-ray diffraction and has lead to the hypothesis that strain plays no role in the properties of LCMO films grown on NGO as a function of thickness [5]. Our samples clearly show (see Fig. 7a) an increase in  $T_p$  and an overall decrease of resistivity on increasing thickness, as reported in [5], but high resolution x-ray measurements of high order reflections using monochromatic radiation, like those shown in Fig. 7(b), have allowed us to determine the out-of-plane lattice parameter as a function of film thickness. On increasing thickness, the out-of-plane lattice parameter decreases towards the distance between (110)



**Fig. 6. Top:** Resistivity of 50-nm LCMO grown on different substrates. The bulk metal-insulator transition temperature is indicated by a dotted line. **Bottom:** Second order reflection for the out-of-plane parameter of the films. Bulk reflections are shown by dotted lines. Data on the LAO-deposited film were taken without a monochromator and  $K_{\beta}$ ,  $K_{\alpha 1}$  and  $K_{\alpha 2}$  peaks can be observed. Data on the NGO-deposited film were taken with very high resolution to resolve film thickness fringes, as a consequence intensity is decreased.



**Fig. 7.** (a) Resistivity as a function of temperature for LCMO/NGO films of different thicknesses. (b) Fourth-order diffraction peak of the out-of-plane parameter. High resolution measurements allowed us to distinguish the contributions of film and substrate. (c) Behavior of  $T_p$  as a function of the out-of-plane order parameter.

planes in the bulk,  $d_{110}$ , indicating that the film grows along the (110) direction. This also points out an increase of the in-plane lattice parameters with thickness. Off-axis measurements are underway to confirm that this increase is due to the relaxation of compressive strain in the plane. In Fig. 7(c) we show that transport properties are intimately connected to this structural relaxation, and that the effect of an apparently negligible substrate mismatch is on the contrary quite significant. This is also confirmed by extracting the activation energy from the fit of high-temperature resistivity data with a small-polaron model in the adiabatic limit [6] ( $\rho = \rho_o \exp(-E_p/kT)$ ) where one finds that the polaron activation energy increases on increasing strain (with activation energy values smaller than that of fully-strained homogeneous films grown on STO [3]).

**References**

[1] A-M. Haghiri-Gosnet and J-P Renard, J. Phys. D: Appl. Phys. **36** (2003) R127.  
 [2] E. Dagotto, "Nanoscale phase separation and colossal magnetoresistance", Springer series in solid-state sciences **136** (2003).

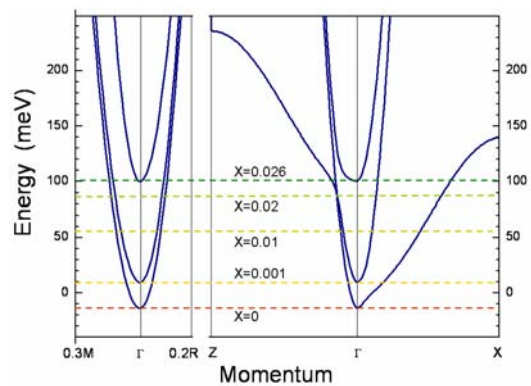
[3] S. Seiro, Y. Fasano, I. Maggio-Aprile, O. Kuffer and Ø. Fischer, J. Magn. Magn. Mater, in press. S. Seiro, Y. Fasano, I. Maggio-Aprile, E. Koller, O. Kuffer, and Ø. Fischer, submitted to PRL.  
 [4] M. Fäth, S. Freisem, A. A. Menovsky, Y. Tomioka, J. Aarts, J. A. Mydosh. Science **285** (1999) 1540.  
 [5] M. Bibes et al, Phys. Rev. B **66** (2002) 134416.  
 [6] D. Emin and T. Holstein, Annals of Physics **53** (1969) 439.

**2.3 THz and Infrared properties of free standing  $\text{SrTi}_{1-x}\text{Nb}_x\text{O}_3$  thin films.**

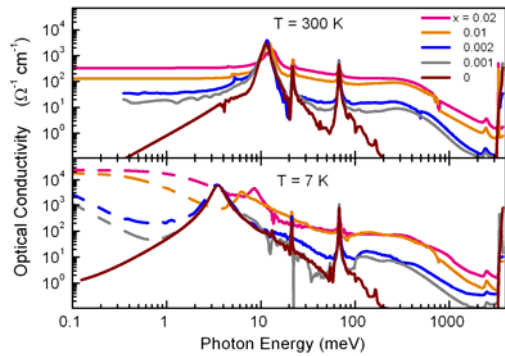
(van der Marel, Triscone)

One of the major questions in the physics of high temperature superconductors and colossal magnetoresistance materials is to what extent electron-phonon coupling is important for the transport anomalies and for superconductivity. An important obstacle in addressing this issue is the complexity of these materials, which are doped Mott-insulators, anti-ferromagnetic, striped, among other possibilities.

In order to separate out the electron-phonon coupling we have studied "free standing" thin films of the doped perovskite  $\text{SrTi}_{1-x}\text{Nb}_x\text{O}_3$  with  $0.0002 < x < 0.02$ . An optical characterization of the electron phonon coupling in STO is interesting in its own right, as it may be a model system for polaron formation. The lowest unoccupied bands of pristine  $\text{SrTiO}_3$  are Ti 3d bands of  $t_{2g}$  character (see Figure 8), which become occupied with electrons upon substituting Nb for Ti. We use THz, infrared, and optical spectroscopy, as well as DC and Hall effect measurements. The main spectral features of the optical conductivity shown in Fig. 9 are, from left to right: The free carrier contribution (leftmost peak in the 7 K spectra, constant for 300 K), optical phonons (three prominent peaks between 0.001 and 0.1 eV), a mid-infrared band (broad shoulder between 0.1 and 1 eV), the  $t_{2g}$ - $e_g$  interband transitions (peak



**Fig. 8.** Detail of the bandstructure of  $\text{SrTi}_{1-x}\text{Nb}_x\text{O}_3$  with Fermi energy indicated for  $x=0, 0.001, 0.01, 0.02$  and  $0.026$ .

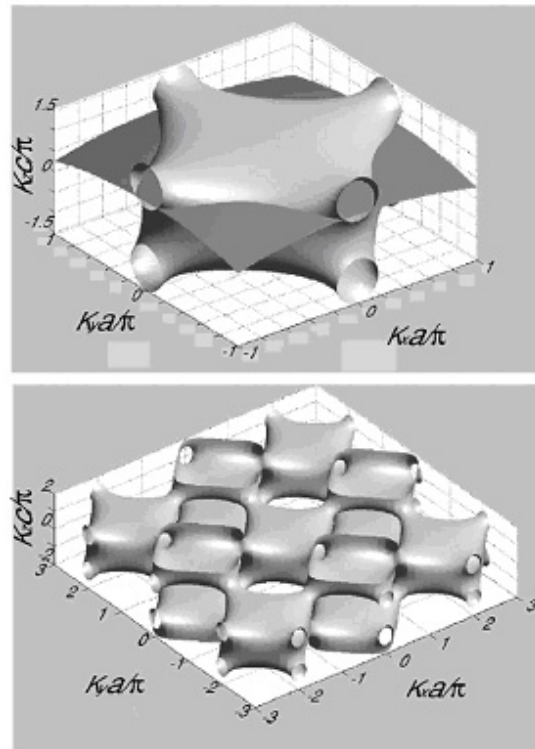


**Fig. 9.** The optical conductivity of  $\text{SrTi}_{1-x}\text{Nb}_x\text{O}_3$  for  $x=0, 0.001, 0.002, 0.01$  and  $0.02$  measured at  $300\text{ K}$  and at  $7\text{ K}$  using 4 different types of spectrometers to cover all spectral ranges shown.

at  $2.7\text{ eV}$ ), and the fundamental  $3\text{ eV}$  charge-transfer gap from oxygen to titanium. The infrared spectra at  $7\text{ K}$  show a very narrow (less than  $2\text{ meV}$  wide) Drude peak, the spectral weight of which reveals a modest mass-enhancement ( $m^*/m_b = 2$ , where  $m^*$  is the effective mass and  $m_b$  is the unrenormalized band-mass) at the lowest carrier concentration. The mass enhancement, the doping dependence thereof, and several other features in the infrared spectra, are clear manifestations of electron-phonon coupling. Upon increasing the charge carrier density the modest mass-renormalization is essentially independent of the doping concentration.

**2.4 ARPES on 214 films.**  
(Margaritondo, Pavuna)

Following years of systematic studies of direct ARPES (no cleavage of samples) on in-situ grown compressively strained high- $T_c$  LSCO-214 films (with enhanced  $T_c$ ), we have now succeeded to demonstrate the role of the tensile strain. The electronic band structure probed by angle-resolved photoemission spectroscopy on thin epitaxial LSCO-214 films under extreme tensile strain shows anomalous features compatible with  $c$ -axis dispersion. This result is in striking contrast with the usual quasi-two-dimensional 2D dispersion observed up to now in most superconducting cuprates, including relaxed and compressively strained LSCO-214 films grown under the same conditions [1]. The data were analyzed using a 3D tight-binding dispersion for a body-centered tetragonal lattice. We relate the enhancement of the  $c$ -axis dispersion to the significant displacement of the apical oxygen induced by epitaxial strain. Ensemble of our data accumulated in the past 10 years tend to suggest that mean-field models developed on two-dimensional *rigid lattices* (like rigid 2D vHs



**Fig. 10.** Fermi surface of tensile strained LSCO-214 films.

or  $t$ - $J$  models) seem inadequate as the data show that cuprates have ‘Napoleon-cake’-like structure in which rigid  $\text{CuO}_2$  planes alternate with softer charge ‘reservoirs’. The latter distorts much more (Fig. 10) than the former and the (local) strain has a major effect on  $T_c$  as independently established also by groups at NTT, IBM and BNL. Those and several other groups are trying to adopt our original approach on direct ARPES on uncleaved in-situ grown correlated electron materials’ films.

**Reference:**  
[1] D. Cloetta, D. Ariosa, C. Cancellieri, M. Abrecht, S. Mitrovic and D. Pavuna, Phys. Rev. B **74**, 014519 (2006).

**2.5 Modulation of the superfluid density in ultrathin high  $T_c$  oxide films.**  
(Martinoli, Triscone)  
and **Local ferroelectric field effect in Nb-doped  $\text{SrTiO}_3$  superconducting films.**  
(financed by Division II)

These two activities are now appearing, as mentioned above, in project 2.

### 3. Novel single photon detectors using low and high $T_c$ superconducting nanostructures

(Blatter, Fischer, Schilling)

In this sub-project, two groups in Geneva and Zurich (Fischer-Schilling) are exploring the use of superconducting meander structures for ultra-fast, ultra-sensitive photon detection. This new type of superconducting single photon detector (SSPD) for the visible and near infrared allows single photon counting with high efficiency ( $>10\%$ ), low dark count rates (recorded false event,  $<5s^{-1}$ ), very high frequencies ( $>GHz$ ) and very low timing jitter ( $<100ps$ ), thus exceeding the performance of semiconductor devices (mainly InGaAs avalanche photodiodes), sometimes by several orders of magnitude [see R. Romestain et al, "Fabrication of superconducting niobium nitride hot electron bolometer for single photon counting", *New Journal of Physics* **6**, 129 (2004)].

Until now, efficient SSPDs are made of very thin (3-5 nm) NbN film sputtered on sapphire and nanopatterned in a meander structure. Part of this project includes a close collaboration with the GAP-optics which is interested in the SSPDs operation for quantum telecommunication (optical) experiments. The Geneva team is also involved in the European (FP 6) project Sinphonia.

The year activity in Geneva has been articulated around three research orientations:

#### a. Investigation on alternative materials:

The objective of this part of the work is to evaluate the possibility of using high  $T_c$  superconductor for SSPD. It means the ability of growing high quality thin films and the ability of patterning the films without deterioration of the superconducting properties. In the family of rare earth (Re) oxide superconductor ( $ReBa_2Cu_3O_{7-\delta}$ , RE-123), Nd-123 is a promising candidate because of its high surface quality (low surface particles density and flatness) and crystalline quality when sputtered on STO, compared to Y-123.

Our experience shows that the critical temperature of the thin films starts to significantly decrease for thicknesses under 25 nm and patterning of NBCO films by optical lithography and chemical etching (using orthophosphoric acid  $H_3PO_4$  (1%)) importantly deteriorates the film. This is illustrated by a 30 K loss in the critical temperature. In this context, we are studying Selective Epitaxial Growth (SEG). This process involves creating

a patterned inhibitor layer upon which the superconducting phase cannot grow. This method allows the superconducting film to be sputtered as the last step of the process, so avoiding its exposure to several contaminations (water, resist, etching...). This technique allowed us to obtain a 100  $\mu m$  wide line exhibiting acceptable changes in the transport behavior (still a 15 K decrease of  $T_c$  and a signature of underdoping). This ongoing study of the SEG of NBCO films will be compared to the result obtained by classical patterning of YBCO films sputtered on  $NdGaO_3$  substrates which provides a lower mismatch than STO.

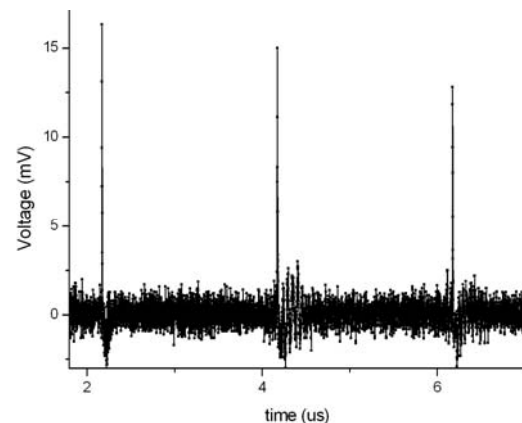
#### b. Characterization set-up:

We have developed a full and flexible electro-optical test set-up for SSPDs. This set-up allows electrical characterization of the devices or films. We also demonstrated the capability of the set-up to detect single photon, as shown Fig. 11 where one sees detected 1310 nm photons generated by a pulsed laser. This flexible set-up will allow us to evaluate the potential of High  $T_c$  material on one hand and to investigate the physics involved in the detection process on the other hand.

#### c. SSPD system:

In the framework of the European project Sinphonia, we have been responsible of characterizing and exploiting a two channels SSPD system fabricated in Moscow.

The characterization of one channel is presented in Fig. 12. It shows the Quantum efficiency (left vertical axis) and the dark count rates (right vertical axis) as a function of the biasing current. 3 measurements performed in Geneva, Moscow and EPFL are presented and show excellent agreement demonstrating the SSPD expected performances and the robustness of the characterization procedures.



**Fig. 11.** Voltage pulses generated by incoming photons with a 120 nm wide stripes NbN meander, fabricated in Moscow.

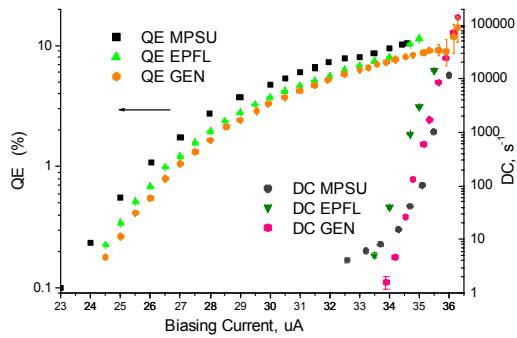


Fig. 12. Characterization of one of the two SSPD channels.

The system has been successively used in the first demonstration of photon bunching of continuously emitted (1510 nm) photons from two different sources.

### Efforts in UNIZH

#### E-beam lithography:

In order to obtain a good detector it is of paramount importance that the complete device is as homogeneous as possible.

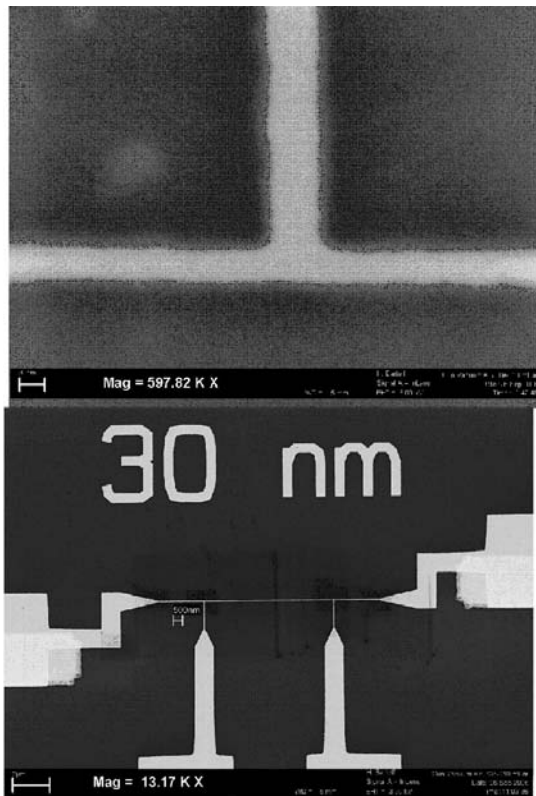


Fig. 13. SEM pictures of a Au/Cr bridge with a width of 30 nm and a thickness of approximately 25 nm created with lift-off. The picture on the bottom shows the bridge and the connection pads that allow for 4-point resistance measurements. On the top we show a blow-up (rotated by 180°) of one of the voltage junctions at maximum resolution.

Already very small variations in  $T_c$ ,  $I_c$  or the cross-sectional area of the strip line lead to a reduced performance or even a complete failure. This implies great demands on the production process of the device. During the report period, we developed a three-step lift-off process that enables us to generate nanometer-sized devices structured from evaporated films, with thicknesses ranging from only a few nanometers to some ten nanometers. The films are evaporated on a silicon substrate and the layout was designed to allow for four point resistivity measurements on our devices.

In the first step, bond pads, orientation marks (for the second optical lithography step and the third electron-beam lithographic step) are created by optical lithography, Cr/Au evaporation and a lift-off. In Fig. 13 we show a SEM picture of a 30 nm wide bridge fabricated. This bridge is made of approximately 25 nm thick Au on top of a roughly 1 nm thick Cr adhesion layer. To demonstrate the feasibility of our process, most structures produced so far are made of Au films. In a next step we plan to use superconducting films.

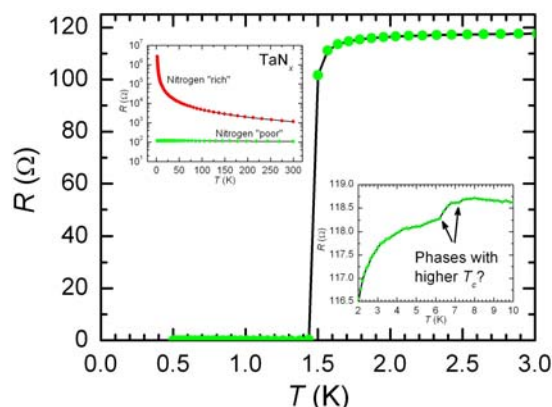
#### Transition metal nitrides:

The detection mechanism of these detectors should work with any superconducting material. There are, however, materials that are better suited than others. If one wants to build a fast detector with a spectral range that is as large as possible, one looks for a material with the following characteristics: The superconducting critical temperature  $T_c$  should be low, because this correlates with a small superconducting energy gap. This is important to push the spectral sensitivity into the low energy, long wavelength range. For the same reason the superconducting coherence length and the diffusion constant for quasi-particles should also be small. In order to make it fast, we need strong electron-electron interactions, which keep relevant time-scales for the quasi-particle multiplication short. These time-scales are temperature dependent and increase at very low temperature. Therefore, optimal  $T_c$ -values are in the range of several Kelvin. For a fast detector it is also important to keep the recovery time short. This limits useful film thicknesses to only a few nanometers. In many respects NbN is a very good material, not only because of its favorable superconducting properties, but also because it is well characterized and there is considerable experimental experience with it. However, it has a relatively high critical temperature limiting its useful spectral range to visible and near-infrared radiation.



As possible alternatives to NbN we are focusing on other transition metal nitrides. With the exception of Cr all neighboring elements to Nb in the periodic table also form superconducting nitrides with  $T_c$  values of several Kelvin. In a first attempt we tried to grow TaN films. Ta was evaporated by means of an e-gun in a  $N_2$  atmosphere at about  $9 \cdot 10^{-5}$  mbar and a small flux of  $N_2^+$ -ions. Ta and N form various stable phases with different N-contents. Adjusting the current density due to the flux of  $N_2^+$ -ions we could tailor the characteristics of the resulting films from semiconductor-like for those films with a high N-content to metallic for films with a reduced amount of N. To prevent oxidation, films with a reduced N-content were protected by a GaN capping layer. The films were deposited onto sapphire and Si substrates held at constant temperatures during evaporation ranging from  $80^\circ\text{C}$  to about  $120^\circ\text{C}$ . Based on previous experience with Ta evaporation in the same vacuum chamber, we expected highly disordered or even amorphous films.

This expectation was confirmed by the temperature dependence of the resistance and by x-ray analysis, which showed no sign of crystalline structure. In the upper inset of Fig. 14 we show corresponding resistance data for two films from room temperature down to below 10 K. The nitrogen-rich film exhibits a clearly non-metallic behavior, whereas the nitrogen-poor film has a small negative temperature coefficient, typical for strongly



**Fig. 14.** Superconducting transition of an approximately 20 nm thick TaN film near 1.45 K. The enlarged view in the lower inset reveals steps in the resistance data, which we attribute to superconducting transitions of small inclusions with higher  $T_c$ . The upper inset shows resistance vs. temperature data for two TaN films with different N-content. Red data points are for a nitrogen rich film of roughly 130 nm in thickness that is clearly non-metallic. The green data are for the 20 nm thick film with much lower N-content.

disordered or amorphous metals. The latter film does become superconducting at a  $T_c \approx 1.45$  K (see Fig. 14), considerably lower than for bulk crystalline TaN with a  $T_c = 14$  K, but still higher than for amorphous Ta ( $T_c = 0.9$  K). In the lower inset of Fig. 14 we show an enlarged view of the resistance data of the metallic TaN film between 2 and 10 K. We observe several small steps in the resistance data that shift and eventually vanish when we increase the measuring current. We interpret these steps as signs of small inclusions in our films with higher  $T_c$ . With further optimization of the deposition parameters and additional annealings of the films at higher temperatures, we aim to increase  $T_c$  into a range where the films might become useful for detector applications.

#### T-dependence of critical current:

One of the key operating parameters of the single-photon detectors is the bias current, which is adjusted to about 90% to 95% of the critical current. The ratio between bias current and critical current directly influences the sensitivity of the detectors. In addition there may be more subtle effects related to the absolute value of the bias current, e.g. caused by the interaction between bias current and vortices that could be present in the strip line. The knowledge of the temperature-dependence of the critical current of the strip line is therefore necessary to choose the best possible operating conditions.

Within standard GL-theory one expects a smooth and continuous increase of the critical current with lower temperatures. Preliminary measurements of the critical current on NbN bridges with widths ranging from  $10 \mu\text{m}$  down to  $300 \text{ nm}$  showed various unexpected kinks and sometimes even steps in their temperature dependence. We have now started to systematically investigate these effects.

#### 4. Giant electroresistive effect in correlated oxide thin films

As mentioned in the beginning of the report, this part of the project was not started. Indeed the work on artificial ferroelectric systems has been developing fast and we focused our efforts in this direction also recently expanding our research towards multiferroic systems.



## Project 6 Industrial applications and pre-application development

**Project leader:** Ø. Fischer (UNIGE)

**Participating members:** M. Abplanalp (ABB), D. Eckert (BRUKER BIOSPIN), Ø. Fischer (UNIGE), R. Flükiger (UNIGE), L. Forró (EPFL), M. Hasler (EPFL), J. Mesot (ETHZ-PSI), R. Nesper (ETHZ), J.-M. Triscone (UNIGE).

**Participating companies:** ABB, BRUKER BIOSPIN, MECSENS, METROLAB, PHASIS, SWISSNEUTRONICS.

**Introduction and overview:** This project has the aim to develop applied projects in the field of MaNEP and to develop collaborations with industry. At the beginning of phase II, 7 groups and 6 companies participate to this project. The topics include applied superconductivity, MaNEP materials for sensors, and applications of thin film technology. Whereas two projects on applied superconductivity started at the beginning of MaNEP and are now steadily progressing, several new developments in other fields started at the beginning of the second phase. These projects, which include new approaches to  $MgB_2$  fabrication, participation in a project to construct a selfshielded magnet for scattering experiments, new materials for high precision low field measurements, gas sensor applications of materials of interest to MaNEP, thin film multilayers for neutron guides, development of new ferroelectric materials, application of ferroelectric materials in high frequency SAW devices and development of thin film ferroelectric devices on Si for MEMS.

### 1. Applied superconductivity

#### Summary:

The collaboration between R. Flükiger and Bruker Biospin on superconducting wires for high field applications builds on a long standing experience of R. Flükiger on superconducting wires and the industrial experience of Bruker Biospin. Over the last years this project has continued to give important results. This year detailed studies of  $T_c$  profiles in the filaments of  $Nb_3Sn$ ,  $Nb_3Al$  and  $MgB_2$  wires have been measured by low temperature calorimetry. These measurements allowed key conclusions about systematical changes between various types of  $Nb_3Sn$  wires. By combining Auger and TEM measurements on various filament bundles, the  $T_c$  distribution found by calorimetry was successfully reconstructed. On the other hand a new compressive stress device (WASP) for measuring the effect of transverse compressive stress on  $J_c$  of  $Nb_3Sn$  wires was constructed and successfully tested up to 21 T and currents up to 1'000 A. The results are important in view of the behavior of various types of  $Nb_3Sn$  wires envisaged for the Next European Dipole (NED) for CERN, but also for the ITER experimental reactor. The group has also obtained improvement of  $J_c$  in bronze route  $Nb_3Sn$  wires produced with a Sn content in the bronze higher than 15.6 wt.%, leading to an increase of  $J_c$  by 25%. Studies of  $MgB_2$  wires with  $B_4C+SiC$  additives obtained by simultaneous addition of  $B_4C$  and  $SiC$  nanosize powders to the initial B and Mg

powders led to a substantial enhancement of  $J_c$  which at 4.2K, reached  $J_c$  values of  $1 \times 10^4$  A/cm<sup>2</sup> at fields as high as 11.3 T. At 20K, this  $J_c$  value was achieved at 4.6 T, which is among the highest reported so far.

The group of R. Nesper has investigated an alternative route to make  $MgB_2$  wires. The patented method for this  $MgB_2$  wire formation [1] was further developed for wire length up to 30 cm. Suitable substrates turned out to be Ni, W, Kanthal and stainless steel. A major problem is still impurities, mainly MgO which assemble in grain boundaries and reduce the critical current. Crack formation by an intermediate shrinking process can be overcome by multiple coatings.

Hole-doped  $Li_{1-x}BC$  and  $Mg_{1-x}(BC)_2$  were predicted to have a much higher  $T_c$  than  $MgB_2$  but did not show SC in our experiments already a year ago obviously due to distortions in the graphene-like layers. We turned our interest towards  $Ca_xB_aC$  phases because of recent reports of SC in electron doped  $CaC_6$  and  $YbC_6$ . The larger Ca is expected to prevent inter-layer BC interactions and enhance the DOS at the Fermi level.  $Ca(BC)_2$  is a semiconductor with a four- and eight- ring layer structure instead of six-rings like in the graphene layers. The Ca-poorer phases  $CaB_2C_4$  and  $CaB_2C_6$ , however, exhibit the six ring layers again.

In the collaboration between the group of Ø. Fischer and M. Decroux with ABB we explore the possibility of future current limiters based

on thin film technology. The origin of this project is that the industry sees numerous possible advantages of such a technology. However, at the beginning of this project two important limitations appeared: 1) Inhomogeneities in the resistance distribution during switching could lead to hot spots and breakdown of the Fault Current Limiter (FCL) and 2) the cost for substrates and thin film deposition is a major limitation for this technology. We decided to approach the first problem first and over recent years we have developed an efficient method of structuring the thin film meanders to distribute the power dissipation. This year we addressed an important problem, when the voltage in the ac power is low. Then the switching is slow and this may lead to local heating. We have demonstrated a modified device in which a current is injected at the moment of the short circuit in a heater deposited on the wafer. It has been demonstrated that in this way it is possible to switch the whole wafer homogeneously. With this result we are very confident that this technology will work technically. However, having brought this technology to a point at which the second limitation mentioned above (i. e. the price of the complete wafer) becomes a central question, it was decided to focus on this point and to investigate the implementation of the developed technology on coated conductors and thereby take advantage of recent developments in this field. This research started early 2007 and first results will be reported in the next progress report.

The FCL project described above is supported by numerical simulations carried out in the group of M. Hasler and B. Dutoit at EPFL. For simulations of YBCO thin films, a new material modeling E-J law has been developed describing the 4 main types of behavior, thermally activated flux flow, flux creep, avalanches leading to flux flow and normal over  $T_c$  regime. An important aspect is that all parameters of this law are temperature dependent and these dependencies are fully implemented.

In 3D modeling, to fully take into account the very high aspect ratio of the thin films, a new method using a scaling factor has been implemented. Physical parameters like electrical and thermal conductivity, thermal capacity have been scaled in order to fit to the real device working parameters like critical current or heat exchange.

The model has been incorporated in the software package FLUX. In order to take into account thermal phenomena during a fault,

coupling between the electromagnetic and thermal models of FLUX has been implemented. This novel numerical method allows studying the local and global behavior of the FCL (current density and temperature profiles) during the superconducting-to-resistive-state transition in case of fault current in voltage source regime. These simulations will be very useful in the future investigations of coated conductors.

In the second phase, MaNEP decided to support a project initially started between PSI and Bruker Biospin. This project is to build a self shielded magnet for use in large facilities like synchrotrons or neutron scattering facilities. Such self shielded magnets with high magnetic fields for scattering experiments have never been realized before, which calls for a very careful assessment of the risks. This magnet is planned not as a pure R&D of a prototype but as a project that has to result in a commercially viable device (concerning price, reliability, ease of operation, operation costs). The planning and assessment finally resulted in the signature of a commercial contract with Bruker Biospin in October 2006. On the technical side, special emphasis was put on the simulation of the coil design; the split region and the variable temperature insert (VTI). Additional evaluations of neutron absorbing steel coatings for the split plates were realized (transmission/reflection measurements, magnetization measurements, mechanical stability at very low temperatures and neutron activation experiments) and on February 1, 2007, a specification review took place, where all detailed specifications have been fixed.

## 1.1 Thermodynamics and critical currents in superconducting wires and tapes for industrial applications

### a) $T_c$ profiles obtained in $Nb_3Sn$ and $MgB_2$ Wires

$Nb_3Sn$  wires. A systematic work was undertaken for determining the  $T_c$  profiles of  $Nb_3Sn$  wires by means of the new calorimetric method described in the MANEP report, Year 5. Low temperature specific heat measurements have been performed on wires prepared by the 3 actually used types of industrial multifilamentary  $Nb_3Sn$  wires: i) Bronze Route, ii) Internal Sn Diffusion and iii) Powder-In-Tube. It is seen from Fig. 1 that the center of the  $T_c$  distribution in the filaments is decreasing in the order PIT→Internal Sn→Bronze Route [2]. An important

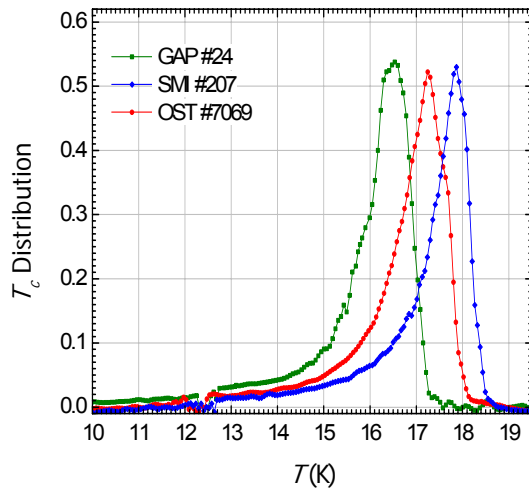


Fig. 1. Distribution of  $T_c$  for three  $Nb_3Sn$  wires obtained by the deconvolution of the calorimetric data.

observation is that the width of the  $T_c$  distribution is nearly the same for the three wire types, although the formation kinetics is quite different. A TEM investigation has revealed Fig.1. Distribution of  $T_c$  for three  $Nb_3Sn$  wires obtained by the deconvolution of the calorimetric data.

Strong differences between the localization of  $Nb_3Sn$  grains with varying  $T_c$  (which is connected to the Sn content): in Bronze Route wires,  $T_c$  decreases radially towards the center of the filament, while in Internal Sn wires (and probably also in PIT wires), the grains with low  $T_c$  are randomly distributed throughout the whole filament.

Since shielding effects are absent in calorimetric measurements, it was possible to show that the variation of  $T_c$  with the Sn content in ternary and quaternary  $Nb_3Sn$  wires is markedly different from that one observed in binary  $Nb_3Sn$  (see Fig. 2). From these

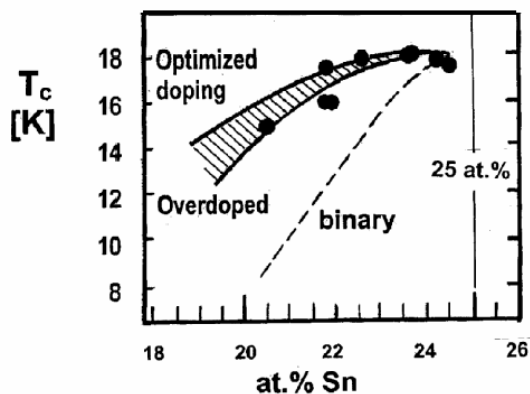


Fig. 2.  $T_c$  vs Sn content relation for alloyed Nb-Sn.

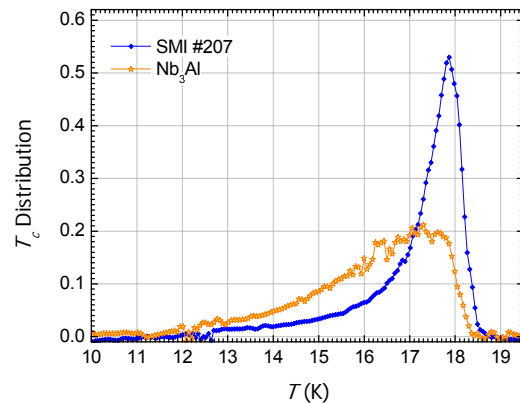


Fig. 3. Comparison of the  $T_c$  distribution of a  $Nb_3Al$  wire with a  $Nb_3Sn$  wire.

measurements, it was also possible to deduce the variation of  $B_{c2}$  with the Sn content for ternary and quaternary  $Nb_3Sn$  wires [3].

The distribution of  $T_c$  in  $Nb_3Al$  wires prepared by the quenching technique at NIMS (Tsukuba, Japan) was determined for the first time and is shown in Fig. 3 [4]. As expected, the  $T_c$  distribution width is rather large ( $\Delta T_c \approx 6$  K), which indicates that further progress is still possible in  $Nb_3Al$  wires.

**MgB<sub>2</sub> wires.** In the case of  $MgB_{1.9}C_{0.1}$ , specific heat measurements show that the C substitution on the B sites modifies the low temperature shoulder related to the second gap. This effect is not visible in the sample doped with SiC. From the distribution of  $T_c$  determined from the deconvolution of the calorimetric data [5], we argue that SiC leads to an inhomogeneous distribution of C (Fig. 4). Our goal is to develop  $MgB_2$  wires with improved formation kinetics, yielding a narrow  $T_c$  distribution as determined by calorimetry.

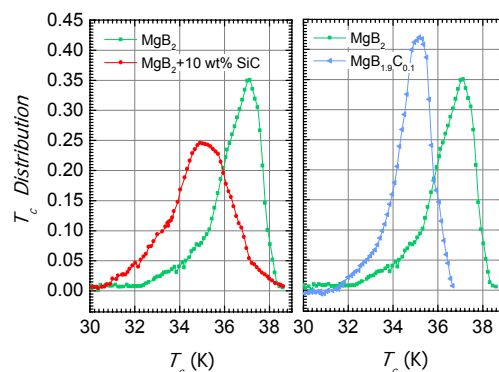
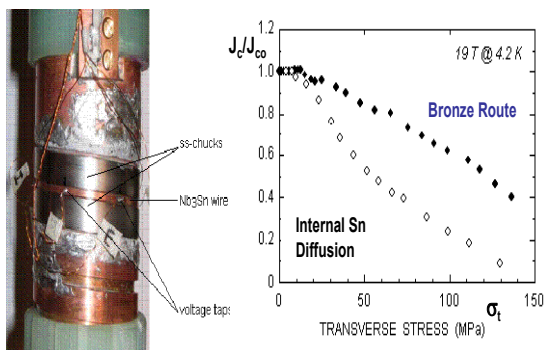


Fig. 4. Distribution of  $T_c$  obtained by the deconvolution of the specific heat data:  $MgB_2$  versus  $MgB_2 + 10$  wt.% SiC (left) and  $MgB_2$  versus  $MgB_{1.9}C_{0.1}$  (right).

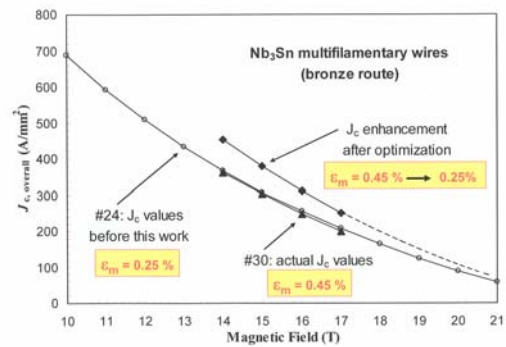
## b) New Device for Measuring the Effect of Transverse Stresses on $J_c$ : the Compressive WASP

Under operation conditions, the conductors of very high field magnets or of large high field systems (e.g. Next European Dipole (NED) for CERN or Tokamak coils for ITER) are submitted to large Lorentz forces, resulting in strong tensile and compressive stresses. In the frame of a collaboration with CERN, we have developed a new device for measuring the effect of transverse compressive stresses on  $J_c$  of  $Nb_3Sn$  wires. The new device was successfully tested up to 21 T and at currents up to 1'000 A [6]. The new compressive WASP rig is shown in Fig. 5a. Measurements on a Bronze Route and an Internal Sn Diffusion wire reveal a very different behaviour of these two wire types: after applying a compressive stress of 120 MPa,  $J_c$  of the former is reduced to 50% of its initial value, while Internal Sn wires exhibit a reduction to 20% (Fig. 5b). This effect is even more pronounced when considering the irreversible behavior: after releasing the compressive stress,  $J_c$  of Bronze Route wires recover to 95% of the initial value, while only 30% of  $J_{c0}$  are recovered for Internal Sn wires, thus indicating a serious degradation in the latter. This difference is attributed to the considerably larger filament diameter ( $\sim 50 \mu m$ ) as well to the presence of voids in the filaments of Internal Sn wires, which favor the formation of nanocracks [6].

The present compressive WASP apparatus is worldwide unique: several demands from various laboratories for the characterization of their  $Nb_3Sn$  wires in view of new large scale devices have been received.



**Fig. 5.** Effect of transverse compressive stress on  $J_c$  of multifilamentary  $Nb_3Sn$  wires. Left: prototype compressive device manufactured at GAP (Compressive WASP). Right: comparison between  $Nb_3Sn$  wires produced by the «Bronze Route» and the «Internal Sn Diffusion» technique (B. Seeber et al., 2006).



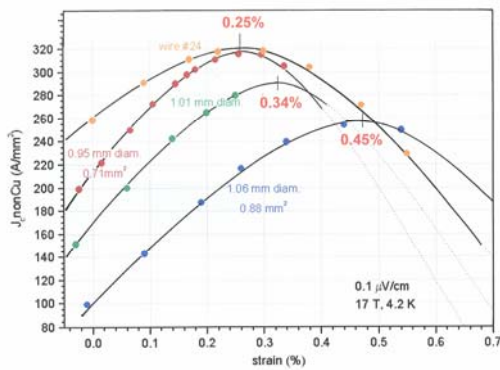
**Fig. 6.**  $J_c$  vs.  $B$  of wires #24 (15.5 wt.%Sn) and #30 (18 wt.%Sn) with very different precompression values. After reduction of the residual Sn content to the equilibrium value of 2 wt.%, an enhancement of  $J_c$  by 25% is expected up to the highest fields.

## c) Improvement of $J_c$ in Bronze Route $Nb_3Sn$ wires

We have succeeded for the first time in forming  $Nb_3Sn$  multifilamentary wires with a Cu-Sn bronze matrix exceeding 15.5 wt.%Sn. At these Sn contents, deformation becomes difficult, due to the presence of the hard  $\delta$  phase precipitates, and new quenching procedures had to be developed (patent submitted). Fig. 6 shows the overall values of  $J_c$  for classical  $Nb_3Sn$  wires (#24) and for the high Sn wire (#30), both with the same Nb content and identical heat treatment conditions ( $600^\circ C/100h + 670^\circ C/150h$ ).  $J_c$  is almost the same, but that the precompression  $\epsilon_m$  (due to the different thermal expansion coefficients) is substantially higher for #30, due to a higher content of residual Sn in the bronze after reaction (4 wt.%Sn compared to 2 wt.%Sn for #24). After optimizing the heat treatment to reach the equilibrium level of 2 wt.% Sn in the residual bronze, an enhancement of  $J_c$  for wire #30 above 25% can be safely expected [7].

The strong effect of precompression  $J_c$  is demonstrated by Fig. 7, where the values of  $\epsilon_m$  of wires #24 and #19, (another wire with higher Sn content in the bronze) are plotted. The  $J_c$  values of the latter were measured after etching away a part of the external bronze. The slight reduction of the wire diameter after etching from 1.05 to 1.01 and finally to 0.95 mm is correlated to a strong reduction of  $\epsilon_m$  which decreases from 0.45% to 0.34% and finally to 0.25%, with strong variations of  $J_c$ , thus justifying the above extrapolation.

The present work has furnished new details about the deformation and the reaction kinetics of Bronze Route  $Nb_3Sn$  wires, as well as about the microstructure of  $Nb_3Sn$  filaments at a nanometric level. The calorimetric



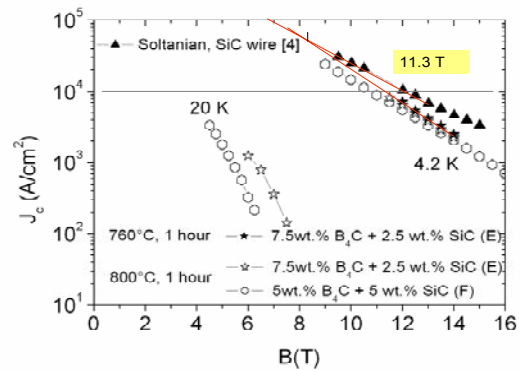
**Fig. 7.**  $J_c$  vs. tensile strain for  $Nb_3Sn$  wires with 15.5 and 18 wt.%Sn, with precompression  $\epsilon_m$  of 0.25 and 0.45%, respectively. Reducing the amount of bronze by etching leads to a reduction of  $\epsilon_m$  from 0.45 to 0.25%.

determination of the  $T_c$  distribution inside the filaments shows that the limits of the bronze route processing are not yet reached.

**d) Enhanced  $J_c$  values in  $MgB_2$  wires by  $B_4C+SiC$  additives**

It is well known that the addition of 10 wt.% SiC nanopowders to the initial Mg + B powder mixture enhances the value of  $B_{c2}$  and  $B_{irr}$  and thus leads to an increase of  $J_c$  at 4.2 K and at fields exceeding 10 T. After having recently reported an enhancement of  $J_c$  for  $B_4C$  additives, the simultaneous addition of various Carbon based additives (in the present case  $B_4C + SiC$ ) to Mg and B powders has been introduced as a new concept in view of further enhancing the superconducting parameters  $B_{c2}$ ,  $B_{irr}$  and  $J_c$  values of *in situ*  $Fe/MgB_2$  wires.

A series of Fe sheathed monofilamentary wires of 1.1 mm diameter with a  $MgB_2$  core of 600  $\mu m$  diameter was prepared with various  $B_4C:SiC$  ratios, the relation being 2.5:7.5, 5:5, 7.5:2.5 and 7.5:7.5 (values in wt. %). After reaction of 1 hour at 760°C, the wire containing 7.5 wt.%  $B_4C$  and 2.5 wt.% SiC powders exhibited a  $J_c$  value of  $1 \times 10^4 A/cm^2$  at 11.3 T and 4.2 K (Fig. 8). Although only 2.5 wt.% SiC were added, these values are considerably above those of ternary wires with  $B_4C$  additions [8], where the same  $J_c$  value is obtained at 10T [9]. The slope  $J_c$  vs. B for the  $B_4C + SiC$  wires is steeper than for SiC additives, the  $J_c$  values at 4.2 K being superior at fields below 9 T. The lattice parameters  $a$  of the  $B_4C + SiC$  added wires exhibit lower values than ternary wires with the same nominal C content, suggesting a higher C content in the  $MgB_2$  phase. The “disorder” in the  $MgB_2$  structure has been characterized as a partial substitution of B by Carbon: a reduction of the domain sizes in the  $c$  direction as well as in-



**Fig. 8.**  $J_c$  vs. B for a  $Fe/MgB_2$  wire with 7.5 wt.%  $B_4C + 2.5$  wt.% SiC additions at 4.2 and 20 K. The data of Soltanian et al. [4], the highest known so far, are added for comparison.

plane to 250 Å and 124 Å has been determined from the FWHM and the breath values of the (110) and (002) peaks. With the simultaneous introduction of  $B_4C + SiC$ , a strong improvement of  $J_c$  and  $B_{irr}$  has been obtained with respect to  $B_4C$  additions. A further enhancement of  $J_c$  is expected when using combinations of additives with and without Carbon, aiming for a further raise of  $J_c$  in wires with multiple additives, as a result of the combination of different mechanisms.

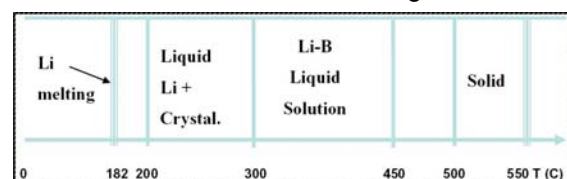
**1.2  $MgB_2$  Wire Formation and Investigations on Related Hole-doped Compounds**

**a)  $MgB_2$  Wire Formation**

$MgB_2$  wire formation was driven through a method which we send in for patent in 2002. In 2006 the patent was granted for the EU, specifically the countries CH, D, E, F, GB, and I; the US version is ready for acceptance and will be granted in 2007 while the Japanese version is still in the checking phase. The method utilizes a low-melting ductile pre-alloy which may be a binary Li/B or a ternary Li/Mg/B form. Such alloy may be cast, coated or shaped into any form and thereafter transformed into  $MgB_2$ . The two-step reaction schemes may be written as follows:



with a thermal treatment according to:

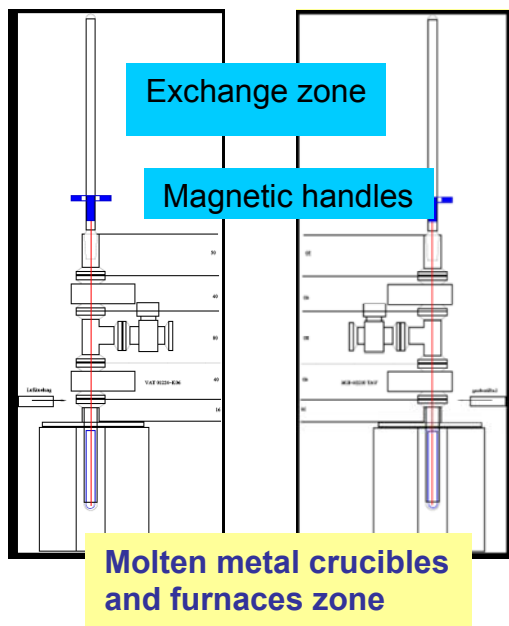


and



The Li/B and the Li/Mg/B melts capture some of the impurities which may be brought into the system through many ways, mainly through impurities of the source materials, especially boron, as well as through the “inert” atmosphere. The procedure has primarily used to coat wires, i.e. ( $\varnothing$  0.5-1 mm): Mo, Pt, Ni, Cu, W, Ag, Kanthal, stainless steel. While Pt, Ag and Cu react with the alloys, coating of Ni, W, Kanthal and stainless steel was successful and led to very pure  $\text{MgB}_2$  films. However, due to shrinking effects (30% volume loss) cracks occur which have to be filled through multiple coating cycles. While the magnetic measurements reveal very pure  $\text{MgB}_2$  conductivities were very bad due to grain boundary impurities (mainly  $\text{MgO}$  and  $\text{Mg}_3\text{N}_2$ ). For this reason a new small volume Schlenk apparatus was constructed which allows to perform all manipulations under inert atmosphere (see scheme 1). By the help of a valve system coated wires at different stages of the procedure can be transferred from one reaction tube to the next one, for example from furnace 1 to 2 or to 3 (for final tempering up to 1100C).

Prior to use we introduced a carbon pre-coating for two reasons: 1. reduction of surface oxygen on the substrate wires; 2. to enhance carbon doping into  $\text{MgB}_2$ . In addition from then on, prior to all experiments lithium and



**Scheme 1.** Small volume inert gas Schlenk line for  $\text{MgB}_2$  wire production.

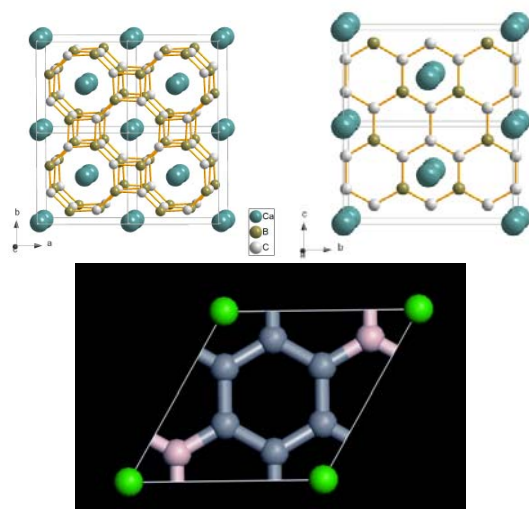
magnesium were distilled and boron was treated in high vacuum at 900C for 24h.

### b) Investigations on $\text{MgB}_2$ Related Hole-doped Compounds

Under-doped  $\text{Li}_{1-x}\text{BC}$  and  $\text{Mg}_{1-y}(\text{BC})_2$  have been prepared and investigated with respect to superconductivity already a year ago [10]. Samples can be prepared up to  $x=0.5$  and  $y=0.78$  but did not show SC down to 4K in magnetic measurements. According to theoretical investigations hole-doping could rise the superconducting  $T_c$  to  $\sim 90\text{K}$  for  $\text{Li}_{0.5}\text{BC}$  [11]. However, we found that on reduction of the Li and Mg contents, respectively, the graphene layers distort.

We started to focus on  $\text{Ca}_x\text{B}_a\text{C}$  phases because of recent reports of SC in electron doped  $\text{CaC}_6$  and  $\text{YbC}_6$  [12]. For  $x=a$  the semiconductor compounds are expected and  $\text{Ca}(\text{BC})_2$  is indeed a semiconductor with a four- and eight- ring layer structure instead of six-rings like in the graphene layers. Up to now we were able to synthesize  $\text{CaB}_2\text{C}_4$  and  $\text{CaB}_2\text{C}_6$  (see Fig. 9) which contain graphene-like layers again, probably because of the larger Ca-Ca distance at such low Ca contents.

They also do belong to the electron-precise  $x=a$  cases. Consequently, semiconducting behaviour was found. At higher synthesis temperatures ( $T > 1000\text{C}$ ) the Ca to B ratio equalizes to one through bond-breaking in the graphene layers. However, at lower temperatures we see possibilities to depopulate the Ca sublattice and thus introduce hole-doping. From DFT band



**Fig. 9.** Crystal structures of  $\text{Ca}(\text{BC})_2$  and  $\text{CaB}_2\text{C}_4$  (top, left and right). Bottom:  $\text{CaB}_2\text{C}_6$ .



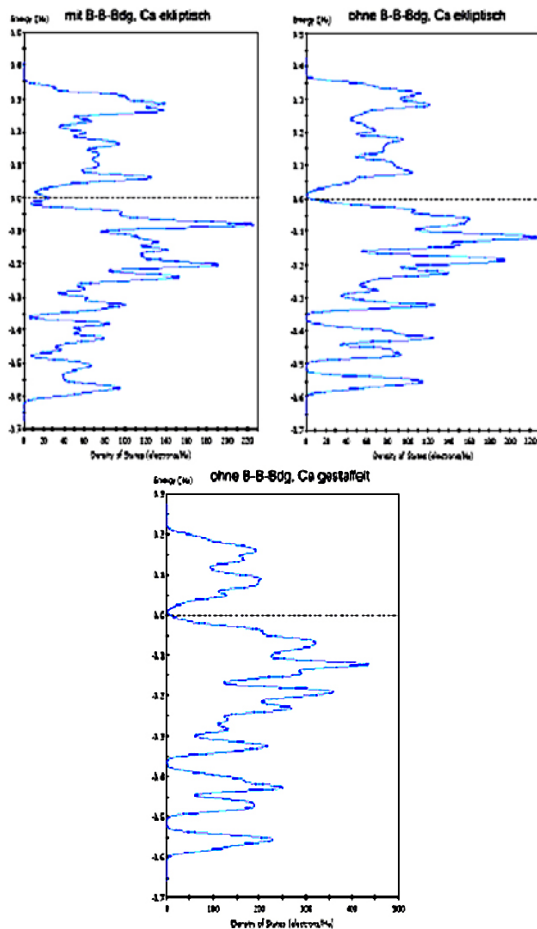


Fig. 10. DFT densities of states for  $\text{CaB}_2\text{C}_4$  for three different B,C orderings.

structure and DOS calculations on  $\text{CaB}_2\text{C}_4$  one can see that the mutual ordering of boron and carbon within and between the layers is of large influence on the electronic structures (cf. Fig. 10).

This seems to be a quite favourable situation for hole doping. The band structure of  $\text{CaB}_2\text{C}_6$  is shown in Figure 11. It is semiconductor with a series of fairly flat band just below the Fermi level.

### 1.3 High $T_c$ thin film fault current limiter

We are currently working on a thin film based Fault Current Limiter (FCL), i.e. a meander of Au/YBCO/CeO on two inches sapphire wafers. This FCL is a device which quickly (few  $\mu\text{s}$ ) limits the current in the electrical network during a short circuit, thanks to its fast superconducting to normal transition. During the last years we have developed a special designed meander with constrictions; the aim of these constrictions is to homogenize the distribution of the dissipated power along the

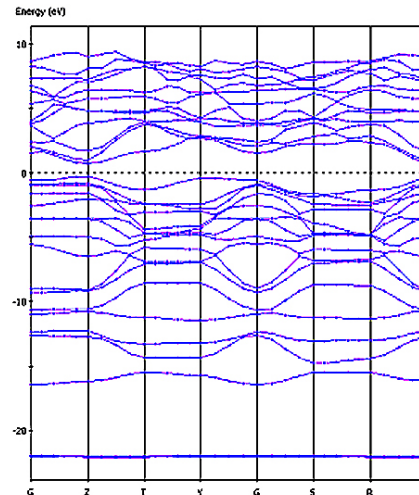
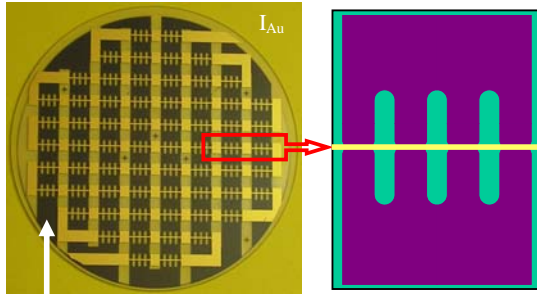


Fig. 11. Bandstructure of  $\text{CaB}_2\text{C}_4$ .

meander. We have successfully tested this design during AC short circuit as long as 60ms. For symmetrical short circuit, the results confirm the benefits of our design; all the constrictions switch at the beginning of the fault and all the lines of the meander are equilibrated very quickly.

However the behavior of our FCL is not optimal during asymmetrical short circuit (short circuit starting at voltages close to zero). These conditions are the most critical for the FCL. This is due to the fact that only a small fraction of the constrictions are switching into the normal state for these low voltages short circuits. After this initial switching, the increase of both the meander resistance (due to the propagation along the meander of the dissipative state and its increase in temperature) and the applied voltage keep the current around  $1.5 J_c$  for a too long time (few ms). This current is too small to turn quickly the other constrictions into the dissipative state but too large to be safely sustained by the connecting path while the normal state region is propagated in them. This can lead, as we have observed few times, to a local burn out of the FCL.

To solve this problem we need to find ways to speed up the transition into the normal state of the other parts of the meander during low voltage short circuits. A first possible solution is to modify the constrictions by including notches. The results on these modified constrictions have been reported last year. However we have observed that these modified constrictions are efficient only if the variation of  $J_c$  across the wafer is less than 5%. This indicates that there is still a room to further improve the performance of our FCL.

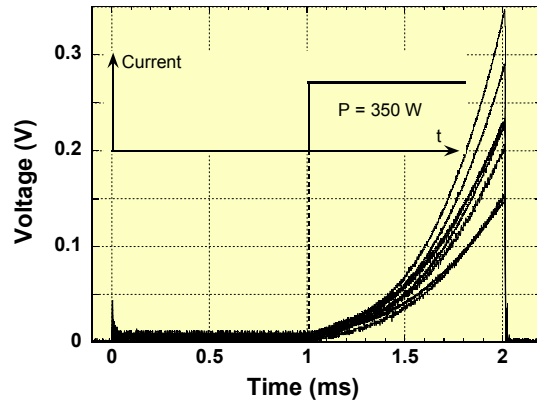


**Fig.12.** Left: View of the backside of a wafer. The white meander is the gold line used for the heating of the superconducting meander. The later is seen, in black, through the transparent substrate. Right: Schematic blow up of one region of the wafer. The heating region (in white) lies exactly underneath the constricted region of the superconducting meander.

Another possible solution is to locally decrease the critical current of the line in such a way that the limited current ( $1.5J_c-2J_c$ ) becomes high enough to quickly switch these parts of the wafer. During this year we have tested this solution in which the basic idea, of what we call the thermally assisted transition, is to heat the lines of the meander locally. A local heating can be obtained by applying a current to a heater line in good thermal contact with the superconducting meander. Since the sapphire is a very good thermal conductor with a thickness of 0.5mm, the heat pulse can be applied from the backside of the wafer. Using a lift-off process, an 80nm gold meander is obtained on the backside of the substrate, as shown in Fig.12. To focus the heat on the superconducting constrictions located on the opposite side, the Au-meander is narrowed (200 $\mu$ m width) at these locations.

To heat the lines a constant DC voltage pulse is applied to the Au meander. This pulse is obtained by the discharge of a capacitance. Our electronic set-up allows us to precisely choose the charging voltage (up to 300V, corresponding to an injected power of 350W) and the delay between the start of the short circuit and the start of the heat pulse.

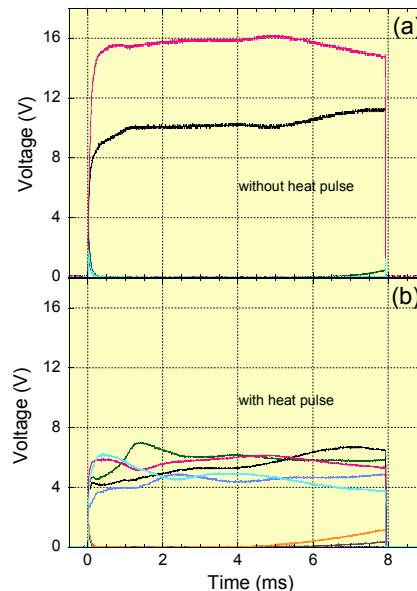
In order to highlight the effect of this thermally assisted transition, we have first tested the behavior of the FCL during constant current pulses. One example of these measurements is shown on Fig.13 for a 2ms current pulse of around 1.5  $J_c$ . We observe that the effect of these thermally assisted transitions is very fast, less than 100 $\mu$ s and takes place in all the lines of the meander. We also studied this effect as a function of the injected power; as expected this effect increases with the injected power.



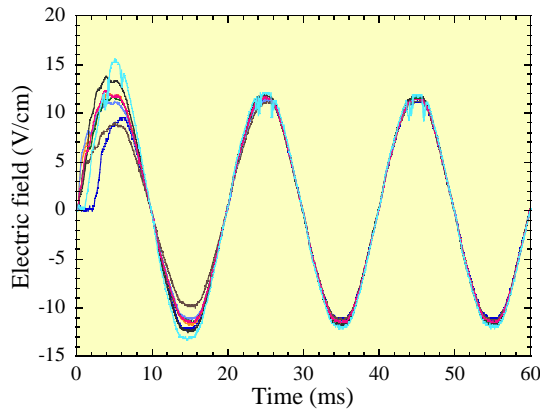
**Fig.13.** Voltage across the 8 lines of the FCL during a current pulse of 16A ( $1.5J_c$ ) starting at  $t=0$ ms. The 350W heat pulse starts at  $t=1$ ms (dotted line).

From the diffusion constant of the sapphire we can estimate, from a simple model of thermal diffusion, which the heat needs only 15 $\mu$ s to go through the 0.5mm of the substrate. This indicates that the fast response time observed in Fig. 13 is due to a thermal effect.

To further highlight this effect we have carefully studied the behavior of our FCL during constant DC low voltage pulses. The improvement of the 340V/12A FCL performance is clearly confirmed, as shown in Fig.14 during a 26V voltage pulse.



**Fig.14.** Voltage across each lines of the meander during a 26V DC voltage pulse without (a) and with (b) a 350W heat pulse starting at  $t=0$ ms. Without the heat pulse only two lines switch whereas 5 lines initially switch, and two later, when the heat pulse is applied.



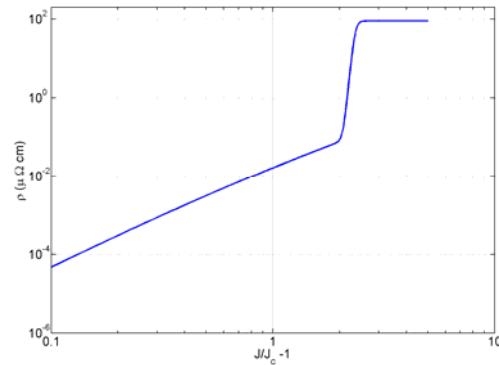
**Fig.15.** Averaged electric field across each line of the wafer during a 60ms AC short circuit starting at  $U=0V$  ( $t=0ms$ ). The heat pulse ( $P=350W$ ) starts also at  $t=0ms$ .

We can observe that five lines have partially switched at the beginning of the short circuit with the heat pulse instead of only two without the heat pulse. The improvement of the normal zone distribution across all the lines is quite impressive when noting that this voltage (26V) represents only 8% of the maximum voltage that this FCL has to sustain.

Finally we have extensively studied the behavior of the FCL during AC short circuit starting at voltages close to zero. A typical result is shown in Fig.15. All the lines switch in the normal state within 2ms after the short circuit and 6 of the 8 lines switch almost instantaneously. This demonstrates the benefit that can be obtained by this thermally assisted transition.

#### 1.4 Modeling of YBCO on sapphire Fault Current Limiters Elements

Properties of HTS materials, such as critical current density and resistivity, is an important factor in devices where over-critical excursions may occur, or when – more generally – the current density locally exceeds the critical current density of the material. This is the case of superconducting fault current limiters (FCLs) where the peak current during a short circuit can easily reach 3-4 times the critical current of the material defined at the nominal temperature. The aim of this work is to provide a numerical simulation method for studying both the electromagnetic and the thermal behaviour of superconducting materials, particularly in over-critical current regime, where the electrical parameters are not constant due to the temperature increase and have to be calculated correspondingly: even when the critical temperature is not reached,



**Fig.16.** Material behavior law.

the resulting power losses lead to important heating which degrades the critical current of superconductors and increases its losses.

##### a) Electrical model

Based on experimental results, different regimes can be distinguished and the electrical behaviour has been modeled as described in our report last year. The resulting  $\rho(J)$  law is shown in Fig. 16 [13-27].

- For  $0 < J < J_c$ , the electrical resistivity is very low. For our purposes the superconducting material can be considered as an almost perfect conductor in this regime. For reasons of numerical stability of the solving algorithm, for avoiding division by zero, a residual resistivity  $\rho_0$  is used for current density lower than or equal to  $J_c$ . This corresponds to the TAFF phenomenon.

- For  $J_c < J < 3 J_c$ , the resistivity of the material has been modeled by a power law relation  $\rho = (E_0/J)(J/J_c - 1)^{n_1}$ , where  $n_1$  and  $E_0$  are two fitting parameters. It has to be noted that  $E_0$  is not the critical electric field  $E_c$  used in the usual  $E - J$  power-law relation.

- When the current density reaches  $3 J_c$ , the material loses its superconducting properties and goes to normal state, where its behaviour is similar to a conventional material. This sharp transition has been modeled with an additional power-law  $E = E_0(J/J_c - 1)^{n_2}$  where  $n_2 > n_1$ . This power-law is not linked with a physical phenomenon, but is used for avoiding discontinuities in the  $\rho - J$  relation. This corresponds to the avalanche phenomenon.

- For  $J > 3 J_c$ , and since the two power-laws are not limited functions, a resistive parallel branch  $\rho_{sat}$  is inserted in order to have a constant resistivity at very large current

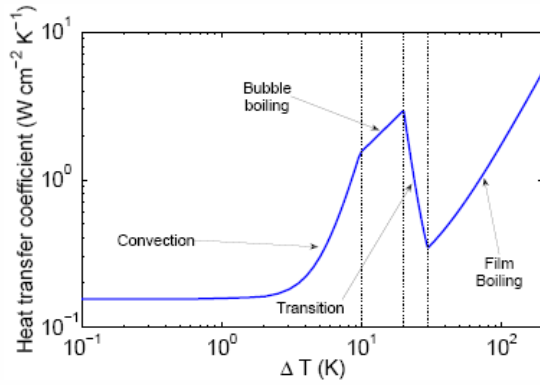


Fig.17.  $N_2$  bath heat exchange as a function of  $T$ .

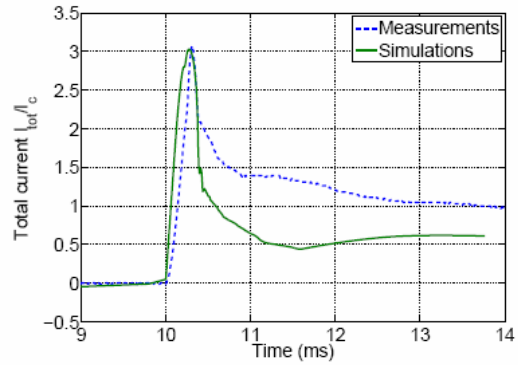


Fig.18. Simulation and measurements comparison.

densities. This resistivity represents the normal state resistivity.

Figure 16 presents the succession of these behaviours as the current increases. In particular, this model allows describing the high current range where the transition from the superconducting to the normal state takes place.

#### b) The thermal model

The thermal model which we use is based on Fourier and heat equations. The thermal exchange with the surrounding environment – liquid nitrogen – is by conduction and convection and it is taken into account by the boundary condition on the outer faces of the device as shown in Figure 17. Coupling is done by alternatively solving thermal and electromagnetic equations sets and adjusting their parameters to the actual temperature value. This is done for each time step.

#### c) Aspect ratio

One central problem in the simulations is the very large aspect ratio of the thin films. Both the critical current  $I_c$  and the resistance depend on the cross section, therefore on the thickness as well. Due to the thickness scaling process [26], the physical properties of the materials have been adapted in order to keep the critical current  $I_c$  and the resistance  $R$  constant.

The resistivity values  $\rho$  have been multiplied by the aspect ratio, since we are interested in over-critical regime, the YBCO material has a resistive electrical behaviour and its resistivity has been adapted in order to have the same resistance as in the real device. In the same way, the resistivity of the gold layer has been adapted too. In addition, we work at industrial

frequencies (50 Hz in this article) without applying any external magnetic field. As a consequence, the magnetic effects are less important than the resistive ones. We assume that the influence of the aspect ratio value on the results can be considered negligible [26].

In the thermal model, multiplying the thicknesses by the aspect ratio leads to multiplying the volume, and the thermal capacity has therefore been divided by the aspect ratio. For the thermal conductivity, anisotropic values have been used: for the x and y axes, the value has been divided by the aspect ratio due to the fact that the section of the layer has been multiplied, whereas for the z axis, it has been multiplied by the aspect ratio because of the modification of the length.

#### d) Comparison between the experimental data and the results obtained with the numerical method.

This 3D FEM model can reproduce the global behaviour of FCLs, and allows studying the effects occurring during a fault caused by the temperature increase.

The model gave results for the current evolution after the fault in qualitative good agreement with experimental data. (Fig. 18). The differences are due to not correct values of the external electrical components like circuit inductance, which need to be estimated more carefully. This work allows the local observation of states variables like temperature as shown in figures 19 and 20.

As YBCO thin film conductors have anisotropic electrical properties, the next stage of this work is to improve the 3D modeling technique by taking into account this effect in the model.

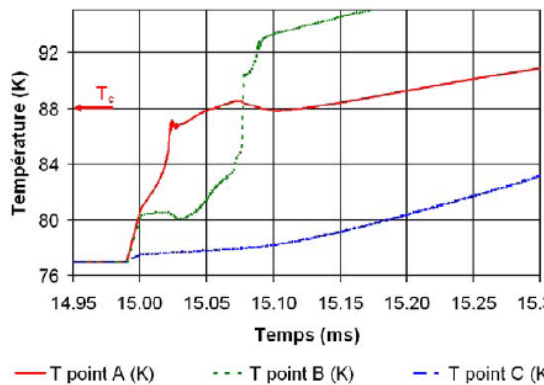


Fig.19. Temperature evolution at selected points.

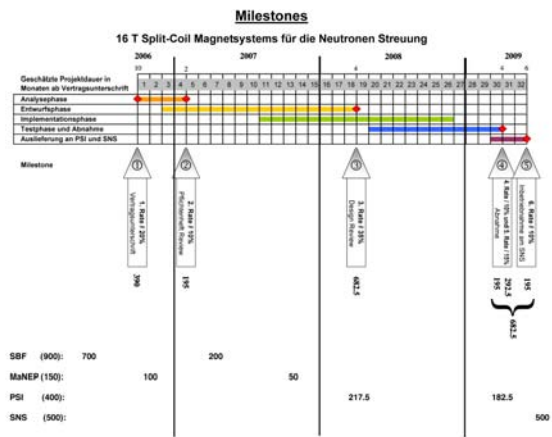


Fig.21. Planning chart and spending profile for the project based on the contract signature date and the contracted milestones.

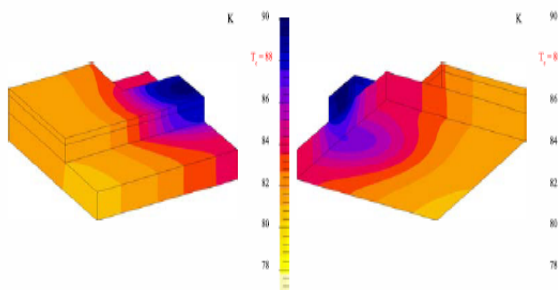


Fig.20. Material temperature YBCO and gold at t=11 ms.

### 1.5 Self Shielded 16T Split Coil Magnet

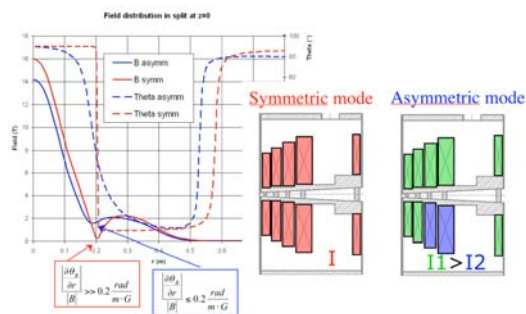
Self shielded magnets for high magnetic fields are today readily available for NMR with maximum fields up to 21 T and a room temperature bore of some centimeters diameter. For scattering methods (X-rays and neutrons) however an axial access and room temperature is by far not satisfactory since these techniques and the problems to be investigated ask for access to most of the scattering plane and temperatures well below or beyond room temperature.

In addition such magnets have to be operated in an environment surrounded by many other instruments and radiation shieldings which will be influenced by an unshielded magnet or exercise large destructive forces on the magnet coils. “From-the-shelf” split coil magnets nowadays reach 15 T but in most of the cases can only be operated – with few exceptions – at fields well below the maximum field due to the reasons mentioned above. The combination of a neutron laboratory with a large experience in high-magnetic fields for scattering experiments and a manufacturer of

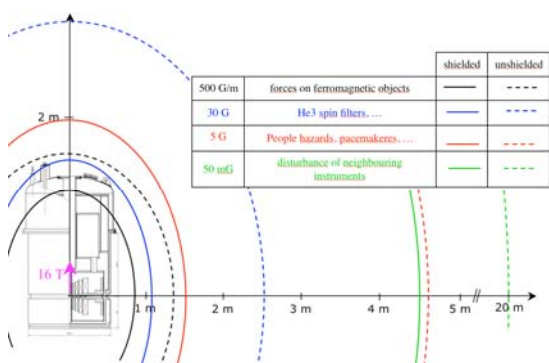
commercial self-shielded NMR magnets provides a unique possibility to realize this demanding combination of self shielding, high magnetic field and access to the scattering plane by a split coil arrangement.

The first magnet of this kind will finally be located at the first 3<sup>rd</sup> generation neutron source (SNS, Oak Ridge, USA) and will there be available to Swiss users. To harmonize the demands of the users (Swiss and US), the final operators (SNS) with the technical feasibility and restrictions assessed by the manufacturer (Bruker) was not an easy task and spanned from technical, over scientific to administrative and financial questions. However, last October the commercial contract was signed and the delivery of the magnet is expected in Spring 2009 for neutron tests at Paul Scherrer Institute (PSI) and a final delivery to SNS typically two months later. The whole process is displayed in Fig. 21 together with the spending profile.

The technical evaluations performed so far concentrate on the specific questions posed by the design of such a magnet which is different from previously manufactured NMR or non-shielded split coil magnets: Split region (design, stability, radiation shielding, neutron transparency, activation), coil design (magnetic shielding, asymmetric mode, field distribution, stray fields) and the VTI which has to be able to accommodate a wide range of custom made inserts (high and low temperatures). Besides some more evaluations of a coating for radiation shielding of the split plates most of the other open questions could be answered and be promoted into the implementation



**Fig.22.** Coils operated in the two different modes (right) and the resulting field profile (left).



**Fig.23.** Magnetic stray fields for shielded and unshielded magnets.

phase. In Fig. 22 the schematic layout of the magnetic coils (symmetric and asymmetric mode) and in Fig. 23 the resulting stray fields are shown.

## 2. MaNEP sensors

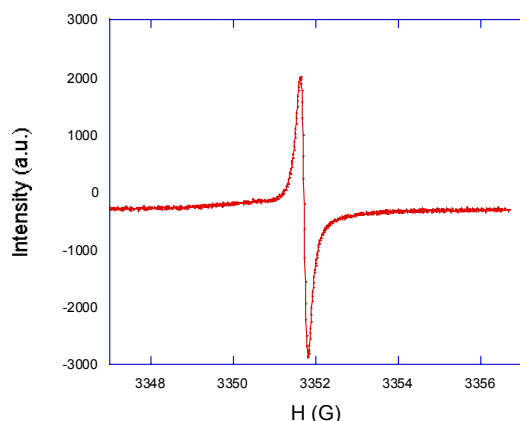
**Summary:** In this subfield of applied projects we are following two routes to use novel materials in the field of sensors. In the first the idea is to find materials with very narrow ESR resonance lines in order to use this for a very precise and absolute low magnetic field determination. In the group of L. Forró a large number of potential candidate materials have been studied and in a collaboration with the company Metrolab the best, like the quasi-one dimensional compound Perylene-AsF<sub>6</sub>, are presently considered for further development. In the second part we are investigating the use of novel materials for gas sensors. In a collaboration between the groups of Ø. Fischer and R. Nesper we have successfully tested the response time of resistive sensors based on MoO<sub>3</sub> nanofibers and shown that very fast response times can be achieved. This measurement used an interdigital device based on SAW device technology. In a further development we have also completed our development of a SAW device to be used as a even more sensitive device. In collaboration with the company Mecsens SA we have carried our studies on Clark type sensors and demonstrated a potential for considerable improvement of such sensors

### 2.1 Recent progress in preparation of materials with a narrow ESR line

The project with Metrolab SA for elaborating a low magnetic field sensor (for geological investigations) based on ESR technique has been continued. Such a sensor needs a material with very narrow ESR line which position would indicate the magnetic field value. The criteria for having a good ESR probe for precise measurements of weak magnetic fields are the following:

- ESR linewidth < 100 mG (ideal 20 mG)
- Spin density  $\geq 10^{26} \text{ m}^{-3}$
- Sample quantity 1 – 10 mm<sup>3</sup>
- Isotropic line
- Working temperature 10 – 40 °C
- Stable composition:  $\Delta g$  is defined better than 10 ppm
- Time stability (but it is not a high priority)
- Price < 1000 CHF

Organic samples can satisfy these requirements, because of the weak spin-orbit coupling, the spin relaxation is slow. However, the test of several organic compounds (electron irradiated kapton, NMP-TCNQ,



**Fig. 24.** ESR linewidth of Perylene-AsF<sub>6</sub> quasi-one-dimensional conductor. The peak-to-peak linewidth is 0.07 G.

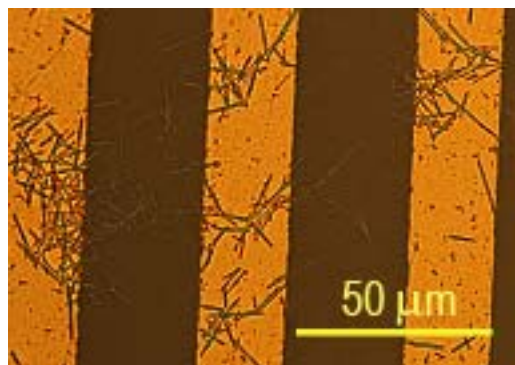
Qn(TCNQ)<sub>2</sub>, Perylene-AsF<sub>6</sub> have revealed, that only the electrically conducting ones are appropriate. In samples with localized electrons, either the spin concentration is too low, or because of the dipolar interaction the linewidth is too broad. It seems that the right material which satisfies all of the above criteria is the quasi-one-dimensional organic metal,

Perylene-AsF<sub>6</sub>, which has an ESR linewidth of 0.07 G at 300 K (Fig. 24). This compound was synthesized by a guest scientist, Dr. Dmitry Konarev from Chernogolovka (Russia). A positive development is that an external consultant of Metrolab, Dr. Giovanni Boero, expert in miniaturization of ESR devices, has joined the project. The first test measurements are foreseen at the beginning of this year.

## 2.2 MaNEP materials for gas detectors

### a) Gas detection with semiconducting oxides and surface acoustic wave (SAW) devices

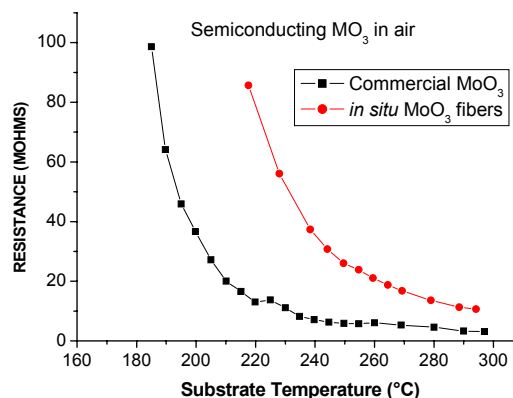
Our aim is to develop new gas sensors based on materials with new electronic properties. Insulating oxides like SnO<sub>2</sub>, WO<sub>3</sub>, and MoO<sub>3</sub> become semiconducting when heated up to 200°C-400°C, and they respond to changes in the surrounding atmosphere with a change in electrical resistance [28]. Recent progress on the 'chemistry of form' of molybdenum and tungsten oxides [29] opens new possibilities to improve the response time and selectivity of oxide-based resistive sensors. In particular, MoO<sub>3</sub> is now available in the shape of nanorods. In order to investigate their sensing behaviour, we have prepared interdigital gold electrode arrays using standard photolithography. The nanorods were deposited on the IDT arrays (Fig. 25) by wet techniques.



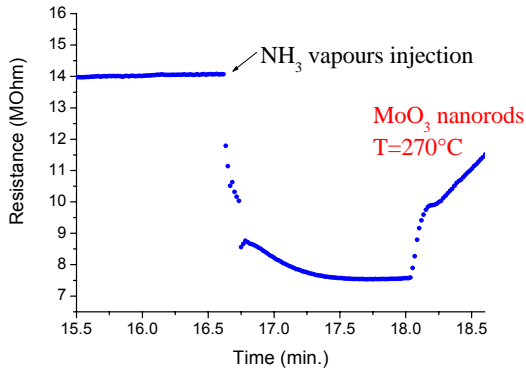
**Fig. 25.** MoO<sub>3</sub> nano-fibers deposited on an alumina substrate with gold interdigitated electrodes (IDTs). Width of the electrodes is 25 μm, and spacing is also 25 μm.

The electrical resistance was measured in a test chamber with a regulated hot plate. Compared to commercial MoO<sub>3</sub> (Fluka), the nanorods become semiconducting at a somewhat higher temperature (Fig. 26).

Gas sensing tests were carried out around 300°C with both nitrogen dioxide and ammonia in a synthetic air background. The resistance of the sensors was monitored using an Agilent 34401 digital multimeter. The sensor response is plotted as a change in resistance versus time, with varying gas concentration. The sensitivity of MoO<sub>3</sub> nanorods to ammonia is shown on Fig. 27. Even if the gas flow in the test chamber has not yet been optimized, the response time of the order of 5 s is fast and compares favourably with MoO<sub>3</sub> sensors reported in the literature [30]. The recovery times, depending on the desorption process and usually much longer, are under investigation. The same sensor showed a similar behaviour upon the injection of a mixture of 5% NO<sub>2</sub> in N<sub>2</sub>. Changes in the free electron density at the grain boundaries are



**Fig. 26.** Electrical resistance of IDT sensors based on commercial MoO<sub>3</sub> and on MoO<sub>3</sub> nanorods.

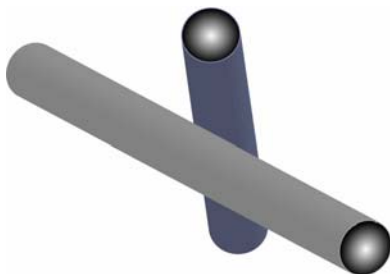


**Fig. 27.** Response of MoO<sub>3</sub> nanorods to the injection of NH<sub>3</sub> vapours in the test chamber, and to the subsequent rinsing inflow of dry air.

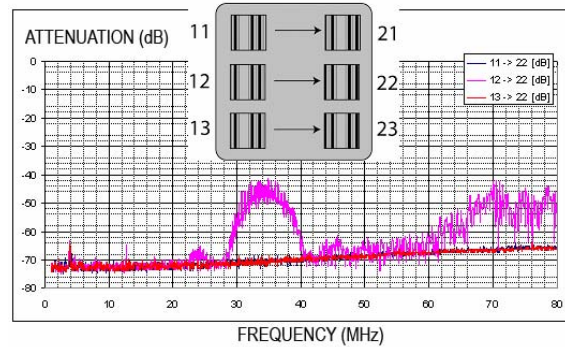
responsible for the sensing mechanism. The response properties are determined by a thin barrier region at the junction between grains. The particular morphology of nanorod-based sensors (Fig. 28) may be responsible for the fast response time.

The transient response time depends on the relative importance of diffusion and reaction rates. Experimental and theoretical work [31] on tin oxide devices has shown that the response time is diffusion limited, and that an improvement in performance may be achieved through a modification in physical properties. The nanorod approach to the sensing layer affects directly the porosity and the kinetics of diffusion. To further investigate the performance of these materials, we will deposit nanofibers on integrated silicon miniature hot-plates (150 μm x 150 μm).

The kinetics of sorption and desorption processes in these materials can be investigated using surface acoustic wave microbalances. SAW devices are also powerful tools for measuring non-percolative electrical conductivity changes in nano-materials [32]. The SAW velocity is perturbed by the



**Fig. 28.** Schematic view of contacts between nanorods. Point- or line-type contacts are dominant when compared to standard granular oxides.

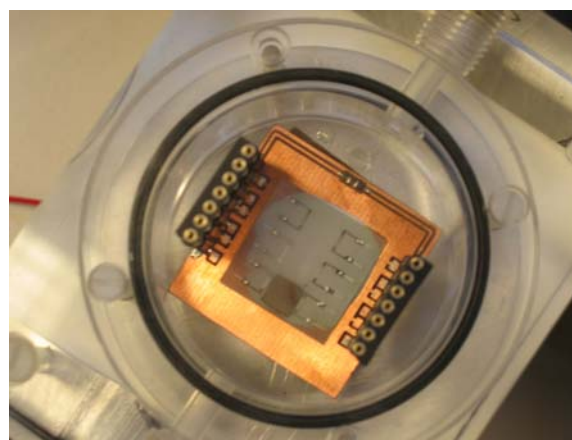


**Fig. 29.** Transmission of a 3-line SAW device. Transmission curve of a LiNbO<sub>3</sub> SAW device with five pair aluminum IDT, showing a peak in transmissivity at the base frequency determined by the geometry.

physical/chemical changes in a sensing layer covering the path of the wave, and this leads to measurable frequency shifts.

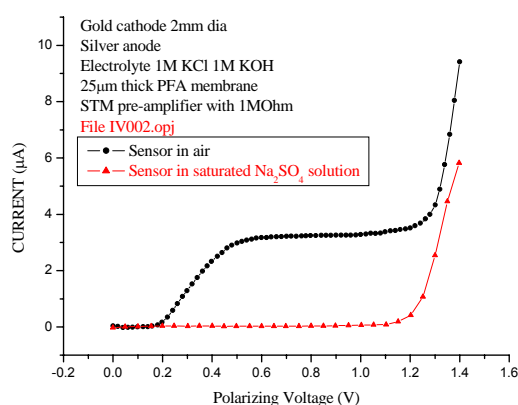
We have thus finished the development of a SAW sensor platform where a SAW device with three transmission lines (Fig. 29) is used as the resonating element in a delay line oscillator circuit at around 36 MHz. There is no crosstalk between transmission lines. Two lines can be used for the deposition of sensing layers and one line for temperature drift compensation. The electronics measures the difference of the resonating frequencies, and since the temperature of the crystal is homogeneous the temperature effect is compensated.

Such a device is shown on Fig. 30 with a 50nm thick palladium film on one transmission line for H<sub>2</sub> detection tests.



**Fig. 30.** LiNbO<sub>3</sub> SAW device with a palladium thin film and temperature compensation transmission line.



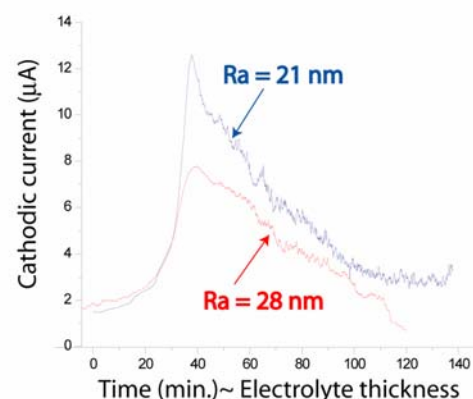


**Fig.31.** Current-voltage diagram of our prototype oxygen sensor. For concentration measurements, the polarizing voltage is set in the plateau where oxygen reduction occurs, around 0.6V. The signal drops to zero when the sensor is immersed in an oxygen-free solution.

#### b) Electrochemical sensors

In this type of sensors the mechanism is based on the reduction of  $O_2$  molecules on a gold cathodic surface. The electrodes are immersed in an electrolyte and covered with a gas permeable hydrophobic membrane. The current circulating between the electrodes is proportional to the gas concentration in the sample. The key parameter to improve the sensitivity of these sensors is thus the ability of the tandem electrolyte layer - cathode surface to generate a higher current for a given oxygen concentration. The best commercial devices perform today at  $1\mu A/mm^2$  in air. In order to experiment different materials and surface morphologies, we have constructed a prototype sensor with interchangeable cathodes ( $\varnothing 2mm$ ). Such a prototype was mounted with a gold cathode having same surface morphology as commercial high-end sensors. The lab sensor achieves the expected current of  $3.1\mu A$  as shown in Fig. 31. The gold cathode roughness was measured with an AFM giving  $R_a=28nm$ .

To investigate the role of the gold surface on the performance of the sensor, we have measured the sensing current for different surface roughnesses as a function of the electrolyte layer thickness. The PFA membrane was removed and the cathode was covered with a thick layer of electrolyte. By placing the sensor vertically in a room with stabilized temperature the electrolyte was allowed to evaporate slowly, and the cathodic current was recorded as a function of time. The



**Fig.32.** Cathodic current as a function of time for two different cathodes. The electrolyte layer thickness is inversely proportional to the time. A thinner functional electrolyte layer and thus a higher peak current is achieved with the smoother surface.

results are shown on Fig. 32 below. As the electrolyte dries, the sensor enters a region where a thin layer of liquid covers the cathode. Oxygen diffusion from air and reduction at the surface occur at an optimum rate resulting in a steep increase of the current. In this region, a plot of the inverse of the current against the electrolyte layer thickness shows the linear behaviour published in the literature [33].

A 30% change in roughness from  $R_a=28nm$  to  $R_a=21nm$  for a polished cathode results in an increase of 60% of the peak current. This result shows the great importance of the microfluidics at the cathode surface, and the potential of improvement for this type of sensors. They can be improved by controlling the cathodic surface structure at the sub-micron scale.

### 3. Thin film preparation and applications

**Summary:** This section of the project is focused on thin film development for applications. In the first part the group of J. Mesot (PSI) studies the use of multilayers for neutron mirrors in collaboration with the company SwissNeutronics. In this part we succeeded in producing  $\text{FeCoV/TiN}_x$  supermirrors for the polarization of cold neutrons with a reflectivity  $R \approx 70\%$  at three times ( $m=3$ ) the critical angle of Ni by using the DC magnetron sputtering technique. In-plane magnetic hysteresis data display a remanent magnetization of about 93%. The Supermirrors are composed of multilayers with graded thickness and achieve a high polarization ( $P \geq 95\%$ ) over a wide angular range.

In the second part the group of J.-M Triscone investigates ferroelectric films for future applications Part of this work is carried out in collaboration with the HES-SO in Geneva and with other groups mentioned at the end of each section. In this work it is shown that thick ferroelectric films can be prepared with a  $T_c$  much higher than the bulk, an effect related to the particular strain state of the layers.

The high frequency properties of epitaxial PZT films have been measured and are found to be far superior to the ones of polycrystalline films.

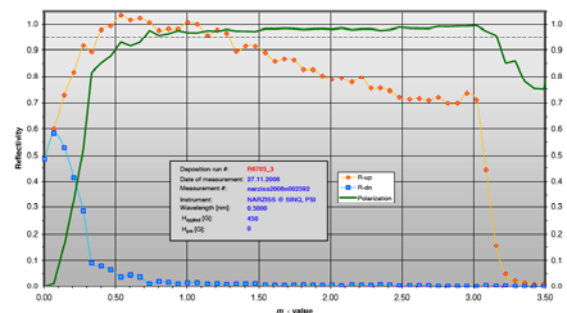
#### 3.1 $\text{FeCoV/TiN}_x$ polarizing supermirrors

Polarizing supermirrors based on various multilayer systems such as Fe/Si and  $\text{FeCoV/TiN}_x$  are used in neutron instrumentation to provide a polarized neutron beam and to analyze the polarization of the scattered beam. They are applied either in reflection or transmission mode. Latter provides the advantage that the beam trajectory is preserved when the polarizing/analyzing device is inserted. Multilayers consisting of magnetic and non-magnetic layers can be used to polarize neutrons due to the different scattering contrasts for neutrons with either up or down polarization. Since the scattering length density (SLD) of Ti matches almost the SLD of FeCoV for one neutron spin state ( $b - p$ ), reactive sputtering enables to tune the SLD of Ti ( $\rightarrow \text{TiN}_x$ ) in order to match precisely the  $b - p$  state of FeCoV. The SLD is supposed to be varied depending on the amount of nitrogen which is incorporated during the growth of the Ti layers. Moreover, the internal stress of the thin films can be manipulated in such a way as

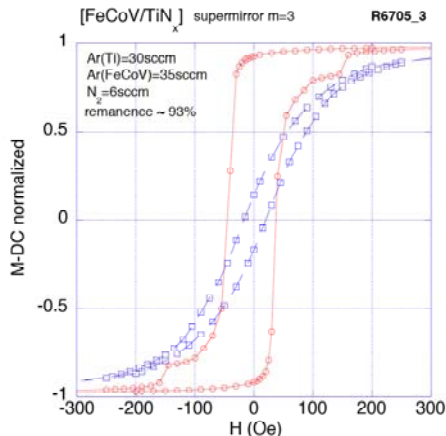
to create an anisotropic distribution, which results in a magnetic anisotropy via magneto-elastic coupling [34]. Due to the magnetic anisotropy the polarizer/analyzer can be used in its 'remanent' state, i.e. at a rather low magnetic field of approximately 10 G (guide field) either with its magnetization parallel or even antiparallel to the applied field. This feature enables to switch the neutron polarization in the experiment by switching the magnetization of the mirror [34, 35].

The goal of the present work is to establish the reactive sputtering process after the refurbishment of the sputtering plant at the Laboratory for Development and Methods, Paul Scherrer Institute, Switzerland. Moreover, it is aimed at improving the performance of  $\text{FeCoV/TiN}_x$  polarizing supermirrors regarding their efficiency and magnetic anisotropy. The  $\text{FeCoV/TiN}_x$  samples were prepared using a Leybold Z600 DC magnetron sputtering system. The sputtering of the ferromagnetic FeCoV layers was carried out in Ar whereas the non-magnetic  $\text{TiN}_x$  layers were reactively sputtered in  $\text{Ar/N}_2$ . In order to achieve a high reflectivity, it is necessary to use very smooth substrates such as float glass and to minimize interdiffusion and interface roughness. The use of TiGd/Ti multilayer absorbers shows considerable improvement of the polarizing properties of the supermirrors. The range of high polarization ( $P \geq 95\%$ ) could be expended down to  $m \approx 0.7$ . In order to measure the performance of the  $\text{FeCoV/TiN}_x$  supermirrors we performed polarized neutron reflectometry (PNR) experiments at the instrument NARZISS (SINQ at PSI).

On this instrument we used a monochromatic ( $\lambda = 0.5 \text{ nm}$ ) and polarized ( $P \approx 95\%$ ) neutron beam. Magnetization measurements were performed in magnetic fields applied parallel and perpendicular to the moving direction of the substrates in the sputtering process.



**Fig. 33** Neutron reflectivity data of a  $m=3.0$   $\text{FeCoV/TiN}_x$  mirror deposited on  $[\text{Ti}(1.3\text{nm})/\text{TiGd}(5\text{nm})]_{25}$  multilayer absorber.



**Fig. 34** In-plane hysteresis loop for a  $m=3.0$  FeCoV/Ti $_x$  supermirror. The red circles and the blue squares represent the measurements along the easy and hard direction of magnetization, respectively.

The intensity of the reflected neutrons of a  $m=3.0$  mirror composed of 300 layers is shown in Fig. 33. As a result of our investigation we were able to produce polarizing supermirrors FeCoV/Ti $_x$  with:

- Polarization up to 98 % for a wide range of the supermirror regime
- High remanence -> operation field of  $\approx 10$  G (See Figure 34)
- Reflectivity of  $\approx 70$  % ( $m=3.0$ )

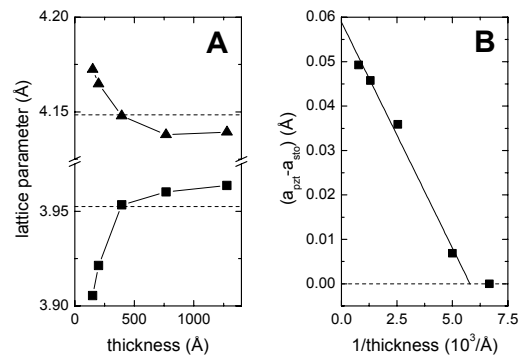
Future experiments will focus on the improvement of the reflectivity and on a better understanding of the origin of the magnetic anisotropy.

### 3.2 Epitaxial Functional Oxides for novel Devices

#### a) Strain relaxation and critical temperature in epitaxial ferroelectric Pb(Zr $_{0.20}$ Ti $_{0.80}$ )O $_3$ thin films

Several recent studies on epitaxial ferroelectric oxide thin films have shown that mechanical constraints can induce large changes in the ferroelectric properties if the strain-polarization coupling is large in the considered materials [36, 37].

Here, we have studied the effect of thickness reduction on the structural and physical properties of epitaxial Pb(Zr $_{0.20}$ Ti $_{0.80}$ )O $_3$  (PZT 20/80) thin films in order to better understand the interplay between strain and ferroelectricity. Using x-ray diffraction, the crystallographic structure and the ferroelectric phase transition temperatures were studied in a series of ferroelectric PZT 20/80 thin films grown onto metallic 0.5% Nb-doped SrTiO $_3$  (Nb-STO) (001) substrates, with thicknesses

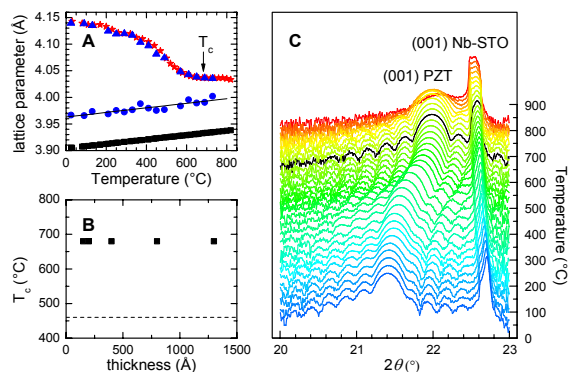


**Fig. 35 A.**  $a$  (square) and  $c$  (triangle) lattice parameters of PZT versus film thickness. Dashed lines are the bulk values. **B.** Difference in PZT and STO in-plane lattice parameters as a function of thickness.

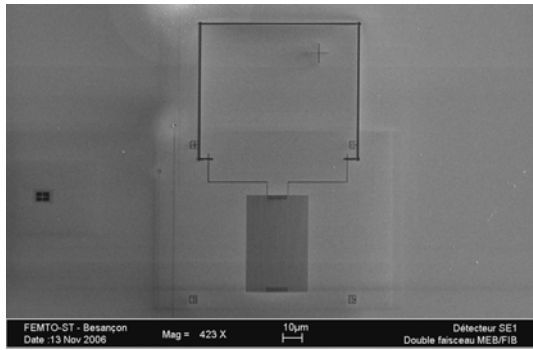
ranging from 150 Å to 1230 Å.

At the growth temperature (500 °C), bulk PZT 20/80 is cubic and paraelectric with a lattice mismatch with the Nb-STO substrates of about -2%. Figure 35 shows the evolution of the lattice parameters at room temperature as a function of film thickness. A 150 Å thick film is found to be pseudomorphic with the Nb-STO substrate: the PZT in-plane lattice parameter reduces to that of STO while the  $c$ -axis parameter elongates. Increasing the thickness induces a progressive relaxation of the strain: the stress is partially relaxed for a 200 Å thick film, and essentially relaxed for a 400 Å thick film [38].

Figure 36A shows the temperature evolution of the  $c$  value for a 1230 Å thick relaxed film. The  $c$  axis shrinks up to 680 °C and then expands. The change in behavior is ascribed to the ferroelectric-paraelectric transition with an estimated  $T_c$  of about 680 °C. The results for



**Fig. 36 (A)**  $c$  and  $a$  axis parameters evolution versus temperature for PZT (triangle and circles respectively) and STO (square) **(B)**  $T_c$  versus PZT film thickness **(C)**  $\theta$ - $2\theta$  scans for a 1230 Å thick film versus temperature.



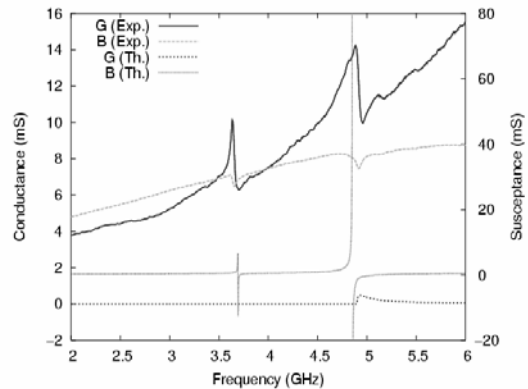
**Fig. 37.** SEM view of the SAW device fabricated by FIB.

all the samples are reported in Figure 36B and, as can be seen, the transition temperature does not vary significantly with thickness, strained and relaxed films displaying a rather similar  $T_c$ .

Because of the large strain-polarization coupling, the modification of the strain state should induce substantial changes in the  $T_c$  of the films and one can expect a  $T_c$  of 1000 °C for the thinnest films (the bulk  $T_c$  is 450°C). As the film thickness is increased and the strain progressively released, the  $T_c$  should approach a value of 680 °C for the thickest relaxed films, a value in good agreement with the data ( $T_c$  is higher than the bulk value since these films, although relaxed, still present a misfit strain of  $-9 \cdot 10^{-3}$  when compared to the cubic paraelectric state, the density of dislocations introduced during the growth being fixed).

These results seem to suggest that, at the growth temperature, it is energetically more favorable for the film to relax in a tetragonal ferroelectric phase than in a cubic paraelectric phase which would require many more dislocations. This is good news for applications since it implies that thick relaxed films can be grown with a critical temperature substantially higher than the bulk.

Finally, an open question is why one does not observe an increase in  $T_c$  for the thinnest films which have a larger misfit strain. For these PZT films, the correlation between  $c/a$ , the polarization and  $T_c$ , used in  $\text{PbTiO}_3$  [39] and demonstrated in  $\text{PbTiO}_3/\text{SrTiO}_3$  superlattices [40] does not seem to hold, an effect possibly due to inhomogeneous strain, for instance due to oxygen vacancies and/or other local defects.



**Fig. 38.** Admittance of a PZT resonator. The thick line is the experimentally measured conductance while the lighter curves are simulations (see text).

*b) Direct writing of high frequency surface acoustic wave devices on epitaxial  $\text{Pb}(\text{Zr}_{0.20}\text{Ti}_{0.80})\text{O}_3$  thin layers using focus ion beam etching*

Here, we pursued our effort on surface acoustic wave (SAW) devices based on epitaxial  $\text{Pb}(\text{Zr}_{0.20}\text{Ti}_{0.80})\text{O}_3$  (PZT) thin films. We have investigated the possibility to fabricate inter-digital transducers (IDT) directly in one process step, by using focused ion beam (FIB) etching techniques on epitaxial PZT layers deposited on  $\text{SrTiO}_3$  single crystal substrates. For that purpose, the FEMTO-ST institute in Besançon has used a FIB machine to directly etch an aluminium layer deposited atop the PZT film. Test devices have been fabricated on PZT epitaxial layers of thicknesses ranging from 100 to 200 nm, allowing for the excitation of 1 micron wavelength Rayleigh-like waves. The test devices (see Fig. 37) correspond to a single-port resonator operating at frequencies ranging from 3 to 5 GHz, depending on the mode order.

Electro-mechanical coupling factors varying from 0.5 to 1.6 % for the first mode and from 0.8% to 2.8% for the second mode have been measured, whereas Q factors in the range of 30-90 were obtained, which are very promising figures according to the literature and the device configuration, far from the optimal one.

The temperature coefficient of the resonance frequency (TCF) was also measured for such a device. A negative TCF of  $-85\text{ppm/K}$  were experimentally found, probably due to the thermo-elastic behaviour of  $\text{SrTiO}_3$ .

Figure 38 shows the superimposition of the experimental admittance of one tested device and the harmonic admittance computed

considering the expected shape of the strip. One can note that resonance frequencies are correctly predicted.

These results show that the high frequency properties of epitaxial PZT films are dramatically superior to the ones of polycrystalline films. This work will be pushed further to see whether such films could be used in specific applications.

(Project in collaboration with Dr S. Ballandras, FEMTO-ST, LPMO, Besançon)

### c) MEMS fabrication based on epitaxial piezoelectric thin films on silicon

The aim of this project is the realization of novel micro-electro-mechanical systems (MEMS) based on epitaxial piezoelectric thin films grown directly on silicon, which should have superior piezoelectric coefficients over conventional piezoelectric thin films. Using SrTiO<sub>3</sub>-buffered silicon substrates, it is possible to grow epitaxial thin films of Pb(Zr<sub>0.2</sub>Ti<sub>0.8</sub>)O<sub>3</sub> and Pb(MgNb)O<sub>3</sub>-PbTiO<sub>3</sub> and take advantage of their high piezoelectric coefficients as actuating/sensing layers in MEMS.

On the fabrication side, we are continuing our efforts in Geneva to acquire the technology allowing SrTiO<sub>3</sub> buffer layers to be produced on silicon. The MBE machine is now operational and we are working on determining the growth parameters and deposition sequence allowing epitaxial SrTiO<sub>3</sub> to be prepared on silicon.

On the MEMS side, since piezoelectric microcantilevers have attracted much attention due to their potential as actuating/sensing platforms, theoretical analysis and computational simulations have been performed to study the behaviour of a cantilever deflected by the piezoelectric layer as a function of various parameters (piezoelectric coefficient, film thickness, applied voltage, cantilever size, electrode configuration, and operating modes). The results show that the epitaxial piezoelectric cantilevers can give higher deflection (actuating mode) and higher voltage sensitivity (sensing mode) compared with conventional piezoelectric cantilevers.

The fabrication of a cantilever requires an etching procedure on the silicon side to define the desirable cantilever thickness down to few micrometers while on the thin film side, the

piezoelectric layer has to be patterned to electrically contact the top and bottom electrodes and to form the cantilever shape. Several wet and dry etching experiments have been performed to establish the different etching procedures for the different materials and their reciprocal compatibility (at this stage the Pb(MgNb)O<sub>3</sub>-PbTiO<sub>3</sub> films used for determining the different necessary etching processes are prepared at the University of Wisconsin, the buffered silicon wafers are produced in Yale).

(Project in collaboration with Prof. de Rooij, IMT, Université de Neuchâtel, Prof. C.B. Eom, University of Wisconsin and Prof. C. H. Ahn, University of Yale)

### References:

- [1] R. Nesper, F. Ottinger, M. Reinoso, M. Wörle, European Patent EP 1368840
- [2] C. Senatore et al., accepted by IEEE Trans. Applied Superconductivity (Proceedings ASC06 Conference)
- [3] D. Uglietti, PhD thesis Univ. Geneva, 2006, to be published
- [4] C. Senatore, to be published
- [5] C. Senatore et al., accepted by IEEE Trans. Applied Superconductivity (Proceedings ASC06 Conference)
- [6] B. Seeber et al., accepted by IEEE Trans. Applied Superconductivity (Proceedings ASC06 Conference)
- [7] R. Flükiger, V. Abächerli, F. Buta, D. Uglietti, B. Seeber, to be published
- [8] R. Flükiger et al., accepted by IEEE Trans. Applied Superconductivity (Proceedings ASC06 Conference)
- [9] P. Lezza et al., Supercond. Sci. Technol. **19** (2006) pp. 1030-1033
- [10] IS. Costanza, Dissertation ETH-Zürich 2006
- [11] J. Nagamatsu, N. Nakagawa, T. Muranaka, Y. Zenitani, J. Akimitsu, Nature **410**, 63 (2001)
- [12] R.P. Smith, *et al.*, Phys. Rev. B **74**, 024505 (2006)
- [13] "Flux" electromagnetic software package, Cedrat S.A., www.cedrat.com
- [14] Meunier G, Le Floch Y and Guerin C 2003 IEEE Trans. Mag. **39** 1729
- [15] Decroux M, Antognazza L, Musolino N, De Chambrier E, Reymond S, Triscone J M, Fischer Ø, Paul W and Chen M 2001 IEEE Trans. Appl. Supercond. **11** 2046
- [16] Duron J, Grilli F, Dutoit B and Stavrev S 2004 Physica C **401** 231
- [17] Rhyner J 1993 Physica C **212** 292
- [18] Stavrev S, Grilli F, Dutoit B, Nibbio N, Vinot E, Klutsch I, Meunier G, Tixador P, Yang Y and Martinez E 2002 IEEE Trans. Magn. **38** 849
- [19] Antognazza L, Decroux M, Reymond S, de Chambrier E, Triscone J M, Paul W, Chen M and Fischer Ø 2002 Physica C **372-376** 1684
- [20] Wesche R 1995 Physica C **246** 186
- [21] Kim H R, Sim J and Hyun O B 2005 IEEE Trans. Appl. Supercond. **15** 2011
- [22] Iwasa Y, Hahn S Y, Lee H, Bascuñán J, Jankowski J, Reeves J, Knoll A, Xie Y Y and Selvamanickam V 2005 IEEE Trans. Appl. Supercond. **15** 1683
- [23] Rettelbach T and Schmitz G J 2003 Supercond. Sci. Tech., **16** 645
- [24] Reymond S, Antognazza L, Decroux M and Fischer Ø 2004 Supercond. Sci. Technol. **17** 522
- [25] Decroux M, Antognazza L, Reymond S, Paul W, Chen M and Fischer Ø 2003 IEEE Trans. Appl. Supercond. **13** 1988

- [26] Duron J, Antognazza L, Decroux M, Grilli F, Stavrev S, Dutoit B and Fischer Ø 2005 IEEE Trans. Appl. Supercond. **15** 1998
- [27] Antognazza L, Decroux M, Therasse M, Fischer Ø and Abplanalp M 2005 IEEE Trans. Appl. Supercond. **15** 1990
- [28] Y. Shimizu and M. Egashira, MRS Bull. **24**, 18 (1999)
- [29] Greta R. Patzke et al., 'One-Step Synthesis of Submicrometer Fibers of MoO<sub>3</sub>', Chem. Mater. **16**, 1126-1134, (2004)
- [30] For a review, see G. Sberveglieri, 'Gas sensors: principles, operation and developments', Kluwer Academic Publishers (1992)
- [31] Julian W. Gardner, Sensors and Actuators B, Volume **1** (1990), pages 166-170
- [32] A. J. Ricco et al., 'Surface acoustic wave gas sensor based on film conductivity changes', Sensors and Actuators **8**, 319-333 (1985)
- [33] J. M. Hale, in 'Measurement of dissolved oxygen', John Wiley & Sons, 1978
- [34] P. Böni, Physica B **234-236** (1997) 1038
- [35] M. Senthil Kumar, P. Böni, J. Appl. Phys. **91** (2002) 3750
- [36] J.H. Haeni et al. Nature **430**, 758 (2004).
- [37] K.J Choi et al. Science **306**, 1005 (2004).
- [38] S. Gariglio et al. submitted to Appl. Phys. Lett.
- [39] C. Lichtensteiger et al. Phys. Rev. Lett. **94**, 047603 (2005)
- [40] M. Dawber et al, Phys Rev Lett. **95**, 177601 (2005), M. Dawber et al. unpublished.

## 3 Knowledge and technology transfer

### 3.1 Introduction

Throughout year 6, Matthias Kuhn has operated the KTT management transition. He built upon the excellent work done by his predecessors (Martin Kugler and Olivier Kuffer) and developed a strategy focused on 1) stimulating MaNEP members to create and protect their inventions and 2) interacting as directly as possible with potential external partners. Means to roll out the strategy were 1) analysis of customer profiles/ needs, 2) internal and external communication. Complementary to his MaNEP contract, Matthias Kuhn works part-time (40%) for the University of Geneva technology transfer office (Unitec). This provides useful horizontal inputs for cross area interaction (i.e. crystallography and physics, see 3.9.7) and best practices in technology transfer.

### 3.2 Marketing and promotion

Based on the significant efforts invested in communication over MaNEP Phase I and based on the direction taken at that time, it was decided to re-focus the KTT audience, i.e. targeting potential new partners for

collaborations or companies interested in acquiring MaNEP licenses.

To this end, several collateral promotions were produced:

- a Powerpoint presentation to be used for prospecting new partners; this material presents MaNEP's organization and promotes research activities with an industrial perspective (usefulness, analogies with Swiss industry products)

- a short flyer (4 pages A5 booklet), which does the same as above in a more condensed way. This document is to be distributed to potential partners.

- a promotional brochure (about 10 pages A4) presenting similar information as the PowerPoint presentation. This work is being done in collaboration with a graphic designer (work in process).

- Aimed at raising the awareness of MaNEP researchers about the importance of KTT and the valorization process, a poster was presented at the 2007 SSP (Swiss Society of Physics) meeting in Zurich (23.02.2007).

### 3.3 Customer prospecting

An analysis of the existing MaNEP database (about 130 industrial entries) and partner rating has been performed and new prospects have been added. The database has been improved so as to allow better interactivity. New fields have been added for enhanced filtering. This database is used in combination with the internet for discovering of potential partners.

Using this database as well as newly established contacts, 10 potential partners were contacted generating 3 expressions of interest and leading to 1 company visit (Manufactures Cartier).

Participation in several industry and professional conferences created new interesting contacts. The list of conferences is provided in the last paragraph: Other forms of technology transfer.

A visit to "Manufactures Cartier R&D" was performed on Jan 29, 2007. Several areas of interest have been identified such as magnetic measurements and contact free polishing.



Cover page of the short flyer

## 3.4 Deals

### ABB:

Following promising results with the ABB partnership (achievement of a 5kV superconducting fault current limiter prototype) and in line with ABB's commitment to pursue the collaboration throughout Phase II, the contract with ABB was renewed. This is a significant achievement for MaNEP.

### Rolex:

MaNEP is a well known and appreciated source of talent. In 2006, Dr. O. Kuffer (former KTT Manager at MaNEP) was hired by Rolex. In his new R&D position, Olivier opened a door for collaboration. The proximity between both groups, the similarities between Rolex needs and the available know-how at MaNEP provided impetus for a good collaboration. Following the signature of a non disclosure agreement (NDA), a contract is currently being signed.

### Bruker Biospin:

PSI through a federal grant started a 30 month new collaboration project with Bruker Biospin. The aim is to build a new product combining the features of Bruker shielded super-magnets and PSI neutron experiments. The end customer is the SNS Project at Oak Ridge

National Laboratory. No device exists to date which has this combination. Publicity about these developments has raised the interest of the X-Ray/synchrotron community. The CHF 0.9 M federal grant requires that the new Bruker/ PSI device be commercialized abroad.

## 3.5 Industrial collaborations

### 3.5.1 ABB

The study of a superconducting fault current limiter (SFCL) by Ø. Fischer and collaborators in Geneva and ABB (M. Abplanalp) continues. Improvements are underway to absorb asymmetrical short circuits where power dissipation is not yet optimal. Research was focused on using a heating metallic layer made of gold, deposited on the flip side of the superconducting meander. Promising results show that the heating speeds up the switching of the meander on the wafer and allows efficient power dissipation. Other routes will be explored in parallel with coated conductors in order to search for reduced production costs. ABB confirms an increase in customer requests for superconducting devices.

### 3.5.2 SwissNeutronics

The collaboration of J. Mesot with SwissNeutronics (P. Böhni), a spin-off from the PSI (Paul Scherrer Institute) continues on the subject of neutron optics. This area of research is critical to increase the yield of neutron sources. Neutron sources are very expensive and price is severely linked to the neutron output. The better neutrons can be guided and transported, the better the beam can be exploited. Ni/Ti supermirrors developed in this collaboration allow doubling the incidence angle at which total reflection takes place, a critical factor for avoiding neutron absorption within the mirror material. Thanks to these developments and the abandonment of activities by competitors in Germany and France, SwissNeutronics enjoys a dominant position in the market.

New developments are taking place in the area of polarizing supermirrors. Such devices allow investigating the magnetism of condensed matter. Prior to hitting the material to investigate, neutrons are polarized in one direction. Analysis of the spin orientation prior to and after reflection allows drawing conclusions about the magnetic properties of the materials.

MaNEP and SwissNeutronics are currently discussing an extension of their collaboration contract.



KTT poster for the SSP meeting at Uni Zurich



### 3.5.3 Bruker Biospin

Historically, the collaboration between Bruker (D. Eckert) and MaNEP (R. Flükiger) has been exemplary, when considering the amount of financing, the results obtained and the number of PhDs transferred from MaNEP to Bruker. Common research aims at developing better superconducting cables for Bruker supermagnets. 3 patent families have been filed to date and a new patent has been filed during MaNEP year 6 (P9024EP patent number). A CTI project is currently being evaluated in Bern on the topic of new alloys for superconducting materials.

The collaboration between Bruker and MaNEP is continuing and the corresponding contract will be signed soon; this contract covers the work of 2 people: (a) Dr Florian Bouta and Damien Zurmuehle.

## 3.6 Other industrial collaborations

### Metrolab Instruments SA

Metrolab is interested in developing new magnetometers to measure weak fields using electron spin resonance (ESR) (0.5-1.0 gauss) with high sensitivity. The end market is geological investigations. Materials of interest to this end must show narrow ESR lines. Up to recently a material of interest was  $N@C_{60}$  diluted in  $C_{60}$ . The problem with this material stemmed from its synthesis, which yielded insufficiently low concentrations of  $N@C_{60}$  in  $C_{60}$ . Scanning of materials has now provided new promising candidates: organic conductors, such as Perylene- $AsF_6$ . These new findings are of special interest to Metrolab and hold the potential for a valuable collaboration with the group of L. Forró at EPFL.

## 3.7 Institutional collaborations

### 3.7.1 Epitaxial ferroelectric films

The group of Prof. J-M Triscone is collaborating with several institutions in the area of applied epitaxial thin film technology:

1) *Domino-InterReg project between UniGe (Geneva, CH), University of Besançon (Besançon, FR), University of Applied Sciences (Geneva, CH), Photline (company, Besançon, France), Phasis Sarl (company, Geneva, CH) and Unaxis (company, Cham, CH)*

One of the aims of this collaboration project is to study opportunities offered by epitaxially grown materials for high frequency applications. It is planned to develop high frequency filters and resonators based on

Surface Acoustic Wave Technology. Results show that the high frequency properties of epitaxial PZT films are dramatically superior to the ones of polycrystalline films.

2) *University of Applied Sciences (UAS, Geneva, CH)*

UAS is developing know-how in the area of thin film synthesis and characterization. These skills are complementary to the ones available at MaNEP. The latter are geared more towards fundamental work. UAS built 2 physical vapor deposition (PVD) setups: molecular beam epitaxy (MBE) and sputtering. On the characterization side, UAS now owns a nano-indentation set up to measure visco-elastic properties of thin films.

3) *IMT – Neuchâtel (Prof. N. F. de Rooij)*

The aim of this collaboration between MaNEP, IMT, University of Wisconsin (Prof. C.B. Eom) and Yale (Prof. C. H. Ahn) is to apply epitaxial piezoelectric thin films to MEMS. Devices under investigation are piezoelectric microcantilevers due to their potential as actuating/sensing platforms. Results show that the epitaxial piezoelectric cantilevers can give higher deflection (actuating mode) and higher voltage sensitivity (sensing mode) as compared to conventional piezoelectric cantilevers (for more details, see the report of Project 6).

### 3.7.2 Symphonia project

This European project aims at developing an optimized superconducting single photon detector. Such devices are of particular strategic importance for quantum telecommunication, where photon counting is required. MaNEP joined this project in 2006 and has 3 main missions related to SSPDs in the visible and near infra-red spectra: 1) evaluate new materials (NbN thin films are currently used on sapphire), like oxide superconductors, 2) develop a characterization setup for SSPDs and 3) Characterize a SSPD system fabricated in Moscow. This system has been successively used in the first demonstration of photon bunching of continuously emitted (1510 nm) photons from two different sources.

### 3.7.3 Project MaCoMuFi

This FP6 European project entitled Manipulating the Coupling in Multiferroic Thin Films started in September 2006. It aims both at understanding these materials better and at developing materials/ setups with novel properties for the industry. The group of Prof. J-M Triscone is actively involved.

### 3.7.4 Project Nanoxyde

This FP6 European project started in 2006. It aims at studying interfaces between oxides so as to discover novel properties. Prototype production is planned in this project. The group of Prof. J-M Triscone is involved in it.

## 3.8 Start-ups

Phasis Sarl a spin-off from MaNEP continues to develop products in line with its strategy:

- Develop, produce and sell high quality epitaxial thin films
- Sub-license new patents in the area of nanoscale object marking
- Develop new resistive sensors based on the surface acoustic wave (SAW) technology.
- Improve electrochemical sensors based on interface improvements.

## 3.9 Other forms of technology transfer

### 3.9.1 Invention disclosures

Invention disclosures represent a key step in the technology transfer process. They precede patent applications.

During this year, one MaNEP invention was disclosed to the University technology transfer office for evaluation. Processing of invention disclosures reported last year is still in progress.

### 3.9.2 Patents

Patent applications reflect both the inventive effort of our scientists and their commitment to bringing their solution to the market. During Year 6, two new patents were filed by MaNEP:

- R. Flükiger patent application relates to new compounds for superconducting applications. It is the fruit of the exemplary collaboration between Bruker BioSpin and MaNEP.
- The patent filed by Phasis, a MaNEP start-up, relates to nanoscale object marking, a strategic field in the context of contemporary counterfeiting.

### 3.9.3 Industry visits on MaNEP site

Dr Céline Lichtensteiger's Prize for her PhD, awarded by Vacheron Constantin watches established tighter bonds with this company. An onsite visit (group leader Prof. J-M Triscone) took place in January 07:

- Visit of the STM and AFM labs.
- Visit of the Crystal growth lab where an exhibition of locally grown crystals was shown.
- MaNEP presentation.
- Visit of Phasis Sàrl (start-up)

The feedback was excellent and the basis for collaboration was set.

Rolex visited our premises in the context of a new confidential collaboration contract. First visit: October 5, 2006.

The visit of Comet AG to MaNEP was cancelled due to a management change in the company. The aim was to exchange ideas about new materials for supercapacitors.

### 3.9.4 MaNEP multimedia presence on internet

The MaNEP website is being redesigned to manage visitor's expectations better. The KTT section has already been partly modified with an updated definition of KTT goals, structure and means.

A reflection took place about means of providing MaNEP with a more focused visibility on the web. This aims at attracting new collaboration partners. Tools are now available, which allow using key words more efficiently. Examples of such tools are Google indexing (for the website), Google AdWords and YouTube. These tools leverage different types of media and technologies. To gain experience with such means, 1 KTT video presentation was posted on YouTube. This video can be found by using the key word "MaNEP" or by using the below link:

- *MaNEP Knowledge and Technology Transfer* (video clip, 1min 27sec)

<http://www.youtube.com/watch?v=kmQXgVa2d38>

A number of other promotional initiatives of promotion were rolled out. Let us mention a campaign on Google AdWords, the participation to the NanoEurope Conference, the MicroNano Day, the Watch Marketing Day, the Integrated sensors Day, etc.

### 3.9.5 KTT via MaNEP e-newsletter

The MaNEP e-newsletter was used several times as a vehicle for KTT related matters:

- Several news articles and internet links were posted, aimed at informing MaNEP researchers about sources of KTT information and about industrial developments in their areas.
- The December 2005 e-newsletter contained 2 articles introducing the new KTT manager (one from O. Fischer and one from M. Kuhn) and his first thoughts about strategy.

- One article was published in the March-April 2006 e-newsletter entitled "Bringing ideas to the community".

### **3.9.6 Service activities**

DynamicMotion SA whose activity is mainly oriented towards small sized electromechanical motion systems commissioned MaNEP for the second time to perform numerical simulations for the optimization of the manufacturing process related to a new strategic product. Research and service contract value: CHF 5k + VAT.

### **3.9.7 Cross functional valorization**

Using information gathered through his activities with Unitec, Matthias Kuhn initiated contacts between two synergetic neighboring groups: the group of Prof. K. Yvon (crystallography) and Phasis.

Prof. K. Yvon's new metal hydrides for hydrogen storage have been tested by Phasis for potential sensor developments.



## 4 Education, training and advancement of women

### 4.1. Education and training

#### 4.1.1 MaNEP Summer School 2006

After the first successful MaNEP summer school in 2004, the second MaNEP School was held in Saas-Fee from 11-16 September 2006. The subject of this school was "Probing the Physics of Low dimensional Systems" and covered an extremely large domain of activities well represented within MaNEP. Sixty three students attended this one week course starting on Monday afternoon and ending on Saturday morning. The lectures were given by 8 teachers who shared this week with the students making it possible for them to establish contact with well recognized researchers in this field. Among the 8 teachers, half were coming from outside of MaNEP, demonstrating our aim to be open to worldwide activities in the MaNEP domains. The school was organized by the local committee chaired by M. Decroux.

This summer school offers to young MaNEP scientists a series of high level lectures illustrating how the unconventional behaviour of low dimensional systems can be probed by different experimental methods.

The week was split into 26 hours of lectures and 2 hours of informal discussion in a Topical meeting. This session gave an opportunity to the students to address questions and

comments to all the teachers. This session was extremely dynamic and we plan to schedule the same concept for the following summer school.

#### 4.1.2 Third MaNEP School

We are already working on the next MaNEP School. As the planning of the academic year changes definitively in September 2007, the date reserved up to now for our school falls exactly at the end of the September session of exams making it quite difficult to continue with our past schedule. Having this school earlier is presently impossible so we are looking to set it in winter sometime in the middle of January 2009 in a period generally not crowded during the winter season. We are in discussion with the hotel owners to see if the next MaNEP School could be a winter school. The idea of a winter school has been unanimously accepted during the MaNEP Forum of January 2007.

#### 4.1.3 Topical Meeting and "Martin Peter colloquium"

This year we had one Topical meeting focused on the subject of Novel Superconductors. Many new materials have been discovered in the last years and interestingly, many old materials were revived since their physical properties were and are so fascinating that deeper characterization with new available techniques is underway. The interest for these novel materials is underlined by the important



*Participants to the 2006 MaNEP Summer school*

number of participant at this meeting: 150 researchers attended this topical meeting which ended with the Martin Peter Colloquium. During this colloquium, Professor P.W. Anderson gave a lesson entitled "Resonance Valence Bond after all: the theory of High  $T_c$ ". This presentation was a perfect conclusion of this interesting one day meeting.

#### 4.1.4 Action initiated by MaNEP outside its domain of activities

To enhance the interest for what is inappropriately called "hard science" and therefore to have more young students attracted by the domain of MaNEP, we have to be active also on a lower level of education. In these actions MaNEP can be seen as an incubator of ideas and has to develop collaborations within each local school administration to promote a positive image of sciences. As MaNEP groups many institutions, a general program is quite impossible to establish, but we believe that local experience can create the necessary dynamics to implement appropriate actions in all institutions participating to MaNEP.

The actions that have been developed during this period addressed the following target:

##### Student exchange program

An exchange program for bachelor and master students is in planning and shall be implemented during MaNEP year 7.

##### Teachers at college (high school or lyceum)

MaNEP has made, in the recent past, several actions to promote physics at the gymnasium school in order to attract more students into the

domain of material sciences. During the last year several actions, described in detail in the report concerning communication and education, have been organized. But the actions at the level of the gymnasium students are not enough since the idea that physics is essentially a technology comes from the teaching history of all the students. It is essential to modify this and therefore we have also to be active at the teaching level. This can be realized by reinforcing the collaboration between ourselves and all the physics teachers. Actions along this line are presently under organization in the framework of the project going under the working title of "PhysicsPark" to be realized by MaNEP and the Department of Physics. This project is discussed in chapter 5 *Public relations*.

It is very important that the domain of MaNEP is first recognized by the teachers acting in high school. This year we have organized a full day of formation on the subject of superconductivity entitled "*Histoire, légendes et développements actuels de la supraconductivité*". 30 teachers attended this one day seminar split into basic courses, demonstrations, an advanced course and 4 PhD presentations ending with laboratory visits. The format of this course was a delicate balance between rigorous and intuitive approaches making possible for the teachers to get a pedagogical approach of this science with many pictures able to illustrate part of their future courses. A CD-rom with all the presentations was offered to the participants to facilitate this important work.



Day of formation dedicated to college teachers

#### 4.1.5 Doctoral School

In the course of this year, we have conducted a reflection aimed to draw the contours of a MaNEP doctoral school. This school is intended to provide the PHD students with a basic knowledge of the experimental and theoretical activities within MaNEP. It is part of a continuing effort of the NCCR to train the new generations of researchers. We plan to welcome the first students in the doctoral program by the end of 2007 in Geneva. The possibility to extend the concept to other groups in the network will be considered in a later step.

Our first lines of thought were to figure out a new recruitment procedure, to imagine ways of improving the support of theses, and to determine the nature of the teaching provided by the doctoral program. The main ideas of the project are summarized below.

The recruitment has been designed in a way which allows for international calls for attracting foreign students while ensuring a maximum flexibility to the PHD advisors in their choice of candidates. In particular, in addition to the existing procedures, the DPMC will organize twice a year a two-day round where the best applicants will have the opportunity to present their ongoing activities in a short seminar, to visit the various labs, and to give their preferences related to PHD work at the DPMC. The students selected in this way will then join the doctoral program under the direction of a PHD advisor, together with the students (local or external) recruited directly by the PHD supervisors.

In order to strengthen the support of PHD students during their thesis, we plan to ask them for short reports and/or seminars on a yearly basis. Furthermore, we ought to organize a monthly informal seminar dedicated to the PHD students. This seminar would serve various purposes, such as discussing recent important publications or achievements in scientific research, training talks before conferences, examining particular practical problems encountered by the students, etc.

The teaching proposed to the students will extend over the first two years of their PHD and come from different sources. In addition to the existing courses (*3ème Cycle de la Physique en Suisse Romande* and various specialized schools like the Saas-Fee MaNEP school), we will set up a general course (equivalent of 2 hours per week for two academic years) covering the main research

activities of the NCCR MaNEP, and given in Geneva. The goal is to provide the students with a common basis of knowledge which should help them understand the main challenges of MaNEP research, encourage communication among them, and perhaps also stimulate collaborations between them. The doctoral school also intends to encourage the transfer of knowledge within the NCCR from the more advanced to the new generation of physicists. To this end, short modules on highly focused scientific questions will be organized in response to explicit requests by the students. In order to diversify the skills of PHD students, we also envisage proposing lessons on topics related to e.g., technology transfer and patents, scientific and public communication, modern computer tools, etc. The MaNEP network will of course be of great value in finding qualified teachers for these short courses.

The various questions related to the project of the MaNEP doctoral school will be collected on a web site which is presently in construction.

## 4.2. Advancement of women

### Introduction

Advancement of women is a long term MaNEP action. As years pass by, specific actions were carried out. Let us mention student internships and collaboration with Equal Opportunities Offices of the academic institutions members of MaNEP. These efforts have led to significant improvement in the position of women within MaNEP. One of the most recent one is the appointment of Patrycja Paruch as *professeure adjointe* at the UNIGE.

After the two successful (2004 and 2005) internships, we have renewed these internships in 2006. The survey made at the end of the two first stages has shown that our communication was not as efficient as we would like and simultaneously we miss the real impact that these internships have on the students. In 2006 we prepared new posters, sooner than in 2005 and sent them to all the project leaders a couple of weeks before the end of the first semester. In addition to the survey we also asked the students to write a short text about their personal experiences during this internship and to focus their statement on what were the impacts that this internship had on their future career. For instance, did it improve their self confidence to manage research; did it modify their career strategy?

This action had the aim to inform us as to why female students start physics studies and if this internship led to a change in the planning of their career. We recall that one important task to promote women in the domain of the physics is first to interest them to this culture. Many young students, independently of their gender, think that physics is essentially a technology and not a culture. As women favour studies based on culture and/or emotion we believe that we have to develop our actions in order to make physics also a choice of culture.

## Internship 2006

In 2006 we had 7 candidates who carried out their internship during the summer period; one at PSI, one at EMPA, two at the EPFL and three in Geneva. All these internships were very successful since these young students were able to carry out very interesting projects. For one student, this internship has allowed both parties to continue their collaboration at the PhD level. We would like to underline the effort made by all the project leaders and their collaborators and to thank them for their implication in our program for promotion of women in sciences.

Hereafter we reproduce part of the text sent by 5 of the 7 students having the chance to participate in our internship in 2006, in order to demonstrate the high degree of satisfaction.

1. *Point n'est réel besoin de m'étendre sur la quantité inespérée de connaissances que j'ai acquises durant ces deux mois, et ce sans à peine ressentir d'effort. La motivation extraordinaire qui était née dès les premiers jours se maintenait, et me poursuit encore*

*aujourd'hui. Et quel bonheur de regarder pour une fois la physique sous un angle autre que celui des cours ! Je considère réellement, avec énormément de gratitude, que ce stage m'aura non seulement confortée dans mes choix d'étude et donné l'envie et le courage de poursuivre, mais surtout apporté, avec l'expérience réelle, une confiance que les meilleurs cours du monde ne sauraient offrir.*

2. *L'existence de ces stages aura joué un rôle considérable dans mon propre parcours. Et j'ai pleine conscience que l'impact psychologique sur l'apport de confiance en soi et l'aperçu de la vie de groupe de recherche aura été absolument nécessaire dans mon cas. En effet, alors que j'étais convaincue, en 3ème année, de ne probablement pas poursuivre mes études au-delà du bachelor, la question du master devient de plus en plus évidente.*

*Sans doute le principe n'est-il pas équitable, mais je ne peux m'en plaindre. Peut-être pourra-t-on un jour élargir le concept de manière à accueillir également des étudiants*

3. *Le seul bémol à ce tableau est la vie extérieure. Durant ce mois, j'ai un peu négligé « l'à côté » tout simplement parce que j'ai vécu cette expérience pleinement. Je me levais AFM, je mangeais AFM, je dormais AFM. Sur le moment, je l'ai remarqué, mais ça ne m'a pas dérangé, plutôt passionné."*

4. *I saw different kinds of topics and how a work can become a real passion. Moreover, the challenges that you can have in such fields is very stimulating. This experience helped me to realize that I really want to work in this*



Internship 2006 posters in French, German and English



*domain. Before my internship at PSI, I was not sure if I wanted to do a thesis but afterwards I changed my mind. In a collaboration involving LNS, SLS and Uni. Neuchâtel, I started my PhD in December 2006 at PSI and I am very delighted about it.*

5. *"The internship was very interesting and indeed gave me confidence in my capabilities to manage research. The internship further confirmed that, independent of academic studies, a lot of skills have to and always can be learned on the spot (new machines, methods, but also new theory). I am very grateful for the experience, however I am currently making a general reevaluation of my further career plans (more specific studies - broader further formation?)."*

These texts highlight the necessity to continue these internships. But as mentioned, women feel that something has to be done also for the male students. As we would like to keep our Advancement of Women program focused on

women students, we are preparing a new concept to interest all the scientific students who want to continue their studies in material sciences with a new program call "Student Exchange". It is worth noting that this program is also in favour of female students.

Finally, to thank the candidates for sending us their feeling about their internship we offered them a "2007 Women diary" based for this year on the spirit of Josephine Baker who always dared to do something new. This way of thinking is clearly the spirit that has to serve as an example for all the students.

For 2007, we already announced the internships with new posters more representative of the reality of the female students within MaNEP. We hope for next year to have pictures of all the 2007 candidates from all MaNEP institutions, so that future candidates can recognise colleagues or friends from the announcement.



## 5 Public relations

This chapter reports on activities of A. Rougemont (communication officer) and A.A. Manuel aimed at the general public and specific audiences since the last report. It covers progress made on PR paper and electronic tools, as well as media features (including TV and radio shows), organization or participation to PR operations as well as ongoing projects that should bloom in year 7.

### Youth oriented efforts

As the list of “PR events and publications” will clearly show, there has been a strong emphasis on the young audience during year 6. Efforts especially concern college students and their teachers, mainly through numerous visits to or from high schools, as well as the building of a strong editorial collaboration (joint creation of contents) around the future “Physiks Park” (working title) in Geneva, a very ambitious project for which MaNEP has been assuming a leading role to this day. If everything proceeds as planned, the Physics Park should be opening its doors to classes at fall 2007. It is also to be noted that more and more attention to MaNEP is paid by institutions situated in the French region surrounding Geneva. As a result, the number of requests for school visits and general infos about MaNEP for all kinds of purposes is steadily growing.

### Exploring new web-based tools

With the idea of exploring a broad variety of PR tools, for both internal and external communication, a mail-and-web-based MaNEP discussion group has been created. The free and convenient solution provided by **Google** has been used. This group was mainly started in the hope of increasing the exchange of high-quality knowledge available within our network especially for the benefit of our PhD and post doc students. Until now, the group has not been very active (some professors have explained they are already too busy with their regular tasks), but we have not yet lost hope of making it as rich and useful a tool as it could be.

<http://groups.google.com/group/MaNEP>

The free broadcasting website **You Tube** is also being tested: 3 MaNEP videos are now available on it. The most successful (nearly 5000 views in 2 months) is a short movie of the model levitating train, which has raised interest shown through comments and questions we received ; it has even lead our Geneva engineer to provide help for the building of a similar set up in Brazil ! The two other videos are slide shows respectively presenting MaNEP and the KTT activity.

[http://www.youtube.com/results?search\\_query=manep&search=Search](http://www.youtube.com/results?search_query=manep&search=Search)

Finally, a MaNEP section in the **Wikipedia (The Free Encyclopedia)** website is currently under preparation.

### Creating new paper documentation

We gradually try to build a full range of PR tools to meet all sorts of needs and audiences. In this perspective two booklets have been created, in French and English, in A4 format (12 pages). One booklet contains a presentation of MaNEP aimed at a general audience (general public, press, school teachers, etc.); the other one is presenting MaNEP's KTT activity and is rather aimed at actual and potential industrial partners.

Both booklets include a back sleeve that allows them to be used both for general presentation purposes as well as for providing documents on new and/or specific issues. Printing should be completed by fall 2007.

The existing short-presentation flyer that had been initially created in French for a specific Geneva event is now also available in English



The new MaNEP presentation booklet

for a broader use within the network. Post-its with MaNEP's new logo and some improvements have been made, both for internal use and as giveaways.

## Improving other existing PR tools

**e-Newsletter:** started in June 2005, the e-Newsletter is mainly meant as a channel available to all members with the idea of making them more familiar with each other, as well as providing fresh news (!) on management projects, research highlights, special achievements, special events, etc.

Seven issues were published during year 6 (January to December 06). This relatively high frequency has allowed it to become something familiar and – it seems – rather appreciated. Calls for contributions work especially well for recent top publications and requests to a specific member to write on a specific subject. They prove less successful when it comes to providing news (awards, events, media features, reading tips, etc.) on a spontaneous basis. An informal poll recently showed strong support for the continuation of the e-Newsletter, though it seems that fewer issues per year would be seen as sufficient. This has still to be decided.

**Website:** benefiting of regular updates, MaNEP's website is still undergoing a massive modification in both structure and content (except for the home page, the design will remain nearly unchanged); these changes are still hidden 'behind the scenes'; they should be completed and made visible by the end of 2007. Initially created in English only, the website will also be made available in French for the sake of the home-institution's local audience - part of them being crucial target-groups (press, politicians, etc.) for the survival of MaNEP in the long run.

## MaNEP in the media

Major research breakthroughs are definitely what the (general) media are hungry for, but they are also a rare thing, the natural pace of fundamental research being such a slow process. As a consequence, having regular exposure in the media is a challenge all NCCR probably share.

However year 6 has shown that MaNEP is gaining always more credibility as a source of top experts and research; for instance, several TV and radio shows as well as the press have relied on our members for expertise and interviews on 'nanotechnology' issues. Prestigious awards received have also been published in newspapers.



*French TV crew "C'est pas sorcier" in MaNEP labs.*

On a regional level MaNEP is now clearly perceived as an asset worth many pages and pictures in a luxury review like *Byblos*.

In year 6 we have also observed a strong interest from the UniGE magazine (Campus) and website which have issued many articles on MaNEP's various activities.

Finally it is worth mentioning that we expect (or at least hope for) a fair share of media attention thanks to an event called the **SupraFête** (read below) to be held in June 2007, at UniGE (Institut de Physique).

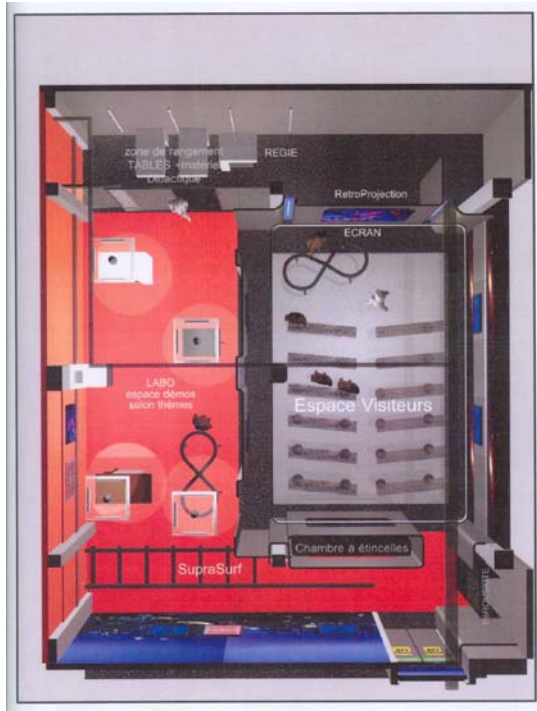
## Preparing the "SupraFête"

2007 marks the 20<sup>th</sup> anniversary of the 1987 (Swiss and German) Nobel Prize which started a new era in superconductivity. During year 6 the preparation of an ambitious 3-day celebration (on June 8-9-10) has kept our Geneva team pretty busy already. The event is aimed at the general public and will consist of a series of conferences (launch with Nobel Prize winner Georg Bednorz confirmed), exhibition with cartoonist Mix & Remix, presentation of MaNEP's KTT activities, showing of a MaNEP movie on superconductivity, demos and activities for children. Feedback will of course be provided in the next Progress Report.

## Plan for a "PhysicsPark"

Since the public event organized in 2002 by MaNEP for its inauguration, the need to for a permanent instrument promoting physical sciences in the Geneva area has emerged. A committee was set up by MaNEP, in collaboration with the Physics Department of UNIGE, to work on a concept.

The first step was to set up a list of themes, selected among local research area, likely to be of interest to the general public. From cosmology to applied physics, particle physics and solid state physics, six fields were selected. For each one, a specific demonstration – or illustration – was designed.



Provisional plan of the show-room to be installed in the physics building of the University of Geneva.

Their construction has started and shall be completed in summer 2007.

The second step was to establish a way to valorise these scientific contents. Collaboration with professionals of the media was initiated leading to the concept of a room of 146 m<sup>2</sup> with two areas: a space for multimedia presentations and a zone for interactive demonstrations. To finance this instrument dedicated to communication of physics, search for sponsors was initiated. The construction costs are almost completely covered thanks to a generous contribution from the H. Dudley Wright Foundation dedicated to the advancement of science and science education. Therefore the construction of the

*PhysicsPark* (working title) should also be completed in summer 2007. Supplementary sponsors were contacted to finance the running costs of the project and a team to manage the exploitation is to be set soon up.

Close contacts with the *Direction de l'Enseignement post-obligatoire du Département de l'Instruction Publique du Canton de Genève* were established as the *PhysicsPark* will be of primary interest for the students of high-schools and junior-high-schools. The positive response of the directions of both the *Collège de Genève* (high-school) and *Cycle d'Orientation* (junior-high-school) allowed us to establish collaborations with the physics teachers of these two education sectors covering 31 schools to work constructively for an appropriate use of the *PhysicsPark*. An important aspect emerged from these contacts: the strong wish of the teachers to benefit from *PhysicsPark* in their teaching. The collaboration is continuing to work along this line, so new demonstrations shall be added to set of six, developed by MaNEP and the Department of Physics.

### MaNEP demos

The set of demonstrations developed within MaNEP in the past years were, this year again, exhibited in a number of public events and shown in primary, junior-high and high schools (see list 8.7, section "Other forms of knowledge transfer").

In addition, the construction of new demos was initiated. The "*SupraSurf*" is the most promising one: it shall allow a seated person to levitate and move along a 6 meter long track. The *SupraSurf* will be uncovered during the *SupraFête* of June 2007. Another smaller levitation setup was also developed. In contrast to other devices, the motion of this mini-train is maintained by an electro-magnetic drive.



## 6 Management

### 6.1 Activities

As a reminder, the NCCR MaNEP is managed by four bodies: The **MaNEP Forum** gathering all MaNEP group leaders and some senior scientists, the **MaNEP Scientific committee** composed of the six MaNEP project leaders, the **MaNEP Management committee** in Geneva composed of all people having a specific responsibility and, last but not least, the new **MaNEP Advisory board** which is just being set up. *(so we're going to present this new structure but we will report on its activity in the next Progress report, because it is planned that this new entity will meet during the next Swiss Workshop MaNEP which will be held in Les Diablerets September 28-30, 2007)*

#### The MaNEP Forum

During this sixth MaNEP year, we have welcomed three new members to the Forum: In August 2006, Prof. **Christian Bernhard** from the University of Fribourg integrated MaNEP. He is a specialist in infrared spectroscopy. At the same date, Dr **Elvezio Morenzoni** from Paul Scherrer Institute where he is in charge of the Low-Energy Muon group, also integrated MaNEP. A new Professor: **Christophe Renner** has just been officially appointed to the Department of Condensed Matter Physics of the University of Geneva and is integrating MaNEP at present as a specialist of Scanning Tunneling Spectroscopy. In addition, Prof Piero Martinoli from the university of Neuchâtel has left the MaNEP Forum because in September 2006 he accepted the presidency of the Università della Svizzera Italiana, but he will actively go on contributing to MaNEP by becoming President of the new MaNEP External Advisory Board...

The MaNEP Forum met twice during this sixth MaNEP year.

The first meeting was held on the 28th of September 2006 in the University of Geneva and the following subjects were brought up for discussion: the appointment of Prof. Renner, the establishment of the new Advisory Board (presented here below), information about MaNEP Phase III, the six MaNEP Internal Workshops, one per MaNEP scientific project (future dates were fixed), and the way to establish the MaNEP Progress report.

On the 18th of January 2007, between the MaNEP Internal Workshops of Projects 1& 2 which gathered the most of MaNEP Forum members, the second meeting of the MaNEP Forum took place in Neuchâtel. The Agenda concerned:

- The year 6 Progress Report
- The decision to carry on the principle of summer internships for young female students or not. It was agreed to carry on.
- The next Swiss MaNEP Workshop 2007 in les Diablerets
- The MaNEP participation in the next Swiss Physical Society Meeting 2008
- Finding a date for the following MaNEP summerschool (which, in fact, is going to become a "winterschool"...) )
- And before closing this meeting, some short scientific communications were presented.

#### The MaNEP Scientific committee

The MaNEP Scientific committee is composed of the six MaNEP scientific project leaders. As in last year, an internal workshop per project was organized:

- Project 1: « Strongly interacting electrons, low-dimensional and quantum fluctuation dominated systems » of which the Project leader is **M. Sigrist** took place in Neuchâtel on January 19th, 2007.
- Project 2: "Superconductivity, unconventional mechanisms and novel materials" of which the Project leader is **D. Van der Marel** took place in Neuchâtel on January 18th, 2007.
- Project 3: "Crystal growth" of which the Project leader is **L. Forró** took place in EPFL, Lausanne on January 26th, 2007.
- Project 4: "Novel materials" of which the Project leader is **J. Hulliger** took place in University of Berne on January 25th, 2007.
- Project 5: "Thin films, artificial materials and novel devices" of which the Project leader is **J-M. Triscone** took place in Neuchâtel on January 17th, 2007.
- Project 6: "Industrial applications and pre-application development" of which the Project leader is **Ø. Fischer** took place in Neuchâtel on January 23rd, 2007.

As last year, these internal workshops were successful and afterwards the Project leaders

made the scientific report of the collaborative project they manage.

The six members of the MaNEP scientific committee met twice formally during this sixth MaNEP year:

The first time on June the 15th of 2006 to discuss the evaluation and progress of the respective projects they manage, to propose a concept and names for a new advisory board, to select a "mobile post-doc" candidate, and to choose dates for next meetings.

The second meeting on September the 1st of 2006 was held to prepare the next MaNEP Topical meeting of September the 27th to select speakers based on abstracts received, to select chairmen, and to discuss the details of the program.

The 6 members of the MaNEP Scientific Committee are also frequently consulted by email by the MaNEP Director so that they can give their opinion concerning the application of a new forum member, and suggest names of speakers to be invited to a MaNEP meeting...

## The MaNEP Management committee

The MaNEP management committee, composed of the Director, deputy Director and people in charge of the administration, education and advancement of women, knowledge and technology transfer, communication and public relations, and website; meets roughly once a month.

The MaNEP management committee organised different tasks and events such as:

- The **MaNEP Summerschool** which took place for the second time in Saas-Fee from September 11-16, 2006 with 78 participants. The subject was "Probing the Physics of Low Dimensional Systems" and 62 students (mainly PhD students) followed the courses.

- The 2006 **Martin Peter Colloquium** took place in the University of Geneva on Wednesday the 27th of September 2006. A topical meeting on Novel Superconductors was organized. Ten talks were given by young MaNEP researchers and a poster session gathered roughly 150 participants. To end this meeting, the Martin Peter Colloquium was given by P.W. Anderson, from Princeton University, USA.

- We have decided to carry on with the concept of "**Mobile Post-Doc**" initiated in MaNEP Phase I. So, 2 positions for 2 young MaNEP researchers aiming to develop an original project using, and within, the MaNEP network were announced in September 2006 and

January 2007. In this "Mobile post-Doc" concept, the project has to be carried out in two or more of the groups participating in MaNEP. This concept is successful in the MaNEP Network because 3 group leaders on average (institutions and/or industrial companies) support an applicant's project. But we notice that applicants give priority to employment security because 2 selected candidates preferred to give up the Mobile Post-doc project in order to take a permanent job position.

In conclusion, one applicant has started as a new mobile post-doc, and we are at present evaluating others projects to choose one or two more Mobile Post-Doc(s).

- On Phase I and in order to favour synergy between MaNEP members, the Director proposed to use part of the money coming from the "Reserve" fund to finance **collaborations** inside MaNEP. 2 cumulative conditions were required: the collaboration had to include a minimum of 2 different MaNEP projects coming from at least 2 different institutions. These collaborations have been a large success on MaNEP Phase I because 8 have been initiated. So at the end of October 2006, we gave a call to MaNEP Forum members to propose that they shared money for new collaborations, under the same conditions as in Phase I. We received 4 new collaboration projects and three are presently being set up.

## The new MaNEP Advisory board

During the last site visit, the MaNEP Review Panel made the following statements: "*The role of the advisory board must be clarified. It should be an independent body including external scientists if its main task is to give advice to the NCCR*" and "*The NCCR should work out a concept to guarantee internal evaluation of the performance within MaNEP*".

Consequently the NCCR MaNEP has established two new advisory organs which also evaluate progress and projects:

On one hand an **External Advisory Board** composed of well known scientists coming from outside Switzerland, and a President who knows the functioning and activities of MaNEP. This External Advisory Board will review the activities of MaNEP and give advice to the Director on future activities. It meets ideally once a year but at least twice during a four year period. The first meeting of the MaNEP External Advisory Board is planned during the Swiss Workshop MaNEP which will be held in Les Diablerets, September 28-30, 2007.



The President is Prof. **Piero Martinoli**, a former MaNEP group leader who is now President of the Università della Svizzera Italiana, and the six members are Prof. **Denis Jérôme** from University Paris Sud Orsay France, Prof. **Robert J. Cava** from Princeton University USA, Prof. **Dave Blank** from the University of Twente Netherlands, Professor **George Sawatzky** from the University of British Columbia Canada, Professor **Andrew Millis** from Columbia University USA and Professor **Antoine Georges** from Ecole Normale Supérieure France.

All these people have been appointed by the MaNEP Director after having consulted the Forum.

On the other hand an **Internal Evaluation Board**, composed of the Scientific Committee and three MaNEP senior scientists who are Profs. **R. Flükiger**, **T.M. Rice** and **H.R. Ott**, is in charge of an internal evaluation. It is planned it meets once a year to discuss each progress report and future directions of MaNEP.

## 6.2 Experiences, recommendations to the SNSF

We still have the same request as last year concerning the SNSF tool NIRA. We ask SNSF, if possible, to make it more flexible to use for the new MaNEP structure which is centred around collaborative projects instead of individual projects. We would like to have a solution which would allow us, when we prepare this report, to treat the scientific part

per collaborative project and the administrative part per individual group leader.

In addition to the inadequacy of NIRA for the structure of MaNEP, its slowness is a real burden for the persons in charge of using NIRA.



## 8.5 Publications

The following lists cover the period from April 1<sup>st</sup> 2005 to March 31<sup>st</sup> 2006:

1. Scientific articles in journals with peer review
2. Scientific articles in journals without peer review
3. Books and scientific articles in anthologies
4. Books
5. Reports

The most important publications are outlined by an asterisk.

The lists are sorted by collaborative project. Lists sorted by group member are available on request.

### 8.5.1 Scientific articles in journals with peer review

#### GRUPE Ph. AEBI

(project 5)

C. BATTAGLIA, H. CERCELLIER, C. MONNEY, M. G. GARNIER, P. AEBI

**Stabilization of silicon honeycomb chains by trivalent adsorbates**  
*EPL* **77**, 36003 1-5 (2007)

F. CLERC, C. BATTAGLIA, M. BOVET, L. DESPONT, C. MONNEY, H. CERCELLIER, M. G. GARNIER, P. AEBI, H. BERGER, L. FORRÓ

**Lattice-distortion-enhanced electron-phonon coupling and Fermi surface nesting in 1T-TaS<sub>2</sub>**

*Phys. Rev. B* **74**, 155114, 1-7 (2006)

L. DESPONT, D. NAUMOVIC, F. CLERC, C. KOITZSCH, M.G. GARNIER, F.J. GARCIA DE ABAJO, M.A. VAN HOVE, P. AEBI

**X-ray photoelectron diffraction study of Cu(111): Multiple scattering investigation**  
*Surf. Sci.* **600**, 380-385 (2006)

\*L. DESPONT, C. LICHTENSTEIGER, C. KOITZSCH, F. CLERC, M.G. GARNIER, F.J. GARCIA DE ABAJO, E. BOUSQUET, P. GHOSEZ, J.-M. TRISCONI, P. AEBI

**Direct evidence for surface ferroelectric polar distortion in ultrathin lead titanate perovskite films**

*Phys. Rev. B* **73**, 094110, 1-6 (2006)

\*L. DESPONT, C. LICHTENSTEIGER, F. CLERC, M.G. GARNIER, F.J. GARCIA DE ABAJO, M.A. VAN HOVE, J.-M. TRISCONI, P. AEBI

**X-ray photoelectron diffraction study of ultra-thin films of PbTiO<sub>3</sub> films**  
*Eur. Phys. J. B* **49**, 141-146 (2006)

L. DESPONT, F. CLERC, M.G. GARNIER, H. BERGER, L. FORRO, P. AEBI

**Multiple scattering investigation of the 1T-TaS<sub>2</sub> surface termination**

*Eur. Phys. J. B* **52**, 421-426 (2006)

C. LICHTENSTEIGER, M. DAWBER, N. STUCKI, J.-M. TRISCONI, J. HOFFMAN, J.-B. YAU, C. H. AHN, L. DESPONT, P. AEBI

**Monodomain to polydomain transition in ferroelectric PbTiO<sub>3</sub> thin films with La<sub>0.67</sub>Sr<sub>0.33</sub>MnO<sub>3</sub> electrodes**

*APL* (accepted)

P. STAROWICZ, C. BATTAGLIA, F. CLERC, L. DESPONT, A. PRODAN, H.J.P. VAN MIDDEN, U. SZERER, A. SZYTULA, M.G. GARNIER, P. AEBI **Electronic Structure of ZrTe<sub>3</sub>**

*Journal of alloy and compounds* (accepted)

#### GRUPE D. BAERISWYL

(projects 1 & 2)

D. BAERISWYL, D. EICHENBERGER, B. GUT **Superconductivity in the two-dimensional Hubbard model?**

*Proc. 30th Int. Conf. of Theoretical Physics (Ustron 2006), to be published in phys. stat. sol. (b).*

D. EICHENBERGER, D. BAERISWYL **Superconducting ground state of the two-dimensional Hubbard model: a variational study** *Proc. 8th Int. Conf. On Materials and Mechanisms of Superconductivity and High Temperature Superconductors (Dresden 2006), to be published in Physica C*

Y. JIANG, T. EMIG **Ordering of geometrically frustrated classical and quantum triangular Ising magnets**

*Phys. Rev. B* **73**, 104452, 1-14 (2006)

Y. JIANG, T. EMIG

**Exotic phases in transverse field triangular Ising antiferromagnets**

*Proc. Int. Conf. On Highly Frustrated Magnetism (Osaka 2006), to be published in J. Phys.: Cond. Mat.*

## GROUPE C. BERNHARD

(project 2)

P. ADLER, A. LEBON, V. DAMLJANOVIC, C. ULRICH, C. BERNHARD, A. BORIS, A. MALIUK, C. LIN, B. KEIMER

**Magnetoresistance effects in  $SrFeO_{3-\delta}$ : Dependence on phase composition and relation to magnetic and charge order**

*Phys. Rev. B* **73**, 094451, 1-16 (2006)

\*J. CHAKHALIAN, J.W. FREELAND, G. SRAJER, J. STREMPFER, G. KHALIULLIN, J. CEZAR, T. CHARLTON, R. DAGLISH, C. BERNHARD, G. CRISTIANI, H.U. HABERMEIER, B. KEIMER **Magnetism at the interface between ferromagnetic and superconducting oxides**  
*Nature Physics* **2**, 244 (2006)

D. CHARALAMBOUS, E. M FORGAN, S. RAMOS, S. P. BROWN, R. J. LYCETT, D. H. UCKO, A. DREW, S. L. LEE, D. FORT, A. AMATO, U. ZIMMERMANN

**Driven vortices in type-II superconductors: A muon spin rotation study**

*Phys. Rev. B* **73**, 104514, 1-9 (2006)

V. DAMLJANOVIC, C. ULRICH, C. BERNHARD, B. KEIMER

**Raman scattering study of  $Ru(Sr,La)_2GdCu_2O_8$**

*Phys. Rev. B* **73**, 172502, 1-4 (2006)

\*Y. KROCKENBERGER, I. FRITSCH, M. PAVELKA, G. CRISTIANI, H. HABERMEIER, LI YU, C. BERNHARD, B. KEIMER, L. ALFF **Superconductivity in epitaxial thin films of  $Na_xCoO_2 \cdot yD_2O$**

*Appl. Phys. Lett.* **88**, 162501, 1-3 (2006)

G. MENON, A. DREW, U. DIVAKAR, S. LEE, R. GILARDI, J. MESOT, F. OGRIN, D. CHARALAMBOUS, E. FORGAN, N. MOMONO, M. ODA, C. DEWHURST, C. BAINES

**\*Muons as local probes of three-body correlations in the mixed state of type-II superconductors**

*Phys. Rev. Lett.* **97**, 177004, 1-4 (2006)

\*H. MOHOTTALA, B. WELLS, J. BUDNICK, W. HINES, C. NIEDERMAYER, C. BERNHARD, A. MOODENBAUGH, F. CHOU **Electronic phase separation in  $La_{2-x}Sr_xCuO_{4+y}$**

*Nature Materials* **5**, 377 (2006)

H. MOHOTTALA, B. WELLS, J. BUDNICK, W. HINES, C. NIEDERMAYER, C. BERNHARD, A. MOODENBAUGH, F. CHOU

**Electronic phase separation in  $La_{2-x}Sr_xCuO_{4+y}$**

*Physica B* **374**, 199 (2006)

T. NACHTRAB, C. BERNHARD, C.T. LIN, D. KÖLLE, R. KLEINER

**The ruthenocuprates: natural superconductor-ferromagnet multilayers**

*Comptes Rendus Physique* **7**, 68-85 (2006)

TRAJNEROWICZ, A. GOLNIK, C. BERNHARD, L. MACHTOUB, C. ULRICH, J. L. TALLON, M. CARDONA

**Isotope effects on the optical phonons of  $YBa_2Cu_4O_8$  studied by far infrared ellipsometry and Raman scattering**

*Phys. Rev. B* **74**, 104513, 1-9 (2006)

## GROUPE G. BLATTER

(projects 1 & 2)

\*A. DE COL, V. B. GESHKENBEIN, G. I. MENON, G. BLATTER

**Surface melting of the vortex lattice, *Phys. Rev. Lett.* **96**, 177001, 1-4 (2006)**

A. DE COL, G. I. MENON, G. BLATTER **Density functional theory of vortex lattice melting in layered superconductors: a mean-field substrate approach**

*Phys. Rev. B* **75**, 014518, 1-10 (2007)

S. D. HUBER, E. ALTMAN, H. P. BUCHLER, G. BLATTER

**Dynamical properties of ultra-cold bosons in an optical lattice**

*Phys. Rev. B* **75**, 085106, 1-12 (2007)

T. SHIBAUCHI, L. KRUSIN-ELBAUM, Y. KASAHARA, Y. SHIMONO, Y. MATSUDA, R. D. MCDONALD, C. H. MIELKE, S. YONEZAWA, Z. HIROI, M. ARAI, T. KITA, G. BLATTER, M. SIGRIST

**Uncommonly high upper critical field of the pyrochlore superconductor  $KOs_2O_6$  below the enhanced paramagnetic limit**

*Phys. Rev. B* **74**, 220506(R), 1-4 (2006)

## GROUPE M. BÜTTIKER

(projects 1 & 2)

\*M. BÜTTIKER

**Detecting and Controlling Electron Correlations**

*Science* **313**, 1587-1588 (2006)

M. BÜTTIKER, S. NIGG,

**Mesoscopic capacitance oscillations**

*Nanotechnology* **18**, 044029, 1-5 (2007)

H. FORSTER, P. SAMUELSSON, S. PILGRAM, M. BÜTTIKER

**Voltage and dephasing probes: a full counting statistics discussion**

*Phys. Rev. B* **75**, 035340, 1-17 (2007)

\*A. N. JORDAN, ALEXANDER N. KOROTKOV, MARKUS BÜTTIKER

**Leggett-Garg Inequality with a Kicked Quantum Pump**

*Phys. Rev. Lett.* **97**, 026805, 1-4 (2006)

\*S. NIGG, R. LOPEZ, M. BÜTTIKER

**Mesoscopic charge relaxation**

*Phys. Rev. Lett.* **97**, 206804, 1-4 (2006)

\*S. PILGRAM, P. SAMUELSSON, H. FORSTER AND M. BÜTTIKER

**Full counting statistics for voltage and dephasing probes**

*Phys. Rev. Lett.* **97** 066801, 1-4 (2006)

\*V. S. RYCHKOV AND M. BÜTTIKER

**Mesoscopic versus Macroscopic division of current fluctuations**

*Phys. Rev. Lett.* **96**, 166806, 1-4 (2006)

P. SAMUELSSON, M. BÜTTIKER

**Quantum state tomography with quantum shot noise**

*Phys. Rev. B* **73**, 041305(R), 1-4 (2006)

B. TRAUZETTEL, A.N. JORDAN, C.W.J. BEENAKKER, M. BÜTTIKER,

**Parity meter for charge qubits: an efficient quantum entangler**

*Phys. Rev. B* **73**, 235331, 1-7 (2006)

## GROUPE L. DEGIORGI

(project 1)

G. CAIMI, L. DEGIORGI, H. BERGER, L. FORRÓ

**Phonon analysis of the S=1 quantum spin systems  $Ni_5Te_4O_{12}X_2$  (X=Cl and Br)**

*J. Phys. Condens. Matter* **18**, 4065-4070 (2006)

G. CAIMI, L. DEGIORGI, H. BERGER, L. FORRO

**Optical evidence for a magnetically driven structural transition in the pin web  $Cu_3TeO_6$**

*Europhys. Lett.* **75**, 496-502 (2006)

L. DEGIORGI, D. JEROME

**Transport and optics in quasi-one-dimensional organic conductors**

*J. Phys. Soc. Jap.* **75**, 051004, 1-10 (2006)

L. DEGIORGI

**The Drude model in correlated systems**

*Ann. Phys.* **15**, 571-584 (2006)

M. PAPAGNO, D. PACILE', G. CAIMI, H. BERGER, L. DEGIORGI, M. GRIONI

**Electronic structure of one-dimensional copper oxide chains in  $LiCu_2O_2$  from angle-resolved photoemission and optical spectroscopy**

*Phys. Rev. B* **73**, 115120, 1-8 (2006)

A. PERUCCHI, L. DEGIORGI, RONGWEI HU, C. PETROVIC, V. F. MITROVIĆ

**Optical investigation of the metal-insulator transition in  $FeSb_2$**

*Eur. Phys. J. B* **54**, 175-183 (2006)

A. SACCHETTI, L. DEGIORGI, T. GIAMARCHI, N. RU, I.R. FISHER

**Chemical pressure and hidden one-dimensional behavior in rare-earth tri-telluride charge-density wave compounds**

*Phys. Rev. B* **74**, 125115, 1-7 (2006)

\*A. SACCHETTI, E. ARCANGELETTI, A. PERUCCHI, L. BALDASSARE, P. POSTORINO, S. LUPI, N. RU, I.R. FISHER, L. DEGIORGI

**Pressure dependence of the charge-density-wave gap in rare-earth tritellurides**

*Phys. Rev. Lett.* **98**, 026401, 1-4 (2007)

## GROUPE Ø. FISCHER

(projects 2, 5 & 6)

L. ANTOGNAZZA, M. DECROUX, M. THERASSE, M. ABPLANALP, J. DURON, B. DUTOIT, Ø. FISCHER

**Thermally assisted transition in thin film based fault current limiter: a way to speed up the normal transition across the wafer**

Accepted for publication in *IEEE Trans. On Applied Superconductivity*

C. DUBOIS, P.-E. BISSON, A.A. MANUEL, Ø. FISCHER, S. REYMOND

**Compact design of a low temperature XY stage scanning tunneling microscope**

*Rev. Sci. Instrum.* **77**, 043712, 1-5 (2006)

C. DUBOIS, N. JENKINS, A.A. MANUEL, N.D. ZHIGADLO, J. KARPINSKI, Ø. FISCHER

**Crystal-edge scanning tunnelling spectroscopy on aluminium-doped magnesium diboride**

*Supercond. Sci. Technol.* **19**, 695-698 (2006)  
doi:10.1088/0953-2048/19/8/002

C. DUBOIS, A. PETROVIC, G. SANTI, CH. BERTHOD, A. A. MANUEL, M. DECROUX Ø. FISCHER, M. POTEL, R. CHEVREL

**Node-like excitations in superconducting  $PbMo_6S_8$  probed by scanning tunneling spectroscopy**

*Phys. Rev. B* **75**, 104501, 1-4 (2007)

C. DUBOIS, G. SANTI, I. CUTTAT, CH. BERTHOD, N. JENKINS, A. A. MANUEL, Ø. FISCHER, G. SCHUCK, J. KARPINSKI

**Scanning Tunneling Spectroscopy in the Superconducting State and in the Vortex Cores of the  $\beta$ -pyrochlore  $KOs_2O_6$**

To be submitted in PRL

J. DURON, F. GRILLI, M. DECROUX, L. ANTOGNAZZA, B. DUTOIT, Ø. FISCHER

**Computer Modeling of YBCO Fault current limiter strips lines in over-critical regime with temperature dependent parameters**

Accepted for publication in *IEEE Trans. On Applied Superconductivity*

J. DURON, F. GRILLI, L. ANTOGNAZZA, M. DECROUX, S. STAVREV, B. DUTOIT, Ø. FISCHER

**Finite-element modeling of superconductors in over-critical regime with temperature dependent resistivity**

*Journal of Physics: Conference series* **43**, 1076 (2006)

J. DURON, F. GRILLI, L. ANTOGNAZZA, M. DECROUX, B. DUTOIT, Ø. FISCHER

**Finite-element modeling of YBCO fault current limiter with temperature dependent parameters**

Submitted to *Superconducting Science and Technology*

Y. FASANO, I. MAGGIO-APRILE, J. KARPINSKI, Ø. FISCHER

**Tunneling and Pseudo Point-contact Spectroscopy on  $YBa_2Cu_4O_8$**

To be published in *Physica C*

L. JANKOVIC, D. GOURNIS, P.N. TRIKALITIS, I. ARFAOUI, T. CREN, P. RUDOLF, M.-H. SAGE, T.T.M. PALSTRA, B. KOOI, J. DE HOSSON, M.A. KARAKASSIDES, K. DIMOS, A. MOUKARIKA, T. BAKAS

**Carbon nanotubes encapsulating superconducting single-crystalline tin nanowires**

*Nano Letters* **6**, 1131-1135 (2006)

A. KOHEN, T. CREN, Y. NOAT, T. PROSLIER, F. GIUBILEO, F. BOBBA, A.M. CUCOLO, N. ZHIGADLO, S.M. KAZAKOV, J. KARPINSKI, W. SACKS, D. RODITCHEV

**Recent progress in vortex studies by tunneling spectroscopy**

*Physica C* **437-438**, 145-148 (2006)

\* A. KOHEN, T. PROSLIER, T. CREN, Y. NOAT, W. SACKS, H. BERGER, D. RODITCHEV

**Probing the superfluid velocity with a superconducting tip: The Doppler shift effect**

*Phys. Rev. Lett.* **97**, 027001, 1-4 (2006)

H. NGUYEN XUAN, S. BEAUQUIS, P. GALEZ, C. JIMENEZ, F. WEISS, M. DECROUX, M. THERASSE

**Tl-based superconducting films by spray pyrolysis and MOCVD**

*J. Phys.: Conf. Ser.* **43281-43284** (2006)

A. PIRIOU, Y. FASANO, E. GIANNINI, Ø. FISCHER

**Doping-dependence of the Vortex Phase Diagram of  $Bi_2Sr_2Ca_2Cu_3O_{10+\delta}$**

To be published in *Physica C*

A. PETROVIC, Y. FASANO, R. LORTZ, M. DECROUX, M. POTEL, R. CHEVREL, Ø. FISCHER

**Unconventional resistive transitions in the extreme type-II superconductor  $Tl_2Mo_6Se_6$**

To be published in *Physica C*

\* TH. PROSLIER, A. KOHEN, Y. NOAT, T. CREN, D. RODITCHEV, W. SACKS

**Probing the superconducting condensate on a nanometer scale**

*Europhys. Lett.* **73**, 962-968 (2006)

W. SACKS, T. CREN, D. RODITCHEV, B. DOUÇOT

**Quasiparticle spectrum of the cuprate  $Bi_2Sr_2CaCu_2O_{8+\delta}$ : Possible connection to the phase diagram**

*Phys. Rev. B* **74**, 174517, 1-15 (2006)

H.R. SALVA, A.A. GHILARDUCCI, A.G. LEYVA, S. SEIRO

**Particle sliding in ceramic  $LaMnO_3$**

*Journal of Magnetism and Magnetic Materials* ( In press)

S. SEIRO, Y. FASANO, I. MAGGIO-APRILE, E. KOLLER, O. KUFFER, Ø. FISCHER

**Temperature Dependence of the Quasiparticle Excitation Spectrum in  $La_{0.77}Ca_{0.23}MnO_3$  films**

Submitted to PRL (2006)

S. SEIRO, Y. FASANO, I. MAGGIO-APRILE, O. KUFFER, Ø. FISCHER

**Homogeneous Spectroscopic Properties in Manganite Films**

*Journal of Magnetism and Magnetic Materials* ( In press)

## GRUPE R. FLÜKIGER (project 6)

- V. ABÄCHERLI, F. BUTA, D. UGLIETTI, C. SENATORE, B. SEEGER, R. FLÜKIGER  
**Investigation on the Effect of Ta Additions on  $J_c$  and  $n$  of  $(Nb,Ti)_3Sn$  Bronze Processed Multifilamentary Wires at High Magnetic Fields**  
Presented at the ASC06 Conference, Accepted for publication in *IEEE Trans. Appl. Supercond.* (2007)
- M. G. ADESSO, M. POLICETTI, S. PACE, D. UGLIETTI, R. FLÜKIGER  
**Common and different features in vortex dynamics of LTS, HTS and  $MgB_2$**   
presented at *CryoPrague*, 17-21 July 2006, Accepted for publication
- M. G. ADESSO, D. UGLIETTI, R. FLÜKIGER, M.P. POLICETTI, S. PACE  
**Phase Transition between the Bragg Glass and a Disordered Phase in  $Nb_3Sn$ , as detected by 3<sup>rd</sup> harmonics of the AC magnetic susceptibility**  
*Phys. Rev. B* **73**, 92513, 1-4 (2006)
- M. G. ADESSO, D. UGLIETTI, R. FLÜKIGER, S. PACE  
 **$Nb_3Sn$  single crystals, polycrystals and multifilamentary wires: common and different features in the magnetic response**  
*J. Phys.: Conference Series* Vol. **43**, 22 (2006)
- M. G. ADESSO, D. UGLIETTI, R. FLÜKIGER, M. POLICETTI, S. PACE  
**Investigations of magnetic behaviour in various type of  $Nb_3Sn$  multifilamentary wires by means of the 1st and 3rd harmonics of the AC magnetic susceptibility**  
*IEEE Trans. Appl. Supercond.* **16**, 1241 (2006)
- R. FLÜKIGER  
**Microstructure, Composition and Critical Current Density in  $Nb_3Sn$  wires»**  
in "State of the Art in Low Temperature Superconducting Materials for Magnet Applications  
*Cryogenics*, Special issue (to be published)
- R. FLÜKIGER, P. LEZZA, M. CESARETTI, C. SENATORE, R. GLADYSHEVSKI  
**Simultaneous Addition of  $B_4C$  +  $SiC$  to  $MgB_2$  wires and consequences for  $J_c$  and  $B_{irr}$**   
Presented at the ASC06 Conference, Accepted for publication in *IEEE Trans. Appl. Supercond.* (2007)
- R. FLÜKIGER, D. UGLIETTI, V. ABÄCHERLI B. SEEGER  
**Asymmetric Behaviour of  $J_c$  ( $\epsilon$ ) in  $Nb_3Sn$  Wires and correlation with the stress induced elastic tetragonal distortion**  
*Supercond. Sci. Technol.*, **18**, 416-423 (2005)
- P. LEZZA, R. GLADYSHEVSKII, H.L. SUO, R. FLÜKIGER  
**Quantitative study of the inhomogeneous distribution of phases in Fe-sheathed ex situ  $MgB_2$  tapes**  
*Supercond. Sci. Technol.* **18**, 753-757 (2005)
- P. LEZZA, R. GLADYSHEVSKII, V. ABÄCHERLI, R. FLÜKIGER  
**Texture gradients in Fe-sheathed ex situ  $MgB_2$  tapes**  
*Supercond. Sci. Technol.* **19**, 286-289 (2006)
- P. LEZZA, C. SENATORE, R. FLÜKIGER  
**Improved critical current densities in  $B_4C$  doped  $MgB_2$  based wires**  
*Supercond. Sci. Technol.* **19**, 1030-1033 (2006)
- P. LEZZA, C. SENATORE, R. GLADYSHEVSKII, R. FLÜKIGER  
**Critical Current Anisotropy and Texture Gradients in ex situ  $MgB_2/Fe$  Tapes**  
Presented at the ASC06 Conference, Accepted for publication in *IEEE Trans. Appl. Supercond.* (2007)
- B. SEEGER, A. FERREIRA, V. ABÄCHERLI, T. BOUTBOUL, L. OBERLI, R. FLÜKIGER  
**Transport Properties up to 1000 A of  $Nb_3Sn$  Wires Under Transverse Compressive Stress**  
Presented at the ASC06 Conference, Accepted for publication in *IEEE Trans. Appl. Supercond.* (2007)
- C. SENATORE, P. LEZZA, R. FLÜKIGER,  
**Critical Current Anisotropy, Pinning Properties and Relaxation Rate of "Ex Situ"  $MgB_2/Fe$  Tapes**  
*Adv. Cryo. Engrg.* **52**, 654-661 (2006)
- C. SENATORE, P. LEZZA, R. FLÜKIGER  
**Determination of the texturing gradient in ex situ  $MgB_2 /Fe$  tapes examined by X-ray diffraction and its effects on the pinning force**  
*J. Appl. Phys.* **100**, 113913, 1-5 (2006)
- C. SENATORE, P. LEZZA, R. LORTZ, O. SHCHERBAKOVA, S.X. DOU, R. FLÜKIGER  
**Specific heat and magnetic relaxation analysis of  $MgB_2$  bulk samples with and without additives**  
Presented at the ASC06 Conference, Accepted for publication in *IEEE Trans. Appl. Supercond.* (2007)
- C. SENATORE, D. UGLIETTI, V. ABÄCHERLI, A. JUNOD, R. FLÜKIGER  
**Specific heat, a method to determine the  $T_c$  distribution in various industrial  $Nb_3Sn$  wires**  
Presented at the ASC06 Conference, Accepted for publication in *IEEE Trans. Appl. Supercond.* (2007)
- C. SENATORE, D. UGLIETTI, R. FLÜKIGER  
**Relaxation Rates of Y-123 and Bi-based Tapes Compared to Low  $T_c$  and  $MgB_2$  Superconductors in View of Persistent Mode Operation in High Field Magnets**  
Submitted to *Appl. Phys.Lett.*
- D. UGLIETTI, V. ABÄCHERLI, M. CANTONI, R. FLÜKIGER  
**Grain growth, Morphology and Composition Profiles in Industrial  $Nb_3Sn$  wires**  
Presented at the ASC06 Conference, Accepted for publication in *IEEE Trans. Appl. Supercond.* (2007)

D. UGLIETTI, V. ABÄCHERLI, B. SEEBER, R. FLÜKIGER

**The effect of Ti addition on Critical Parameters and Transport Properties of Quaternary (Nb,Ta,Ti)<sub>3</sub>Sn Wires**

*Supercond. Sci. Technol.* **19**, 1185-1190 (2006)

D. UGLIETTI, B. SEEBER, V. ABÄCHERLI, M. CANTONI, R. FLÜKIGER

**Strain and Field Scaling Laws for Internal Sn and Bronze Nb<sub>3</sub>Sn Wires up to 21 T**

*Adv. Cryo. Engrg.*, **52** (2006)

D. UGLIETTI, B. SEEBER, V. ABÄCHERLI, W.L. CARTER, R. FLÜKIGER

**Critical Current vs. Applied Strain for Industrial Y-123 Coated Conducors at Various Temperatures and Magnetic Fields up to 19 T**

*Supercond. Sci. Technol.* **19**, 869-872 (2006)

Y. WANG, C. SENATORE, V. ABÄCHERLI, D. UGLIETTI, R. FLÜKIGER

**Specific Heat of Nb<sub>3</sub>Sn Wires**

*Supercond. Sci. Technology* **19**, 263-266 (2006)

## GROUPE L. FORRÓ

(projects 1 & 6)

A. AKRAP, N. BARISIC, L. FORRÓ, D. MANDRUS, B.C. SALES

**High pressure resistivity and thermoelectric power in Yb<sub>14</sub>MnSb<sub>11</sub>**

*Physical Review B* (accepted)

A. AKRAP, E. TUTIS, S. M. KAZAKOV, N. D. ZHIGADLO, J. KARPINSKI, L. FORRÓ

**Manifestations of the features of the density of states in the transport properties of KO<sub>2</sub>O<sub>6</sub>** *Physical Review B* (accepted)

A. AKRAP, T. WELLER, M. ELLERBY, S.S. SAXENA, G. CSANYI, L. FORRÓ

**C<sub>6</sub>Yb and graphite: a comparative high pressure transport study**

*Physical Review B* (accepted)

G. CAIMI, L. DEGIORGI, H. BERGER, L. FORRÓ

**Optical evidence for a magnetically driven structural transition in the spin web Cu<sub>3</sub>TeO<sub>6</sub>**

*Europhys Letters* **75**, 496-502 (2006)

G. CAIMI, L. DEGIORGI, H. BERGER, L. FORRÓ

**Phonon analysis of the S=1 quantum spin systems Ni<sub>5</sub>Te<sub>4</sub>O<sub>12</sub>X<sub>2</sub> (X = Cl and Br)**

*Journal of Physics -Condensed Matter* **18**, 4065-4070 (2006)

\*I. KEZSMARKI, G. Y. MIHALY, R. GAAL, N. BARISIC, A. AKRAP, H. BERGER, L. FORRÓ, C. C. HOMES, L. MIHALY

**Separation of orbital contributions to the optical conductivity of BaVS<sub>3</sub>**

*Physical Review Letters* **96**, 186402, 1-4 (2006)

H.L. LIU, M. QUIJADA, D.B. ROMERO, D.B. TANNER, A. ZIBOLD, G.L. CARR, H. BERGER, L. FORRO, L. MIHALY, G. CAO, B.H. O, J.T. MARKERT, J.P. RICE, M.J. BURNS, K.A. DELIN

**Drude behavior in the far-infrared conductivity of cuprate superconductors**

*Annalen Der Physik* **15**, 606-618 (2006)

\*L. MIHALY, B. DORA, A. VANYOLOS, H. BERGER, L. FORRÓ

**Spin-lattice interaction in the quasi-one-dimensional helimagnet LiCu<sub>2</sub>O<sub>2</sub>**

*Physical Review Letters* **97**, 067206, 1-4 (2006)

R.P. SMITH, A. KUSMARTSEVA, Y.T.C. KO, S.S. SAXENA, A. AKRAP, L. FORRÓ, M. LAAD, T.E. WELLER, M. ELLERBY, N.T. SKIPPER

**Pressure dependence of the superconducting transition temperature in C<sub>6</sub>Yb and C<sub>6</sub>Ca**

*Physical Review B* **74**, 024505, 1-4 (2006)

## GROUPE T. GIAMARCHI

(projects 1 & 2)

L. BENFATTO, C. CASTELLANI, T. GIAMARCHI

**Signatures of Kosterlitz-Thouless behavior in anisotropic layered superconductors**

cond-mat/0609287, accepted to PRL (2007)

\*C. BERTHOD, T. GIAMARCHI, S. BIERMANN, A. GEORGES

**Breakup of the Fermi surface near the Mott transition in low-dimensional systems**

*Phys. Rev. Lett.* **97**, 136401, 1-4 (2006)

M. A. CAZALILLA, A. F. HO, T. GIAMARCHI

**Interacting Bose gases in quasi-one dimensional optical lattices**

*New. J. Phys.* **8**, 158, 1-55 (2006)

L. F. CUGLIANDOLO, P. LE DOUSSAL, T. GIAMARCHI



**Dynamic Compressibility and aging in Wigner crystals and quantum glasses**

\*Phys. Rev. Lett. **96**, 217203, 1-4 (2006)

A. IUCCI, M. A. CAZALILLA, A. F. HO, T. GIAMARCHI

**Energy absorption of a Bose gas in a periodically modulated optical lattice**

Phys. Rev. A **73**, 041608(R), 1-4 (2006)

T. JARLBORG

**Effects of spin-phonon interaction within the CuO plane of high- $T_c$  superconductors**

Physica C (in press)

\*C. KOLLATH, A. IUCCI, T. GIAMARCHI, W. HOFSTETTER, U. SCHOLLWOCK

**Spectroscopy of ultracold atoms by periodic lattice modulations**

Phys. Rev. Lett. **97**, 050402, 1-4 (2006)

C. KOLLATH, A. IUCCI, I. P. MCCULLOCH, T. GIAMARCHI

**Modulation spectroscopy with ultracold fermions in an optical lattice**

Phys. Rev. A **74**, 041604(R), 1-4 (2006)

C. KOLLATH, U. SCHOLLWÖCK

**Cold Fermi gases: A new perspective on spin-charge separation**

New J. Phys. **8**, 220, 1-18 (2006)

U. LONDON, T. GIAMARCHI, D. ORGAD

**Disorder effects in fluctuating one-dimensional interacting systems**

Phys. Rev. B **73**, 134201, 1-14 (2006)

E. ORIGNAC, A. ROSSO, R. CHITRA, T. GIAMARCHI

**Coulombian Disorder in Periodic Systems: Effect of unscreened charged impurities**

Phys. Rev. B **73**, 035112, 1-11 (2006)

P. PARUCH, T. GIAMARCHI, T. TYBELL, J. M. TRISCONI

**Nanoscale studies of domain wall motion in epitaxial ferroelectric thin films**

J. Applied Physics **100**, 051608, 1-10 (2006)

\*P. PEDRAZZINI, H. WILHELM, D. JACCARD, T. JARLBORG, M. SCHMIDT, M. HELFLAND, L. AKSELRUD, H.Q. YUAN, U. SCHWARZ, YU. GRIN, F. STEGLICH

**Metallic State in Cubic FeGe Beyond Its Quantum Critical Phase Transition**

Phys. Rev. Lett. **98**, 047204, 1-4 (2007)

A. SACCHETTI, L. DEGIORGI, T. GIAMARCHI, N. RU, I. R. FISCHER

**Chemical pressure and hidden one-dimensional behavior in rare-earth tri-telluride charge-density wave compounds**

Phys. Rev. B **74**, 125115, 1-7 (2006)

C. WEBER, A. LAEUCHLI, F. MILA, T. GIAMARCHI

**Magnetism and superconductivity of strongly correlated electrons on the triangular lattice**

Phys. Rev. B **73**, 014519, 1-10 (2006)

**GRUPE M. GRIONI**

(projects 1 & 2)

C. R. AST, D. PACILÉ, M. PAPAGNO, TH. GLOOR, F. MILA, S. FÉDRIGO, G. WITTICH, K. KERN, H. BRUNE, M. GRIONI

**Orbital selective overlayer-substrate hybridization in a Pb monolayer on Ag(111)**

Phys. Rev. B **73**, 245428, 1-6 (2006)

S. COLONNA, F. RONCI, A. CRICENTI, L. PERFETTI, H. BERGER, M. GRIONI

**Scanning tunneling microscopy observation of a Mott insulator phase at the 1T-TaSe<sub>2</sub> surface**

Jap. J. Appl. Phys. **45**, N°3B, 1950-1952 (2006)

C. DALLERA, O. WESSELY, M. COLARIETI-TOSTI, O. ERIKSSON, R. AHUJA, B. JOHANSSON, M.I. KATSNELSON, E. ANNESE, J.-P. RUEFF, G. VANKO, L. BRAICOVICH, AND M. GRIONI

**Understanding mixed valent materials: Effects of dynamical core-hole screening in high-pressure x-ray spectroscopy**

Phys. Rev. B **74**, 081101(R), 1-4 (2006)

G. GHIRINGHELLI, A. PIAZZALUNGA, C. DALLERA, G. TREZZI, L. BRAICOVICH, T. SCHMITT, V.N. STROCOV, R. BETEMPS, L. PATTHEY, X. WANG, M. GRIONI

**SAXES, a high resolution spectrometer for resonant x-ray emission in the 400-1600 eV energy range**

Rev. Sci. Instrum. **77**, 113108, 1-9 (2006)

M. MEDARDE, C. DALLERA, M. GRIONI, J. VOIGT, A. PODLESNYAL, E. POMJAKUSHINA, K. CONDER, TH. NEISIUS, O. TJERNBERG, S.N. BARILO

**The low-temperature spin-state transition in LaCoO<sub>3</sub> investigated using resonant x-ray absorption at the Co K edge**

Phys. Rev. B **73**, 054424, 1-10 (2006)

L. MORESCHINI, C. DALLERA, J.J. JOYCE, J.L. SARRAO, E.D. BAUER, V. FRITSCH, S. BOBEV, E. CARPENE, S. HUOTARI, G. VANKO, G. MONACO, P. LACOVIG, G. PANACCIONE, A. FONDACARO, G. PAOLICELLI, P. TORELLI, AND M. GRIONI

**A comparison of bulk-sensitive spectroscopic probes of Yb valence in Kondo systems**  
*Phys. Rev. B* **75**, 035113, 1-7 (2007)

D. PACILÉ, C.R. AST, M. PAPGNO, C. DA SILVA, L. MORESCHINI, M. FALUB, A.P. SEITSONEN, M. GRIONI

**Electronic structure of an ordered Pb/Ag(111) surface alloy: Theory and experiment**  
*Phys. Rev. B* **73**, 245429, 1-6 (2006)

M. PAPAGNO, D. PACILÉ, G. CAIMI, H. BERGER, L. DEGIORGI, M. GRIONI

**Electronic structure of one-dimensional copper chains in  $\text{LiCu}_2\text{O}_2$  from angle-resolved photoemission and optical spectroscopy**  
*Phys. Rev. B* **73**, 115120, 1-8 (2006)

X. WANG, H. MICHOR, M. GRIONI

**Probing the nature of the Ce 4f states in  $\text{CeX}_9\text{Si}_4$  ( $X=\text{Ni, Co}$ ) by high-energy spectroscopies**  
*Phys. Rev. B* **75**, 035127, 1-5 (2007)

## GRUPE M. HASLER

(project 6)

J. DURON, F. GRILLI, L. ANTOGNAZZA, M. DECROUX, B. DUTOIT, O. FISCHER

**Finite-element modelling of YBCO fault current limiter with temperature dependent parameters**

*Superconductor Science and Technology*, vol. **20**, no. 3 (2007)

J. DURON, F. GRILLI, L. ANTOGNAZZA, M. DECROUX, S. STAVREV, B. DUTOIT, O. FISCHER

**Finite-element modelling of superconductors in over-critical regime with temperature dependent resistivity**  
*7th European Conference on Applied Superconductivity*, vol. *Journal of Physics of Conference Series*, pp. 1076-1080 (2006)

S. STAVREV, F. GRILLI, B. DUTOIT, S. ASHWORTH

**Finite-element analysis and comparison of the AC loss performance of BSCCO and YBCO conductors**

*7th European Conference on Applied Superconductivity*, vol. *Journal of Physics of Conference Series*, pp. 581-586 (2006)

## GRUPE J. HULLIGER

(project 4)

G. COUDERC, J. B. WILLEMS, B. TRUSCH, J. HULLIGER

**Optical recognition of local reaction products in ceramic combinatorial syntheses**

*Mater. Res. Bull.* 2007 (in press)

L. DESSAUGES, J. B. WILLEMS, D. FAVRE, C. BOHRER, F. HELBLING, J. HULLIGER

**Theory of high gradient attractive magnetic separation of superconducting materials and its experimental verification by  $\text{YBa}_2\text{Cu}_3\text{O}_x$  particles**  
*Supercond. Sci. Technol.* **19**, 748-755 (2006)

## GRUPE J. KARPINSKI

(projects 3 & 4)

M. BRÜHWILER, B. BATLOGG, S. M. KAZAKOV, J. KARPINSKI

**Mass enhancement, correlations, and strong-coupling superconductivity in the  $\beta$ -pyrochlore  $\text{KOs}_2\text{O}_6$**

*Physical Rev. B* **73**, 094518, 1-10 (2006)

M. BRÜHWILER, B. BATLOGG, S.M. KAZAKOV, CH. NIEDERMAYER, J. KARPINSKI

**$\text{Na}_x\text{CoO}_2$ : Enhanced low-energy excitations of electrons on a 2d triangular lattice**  
*Physica B: Condensed Matter* **378-380**, 630-631, (2006)

M. BRÜHWILER, S.M. KAZAKOV, J. KARPINSKI, B. BATLOGG

**Large mass enhancement in  $\text{RbOs}_2\text{O}_6$**

*Journal of Physics and Chemistry of Solids* **67**, 493-496 (2006)

R. CUBITT, C.D. DEWHURST, M.R. ESKILDSEN, S.J. LEVETT, A. MATADEEN, J. JUN, S.M. KAZAKOV, J. KARPINSKI, S.L. BUD'KO, N.E. ANDERSON, P.C. CANFIELD

**Penetration depth anisotropy in  $\text{MgB}_2$  single crystals and powders**

*Journal of Physics and Chemistry of Solids* **67**, 493-496 (2006)

D. DAGHERO, R.S. GONNELLI, G.A. UMMARINO, A. CALZOLARI, VALERIA DELLAROCCHA, V.A. STEPANOV, S.M. KAZAKOV, J. JUN, J. KARPINSKI

**Effect of the magnetic field on the gaps of  $\text{MgB}_2$ : A directional point-contact study**

*Journal of Physics and Chemistry of Solids* **67**, Issues 1-3, 424-427 (2006)

D. DICASTRO, M. ORTOLANI, E. CAPPELLUTI, U. SCHADE, N.D. ZHIGADLO, J. KARPINSKI

**Infrared properties of  $\text{Mg}_{1-x}\text{Al}_x(\text{B}_{1-y}\text{C}_y)_2$  single crystals in the normal and superconducting state**  
*Phys. Rev. B* **73**, 174509, 1-12 (2006)

C. DUBOIS, N. JENKINS, A.A. MANUEL, O. FISCHER, N.D. ZHIGADLO, J. KARPINSKI

**Crystal-edge scanning tunneling spectroscopy on aluminium-doped magnesium diboride**  
*Supercond. Sci. Technol.* **19**, 695-698 (2006)

J.L. GAVILANO, B. PEDRINI, K. MAGISHI, M. WELLER, J. HINDERER, H.R. OTT, S.M. KAZAKOV, J. KARPINSKI

**Localized versus itinerant magnetic moments in  $\text{Na}_{0.7}\text{CoO}_2$**   
*Phys. Rev. B* **74**, 064410, 1-10 (2006)

R.S. GONNELLI, D. DAGHERO, A. CALZOLARI, G.A. UMMARINO, M. TORTELLO, V.A. STEPANOV, N.D. ZHIGADLO, K. ROGACKI, J. KARPINSKI, C. PORTESI, E. MONTICONE, D. MIJATOVIC, D. VELDHUIS, A. BRINKMAN

**Recent achievements in  $\text{MgB}_2$  physics and applications: A large-area SQUID magnetometer and point-contact spectroscopy measurements**  
*Physica C: Superconductivity, Volume* **435**, 59-65 (2006)

\* R.S. GONNELLI, D. DAGHERO, G.A. UMMARINO, A. CALZOLARI, M. TORTELLO, V.A. STEPANOV, N. D. ZHIGADLO, K. ROGACKI, J. KARPINSKI, F. BERNARDINI, S. MASSIDDA

**The effect of magnetic impurities in a two-band superconductor: A point-contact study of Mn-substituted  $\text{MgB}_2$  single crystals**  
*Phys. Rev. Lett.* **97**, 037001, 1-4 (2006)

R.S. GONNELLI, D. DAGHERO, G.A. UMMARINO, A. CALZOLARI, VALERIA DELLAROCCHA, V.A. STEPANOV, S.M. KAZAKOV, J. JUN, J. KARPINSKI

**A point-contact study of the superconducting gaps in Al-substituted and C-substituted  $\text{MgB}_2$  single crystals**  
*Journal of Physics and Chemistry of Solids* **67**, Issues 1-3, 360-364 (2006)

V. GURITANU, A.B. KUZMIENKO, D. VAN DER MAREL, S.M. KAZAKOV, J. KARPINSKI

**Anisotropic optical conductivity and two colors of  $\text{MgB}_2$**   
*Physical Rev. B* **73**, 104509, 1-11 (2006)

R. KHASANOV, A. SHENGELAYA, K. CONDER, E. MORENZONI, I.M. SAVIC, J. KARPINSKI, H. KELLER

**Correlation between oxygen isotope effects on transition temperature and magnetic penetration depth in high-temperature superconductors close to optimal doping**  
*Phys. Rev. B* **74**, 064504, 1-6 (2006)

V.G. KOGAN, R. PROZOROV, S.L. BUD'KO, P.C. CANFIELD, J.R. THOMSON, J. KARPINSKI, N.D. ZHIGADLO, P. MIRANOVI

**Effect of field-dependent core size on reversible magnetization of high- $K$  superconductors**  
*Phys. Rev. B* **74**, 184521, 1-10 (2006)

A. KOHEN, F. GIUBILEO, F. BOBBA, T. PROSLIER, N. ZHIGADLO, S.M. KAZAKOV, J. KLEIN, J. KARPINSKI, A.M. CUCOLO, D. RODITCHEV

**Lazy Fisherman' method of vortex analysis: application to  $\text{MgB}_2$**   
*Journal of Physics and Chemistry of Solids* **67**, 442-446 (2006)

A. KOHEN, T. CREN, Y. NOAT, T. PROSLIER, F. GIUBILEO, F. BOBBA, A.M. CUCOLO, N. ZHIGADLO, S.M. KAZAKOV, J. KARPINSKI, W. SACHS, D. RODITCHEV

**Recent progress in vortex studies by tunneling spectroscopy**  
*Physica C: Superconductivity* **437-438**, 145-148 (2006)

C. KRUTZLER, M. ZEHETMAYER, M. EISTERER, H.W. WEBER, N.D. ZHIGADLO, J. KARPINSKI, A. WISNIEWSKI

**Anisotropic reversible mixed-state properties of superconducting carbon doped  $\text{Mg}(\text{B}_{1-x}\text{C}_x)_2$  single crystals**  
*Phys. Rev. B* **74**, 144511, 1-10 (2006)

G. LAMURA, A. GAUZZI, S.M. KAZAKOV, J. KARPINSKI, A. ANDREONE

**High-resolution measurements of the magnetic penetration depth on  $\text{YBa}_2\text{Cu}_3\text{O}_7$  single crystals**  
*Journal of Physics and Chemistry of Solids* **67**, 447-449 (2006)

E. LIAROKAPIS, D. LAMPAKIS, D. PALLES, J. KARPINSKI AND C. PANAGOPOULOS

**A Raman view of local lattice distortions and charge transfer in cuprates**  
*Journal of Physics and Chemistry of Solids volume* **67**, Issues 9-10, 2065-2071 (2006)

A. MIALITSIN, B. S. DENNIS, N. D. ZHIGADLO, J. KARPINSKI, G. BLUMBERG

**Anharmonicity and self-energy effects of  $E_{2g}$  phonon in  $\text{MgB}_2$**   
*Phys. Rev. B* **75**, 020509(R) (2007)

D. PAL, L. DEBEER-SCHMITT, T. BERA, R. CUBITT, C.D. DEWHURST, J. JUN, N. D. ZHIGADLO, J. KARPINSKI, V. G. KOGAN, M. ESKILDSEN

**Measuring the penetration depth anisotropy in  $\text{MgB}_2$  using small-angle neutron scattering**  
*Physical Rev. B* **73**, 012513, 1-4 (2006)

P. PARISIADES, D. LAMPAKIS, D. PALLES, E. LIAROKAPIS, J. KARPINSKI

**The relation of the broad band with the  $E_{2g}$  phonon and superconductivity in the  $\text{Mg}(\text{B}_{1-x}\text{C}_x)_2$  compound**

*Journal of Magnetism and Magnetic Materials, In Press, Corrected Proof, Available online 10 November, 1-3 (2006)*

B. PEDRINI, S. WESSEL, J.L. GAVILANO, H.R. OTT, S.M. KAZAKOV, J. KARPINSKI

**Quenching of the Haldane gap in  $\text{LiVSi}_2\text{O}_6$  and related compounds**  
*European Physical Journal B (In print)*

B. PEDRINI, S. WEYENETH, J.L. GAVILANO, J. HINDERER, M. WELLER, H.R. OTT, S.M. KAZAKOV, J. KARPINSKI

**Magnetic transition in  $\text{Na}_{0.5}\text{CoO}_2$  at 88 K**

*Physica B: Condensed Matter* **378-380**, 861-862 (2006)

K. ROGACKI, B. BATLOGG, J. KARPINSKI, N.D. ZHIGADLO, G. SCHUCK, S.M. KAZAKOV, P. WÄGLI, R. PUZNAK, A. WISNIEWSKI, F. CARBONE, A. BRINKMAN, D. VAN DER MAREL, **Strong magnetic pair breaking in Mn substituted  $\text{MgB}_2$**

*Phys. Rev. B* **73**, 174520, 1-8 (2006)

G. SCHUCK, S.M. KAZAKOV, K. ROGACKI, N.D. ZHIGADLO, J. KARPINSKI

**Crystal growth, structure, and superconducting properties of  $\beta$ -pyrochlores  $\text{KOs}_2\text{O}_6$**

*Physical Rev. B* **73**, 144506, 1-9 (2006)

A.V. SOLOGUBENKO, N.D. ZHIGADLO, J. KARPINSKI, H.R. OTT

**Thermal conductivity of Al-doped  $\text{MgB}_2$ : Impurity scattering and the validity of the Wiedemann-Franz law**

*Phys. Rev. B* **74**, 184523, 1-6 (2006)

S. STREULE, M. MEDARDE, A. PODLESNYAK, E. POMJAKUSHINA, K. CONDER, S. KAZAKOV, J. KARPINSKI, J. MESOT

**Short-range charge ordering in  $\text{Ho}_{0.1}\text{Sr}_{0.9}\text{CoO}_{3-x}$  ( $0.15 < x < 0.49$ )**

*Physical Rev. B* **73**, 024423, 1-8 (2006)

A. WISNIEWSKI, R. PUZNAK, J. JUDEK, C. KRUTZLER, M. EISTERER, H.W. WEBER, J. JUN, S.M. KAZAKOV, J. KARPINSKI

**Comparison of the influence of carbon substitution and neutron induced defects on the upper critical field and flux pinning in  $\text{MgB}_2$  single crystals**

*Supercond. Sci. Technol.* **20**, 256-260 (2007)

\* S. WU, P. GEISER, J. JUN, J. KARPINSKI, J.-R. PARK, R. SOBOLEWSKI

**Long-lived, coherent Acoustic phonon oscillations in GaN single crystals**

*Applied Physics Letters* **88**, 041917, 1-3 (2006)

M. ZEHETMAYER, M. EISTERER, R.MÜLLER, M.WEIGAND, J.JUN, S. M. KAZAKOV, J. KARPINSKI, H. W. WEBER

**Flux pinning in neutron irradiated  $\text{MgB}_2$  single crystals**

*Journal of Physics: Conference Series* **43**, 651-654, 7th European Conference on Applied Superconductivity (2006)

M. ZEHETMAYER, C. KRUTZLER, M. EISTERER, J. JUN, S.M. KAZAKOV, J. KARPINSKI AND H.W. WEBER

**Effect of disorder on the irreversible magnetic properties of single crystalline  $\text{MgB}_2$ : comparison of carbon doping and neutron irradiation**

*Physica C: Superconductivity, Volumes 445-448*, 65-68 (2006)

## GRUPE H. KELLER

(project 2)

A. R. BISHOP, A. BUSSMANN-HOLDER, O.V. DOLGOV, A. FURRER, H. KAMIMURA, H. KELLER, R. KHASANOV, R.K. KREMER, D. MANSKE, K.A. MÜLLER, A. SIMON

**Real and marginal isotope effects in cuprate superconductors**

*Journal of Superconductivity* (accepted)

A. BUSSMANN-HOLDER, R. KHASANOV, A. SHENGELAYA, A. MAISURADZE, F. LA MATTINA, H. KELLER, K. A. MÜLLER

**Mixed order parameter symmetries in cuprate superconductors**

*Europhys. Lett.* **77**, 27002, 1-4 (2007)

R. KHASANOV, A. SHENGELAYA, D. DI CASTRO, D.G. ESHCHENKO, I.M. SAVICH, K. CONDER, E. POMJAKUSHINA, J. KARPINSKI, S.M. KAZAKOV, H. KELLER

**Magnetic field dependence of the oxygen isotope effect on the magnetic penetration depth in hole-doped cuprate superconductors**

*Phys. Rev. B, Rapid communications*, (accepted)

\* R. KHASANOV, A. SHENGELAYA, A. MAISURADZE, F. LA MATTINA, A. BUSSMANN-HOLDER, H. KELLER, AND K.A. MÜLLER **Experimental evidence for two gaps in the high-temperature  $\text{La}_{1.83}\text{Sr}_{0.17}\text{CuO}_4$  superconductor**

*Phys. Rev. Lett.* **98**, 057007, 1-4 (2007)

R. KHASANOV, A. SHENGELAYA, K. CONDER, E. MORENZONI, I.M. SAVIC, J. KARPINSKI, H. KELLER

**Correlation between oxygen isotope effects on transition temperature and magnetic penetration depth in high-temperature superconductors close to optimal doping**

*Phys. Rev. B* **74**, 064504, 1-6 (2006)

\* R. KHASANOV, P. S. HÄFLIGER, N. SHITSEVALOVA, A. DUKHNENKO, H. KELLER **Pressure effect on the Ginzburg-Landau parameter  $\kappa = \lambda/\xi$**

*Phys. Rev. Lett.* **97**, 157002, 1-4 (2006)

R. KHASANOV, I.L. LANDAU, C. BAINES, F. LA MATTINA, K. TOGANO, H. KELLER

**Muon-spin-rotation measurements of the penetration depth in  $\text{Li}_2\text{Pd}_3\text{B}$**

*Phys. Rev. B* **73**, 214528, 1-6 (2006)

I. L. LANDAU, R. KHASANOV, K. TOGANO, H. KELLER

**Temperature dependences of the upper critical field and the Ginzburg-Landau parameter of  $\text{Li}_2\text{Pd}_3\text{B}$  from magnetization measurements**

*Physica C* **451**, 134-138 (2007)

E. MORENZONI, R. KHASANOV, H. LUETKENS, T. PROKSCHA, A. SUTER

**Surface and thin film studies with polarized low energy muons**

*Journal of Neutron Research*, **14**, 269, (2006)

T. PROKSCHA, E. MORENZONI, K. DEITERS, F. FOROUGH, D. GEORGE, R. KOBLER, A. SUTER, V. VRANKOVIC

**The new high-intensity surface muon beam  $\mu\text{E4}$  for the generation of low-energy muons at PSI** *Physica B* **374-375**, 460-464 (2006)

V. G. STORCHAK, D. G. ESHCHENKO, H. LUETKENS, E. MORENZONI, R. L. LICHTI, S. F. MARENKIN, O. N. PASHKOVA, J. H. BREWER

**Room temperature ferromagnetism in III-V and II-IV-V<sub>2</sub> dilute magnetic semiconductors**

*Physica B* **374-375**, 430-432 (2006)

V. G. STORCHAK, D.G. ESHCHENKO, J. H. BREWER, S. P. COTTRELL, R. L. LICHTI

**Muonium in InSb: Shallow acceptor versus deep trap or recombination center**

*Phys. Rev. B* **73**, 081203, 1-4 (2006)

V. G. STORCHAK, D. G. ESHCHENKO, J. H. BREWER, S. P. COTTRELL

**Formation and dynamics of muonium centers in semiconductors**

*Physica B* **374-375**, 398-401 (2006)

V. G. STORCHAK, D. G. ESHCHENKO, J. H. BREWER

**Quantum diffusion of muonium atoms in solids: Localization vs. band-like propagation**

*Physica B* **374-375**, 347-350 (2006)

A. SUTER, E. MORENZONI, N. GARIFIANOV, R. KHASANOV, E. KIRK, H. LUETKENS, T. PROKSCHA, M. HORISBERGER

**Nonlocal Meissner screening**

*Physica B* **374-375**, 243-246 (2006)

## GRUPE G. MARGARITONDO

(project 3)

R. BECKER, H. BERGER

**Reinvestigation of  $\text{Ni}_3\text{TeO}_6$**

*Acta Crystallographica Section E* **62**, i256-i257 (2006)

R. BECKER, H. BERGER

**A new synthetic copper cobalt tellurate  $\text{Cu}_2\text{CoTeO}_6$**

*Acta Crystallographica Section E* **62**, i261-i262 (2006)

R. BECKER, H. BERGER

**Reinvestigation of  $\text{CuSe}_2\text{O}_5$**

*Acta Crystallographica Section E* **62**, i256-i257(2006)

R. BECKER, M. JOHNSON, H. BERGER

**A new synthetic cobalt tellurate:  $\text{Co}_3\text{TeO}_6$**

*Acta Crystallographica Section C - Crystal Structure Communications* **62**, i67-i69 (2006)

R. BECKER, H. BERGER, M. JOHNSON, M. PRESTER, Z. MAROHNIC, M. MILJAK, M. HERAK

**Crystal structure and magnetic properties of  $\text{Co}_2\text{TeO}_3\text{Cl}_2$  and  $\text{Co}_2\text{TeO}_3\text{Br}_2$**

*Journal of Solid State Chemistry*, **179**, 877-883 (2006)

R. BECKER, M. JOHNSON, H. BERGER, M. PRESTER, I. ZIVKOVIC, D. DROBAC, M. MILJAK, M. HERAK

**Crystal structure and magnetic properties of  $\text{Co}_7(\text{TeO}_3)_4\text{Br}_6$  - A new cobalt telluritebromid**

*Solid State Science* **8**, 836-842 (2006)

M. BIMBI, G. ALLODI, R. DE RENZI, G. MAZZOLI, H. BERGER, A. AMATO

**The Verwey transition in  $\text{Fe}_3\text{O}_4$  : A single crystal muon investigation**

*Physica B : Condensed Matter* **374-375**, 51-54 (2006)

\*S. V. BORISENKO, A. A. KORDYUK, A. KOITZSCH, J. FINK, J. GECK, V. ZABOLOTNYY, M. KNUPFER, B. BÜCHNER, H. BERGER, M. FALUB, M. SHI, J. KREMPASKY, L. PATTHEY

**Parity of the Pairing Bosons in a High-Temperature  $\text{Pb-Bi}_2\text{Sr}_2\text{CaCu}_2\text{O}_8$  Bilayer Superconductor by Angle-Resolved Photoemission Spectroscopy**

*Phys. Rev. Lett.* **96**, 067001, 1-4 (2006)

G. CAIMI, L. DEGIORGI, H. BERGER, L. FORRÓ, **Optical evidence for magnetically**

**driven structural transition in the spin web  $\text{Cu}_3\text{TeO}_6$**   
*Europhys. Lett.* **75**, 496-502 (2006)

G. CAIMI, L. DEGIORGI, H. BERGER, L. FORRÓ

**Phonon analysis of the  $S = 1$  quantum spin systems  $\text{Ni}_5\text{Te}_4\text{O}_{12}\text{X}_2$  ( $\text{X} = \text{Cl}$  and  $\text{Br}$ )**  
*J. Phys. Condensed Matter* **18**, 4065-4070 (2006)

F. CARBONE, A.B. KUZMENKO, H.J.A. MOLEGRAAF, E. VANHEUMEN, V. LUKOVAC, F. MARSIGLIO AND D. VAN DER MAREL, K. HAULE, G. KOTLIAR, H. BERGER, P.H. KES

**Doping Dependence of the Redistribution of Optical Spectral Weight in  $\text{Bi}_2\text{Sr}_2\text{CaCu}_2\text{O}_{8+\delta}$**   
*Physical Review B* **74**, 064510, 1-8 (2006)

F. CLERC, C. BATTAGLIA, M. BOVET, L. DESPONT, C. MONNEY, H. CERCELLIER, M. G. GARNIER, P. AEBI, H. BERGER, L. FORRO

**Lattice-distortion-enhanced electron-phonon coupling and Fermi surface nesting in  $1\text{T-TaS}_2$**   
*Physical Review B* **74**, 155114, 1-7 (2006)

D. CLOETTA, D. ARIOSA, C. CANCELLIERI, M. ABRECHT, S. MITROVIC, D. PAVUNA  
**Three-dimensional dispersion induced by extreme tensile strain in  $\text{La}_{2-x}\text{Sr}_x\text{CuO}_4$  films**  
*Physical Review B* **74**, 014519, 1-7 (2006)

S. COLONNA, F. RONCI, A. CRICENTI, L. PERFETTI, H. BERGER, M. GRIONI  
**Scanning tunneling microscopy observation of a mott-insulator phase at the  $1\text{T-TaSe}_2$**   
*Japanese Journal of Applied Physics* **45**, N°3B, 1950-1952 (2006)

S. J. CROWE, M. R. LEES, D. MCK. PAUL, R. I. BEWLEY, J. TAYLOR, G. MCINTYRE, O. ZAHARKO, H. BERGER  
**Effect of externally applied pressure on the magnetic behavior of  $\text{Cu}_2\text{Te}_2\text{O}_5(\text{Br}_x\text{Cl}_{1-x})_2$**   
*Phys. Rev. B* **73**, 144410, 1-6 (2006)

J. DEISENHOFER, R. M. EREMINA A. PIMENOV, T. GAVRILOVA, H. BERGER, M. JOHNSON, P. LEMMENS, H.-A. KRUG VON NIDDA, A. LOIDL, K.-S. LEE, M.-H. WHANGBO  
**Structural and magnetic dimers in the spin-gapped system  $\text{CuTe}_2\text{O}_5$**   
*Physical Review B* **74**, 174421, 1-8 (2006)

L. DESPONT, F. CLERC, M. G. GARNIER, H. BERGER, AND L. FORRO, P. AEBI  
**Multiple scattering investigation of the  $1\text{T-TaS}_2$  surface termination**  
*Eur. Phys. J.B.* **52**, 421-426 (2006)

D. V. EVTUSHINSKY, A. A. KORDYUK, S. V. BORISENKO, V. B. ZABOLOTNYY, M. KNUPFER, J. FINK, B. BUECHNER. A. V. PAN, A. ERB, C. T. LIN, H. BERGER  
**Unadulterated spectral function of low-energy quasi particles in  $\text{Bi}_2\text{Sr}_2\text{CaCu}_2\text{O}_{8+\delta}$**   
*Physical Review B* **74**, 172509, 1-4 (2006)

J. FINK, S. BORISENKO, A. KORDYUK, A. KOITSCH, J. GECK, V. ZABOLOTNYY, M. KNUPFER, B. BÜCHNER, H. BERGER  
**Dressing of the charge carriers in high  $-T_c$  superconductors**  
*Review Artikels in Book-Hüfners «Very high resolution photoemission spectroscopy»* (2006)

J. FINK, A. KOITZSCH, J. GECK, V. ZABOLOTNYY, M. KNUPFER, B. BÜCHNER, A. CHUBUKOV, H. BERGER  
**Reevaluation of the coupling to a bosonic mode of the charge carriers in  $(\text{Bi,Pb})_2\text{Sr}_2\text{CaCu}_2\text{O}_{8+\delta}$  at the antinodal point**  
*Physical Review B* **74**, 165102, 1-12 (2006)

\* J. GECK, M. V. ZIMMERMANN, H. BERGER, S.V. BORISENKO, H. ESCHRIG, K. KOEPERNIK, M. KNUPFER, B. BÜCHNER  
**Stripe correlations in  $\text{Na}_{0.75}\text{CoO}_2$**   
*Phys. Rev. Lett.* **97**, 106403, 1-4 (2006)

M. GROBOSCH, R. SCHUSTER, T. PICHLER, M. KNUPFER, H. BERGER  
**Analysis of the anisotropy of excitons in pentacene single crystals**  
*Physical Review B* **74**, 155202, 1-6 (2006)

Z. JAGLICIC, J. DOLINSEK, A. BILUSIC, A. SMONTARA, Z. TRONTELJ, H. BERGER  
**Searching for magnetic frustration-like properties in tetrahedral spin systems  $\text{Cu}_2\text{Te}_2\text{O}_5(\text{Br}_{1-x}\text{Cl}_x)_2$**   
*Physica B* **382**, 209-212 (2006)

Z. JAGLICIC, S. EL SHAWISH, A. JEROMEN, A. BILUSIC, A. SMONTARA, Z. TRONTELJ, J. BONCA, J. DOLINSEK, H. BERGER  
**Magnetic ordering and ergodicity in the  $\text{Cu}_2\text{Te}_2\text{O}_5\text{X}_2$  family of frustrated quantum magnets**

*Physical Review B* **73**, 214408, 1-9 (2006)

\*I. KEZSMARKI, G. MIHALY, R. GAAL, N. BARISIC, A. AKRAP, H. BERGER, L. FORRO, C. C. HOMES, L. MIHALY

**Separation of orbital contributions to the optical conductivity of  $BaVS_3$**

*Phys. Rev. Lett.* **96**, 186402, 1-4 (2006)

M. KNUPFER, H. BERGER

**Dispersion of electron-hole excitations in pentacene along (100)**

*Chemical Physics* **325**, 92-98 (2006)

\*A. KOHEN, TH. PROSLIER, T. CREN, Y. NOAT, W. SACKS, H. BERGER, D. RODITCHEV

**Probing the superfluid velocity with a superconducting tip : the Doppler shift effect**

*Phys. Rev. Lett.* **97**, 027001, 1-4 (2006)

A. A. KORDYUK, S. V. BORISENKO, A. KOITZSCH, J. FINK, M. KNUPFER, B. BUECHNER, H. BERGER

**Life of the nodal quasiparticles in Bi-2212 as seen by ARPES**

*Journal of Physics and Chemistry of solids* **67**, 201-207 (2006)

\*A. Kordyuk, S. V. Borisenko, V. B. Zabolotnyy, J. Geck, M. Knupfer, J. Fink, B. Büchner, C. T. Lin, B. Keimer, H. Berger, Seiki Komiyama, Y. Ando

**Constituents of the Quasiparticle Spectrum Along the Nodal Direction of High- $T_c$  Cuprates**

*Phys. Rev. Lett.* **97**, 017002, 1-4 (2006)

T. KROLL, M. KNUPFER, J. GECK, C. HESS, T. SCHWIEGER, G. KRABBES, C. SEKAR, D. R. BATCHELOR, H. BERGER, J. FINK, B. BUECHNER

**X-ray absorption spectroscopy on layered cobaltates  $Na_2CoO_2$**

*Physical Review B* **74**, 115123, 1-6 (2006)

H.L. LIU, M. QUIJADA, D.B. ROMERO, D.B. TANNER, A. ZIBOLD, G.L. CARR, H. BERGER, L. FORRO, L. MIHALY, G. CAO, BEOM-HOAN O, J.T. MARKERT, J.P. RICE, M.J. BURNS, K.A. DELIN

**Drude behavior in the far-infrared conductivity of cuprate superconductors**

*Annalen der Physik (Leipzig)* **15** (7-8), 606-618 (2006)

\*A. MANS, I. SANTOSO, Y. HUANG, W. K. SIU, S. TAVODDOD, V. ARPIAINEN, M.

LINDROSS, H.

BERGER, V.N. STROCOV, M. SHI, L. PATTHEY, M.S. GOLDEN

**Experimental proof of a structural origin for the shadow fermi surface of  $Bi_2Sr_2CaCu_2O_{8-\delta}$**

*Phys. Rev. Lett.* **96**, 107007, 1-4 (2006)

L. MIHALY, T. FEHÉR, B. DORA, B. NAFRADI, H. BERGER, L. FORRO

**Spin resonance in the ordered magnetic state of  $Ni_5(TeO_3)_4Cl_2$**

*Phys. Rev. B* **74**, 174403, 1-9 (2006)

M. PAPAGNO D. PACILE, G. CAIMI, H. BERGER, L. DEGIORGI, M. GRIONI

**Electronic structure of one-dimensional copper oxide chains in  $LiCu_2O_2$  from angle-resolved photoemission and optical spectroscopy**

*Phys. Rev. B* **73**, 11512, 1-8 (2006)

\*L. PERFETTI, P. LOUKAKOS, M. LISOWSKI, U. BOVENSIEPEN, H. BERGER, S. BIERMANN, P. S. CORNAGLIA, A. GEORGES, M. WOLF

**Time Evolution of the Electronic Structure of  $1T-TaS_2$  through the Insulator-Metal Transition**

*Phys. Rev. Lett.* **97**, 067402, 1-4 (2006)

A. PERUCCHI, L. DEGIORGI, H. BERGER

**Infrared signature of the charge-density-wave gap in  $ZrTe_3$**

*European Physical Journal B* **48**, 489-493 (2006)

V. N. STROCOV, E. E. KRASOVSKII, W. SCHATTKE, N. BARRETT, H. BERGER, D. SCHRUPP, R. CLAESSEN

**Three-dimensional band structure in layered  $TiTe_2$  : Photoemission final-state effects**

*Physical Review B* **74**, 195125, 1-14 (2006)

\*V. B. ZABOLOTNYY, S. V. BORISENKO, A. A. KORDYUK, J. FINK, J. GECK, A. KOITZSCH, M. KNUPFER, B. BUECHNER, H. BERGER, A. ERB, C. T. LIN, B. KEIMER, R. FOLLATH

**Effect of Zn and Ni Impurities on the Quasiparticle Renormalization of Superconducting Bi-2212**

*Phys. Rev. Lett.* **96**, 037003, 1-4 (2006)

O. ZAHARKO, H. RONNOW, J. MESOT, S. CROWE, D. MCK PAUL, P.J. BROWN, A. DAOUD-ALADINE, A. MEENTS, A. WAGNER, M. PRESTER, H. BERGER

**Incommensurate magnetic ordering in  $Cu_2Te_2O_5X_2$  ( $X = Cl, Br$ ) studied by single crystal neutron diffraction**

*Phys. Rev. B* **73**, 064422, 1-7 (2006)

**GROUPE J. MESOT**

(projects 1, 2, 3 & 6)

- J. CHANG, J. MESOT, R. GILARDI, J. KOHLBRECHER, A.J. DREW, U. DIVAKAR, S.J. LISTER, S.L. LEE, S.P. BROWN, D. CHARALAMBOUS, E.M. FORGAN, C.D. DEWHURST, R. CUBITT, N. MONOMO, M. ODA  
**Neutron scattering investigations of the Abrikosov state of high-temperature superconductors**  
*Physica B* **35-37**, 385-386 (2006)
- \* J. CHANG, A.P. SCHNYDER, R. GILARDI, H.M. RØNNOW, S. PAILHES, N.B. CHRISTENSEN, CH. NIEDERMAYER, D.F. MCMORROW, A. HIESS, A. STUNAUT, M. ENDERLE, B. LAKE, I. SOBOLEV, N. MOMONO, M. ODA, M. IDO, C. MUDRY, J. MESOT  
**Magnetic-field induced spin excitations and renormalized spin gap in  $La_{1.895}Sr_{0.105}CuO_4$**   
*Phys. Rev. Lett.* **98**, 077004, 1-4 (2007)
- S.J. CROWE, M.R. LEES, D.M.K. PAUL, R.I. BEWELY, J. TAYLOR, G. MCINTYRE, O. ZAHARKO, H. BERGER  
**Effect of externally applied pressure on the magnetic behavior of  $Cu_2Te_2O_5(Br_xCl_{1-x})_2$**   
*Phys. Rev. B* **73**, 144410, 1-6 (2006)
- A.J. DREW, D.O.G. HERON, U.K. DIVAKAR, S.L. LEE, R. GILARDI, J. MESOT, F.Y. OGRIN, D. CHARALAMBOUS, N.M. MONOMO, M. ODA, C. BAINES  
**mSR measurements on the vortex lattice of  $La_{1.83}Sr_{0.17}CuO_4$**   
*Physica B* **374-375**, 203-206 (2006)
- A. FURRER, CH. RÜEGG  
**Bose-Einstein condensation in magnetic materials**  
*Physica B* **385-386**, 295-300 (2006)
- P.S. HÄFLIGER, A. PODLESNYAK, K. CONDER, A. FURRER  
**Pressure effect on the pseudogap in the optimally doped high-temperature superconductor  $La_{1.81}Sr_{0.15}Ho_{0.04}Cu^{16}O_4$**   
*Europhys. Lett.* **73**, 260-266 (2006)
- P.S. HÄFLIGER, A. PODLESNYAK, K. CONDER, E. POMJAKUSHINA, A. FURRER  
**Pseudogap of the high-temperature superconductor  $La_{1.96-x}S_xHo_{0.04}CuO_4$  as observed by neutron crystal-field spectroscopy**  
*Phys. Rev. B* **74**, 184520, 1-13 (2006)
- \* G.I. MENON, A. DREW, U.K. DIVAKAR, S.L. LEE, R. GILARDI, J. MESOT, F.Y. OGRIN, D. CHARALAMBOUS, E.M. FORGAN, N. MOMONO, M. ODA, C. DEWHURST, C. BAINES  
**Muons as Local Probes of Three-Body Correlations in the Mixed State of Type-II Superconductors**  
*Phys. Rev. Lett.* **97**, 177004, 1-4 (2006)
- \* H.E. MOHOTTALA, B.O. WELLS, J.I. BUDNICK, W.A. HINES, CH. NIEDERMAYER, L. UDBY, CH. BERNHARD, A.R. MOODENBAUGH, F.C. CHOU  
**Phase separation in superoxygenated  $La_{2-x}Sr_xCuO_{4-y}$**   
*Nature materials* **5**, 377-382 (2006)
- \* J. PADIYATH, J. STAHN, M. HORISBERGER  
**Multilayers with tailored blurred interfaces**  
*Appl. Phys. Lett.* **89**, 113123, 1-3 (2006)
- A. PODLESNYAK, S. STREULE, K. CONDER, E. POMJAKUSHINA, J. MESOT, A. MIRMELSTEIN, P. SCHUTZENDORF, R. LENGSDORF, M.M. ABD-ELMEGUID  
**Pressure effects on crystal structure, magnetic and transport properties of layered perovskite  $TbBaCo_2O_{5.5}$**   
*Physica B* **378-380**, 537-538 (2006)
- \* A. PODLESNYAK, S. STREULE, J. MESOT, M. MEDARDE, E. POMJAKUSHINA, K. CONDER, A. TANAKA, M.W. HAVERKORT, D.I. KHOMSKII  
**Spin-State Transition in  $LaCoO_3$ : Direct Neutron Spectroscopic Evidence of Excited Magnetic States**  
*Phys. Rev. Lett.* **97**, 274208, 1-4 (2006)
- E. POMJAKUSHINA, K. CONDER, V. POMJAKUSHIN  
**Orbital order-disorder transition with volume collapse in  $HoBaCo_2O_{5.5}$ : A high-resolution neutron diffraction study**  
*Phys. Rev. B* **73**, 113105, 1-4 (2006)
- \* H.M. RØNNOW, CH. RENNER, G. AEPPLI, T. KIMURA, Y. TOKURA  
**Polarons and confinement of electronic motion to two dimensions in a layered manganite**  
*Nature* **440**, 1025-1028 (2006)
- S. STREULE, M. MEDARDE, A. PODLESNYAK, E. POMJAKUSHINA, K. CONDER, S. KAZAKOV, J. KARPINSKI, J. MESOT  
**Short-range charge ordering in  $Ho_{0.1}Sr_{0.9}Co_{3-x}$  ( $0.15 \leq x \leq 0.49$ )**  
*Phys. Rev. B* **73**, 024423, 1-8 (2006)
- S. STREULE, A. PODLESNYAK, D. SHEPTYAKOV, E. POMJAKUSHINA, M. STINGACIU, K. CONDER, M. MEDARDE, M.V. PATRAKEEV, I.A. LEONIDOV, V.L. KOZHEVNIKOV, J. MESOT  
**High-temperature order-disorder transition and polaronic conductivity in  $PrBaCo_2O_{5.48}$**   
*Phys. Rev. B* **73**, 094203, 1-5 (2006)
- S. STREULE, A. PODLESNYAK, E. POMJAKUSHINA, K. CONDER, D. SHEPTYAKOV, M. MEDARDE, J. MESOT  
**Oxygen order-disorder phase transition in  $PrBaCo_2O_{5.48}$  at high temperature**  
*Physica B* **378-380**, 539-540 (2006)



O. ZAHARKO, H. RØNNOW, J. MESOT, S.J. CROWE, D.MCK. PAUL, P.J. BROWN, A. DAOUD-ALADINE, A. MEENTS, A. WAGNER, M. PRESTER, H. BERGER

**Incommensurate magnetic ordering in  $\text{Cu}_2\text{Te}_2\text{O}_5\text{X}_2$  ( $\text{X}=\text{Cl},\text{Br}$ ) studied by single crystal neutron diffraction**

*Phys. Rev. B* **73**, 964422, 1-7 (2006)

## GROUPE F. MILA

(Project 1)

C. R. AST, D. PACILE, M. PAPAGNO, T. GLOOR, F. MILA, S. FEDRIGO, G. WITTICH, K. KERN, H. BRUNE, M. GRIONI

**Orbital selective overlayer-substrate hybridization in a Pb monolayer on Ag(111)**

*Phys. Rev. B* **73**, 245428, 1-6 (2006)

\* M. CLÉMANCEY, H. MAYAFFRE, C. BERTHIER, M. HORVATIC, J.-B. FOUET, S. MIYAHARA, F. MILA, B. CHIARI, O. PIOVESANA

**Field Induced Staggered Magnetization and Magnetic Ordering in  $\text{Cu}_2(\text{C}_5\text{H}_{12}\text{N}_2)_2\text{Cl}_4$**

*Phys. Rev. Lett.* **97** 167204, 1-4 (2006)

J.-B. FOUET, F. MILA, D. CLARKE, H. YOUK, O. TCHERNYSHYOV, P. FENDLEY, R. M. NOACK

**Condensation of magnons and spinons in a frustrated ladder**

*Phys. Rev. B* **73**, 214405, 1-15 (2006)

\* A. LÄUCHLI, F. MILA, K. PENC

**The quadrupolar phases of the  $S=1$  bilinear-biquadratic Heisenberg model on the triangular lattice**

*Phys. Rev. Lett.* **97**, 087205, 1-4 (2006)

V.V. MAZURENKO, F. MILA, V.I. ANISIMOV

**Electronic Structure and Exchange Interactions of  $\text{Na}_2\text{V}_3\text{O}_7$**

*Phys. Rev. B* **73**, 014418, 1-6 (2006)

M. MAMBRINI, A. LÄUCHLI, D. POILBLANC, F. MILA

**Plaquette valence bond solid in the frustrated Heisenberg quantum antiferromagnet on the square lattice**

*Phys. Rev. B* **74**, 144422, 1-11 (2006)

F. MILA, F. VERNAY, A. RALCO, F. BECCA, P. FAZEKAS, K. PENC

**The emergence of Resonating Valence Bond physics in spin-orbital models**

To appear in *J. Phys. Condens. Matter, Proceedings of HFM2006*

D. POILBLANC, F. ALET, F. BECCA, A. RALCO, F. TROUSSELET, FRÉDÉRIC MILA

**Doping quantum dimer models on the square lattice**

*Phys. Rev. B* **74**, 014437, 1-5 (2006)

D. POILBLANC, A. LÄUCHLI, M. MAMBRINI, F. MILA

**Spinon confinement around a vacancy in frustrated quantum antiferromagnets**

*Phys. Rev. B* **73**, 100403(R) (2006)

D. POILBLANC, M. MAMBRINI, A. LAEUCHLI, F. MILA

**Exotic phenomena in doped quantum magnets**

To appear in *J. Phys. Condens. Matter, Proceedings of HFM2006*

A. RALCO, M. FERRERO, F. BECCA, D. IVANOV, F. MILA

**Dynamics of the quantum dimer model on the triangular lattice: Soft modes and local resonating valence-bond correlations**

*Phys. Rev. B* **74**, 134301, 1-6 (2006)

K. P. SCHMIDT, J. DORIER, A. LÄUCHLI, F. MILA

**Single-particle versus pair condensation of hard-core bosons with correlated hopping**

*Phys. Rev. B* **74**, 174508, 1-7 (2006)

F. VERNAY, A. RALCO, F. BECCA, F. MILA

**Identification of an RVB liquid phase in a quantum dimer model with competing kinetic terms**

*Phys. Rev. B* **74**, 054402, 1-7 (2006)

C. WEBER, A. LÄUCHLI, F. MILA, T. GIAMARCHI

**Magnetism and superconductivity of strongly correlated electrons on the triangular lattice**

*Phys. Rev. B* **73**, 014519, 1-10 (2006)

C. WEBER, D. POILBLANC, S. CAPPONI, F. MILA, C. JAUDET

**Bond-order modulated staggered flux phase for the  $t$ - $J$  model on the square lattice**

*Phys. Rev. B* **74**, 104506, 1-10 (2006)

## GROUPE R. NESPER

(projects 4 & 6)

A. MICHAILOVSKI, R. KIEBACH, W. BENSCH, J.-D. GRUNWALDT, A. BAIKER, S. KOMARNENI, G. R. PATZKE

**Morphological and Kinetic Studies on Hexagonal Tungstates**

*Chem. Mater.* **19**, 185-197 (2007)

\* A. TAURINO, A. FORLEO, L. FRANCIOSO, P. SICILIANO, M. STALDER, R. NESPER

**Synthesis, electrical characterization, and gas sensing properties of molybdenum oxide nanorods**

*Appl. Phys. Lett.* **88**, 152111, 1-3 (2006)

M. WÖRLE, R. NESPER, T. CHATTERJI

**LiB<sub>x</sub> (0.82 < x ≤ 1.0) - an Incommensurate Composite Structure below 150 K**  
*Z. Anorg. Allg. Chem.* **632**, 1737-1742 (2006)

## GROUPE H. - R. OTT

(project 1)

A. BILUSIC, A. SMONTARA, J. DOLINSEK, P. MCGUINNESS, H. R. OTT  
**Phonon scattering in quasicrystalline i-Al<sub>72</sub>Pd<sub>19.5</sub>Mn<sub>8.5</sub>: A study of the low-temperature thermal conductivity**  
*J. of Alloys and Comp.*, online available, 7th July (2006)

J. L. GAVILANO, E. FELDER, D. RAU, H. R. OTT, P. MILLET, F. MILA, T. CHICOREK, A. C. MOTA  
**Na<sub>2</sub>V<sub>3</sub>O<sub>7</sub>: An unusual low-dimensional Quantum magnet**, *Physica B* **378-380**, 123-124 (2006)  
 J. HINDERER, S.M. WEYENETH, M. WELLER, J.L. GAVILANO, E. FELDER, F. HULLIGER, H. R. OTT  
**NMR study of CeTe at low temperatures**  
*Physica B* **378-380**, 765-766 (2006)

\* J.L. GAVILANO, B. PEDRINI, K. MAGISHI, J. HINDERER, M. WELLER, H.R. OTT, S. M. KAZAKOV, J. KARPINSKI  
**Localized versus itinerant magnetic moments in Na<sub>0.7</sub>CoO<sub>2</sub>**  
*Phys. Rev. B* **74**, 064410 (2006)

\* H.R. OTT  
**Heavy electrons and non-Fermi liquids, the early times**  
*Physica B*, 378-380, 1-6 (2006)

\* B.PEDRINI, S.WESSEL, J.L. GAVILANO, H.R. OTT, S.M. KAZAKOV, J. KAPINSKI, **Quenching of the Haldane gap in LiVSi<sub>2</sub>O<sub>6</sub> and related compounds**  
 Accepted. for publication in *Eur. Phys. J B*, in print.

\* B.PEDRINI, S.WESSEL, J.L. GAVILANO, H.R. OTT, S.M. KAZAKOV, J. KAPINSKI, **Quenching of the Haldane gap in LiVSi<sub>2</sub>O<sub>6</sub> and related compounds**  
 Accepted. for publication in *Eur. Phys. J B*, in print.

B. PEDRINI, S. WEYENETH, J. L. GAVILANO, J.HINDERER, M. WELLER, H.R. OTT, S.M. KAZAKOV, J. KARPINSKI  
**Magnetic transition in Na<sub>0.5</sub>CoO<sub>2</sub> at 88K**  
*Physica B* **378-380**, 861-862 (2006)

M. WELLER, J. HINDERER, J. L. GAVILANO, B. PEDRINI, D. RAU, I. SHEIKIN, M. CHIAO, H.R. OTT  
**NQR studies of CePd<sub>2</sub>In under hydrostatic pressure**  
*Physica B* **378-380**, 829-830 (2006)

\* A.V. SOLOGUBENKO, N. D. ZHIGADLO, J. KARPINSKI, H. R. OTT  
**Thermal conductivity of Al-doped MgB<sub>2</sub>: Impurity scattering and the validity of the Wiedemann-Franz law**  
*Phys. Rev. B* **74**, 184523 (2006)

## GROUPE A. SCHILLING

(projects 4 & 5)

A. ENGEL, A. SEMENOV, H.-W. HÜBERS, K. IL'IN, M. SIEGEL  
**Fluctuation effects in superconducting nanostrips**  
*Physica C* **444**, 12-18 (2006)

A. SCHILLING, M. REIBELT  
**Low-temperature differential-thermal analysis to measure variations in entropy**  
*Rev. Sci. Instrum.*, accepted for publication (2007)

## GROUPE L. SCHLAPBACH

(projects 1, 3 & 4)

R. AGUIAR, D. LOGVINOVICH, A. WEIDENKAFF, A. RELLER, S.G. EBBINGHAUS  
**The vast colour spectrum of ternary metal oxynitride pigments, Dyes and Pigments**  
<http://dx.doi.org/10.1016/j.dyepig.2006.08.029> (In press)

R. AGUIAR, A. WEIDENKAFF, C.W. SCHNEIDER, D. LOGVINOVICH, A. RELLER, S. EBBINGHAUS,  
**Syntheses and Properties of Oxynitrides (La, Sr)Ti(O, N)<sub>3</sub> thin films**  
*Progr. in Solid State Chem.*, (In press)

U. BANGERT, U. FALKE, A. WEIDENKAFF  
**Nature of domains in Lanthanum Calcium Cobaltite Perovskite revealed by atomic resolution Z-contrast and electron energy loss spectroscopy**  
*Mat. Sci. Eng.*, **133**, 30-36 (2006)

U. BANGERT, U. FALKE, A. WEIDENKAFF  
**Ultra-high resolution EEL studies of domains in Perovskite**  
*Journal of Physics* **26**, 17-20 (2006)

\* G. BUCHS, P. RUFFIEUX, P. GROENING, O. GROENING  
**Scanning tunneling microscopy investigations of hydrogen plasma-induced electron scattering centers on single-walled carbon nanotubes**  
*Appl. Phys. Lett.* **90**, 013104, 1-3 (2007)

G. BUCHS, P. RUFFIEUX, P. GROENING, O. GROENING

**Creation and STM/STS investigations of hydrogen ions induced defects on single-walled carbon nanotubes**

*Journal of Physics: Conference Series (In press)*

L. BOCHER, M.H. AGUIRE, R. ROBERT, A. WEIDENKAFF

**Chimie douce synthesis method and thermal investigations on perovskite-type titanate phases**

*TCA (In press)*

S. CANULESCU, T. LIPPERT, H. GRIMMER, A. WOKAUN, R. ROBERT, D. LOGVINOVICH, M. DOEBELI, A. WEIDENKAFF

**Structural Characterization and Magnetoresistance of Manganates Thin Films and Fe-doped Manganates**

*Appl. Surf. Sci.* **252**, 4599-4603 (2006)

S. CANULESCU, T. LIPPERT, A. WOKAUN, M. DÖBELI, A. WEIDENKAFF, R. ROBERT, D. LOGVINOVICH

**The effect of the fluence of the plume species on the properties of La- Ca- Mn- O thin films prepared by pulsed laser deposition**

*Appl. Surf. Sci.*, (In press)

S. CANULESCU, T. LIPPERT, A. WOKAUN, R. ROBERT, D. LOGVINOVICH, A. WEIDENKAFF

**Preparation of epitaxial  $\text{La}_{0.6}\text{Ca}_{0.4}\text{Mn}_x\text{Fe}_{1-x}\text{O}_3$  ( $x=0, 0.2$ ) Thin Films: Variation of the Oxygen Content**

*Progr. in Solid State Chem.*, (In press)

T. LIPPERT, M.J. MONTENEGRO, M. DÖBELI, A. WEIDENKAFF, S. MÜLLER, P.R. WILLMOTT, A. WOKAUN

**Perovskite Thin Films Deposited by Pulsed Laser Ablation as Model Systems for Electrochemical Applications**

*Progr. in Solid State Chem.*, (In press)

D. LOGVINOVICH, A. BÖRGER, A. DÖBELI, M. EBBINGHAUS, S.G. RELLER, A. WEIDENKAFF

**A, Synthesis and physical chemical properties of Ca substituted  $\text{LaTiO}_2\text{N}$**

*Progr. in Solid State Chem.*, (In press)

A. WEIDENKAFF, U. BANGERT, M. AGUIRE

**Structure and composition of nanoscopic domains in functional perovskite-type materials**  
*Chimia*, **60**, 742-748 (2006)

## GRUPE M. SIGRIST

(projects 1 & 2)

D.F. AGTERBERG, P.A. FRIGERI, R.P. KAUR, A. KOGA, M. SIGRIST

**Magnetic fields and superconductivity without inversion symmetry in  $\text{CePt}_3\text{Si}$**

*Physica B* **378-380**, 351-354 (2006)

E. BASCONES, T.M. RICE

**Spin susceptibility of underdoped cuprates: The case of ortho-II  $\text{YBa}_2\text{Cu}_3\text{O}_{6.5}$**

*Phys. Rev. B* **74**, 134501, 1-5 (2006)

E. BAUER, I. BONALDE, A. EICHLER, G. HILSCHER, Y. KITAOKA, R. LACKNER, ST. LAUMANN, H. MICHOR, M. NICKLAS, P. ROGL, E.W. SCHEIDT, M. SIGRIST, M. YOGI

**$\text{CePt}_3\text{Si}$ : Heavy Fermion Superconductivity and Magnetic Order with Inversion Symmetry**,  
*AIP Conference Proceedings* **850**, 1-8 (2006)

\*B. BINZ, H.B. BRAUN, T.M. RICE, M. SIGRIST

**Magnetic domain formation in itinerant metamagnets**,

*Phys. Rev. Lett.* **96**, 196406, 1-4 (2006)

\*Y. CHAN, T.M. RICE, F.C. ZHANG

**Rotational Symmetry Breaking in the Ground State of Sodium-Doped Cuprate Superconductors**

*Phys. Rev. Lett.* **97**, 237004, 1-4 (2006)

P.A. FRIGERI, D.F. AGTERBERG, I. MILAT, M. SIGRIST

**Phenomenological theory of the s-wave state in superconductors without an inversion center**

*Eur. Phys. J. B* **54**, 435-448 (2006)

P. A. FRIGERI, M. SIGRIST, D.F. AGTERBERG

**Characterization of the "s-wave" state in parity-violating superconductors**

*Physica B* **378-380**, 900-901 (2006)

P. GENTILE, C. NOCE, M. SIGRIST

**Role of spin exchange on the coexistence of superconductivity and itinerant ferromagnetism in a two carrier model**

*Physica B* **378-80**, 550-551 (2006)

N. HAYASHI, Y. KATO, P. A. FRIGERI, K. WAKABAYASHI, M. SIGRIST

**Basic Properties of a Vortex in a Noncentrosymmetric Superconductor**

*Physica C* **437-438**, 96-99 (2006)

N. HAYASHI, K. WAKABAYASHI, P. A. FRIGERI, Y. KATO, M. SIGRIST

**Spatially Resolved NMR Relaxation Rate in a Noncentrosymmetric Superconductor**

*Physica B* **378-380**, 388-390 (2006)

M. INDERGAND, C. HONERKAMP, A. LÄUCHLI, D. POILBLANC, M. SIGRIST

**Plaquette bond order wave in the quarter-filled extended Hubbard model on the checkerboard lattice**

*Phys. Rev. B* **75**, 045105, 1-7 (2007)

M. INDERGAND, A. LÄUCHLI, S. CAPPONI, M. SIGRIST

**Modeling bond-order wave instabilities in doped frustrated antiferromagnets: Valence bond solids at fractional filling**

*Phys. Rev. B* **74**, 064429, 1-11 (2006)

M. INDERGAND, M. SIGRIST

**Existence of Long-Range Magnetic Order in the Ground State of Two-Dimensional Spin-1/2 Heisenberg Antiferromagnets**

*Prog. Theor. Phys.* **117**, N°1, 1-15 (2007)

A.V. LUKOYANOV, V.V. MAZURENKO, V.I. ANISIMOV, M. SIGRIST, T.M. RICE

**The semiconductor-to-ferromagnetic-metal transition in FeSb<sub>2</sub>**

*Eur. Phys. J. B* **53**, 205 (2006)

Y. NAGAI, Y. KATO, N. HAYASHI,  
**Analytical result on electronic states around a vortex core in a noncentrosymmetric superconductor**

*J. Phys. Soc. Jpn.* **75**, 043706, 1-14 (2006)

Y. NAGAI, Y. UENO, Y. KATO, N. HAYASHI  
**Analytical formulation of the local density of states around a vortex core in unconventional superconductors**

*J. Phys. Soc. Jpn.* **75**, 104701, 1-4 (2006)

\*S. PILGRAM, T.M. RICE, M. SIGRIST  
**Role of inelastic tunneling through the barrier in scanning tunneling microscope experiments on cuprates superconductors**

*Phys. Rev. Lett.* **97**, 117003, 1-4 (2006)

A.P. SCHNYDER, D. MANSKE, C. MUDRY, M. SIGRIST

**Theory for Inelastic Neutron Scattering in Orthorhombic High-T<sub>c</sub> Superconductors**

*Phys. Rev. B* **73**, 224523, 1-8 (2006)

T. SHIBAUCHI, L. KRUSIN-ELBAUM, Y. KASAHARA, Y. SHIMONO, Y. MATSUDA, R. D. MCDONALD, C. H. MIELKE, S. YONEZAWA, Z. HIROI, M. ARAI, T. KITA, G. BLATTER, M. SIGRIST

**Uncommonly high upper critical field of the pyrochlore superconductor KOs<sub>2</sub>O<sub>6</sub> below the enhanced paramagnetic limit**

*Phys. Rev. B* **74**, 220506(R), 1-4 (2006)

A.O. SHORIKOV, V.I. ANISIMOV, M. SIGRIST  
**A band structure analysis of the coexistence of superconductivity and magnetism in (Ho,Dy)Ni<sub>2</sub>B<sub>2</sub>C**

*J. Phys. Condens. Matter* **18**, 5973 (2006)

M. SIGRIST, D.F. AGTERBERG, P.A. FRIGERI, N. HAYASHI, R.P. KAUR, A. KOGA, I. MILAT, K. WAKABAYASHI

**Unconventional superconductivity in non-centrosymmetric materials**

*AIP Conference Proceedings* **816**, 1-12 (2006)

S. TREBST, H. MONIEN, A. GRZESIK, M. SIGRIST

**Quasiparticle Dynamics in the Kondo Lattice Model at Half Filling**

*Phys. Rev. B* **73**, 165101, 1-7 (2006)

K.Y. YANG, T.M. RICE, F.C. ZHANG  
**Phenomenological theory of the pseudogap state**

*Phys. Rev. B* **73**, 174501,1-10 (2006)

\*H. Q. YUAN, D. F. AGTERBERG, N. HAYASHI, P. BADICA, D. VANDERVELDE, K. TOGANO, M. SIGRIST, M. B. SALAMON  
**S-Wave Spin-Triplet Order in Superconductors without Inversion Symmetry: Li<sub>2</sub>Pd<sub>3</sub>B and Li<sub>2</sub>Pt<sub>3</sub>B**

*Phys. Rev. Lett.* **97**, 017006, 1-4 (2006)

## GRUPE J.- M. TRISCONE

(projects 5 & 6)

\*C.H. AHN, A. BATTACHARYA, A.M. GOLDMAN, M. DI VENTRA, J.N. ECKSTEIN, C. DANIEL FRISBIE, M.E. GERSHENSON, I.H. INOUE, J. MANNHART, A. MILLIS, A. MORPURGO, D. NATELSON, J.-M. TRISCONE

**Electrostatic modification of novel materials**  
*Review of Modern Physics* **78**, 1185, 1-28 (2006)

E. COURJON, N. BODIN, G. LENGAIN, L. GAUTHIER-MANUEL, W. DANIAU, S. BALLANDRAS, P. PARUCH, J.-M. TRISCONE, J. HAUDEN

**Fabrication of periodically poled domains as transducers on LiNbO<sub>3</sub>**

*Submitted to IFCS 2006*

M. DAWBER, C. LICHTENSTEIGER, P. PARUCH, J.-M. TRISCONE

**Advanced fabrication and characterization of epitaxial ferroelectric thin films and multilayers**

*IEEE Transactions on Ultrasonics, Ferroelectric and Frequency Control* **53**, 2261 (2006)

\* L. DESPONT, C. LICHTENSTEIGER, C. KOITZSCH, F. CLERC, M.G. GARNIER, F.J. GARCIA DE ABAJO, E. BOUSQUET, PH. GHOSEZ, J.-M. TRISCONE, P. AEBI

**Direct evidence for surface ferroelectricity in ultra-thin perovskite films**

*Physical Review B* **73**, 094110, 1-6 (2006)

C. LICHTENSTEIGER, M. DAWBER, N. STUCKI, J.-M. TRISCONI, J. HOFFMAN, J.-B. YAU, C.H. AHN, L. DESPONT, P. AEBI  
**Monodomain to polydomain transition in ferroelectric  $\text{PbTiO}_3$  thin films with  $\text{La}_{0.67}\text{Sr}_{0.33}\text{MnO}_3$  electrodes.**  
 APL (To appear)

\*D. MATTHEY, N. REYREN, T. SCHNEIDER, AND J.-M. TRISCONI  
**Electric field effect modulation of the transition temperature, mobile carrier density and in-plane penetration depth of  $\text{NdBa}_2\text{Cu}_3\text{O}_{7-\delta}$  thin films**  
*Physical Review Letters* **98**, 57002 (2007)

P. PARUCH, J.-M. TRISCONI  
**High-temperature ferroelectric domain stability in epitaxial  $\text{PbZr}_{0.2}\text{Ti}_{0.8}\text{O}_3$  thin films**  
*Applied Physics Letters* **88**, 162907, 1-3 (2006)

\*K. TAKAHASHI, D. JACCARD, M. GABAY, K. SHIBUYA, T. OHNISHI, M. LIPPMAA, J.-M. TRISCONI  
**Local on-off switching of 2-D superconductivity with ferroelectric field effect**  
*Nature* **441**, 195-198 (2006)

## GROUPE M. TROYER

(project 1)

A. F. ALBUQUERQUE, F. ALET, P. CORBOZ, P. DAYAL, A. FEIGUIN, S. FUCHS, L. GAMPER, E. GULL, S. GÜRTLER, A. HONECKER, R. IGARASHI, M. KÖRNER, A. KOZHENIKOV, A. LÄUCHLI, S. R. MANMANA, M. MATSUMOTO, I.P. McCULLOCH, F. MICHEL, R. M. NOACK, G. PAWLOWSKI, L. POLLET, T. PRUSCHKE, U. SCHOLLWÖCK, S. TODO, S. TREBST, M. TROYER, P. WERNER, S. WESSEL (ALPS COLLABORATION)  
**The ALPS project release 1.3: open source software for strongly correlated systems**  
*Journal of Magnetism and Magnetic Materials* (In press)

\*M. BONINSEGNI, A. KUKLOV, L. POLLET, N. PROKOF'EV, B. V. SVISTUNOV, M. TROYER  
**Fate of vacancy-induced supersolidity in  $^4\text{He}$**   
*Phys. Rev. Lett.* **97**, 080401, 1-4 (2006)

\*E. BUROVSKI, N. PROKOF'EV, B. SVISTUNOV, M. TROYER  
**Critical Temperature and Thermodynamics of Attractive Fermions at Unitarity**  
*Phys. Rev. Lett.* **96**, 160402, 1-4 (2006)

E. BUROVSKI, N. PROKOF'EV, B. SVISTUNOV, M. TROYER  
**The Fermi-Hubbard Model at Unitarity**  
*New J. Phys.* **8**, 153, 1-29 (2006)

A. FEIGUIN, S. TREBST, A. LUDWIG, M. TROYER, A. KITAEV, Z. WANG, M. FREEDMAN  
**Interacting anyons in topological quantum liquids: The golden chain**  
*Phys. Rev. Lett.* (in press)

O. GYGI, H. KATZGRABER, M. TROYER  
**Simulations of ultracold bosonic atoms in optical lattices with anharmonic traps**  
*Phys. Rev. A* **73**, 063606, 1-7 (2006)

K. HARADA, N. KAWASHIMA, M. TROYER  
**Dimer-quadrupolar quantum phase transition in the quasi-one-dimensional Heisenberg model with biquadratic interactions**  
*J. Phys. Soc. Jap.* **76**, 013703, 1-4 (2007)

H. KATZGRABER, A. ESPOSITIO, M. TROYER  
**Ramping fermions in optical lattices across a Feshbach resonance**  
*Phys. Rev. A* **74**, 043602, 1-8 (2006)

H. KATZGRABER, S. TREBST, D. A. HUSE, M. TROYER  
**Feedback-optimized parallel tempering Monte Carlo**  
*J. Stat. Mech.* P03018, 1-22 (2006)

A. KUKLOV, N. PROKOF'EV, B. SVISTUNOV, M. TROYER  
**Deconfined criticality, runaway flow in the two-component scalar electrodynamics and weak first-order superfluid-solid transitions**  
*Ann. of Phys.* **321**, 1602-1621 (2006)

\*L. POLLET, M. TROYER, K. VAN HOUCKE, S. M. A. ROMBOUTS  
**Phase diagram of Bose-Fermi mixtures in one-dimensional optical lattices**  
*Phys. Rev. Lett.* **96**, 190402, 1-4 (2006)

S. TREBST, U. SCHOLLWÖCK, M. TROYER, P. ZOLLER  
**d-wave resonating valence bond states of ultracold fermionic atoms in optical lattices**  
*Phys. Rev. Lett.* **96**, 250402, 1-4 (2006)

S. TREBST, P. WERNER, M. TROYER, K. SHTENDEL, C. NAYAK  
**Breakdown of a topological phase: Quantum phase transition in a loop gas model with tension**

*Phys. Rev. Lett.* (in press)

\*P. WERNER, A. COMANAC, L. DE MEDICI,  
A.J. MILLIS, M. TROYER

***A continuous-time solver for quantum impurity models***

*Phys. Rev. Lett.* **97**, 076405, 1-4 (2006)

## **GROUPE D. VAN DER MAREL**

(project 1, 2, 3 & 5)

K. S. BURCH, S. V. DORDEVIC, F. P. MENA,  
A. B. KUZMENKO, D. VAN DER MAREL, J. L.  
SARRAO, J. R. JEFFRIES, E. D. BAUER, M.  
B. MAPLE, D. N. BASOV

***Optical signatures of momentum-dependent hybridization of the local moments and conduction electrons in Kondo lattices***

*Phys. Rev. B* **75**, 054523, 1-6 (2007)

F. CARBONE, A. B. KUZMENKO, H. J. A.  
MOLEGRAAF, E. VAN HEUMEN, E.  
GIANNINI, D. VAN DER MAREL

***In-plane optical spectral weight transfer in optimally doped  $\text{Bi}_2\text{Sr}_2\text{Ca}_2\text{Cu}_3\text{O}_{10}$***

*Phys. Rev. B* **74**, 024502, 1-10 (2006)

F. CARBONE, A. B. KUZMENKO, H. J. A.  
MOLEGRAAF, E. VAN HEUMEN, V.  
LUKOVAC, F. MARSIGLIO, D. VAN DER  
MAREL, K. HAULE, G. KOTLIAR, H.  
BERGER, S. COURJAULT, P. H. KES, AND  
M. LI

***Doping dependence of the redistribution of optical spectral weight in  $\text{Bi}_2\text{Sr}_2\text{CaCu}_2\text{O}_{8+\delta}$***

*Phys. Rev. B* **74**, 064510, 1-8 (2006)

F. CARBONE, M. ZANGRANDO, A.  
BRINKMAN, A. NICOLAOU, F. BONDINO, E.  
MAGNANO, A.A. NUGROHO, TH.  
JARLBORG, D. VAN DER MAREL

***Electronic structure of  $\text{MnSi}$ : The role of electron-electron interactions***

*Phys. Rev. B* **73**, 085114 (2006)

J. DEISENHOFER, R. M. EREMINA, A.  
PIMENOV, T. GAVRILOVA, H. BERGER, M.  
JOHNSSON, P. LEMMENS, H.-A. KRUG VON  
NIDDA, A. LOIDL, K.-S. LEE, M.-H.  
WHANGBO

***Structural and magnetic dimers in the spin-gapped system  $\text{CuTe}_2\text{O}_5$***

*Physical Review B* **74**, 174421, 1-8 (2006)

D. L. FENG, Z.-X. SHEN, X. J. ZHOU, K. M.  
SHEN, D. H. LU, D. VAN DER MAREL

***Puzzles about 1/8 magic doping in cuprates***

*Journal of Physics and Chemistry of Solids*  
**67**,198-200 (2006)

G. GURITANU, A .B. KUZMENKO, D. VAN  
DER MAREL, S. M. KAZAKOV, N. D.  
ZHIGADLO, J. KARPINSKI

***Anisotropic optical conductivity and two colors of  $\text{MgB}_2$***

*Phys. Rev. B* **73**, 104509, 1-11 (2006)

A. B. KUZMENKO

***Kramers-kronig constrained variational analysis of optical spectra***

*Rev. Sci. Instrum.* **76**, 083108 (2005)

A. B. KUZMENKO, H.J.A. MOLEGRAAF, F.  
CARBONE, D. VAN DER MAREL

***Temperature-modulation analysis of superconductivity-induced transfer of in-plane spectral weight in  $\text{Bi}_2\text{Sr}_2\text{CaCu}_2\text{O}_8$***

*Phys. Rev. B* **72**, 144503, 1-9 (2005)

F. MARSIGLIO

***Sum rule from suppression of inelastic scattering in the superconducting state***

*Phys. Rev. B* **73**, 064507, 1-7 (2006)

F. MARSIGLIO, F. CARBONE, A.  
KUZMENKO, D. VAN DER MAREL

***Intraband Optical Spectral Weight in the presence of a van Hove singularity: application to  $\text{Bi}_2\text{Sr}_2\text{CaCu}_2\text{O}_{8+\delta}$***

*Phys. Rev. B* **74**, 174516, 1-10 (2006)

F.P. MENA, J.F. DITUSA, D. VAN DER  
MAREL, G. AEPPLI, D.P. YOUNG, A.  
DAMASCELLI, J.A. MYDOSH

***Suppressed reflectivity due to spin-controlled localization in a magnetic semiconductor***

*Phys. Rev. B* **73**, 085205, 1-7 (2006)

F. P. MENA, D. VAN DER MAREL, J. L.  
SARRAO

***Optical conductivity of  $\text{CeMIn}_5$  ( $M=\text{Co, Rh, Ir}$ )***

*Phys. Rev. B* **72**, 045119, 1-6 (2005)

K. ROGACKI, B. BATLOGG, J. KARPINSKI, N.D.  
ZHIGADLO, G. SCHUCK, S.M. KAZAKOV, P.  
WAGLI, R. PUZNIAK, A. WISNIEWSKI, F.  
CARBONE, A. BRINKMAN, D. VAN DER MAREL

***Strong magnetic pair breaking in Mn substituted  $\text{MgB}_2$  single crystals***

*Cond-mat/0510227* (2005)

K. ROGACKI, B. BATLOGG, J. KARPINSKI,  
N. D. ZHIGADLO, G. SCHUCK, S. M.  
KAZAKOV, P. WAGLI, R. PUZNIAK, A.  
WISNIEWSKI, F. CARBONE, A. BRINKMAN,  
D. VAN DER MAREL

**Strong magnetic pair breaking in Mn substituted  $MgB_2$  single crystals**  
*Phys. Rev. B* **73**, 174520, 1-8 (2006)

P. ROMANIELLO, P. L. DE BOEIJ, F. CARBONE, D. VAN DER MAREL  
**Optical properties of bcc transition metals in the range 0–40 eV**  
*Phys. Rev. B* **73**, 075115, 1-16 (2006)

J. TEYSSIER, A. B. KUZMENKO, D. VAN DER MAREL, F. MARSIGLIO, V. FILIPPOV, N. SHITSEVALOVA  
**Optical properties and electronic structure of  $ZrB_{12}$**   
*Phys. Rev. B* (In press)

J. TEYSSIER, A. KUZMENKO, D. VAN DER MAREL, R. LORTZ, A. JUNOD, V. FILIPPOV, N. SHITSEVALOVA  
**Electronic and optical properties of  $ZrB_{12}$  and  $YB_6$ . Discussion on electron-phonon coupling**  
*Physica Status Solidi c* **3**, 3114-3117 (2006)

D. VAN DER MAREL  
**Optical spectroscopy of plasmons and excitons in cuprate superconductors**  
*Journal of Superconductivity* **17**, 559-575 (2004), in *Festschrift dedicated to Professor Michael Trinkham on the occasion of his 75<sup>th</sup> birthday*

## 8.5.2 Scientific articles in journals without peer review

### Group G. Blatter

(projects 1 & 2)

T. ESSLINGER, G. BLATTER,  
**Atomic gas in flatland**  
*News & Views, Nature* **441**, 1053 (2006)

### Group T. Giamarchi

(projects 1 & 2)

G. LEON, T. GIAMARCHI  
**Hall effect in quasi one-dimensional organic conductors**  
*J. Low Temp. Phys.* **142**, 315-319 (2006)

C. J. BOLECH, T. GIAMARCHI  
**Tunnelling in organic Superconductors**  
*J. Low Temp. Phys.* **142**, 221-227 (2006)

A. ROSSO, E. ORIGNAC, R. CHITRA, T. GIAMARCHI  
**Coulombian Disorder in Charge Density Waves**

\*D. VAN DER MAREL  
**Electrons living apart together**  
*Nature Physics* **2**, 585-586 (2006)

D. VAN DER MAREL, F. CARBONE, A. B. KUZMENKO, E. GIANNINI  
**Scaling properties of the optical conductivity of Bi-based cuprates**  
*Annals of Physics* **321**, 1716–1729 (2006)

E. VAN HEUMEN, R. LORTZ, A.B. KUZMENKO, F. CARBONE, D. VAN DER MAREL, X. ZHAO, G. YU, Y. CHO, N. BARISIC, M. GREVEN, C.C. HOMES, S.V. DORDEVIC  
**Optical and thermodynamic properties of the high-temperature superconductor  $HgBa_2CuO_{4+\delta}$**   
*Phys. Rev. B* **75**, 054522, 1-10 (2007)

D.V. ZAKHAROV, J. DEISENHOFER, H.-A. KRUG VON NIDDA, P. LUNKENHEIMER, J. HEMBERGER, A. LOIDL, R. CLAESSEN, M. HOINKIS, M. KLEMM, M. SING, M.V. EREMIN, S. HORN, A. LOIDL,  
**Spin dynamics in the low-dimensional magnet  $TiOCl$**   
*Physical Review B* **73**, 094452 (2006)

*J. de Phys. IV* **131**, 179-182 (2006)

R. CHITRA, T. GIAMARCHI  
**Zero field Wigner glass**  
*J. de Phys. IV* **131**, 163-166 (2006)

A. B. KOLTON, A. ROSSO, T. GIAMARCHI,  
**Non equilibrium relaxation of an elastic string in random media**  
*J. de Phys. IV* **131**, 189-190 (2006)

C. KOLLATH  
**Separation of spin and charge in cold Fermi-gases**  
*J. Phys. B* **39**, 65-75 (2006)

T. JARLBORG  
**Spin-Phonon coupling in High-Tc Copper Oxides**  
*24th Int. Conf. on Low Temp. Phys.*, Eds. Y. Takano et al., AIP, p 549 (2006)

### Group F. Mila

(project 1)

D. POILBLANC, C. WEBER, F. MILA, M. SIGRIST  
**Checkerboard order in the t-J model on the square lattice**  
to appear in the Proceedings of ICM2006

## Group M. Troyer

(project 1)

S. TREBST, M. TROYER  
**Optimized Ensembles for Classical and Quantum Systems in Computer Simulations in Condensed Matter: Systems: From Materials to Chemical Biology**  
Volume 1 edited by M. Ferrario, G. Ciccotti and K. Binder (Springer Verlag 2006)

### 8.5.3 Scientific articles in anthologies

A ENGEL, A. SEMENOV, H.-W. HÜBERS, K. IL'IN, M. SIEGEL

**Electric noise and local photon-induced nonequilibrium states in a current-carrying nanostructured superconductor**

Barry P. Martins, *New Frontiers in Superconductivity Research*, 153-189, Nova Science Publishers. Inc., New York (2006)

(projects 4 & 5, group Schilling)

Ø. FISCHER, M. KUGLER, I. MAGGIO-APRILE, CH. BERTHOD, CH. RENNER

**Scanning tunneling spectroscopy of high-temperature superconductors**

*Review of Modern Physics*; **79**, 353, (2007), 65 pages, 62 figures.

(projects 2, 5 & 6, group Fischer)

T. GIAMARCHI

**Strong correlation in low dimensional systems**

In "Lectures on the physics of Highly correlated electron systems X"

AIP conference proceeding 846 (2006)

(projects 1 & 2, group Giamarchi)

T. GIAMARCHI

**From Luttinger to Fermi liquids in organic conductors**

In "The physics of organic superconductors"

To be published by Springer, ed. A Lebed (2007)

(projects 1 & 2, group Giamarchi)

N. HAYASHI, M. SIGRIST

**Kukan hanten taishosei no nai kei deno choudendou**

*Kotai-Butsuri* **41**, 631 (2006)

(projects 1 & 2, group Sigrist)

### 8.5.4 Books

A. BUSSMANN-HOLDER, H. KELLER

**Polaron Effects in High-Temperature Cuprate Superconductors**

in *Polarons in Advanced Materials*, ed. A.S. Alexandrov, Canopus Publishing Bristol 2007 ( in press)

(project 2, group Keller)

A. FURRER, A. PODLESNYAK

**Crystal-Field Spectroscopy**

*Handbook of Applied Solid State Spectroscopy*, ed. by D.R. Vij (Springer, New York, 2006), p. 257

(projects 1, 3 & 6, group Mesot)

R. KHASANOV, A. SHENGELAYA, A. BUSSMANN-HOLDER, H. KELLER

**Two-gap superconductivity in the cuprate superconductor  $La_{1.83}Sr_{0.17}CuO_4$ , in High- $T_c$  Superconductors and Related Transition Metal Oxides**

Eds. A. Bussmann-Holder and H. Keller, Springer, Berlin, 2007 ( in press)

(project 2, group Keller)

CH. RENNER, H. M. RØNNOW

**Scanning Tunneling Microscopy and Spectroscopy of Manganites**

chapter in *Scanning Probe Microscopy: Electrical and Electromechanical Phenomena at the Nanoscale*

Ed. S. V. Kalinin, A. Gruverman, Springer (October 2006)

(projects 1, 3 & 6 group Mesot)

### 8.5.5 Reports

H. BARTOLF, A. ENGEL, A. SCHILLING

**Superconducting Single Photon Detectors, in Electron beam applications at ETH Zürich**

Franck Robin, Raith Application Note 2006, Raith GmbH (2006)

(projects 4 & 5, group Schilling)



## 8.6 Lectures, seminars and colloquia

### 8.6.1 Lectures at congresses

- V. ABÄCHERLI, F. BUTA, D. UGLIETTI, C. SENATORE, B. SEEBER, R. FLÜKIGER, *Investigation on the Effect of Ta Additions on  $J_c$  and  $n$  of  $(Nb,Ti)_3Sn$  Bronze Processed Multi-filamentary Wires at High Magnetic Fields*, ASC06 Conference, Seattle, USA, August 27 - September 1, 2006 (project 6, Group of Flükiger)
- M. G. ADESSO, M. POLICHETTI, S. PACE, D. UGLIETTI, R. FLÜKIGER, *Common and different features in vortex dynamics of LTS, HTS and  $MgB_2$* , CryoPrague 2006, Prague, Czech Republic, July 17-21, 2006 (project 6, Group of Flükiger)
- P. AEBI, *Angle-resolved Photoemission Spectroscopy Using Synchrotron Radiation*, 8th International School and Symposium on Synchrotron Radiation in Natural Sciences, Zakopane, Poland, June 14, 2006 (project 5, Group of Aebi)
- P. AEBI, *ARPES on CDW compounds*, Workshop on statistical and low dimensional systems, Nancy, France, May 18, 2006 (project 5, Group of Aebi)
- P. ALLENSPACH, *Continuous and Pulsed Neutron Sources*, International Summer School, "Neutron Techniques in Molecular Magnets", Jaca, Spain, September 6, 2006 (projects 1, 3 & 6, Group of Mesot)
- P. ALLENSPACH, *Novel Neutron Optics Based on Supermirrors*, WINS Berlin, Germany, September 29 - October 1, 2006 (projects 1, 3 & 6, Group of Mesot)
- L. ANTOGNAZZA, *Thermally assisted transition in thin films based FCL: a way to speed up the normal transition across the wafer*, Applied Superconductivity Conference 2006, Seattle, USA, August 27 - September 1, 2006 (projects 2, 5 & 6, Group Fischer)
- D. BAERISWYL, *Variational studies: from conjugated polymers to high- $T_c$  superconductors*, Workshop on Strongly Correlated Electrons, Schloss Ringberg, Germany, May 2006 (project 2, Group Baeriswyl)
- D. BAERISWYL, *Superconductivity in the repulsive Hubbard model*, 30th Int. Conf. of Theoretical Physics, Ustron, Poland, September 2006 (project 2, Group Baeriswyl)
- D. BAERISWYL, *Superconductivity in the repulsive Hubbard model*, Workshop "From Memory to Future", Institute of Scientific Interchange, Torino, Italy, November 2006 (project 2, Group Baeriswyl)
- H. BARTOLF, *Lift-off technique for the fabrication of nanostructures*, SPS Jahrestagung 2007, Zürich, February 20-21, 2007 (projects 4 & 5, Group of Schilling)
- C. BERNHARD, *Competition between high  $T_c$  superconductivity and ferromagnetism in oxide multilayers*, Conference on "Trends in future electronics: Quantum digital circuits, materials with exceptional electronic properties, novel device concepts and applications", Bordeaux, France, May 6-10, 2006 (project 2, Group of Bernhard)
- C. BERNHARD, *Spin state transition and magnetic order in  $Na_xCoO_2$  at  $x>0.7$* , Conference on "Self-organized strongly correlated electron systems", Seillac, France, May 29-31, 2006 (project 2, Group of Bernhard)
- C. BERNHARD, *The anomalous c-axis conductivity of the cuprate HTSC probed by infrared ellipsometry*, M<sup>2</sup>S HTSC VIII, 8<sup>th</sup> International Conference on Materials and Mechanisms of Superconductivity and High Temperature Superconductors, Dresden, Germany, July 9-14, 2006 (project 2, Group of Bernhard)
- C. BERNHARD, *Magnetic order, anomalous transport, and spin state transition in  $Na_xCo_2$  at  $x>0.70$* , First Swiss-Japanese Workshop on the Applications and on novel developments in muon spectroscopy on novel materials, Tsukuba, Japan, September 28-30, 2006 (project 2, Group of Bernhard)
- C. BERTHOD, T. GIAMARCHI, S. BIERMANN, A. GEORGES, *Fermi surface pockets and Luttinger sum rule in low-dimensional systems*, 2007 APS March Meeting Denver, CO, USA, March 5-9, 2007 (projects 1 & 2, Group of Giamarchi)
- C. BERTHOD, T. GIAMARCHI, S. BIERMANN, A. GEORGES, 2006 Swiss Physical Society - MaNEP Meeting Lausanne-EPFL, Switzerland, February 13-14, 2006 (projects 1 & 2, Group of Giamarchi)
- C. BERTHOD, T. GIAMARCHI, S. BIERMANN, A. GEORGES, Martin Peter Colloquium, Geneva-DPMC, Switzerland, September 27, 2006 (projects 1 & 2, Group of Giamarchi)
- C. BERTHOD, G. LEVY, Ø. FISCHER, 2007 APS March Meeting, Denver, CO, USA, March 5-9, 2007 (projects 1 & 2, Group of Giamarchi)

- G. BLATTER, *Vortex Matter*, International Conference on Frontiers of Condensed Matter Physics, Minnesota, Minneapolis, May 2006 (projects 1 & 2, Group of Blatter)
- G. BLATTER, *Using qubits for measuring fidelity in mesoscopic systems*, Advanced Research Workshop "Meso-06" on Mesoscopic and strongly correlated electron systems - 4, Nanoscale superconductivity and magnetism, Chernogolovka, Russia, June, 2006 (projects 1 & 2, Group of Blatter)
- G. BLATTER, *Vortex Matter in Layered Superconductors*, Three Lectures at the Winter School on Unconventional Superconductivity, Brasilia, Brasil, July/August 2006 (projects 1 & 2, Group of Blatter)
- L. BOCHER, R. ROBERT, D. LOGVINOVICH, A. WEIDENKAFF, *Cationic and Anionic Substitution in Functional Perovskite-type Phases*, SCS meeting, University of Zürich, October 13, 2006 (projects 1, 3 & 4, Group of Schlapbach)
- G. BUCHS, *STM/ STS Investigations of Single-Walled Carbon Nanotubes Defects Induced by Low-Energy Hydrogen Ions*, ICNT2006: International Conference on Nanoscience and Technology, Basel, August 01, 2006 (projects 1, 3 & 4, Group of Schlapbach)
- Z. BUKOWSKI, N.D. ZHIGADLO, G. SCHUCK, B. BATLOGG, J. KARPINSKI, *Na<sub>2</sub>Os<sub>2</sub>O<sub>6.5</sub>-new metallic pyrochlore synthesized under high pressure*, 8th International Conference on Materials and Mechanism of Superconductivity and High Temperature Superconductors, M<sup>2</sup>S-HTSC VIII, Dresden, Germany, July 9-14, 2006 (projects 3 & 4, Group of Karpinski)
- Z. BUKOWSKI, N.D. ZHIGADLO, M. BRÜHWILER, B. BATLOGG, J. KARPINSKI, *High-pressure growth of Rb, K and Na osmate single crystals with the pyrochlore structure*, Swiss Physical Society-MaNEP Meeting, Lausanne, Switzerland, February 13-14, 2006 (projects 3 & 4, Group of Karpinski)
- Z. BUKOWSKI, *Single crystal growth and properties of superconducting  $\beta$ -pyrochlore osmates KOs<sub>2</sub>O<sub>6</sub> and RbOs<sub>2</sub>O<sub>6</sub> Novel pyrochlore compounds synthesized under high pressure*, 2006 Martin Peter Colloquium and MaNEP Topical Meeting on "Novel Superconductors", Geneva, Switzerland, September 27, 2006 (projects 3 & 4, Group of Karpinski)
- M. BÜTTIKER, *Transport in Nanostructures*, four lectures at the 2nd Capri Spring School on, Island of Capri, Italy, April 2 - 9, 2006 (projects 1 & 2, Group of Büttiker)
- M. BÜTTIKER, *Dephasing and inelastic scattering from voltage probes*, International seminar and workshop on "Quantum Coherence, Noise and Decoherence in Nanostructures", Dresden, Germany, May 21-26, (2006) (projects 1 & 2, Group of Büttiker)
- M. BÜTTIKER, *Departures from Onsager Symmetries in non-linear conduction*, Frontiers in Condensed Matter Theory, William I. Fine Theoretical Physics Institute, University of Minnesota, Minneapolis, USA, May 4 - 7, 2006 (projects 1 & 2, Group of Büttiker)
- M. BÜTTIKER, *Mesoscopic Capacitors*, First Conference on Quantum Control, Fudan University, Shanghai, China, June 2 - 3, 2006 (projects 1 & 2, Group of Büttiker)
- M. BÜTTIKER, *"Testing the quantum-ness of qubits"*, informal presentation at the workshop "Interactions, Coherence and Control in Mesoscopic Systems", Aspen Institute of Physics, Aspen, Colorado, USA, July 13, 2006 (projects 1 & 2, Group of Büttiker)
- M. BÜTTIKER, *Mesoscopic Capacitors*, International Conference of Nanoscience and Nanotechnology, Basel, Switzerland, July 31, 2006 (projects 1 & 2, Group of Büttiker)
- M. BÜTTIKER, *"Mesoscopic Capacitors"*, workshop on "Quantum Pumping", Lewiner Institute for Theoretical Physics, Technion, Haifa, Israel, January 12, 2007 (projects 1 & 2, Group of Büttiker)
- H. CERCELLIER, *ARPES and STM/STS study of the electronic properties of 1-TiSe<sub>2</sub>*, Nancy, France May 19, 2006 (project 5, Group of Aebi)
- J. CHANG, *High- and low- energy electronic responses in high temperature superconductors*, 5th International Conference Stripes, Roma, Italy, December 17-19, 2006 (projects 1, 3 & 6, Group of Mesot)
- A. DE COL, *Surface Melting of the Vortex Lattice*, 8-th Int. Conf. on Materials and Mechanisms of Superconductivity - High-Temperature Superconductors (M<sub>2</sub>SHTSC), Dresden, Germany, July 2006 (projects 1 & 2, Group of Blatter)
- A. DE COL, *Surface Melting of the Pancake Vortex Lattice in Layered Superconductors*, The 11-th International Workshop on Vortex Matter, Wrocław, Poland, July 2006 (projects 1 & # 2, Group of Blatter)
- K. CONDER, *Layered perovskite cobaltites*, Solid State Seminar at Physics Institute University of Zurich, November 1, 2006 (projects 1, 3 & 6, Group of Mesot)
- K. CONDER, A. PODLESNYAK, E. POMJAKUSHINA, M. STINGACIU, *Layered cobaltites: synthesis, oxygen nonstoichiometry, transport and magnetic properties*, E-MRS Fall Meeting 2006, Warsaw, Poland September 4-8, 2006, (projects 1, 3 & 6, Group of Mesot)

- K. CONDER, M. STINGACIU, E. POMJAKUSHINA, A. PODLESNYAK, *Structural, magnetic and transport properties of layered cobaltites  $\text{LnBaCo}_2\text{O}_{5+x}$* , International Conferences on Modern Materials and Technologies (CIMTEC 2006), Acireale, Sicily, Italy, June 4-9, 2006 (projects 1, 3 & 6, Group of Mesot)
- M. DAWBER, *Tailoring the electrical properties of ferroelectric superlattices*, Rank Prize Mini-Symposium on nanostructured electro-optic arrays, Grasmere, UK, September 11-14, 2006 (projects 5 & 6, Group of Triscone)
- M. DAWBER, *Controlling ferroelectricity in  $\text{PbTiO}_3/\text{SrTiO}_3$  superlattices*, 18th International Symposium on Integrated Ferroelectrics, Honolulu, Hawaii, USA, April 23-27, 2006 (projects 5 & 6, Group of Triscone)
- M. DAWBER, *Phase transitions in ferroelectric superlattices*, APS March Meeting 2006, Baltimore, Maryland, USA, March 12-18, 2006 (projects 5 & 6, Group of Triscone)
- L. DEGIORGI, *Magneto-optical evidence of double exchange in a percolating lattice*, Internal MaNEP Workshop 2006, Neuchatel, Switzerland, February 6 2006 (project 1, Group of Degiorgi)
- L. DEGIORGI, *Optical evidence for a magnetically driven structural transition in the spin web  $\text{Cu}_3\text{TeO}_6$* , March Meeting of the American Physical Society, Baltimore, U.S.A. March 13-17 2006 (project 1, Group of Degiorgi)
- L. DEGIORGI, *Magneto-optical evidence of double exchange in a percolating lattice*, March Meeting of the American Physical Society, Baltimore, U.S.A. March 13-17 2006 (project 1, Group of Degiorgi)
- L. DEGIORGI, *Magneto-optical evidence of double exchange in a percolating lattice*, International Conference on Low Energy Electrodynamics in Solids 2006, July 1-6 2006, Tallinn, Estonia (project 1, Group of Degiorgi)
- J. DEISENHOFER, P. GHIGNA, F. MAYR, A. LOIDL, D VAN DER MAREL, *Optical properties of the 1D antiferromagnet  $\text{KCuF}_3$* , APS March Meeting, Denver, USA, March 7, 2007 (projects 2, 5 & 6, Group of Van der Marel)
- C. DUBOIS, *Scanning Tunneling Spectroscopy on the Pyrochlore Superconductor  $\text{KOs}_2\text{O}_6$* , APS March Meeting, Denver, Colorado, USA, March 07, 2007 (projects 2, 5 & 6, Group of Fischer)
- D. EICHENBERGER, *Search for d-wave superconductivity in the repulsive Hubbard model*, Annual Meeting of the Swiss Physical Society, Lausanne, Switzerland, February 2006 (project 2, Group Baeriswyl)
- D. EICHENBERGER, *Superconductivity in the two-dimensional repulsive Hubbard model*, Martin Peter Colloquium and Manep Topical Meeting on Novel Superconductors, Geneva, Switzerland, September 2006 (project 2, Group Baeriswyl)
- Y. FASANO, *The tunneling detected pseudogap phase on cuprates: evidence from  $\text{YBa}_2\text{Cu}_4\text{O}_8$* , Swiss Physical Society, Zürich, February 21, 2007 (projects 2, 5 & 6, Group of Fischer)
- Ø. FISCHER, *Vortex cores in  $\text{Kos}_2\text{O}_6$ ,  $\text{PbMo}_6\text{S}_8$  and high temperature superconductors observed by STM*, M2S-HTSVIII, Dresden, Germany, July 10-14, 2007 (projects 2, 5 & 6, Group of Fischer)
- Ø. FISCHER, *Scanning Tunneling Spectra on HTS: The interplay of the gap, the bosonic mode and the van Hove singularity*, LEES 2006, Tallinn, Estonia, (projects 2, 5 & 6, Group of Fischer)
- Ø. FISCHER, *Temperature Dependence of the Quasiparticle Excitation Spectrum in Colossal Magnetoresistive Manganites*, SSCES, May 27-31, Seillac, France (projects 2, 5 & 6, Group of Fischer)
- Ø. FISCHER, *Tunnelling Spectroscopy*, Summerschool NEEM, Aussois, France, May-June 2006 (projects 2, 5 & 6, Group of Fischer)
- Ø. FISCHER, *Thin films of cuprates: From 2D physics to future applications*, Workshop in honor of Piero Martinoli, Neuchâtel, Switzerland, September 22, 2006 (projects 2, 5 & 6, Group of Fischer)
- Ø. FISCHER, *Local probes applied to the study of materials with novel electronic properties*, MaNEP Summer school, Saas Fee, September 11-16, 2006 (projects 2, 5 & 6, Group of Fischer)
- R. FLÜKIGER, P. LEZZA, M. CESARETTI, C. SENATORE, R. GLADYSHEVSKI, *Simultaneous Addition of  $\text{B}_4\text{C}$  +  $\text{SiC}$  to  $\text{MgB}_2$  wires and consequences for  $J_c$  and  $B_{irr}$* , ASC06 Conference, Seattle, USA, August 27 - September 1, 2006 (project 6, Group of Flükiger)
- A. FURRER, *Barocaloric Cooling: A precursor and spin-off of the Discovery of High-Temperature Superconductivity*, International Symposium in Honor of J.G. Bednorz and K.A. Müller, Zurich, Switzerland, March 27-30, 2006 (projects 1, 3 & 6, Group of Mesot)
- F. HASSLER, *Using Qubits for Measuring Full Counting Statistics*, QSIT Workshop, Arosa, Switzerland, January, 2006 (projects 1 & 2, Group of Blatter)
- F. HASSLER, *Superconducting Tetrahedral Qubit with Broken Symmetry*, Meeting on Quantum Systems for Information Technology (QSIT), Engelberg, Switzerland, March, 2006 (projects 1 & 2, Group of Blatter)

- F. HASSLER, *Stability and Noise in Tetrahedral Qubits*, ESF Workshop on Trends in future electronics, Bordeaux, France, May 2006 (projects 1 & 2, Group of Blatter)
- S. HUBER, *Shaking Atoms in an Optical Lattice*, QSIT Workshop, Arosa, Switzerland, January, 2006 (projects 1 & 2, Group of Blatter)
- J.L. GAVILANO, *Some Open Issues in the Magnetism of  $\text{Na}_x\text{CoO}_2$* , First International Workshop on the Physical Properties of Lamellar Cobaltates, Université Paris-Sud, Orsay, France, July 16-19, 2006 (projects 1, 3 & 6, Group of Mesot)
- J.L. GAVILANO, B. PEDRINI, M. WELLER, J. HINDERER, H.R. OTT, S.M. KAZAKOV, J. KARPINSKI, *Itinerant Versus Localized Spins in  $\text{Na}_x\text{CoO}_2$* , Joint Swiss-Russian Workshop on Quantum Magnetism and Polarized Neutrons, Laboratory for Neutron Scattering, Paul Scherrer Institut, Villigen PSI, Switzerland, March 1-4, 2006 (projects 1, 3 & 6, Group of Mesot)
- V. GESHKENBEIN, *Dynamic approach for the strong pinning*, International Conference on Frontiers of Condensed Matter Physics, Minnesota, Minneapolis, USA, May 2006 (projects 1 & 2, Group of Blatter)
- V. GESHKENBEIN, *Strong pinning: dynamic approach*, Landau Days 2006, Chernogolovka, Russia, June, 2006 (projects 1 & 2, Group of Blatter)
- V. GESHKENBEIN, *Dynamic approach for strong pinning*, The 11th International Workshop on Vortex Matter, Wroclaw, Poland, July 2006 (projects 1 & 2, Group of Blatter)
- V. GESHKENBEIN, *Lectures on Superconductivity*, Kiev, Ukraine, March, 2006 (projects 1 & 2, Group of Blatter)
- T. GIAMARCHI, Conférence "Frontiers of Condensed Matter Theory", Minneapolis, USA, May 4-7, 2006 (projects 1 & 2, Group of Giamarchi)
- T. GIAMARCHI, INSTANS Summer Conference, Como, Italy, June 12-16 2006 (projects 1 & 2, Group of Giamarchi)
- T. GIAMARCHI, 11th Itsykson meeting, "Strongly correlated electrons", SACLAY, France, June 21-23, 2006 (projects 1 & 2, Group of Giamarchi)
- T. GIAMARCHI, International Conference on "Low Energy Electrodynamics of Solids" (LEES), Tallinn, Estonia, July 1-6, 2006 (projects 1 & 2, Group of Giamarchi)
- T. GIAMARCHI, School and conference "Modelling elastic manifolds, from soft condensed matter to biomolecules", ICTP Trieste, July 24-29, 2006 (projects 1 & 2, Group of Giamarchi)
- T. GIAMARCHI, Workshop "Stochastic Geometry and Field Theory: From Growth Phenomena to Disordered Systems", KITP Santa-Barbara, August-Sept, 2006 (projects 1 & 2, Group of Giamarchi)
- T. GIAMARCHI, 10th Joint MMM/Intermag Conference, Baltimore, January 7-11, 2006 (projects 1 & 2, Group of Giamarchi)
- R. GILARDI, *New high-field actively shielded split-coil magnet for neutron scattering*, 3rd Workshop on Inelastic Neutron Spectrometers, Berlin, September 29-30, 2006 (projects 1, 3 & 6, Group of Mesot)
- O. GRÖNING, *Low energy H-ion induced defects on graphite and single walled carbon nanotubes characterized by STM and STS*, Workshop on Statistical Physics and Low Dimensional Systems, Nancy, France, May 17-19, 2006 (projects 1, 3 & 4, Group of Schlapbach)
- O. GRÖNING, *Low energy H-ion induced defects on single-walled carbon nanotubes*, Sino-Swiss Cooperation Symposium on Material Science 2006, ETH, Zürich, Switzerland, October 30 - November 2, 2006 (projects 1, 3 & 4, Group of Schlapbach)
- E. GULL, *The ALPS DMFT Framework*, ALPS DMFT Workshop, Universität Göttingen, Göttingen, Deutschland, December 7, 2006 (project 1, Group of Troyer)
- N. HAYASHI, *dc Josephson current between spin-singlet and noncentrosymmetric superconductors*, 2006 Autumn Meeting of the Physical Society of Japan, Chiba, Japan, Sept. 25-29, 2006 (projects 1 & 2, Group of Sigrist)
- A. IUCCI, 2007 APS March Meeting, Denver, CO, USA, March 5-9, 2007 (projects 1 & 2, Group of Giamarchi)
- T. JARLBORG, 2007 APS March Meeting Denver, CO, USA, March 5-9, 2007 (projects 1 & 2, Group of Giamarchi)
- D. JACCARD, *Is pressure an ideal experimental parameter?*, High pressure PSI workshop, Villigen, Switzerland, January 25, 2006 (projects 5 & 6, Group of Triscone)
- D. JACCARD, *Ferromagnetic spin-fluctuation mediated superconductivity in high pressure iron*,  $\text{M}_2\text{S-HTSC}$  VII Conf, Dresden, Germany, July 9-14, 2006 (projects 5 & 6, Group of Triscone)
- Y. JIANG, *Phase transitions in quantum triangular Ising antiferromagnets*, contributed talk, Summer School of Quantum Magnetism, Les Houches, France, June 2006 (project 2, Group Baeriswyl)
- Y. JIANG, *Phase transitions in quantum triangular Ising antiferromagnets*, IFCAM Workshop on Spin Currents, Sendai, Japan, August 2006 (project 2, Group Baeriswyl)
- J. KARPINSKI, *Magnetic and non-magnetic substitutions in  $\text{MgB}_2$  single crystals influence on superconducting*

- properties and structure*, Am. Phys. Soc. Meeting, Baltimore, USA, March 11-17, 2006 (projects 3 & 4, Group of Karpinski)
- J. KARPINSKI, *Influence of magnetic and non-magnetic substitutions in MgB<sub>2</sub> single crystals, on superconducting properties and structure*, Conference: Ceramic Congress CIMTEC Acireale, Sicily, June 4-9, 2006 (projects 3 & 4, Group of Karpinski)
  - J. KARPINSKI, *Influence of substitutions, defects and inhomogeneities on superconducting properties and structure of boride and oxide superconductors*, Conference: From Solid State Physics to Biophysics, Cavtat, Croatia, June 24 - July 1, 2006 (projects 3 & 4, Group of Karpinski)
  - J. KARPINSKI, *MgB<sub>2</sub> single crystals, Influence of magnetic and non-magnetic substitutions on superconducting properties and structure*, Conference: EMRS Warsaw, Poland, September 4-8, 2006 (projects 3 & 4, Group of Karpinski)
  - J. KARPINSKI, *Influence of magnetic and non-magnetic substitutions in MgB<sub>2</sub> single crystals, on superconducting properties and structure*, Workshop: Controlled Mesoscopic Phase Separation, Heraklion, Greece, October 24 - November 4, 2006 (projects 3 & 4, Group of Karpinski)
  - J. KARPINSKI, K. ROGACKI, G. SCHUCK, S.M. KAZAKOV, N.D. ZHIGADLO, *Crystal growth, structural studies and superconducting properties of  $\beta$ -pyrochlore KOs<sub>2</sub>O<sub>6</sub>*, 8th International Conference on Materials and Mechanism of Superconductivity, M<sup>2</sup>S-HTSC VIII, Dresden, Germany, July 9-14, 2006 (projects 3 & 4, Group of Karpinski)
  - J. KARPINSKI, N.D. ZHIGADLO, K. ROGACKI, B. BATLOGG, G. SCHUCK, R. PUZNIAK, A. WISNIEWSKI, R.S. GONNELLI, *Magnetic and non-magnetic substitutions in MgB<sub>2</sub> single crystals: influence on superconducting properties and structure*, 8th International Conference on Materials and Mechanism of Superconductivity and High Temperature Superconductors, M<sup>2</sup>S-HTSC VIII, Dresden, Germany, July 9-14, 2006 (projects 3 & 4, Group of Karpinski)
  - J. KARPINSKI, N.D. ZHIGADLO, K. ROGACKI, B. BATLOGG, G. SCHUCK, R. PUZNIAK, A. WISNIEWSKI, R. GONNELLI, *Magnetic and non-magnetic substitutions in MgB<sub>2</sub> single crystals: influence on superconducting properties and structure*, Swiss Physical Society-MaNEP Meeting, Lausanne, Switzerland, February 13-14, 2006 (projects 3 & 4, Group of Karpinski)
  - J. KARPINSKI, *MgB<sub>2</sub> single crystals, influence of magnetic and non-magnetic substitution and hole and electron doping on superconducting properties and structure*, 2006 Martin Peter Colloquium and MaNEP Topical Meeting on "Novel Superconductors", Geneva, Switzerland, September 27, 2006, (projects 3 & 4, Group of Karpinski)
  - H. KELLER, *Unconventional isotope effects in cuprate superconductors - what can we learn from them?*, Conference on Lattice Effects in Superconductors, Santa Fe, USA, April 17-20, 2006 (project 2, Group Keller)
  - H. KELLER, *Unconventional isotope effects in cuprate superconductors*, Third Meeting of CoMePhS, Paris, France, June 17-19, 2006 (project 2, Group Keller)
  - H. KELLER, *Unconventional isotope effects in cuprate high-temperature superconductors*, 8th International Conference on Materials and Mechanisms of Superconductivity and High Temperature Superconductors (M<sup>2</sup>S 2006 Dresden), Dresden, Germany, July 9-14, 2006 (project 2, Group Keller)
  - H. KELLER, *Vortex matter and unconventional isotope effects in cuprate superconductors*, First Swiss-Japanese workshop on the applications and on new developments in muon spectroscopy on novel materials, KEK, Tsukuba, Japan, September 28-30, 2006 (project 2, Group Keller)
  - H. KELLER, *Unconventional isotope effects in cuprate high-temperature Superconductors*, Miniworkshop on Isotope Effect in HTSC Cuprates: Experiment vs. Theory, National Institute of Advanced Industrial Science and Technology (AIST) Tsukuba, Japan September 29, 2006 (project 2, Group Keller)
  - H. KELLER, *Experimental evidence for two gaps in cuprate high-temperature superconductors*, Sixth International Conference on New Theories, Discoveries, and Applications of Superconductors and Related Materials, Sydney, Australia, January 9-11, 2007 (project 2, Group Keller)
  - C. KOLLATH, Wilhelm and Else Heraeus seminar on "Nonequilibrium Transport of Strongly Correlated Systems: Towards Simulation of Novel Devices", Bad Honnef, Germany, February 2007 (projects 1 & 2, Group of Giamarchi)
  - C. KOLLATH, Conference on "Thermal Transport and Relaxation: Foundations and Perspectives" Bad Honnef, Germany, January 2007 (projects 1 & 2, Group of Giamarchi)
  - C. KOLLATH, International Workshop on "Dynamics and Relaxation in Complex Quantum and Classical Systems and Nanostructures", Max-Planck Institut in Dresden, Germany, August 2006 (projects 1 & 2, Group of Giamarchi)
  - C. KOLLATH, International Workshop on "Non-equilibrium Dynamics in Interacting Systems" Max-Planck Institut in Dresden

- Germany, April 2006 (projects 1 & 2, Group of Giamarchi)
- C. KOLLATH, Workshop "Non-equilibrium phenomena in strongly correlated quantum systems" Harvard University, USA, February 2006 (projects 1 & 2, Group of Giamarchi)
  - C. KOLLATH, Korrelationstage 2007, Dresden, Germany, February 2007 (project # 1 & 2, Group of Giamarchi)
  - C. KOLLATH, Spring meeting of the German physical society (DPG), Frankfurt, Germany, March 2006 (projects 1 & 2, Group of Giamarchi)
  - A. KUZMENKO, D. VAN DER MAREL, F. CARBONE, F. MARSIGLIO, *Spectral Weight Oracle: Model-Independent Sum Rule Analysis Based on Limited-Range Spectral Data*, APS March Meeting, Denver, USA, March 7, 2007 (projects 2, 5 & 6, Group of Van der Marel)
  - G. LEON, 2007 APS March Meeting Denver, CO, USA, March 5-9, 2007 (project # 1 & 2, Group of Giamarchi)
  - G. LEVY, *Scanning Tunneling Spectra on HTS: The interplay of the gap, the bosonic mode and the van Hove singularity*, Swiss Physical Society, Zürich, February 21, 2007 (projects 2, 5 & 6, Group of Fischer)
  - P. LEZZA, C. SENATORE, R. GLADYSHEVSKII, R. FLÜKIGER, *Critical Current Anisotropy and Texture Gradients in ex situ MgB<sub>2</sub>/Fe Tapes*, ASC06 Conference, Seattle, USA, August 27 - September 1, 2006 (project 6, Group of Flükiger)
  - D. LOGVINOVICH, *Synthesis and Characterisation of Oxynitride Perovskites*, Workshop, Substitutionseffekte in ionischen Festkörpern, Rauscholzhausen, August 22-24, 2006 (projects 1, 3 & 4, Group of Schlapbach)
  - D. LOGVINOVICH, *Synthesis and physical chemical properties of SrMoO<sub>3-x</sub>N<sub>x</sub> (x > 1)*, SCS meeting, University of Zürich, October 13, 2006 (projects 1, 3 & 4, Group of Schlapbach)
  - I. MAROZAU, A. SHKABKO, T. LIPPERT, L. SCHLAPBACH, A. WOKAUN, A. WEIDENKAFF, *Pulsed Laser Deposition of epitaxial SrTiO<sub>3</sub>:N films*, SPS meeting 2007, Zürich, Febr. 20-21, 2007 (projects 1, 3 & 4, Group of Schlapbach)
  - F. MARSIGLIO, F. CARBONE, A. KUZMENKO, D. VAN DER MAREL, *Intraband Optical Spectral Weight in the presence of a van Hove singularity: application to Bi<sub>2</sub>Sr<sub>2</sub>CaCu<sub>2</sub>O<sub>8+d</sub>*, APS March Meeting, Denver, USA, March 8, 2007 (projects 2, 5 & 6, Group of Van der Marel)
  - M. MEDARDE, C. DALLERA, M. GRIONI, TH. NEISIUS, J.A. ALONSO, M.J. SAYAGUES AND M.T. CASAIS, *2Ni<sup>3+</sup> → Ni<sup>3+d</sup> + Ni<sup>3-d</sup> charge disproportionation in RNiO<sub>3</sub> perovskites (r=rare earth): implications for the stability of the magnetic structure*, Seminar, Laboratorium für Neutronenstreuung, ETH Zürich and PSI Villigen, Villigen, Switzerland, May 18, 2006 (projects 1, 3 & 6, Group of Mesot)
  - J. MESOT, *Interplay between electronic and magnetic degrees of freedom in 3d-metal oxides*, International Workshop on Self-Organized Strongly Correlated Electron Systems, Seillac, France, May 28 - June 1, 2006 (projects 1, 3 & 6, Group of Mesot)
  - J. MESOT, *Neutron and Photon Spectroscopies of Highly Correlated Electron Systems*, Rencontres LLB/Soleil: électrons fortement corrélés, Saclay, France, June 22-23, 2006 (projects 1, 3 & 6, Group of Mesot)
  - J. MESOT, *Momentum Resolved Neutron and ARPES Investigations of HTSC*, Conference on Low Energy Electrodynamics in Solids (LEES06), Tallinn, Estonia, July 2-6, 2006 (projects 1, 3 & 6, Group of Mesot)
  - J. MESOT, *Neutron Scattering Investigations of the Abrikosov State of High-Temperature Superconductors*, 8th International Conference on Materials and Mechanisms on Superconductivity (M<sub>2</sub>S-HTSC VIII), Dresden, Germany, July 9-14, 2006 (projects 1, 3 & 6, Group of Mesot)
  - J. MESOT, *Elementary scattering*, 5th PSI Summer School on Condensed Matter Research: Neutron, X-ray and Muon Studies of Nano Scale Structures, Zuoz, Switzerland, August 19-26, 2006 (projects 1, 3 & 6, Group of Mesot)
  - J. MESOT, *Neutron- and photon-based spectroscopies*, Second MaNEP summer school: Probing the Physics of Low Dimensional Systems, Saas-Fee, Switzerland, September 11-16, 2006 (projects 1, 3 & 6, Group of Mesot)
  - J. MESOT, *Neutron scattering of low-dimensional systems*, Workshop on Polarized Neutrons in Condensed Matter Investigations (PNCMI 2006), Berlin, Germany, September 25-28, 2006 (projects 1, 3 & 6, Group of Mesot)
  - F. MILA, *Lectures on Quantum Magnetism*, Summer school on « Aussois, May 27 - June 2, 2006 (project 1, Group of Mila)
  - F. MILA, *Looking for exotic ground states in quantum antiferromagnets*, International Conference "From Solid State To BioPhysics III", Dubrovnik, June 24 - July 1, 2006 (project 1, Group of Mila)
  - F. MILA, *From orbital degeneracy to RVB spin liquids*, International conference "Highly Frustrated Magnetism 2006", Osaka, August 15-19, 2006 (project 1, Group of Mila)
  - F. MILA, *Phase Transitions in Bosonic Models of Frustrated Quantum Magnets*, International Focus Workshop on "Mobile Fermions and Bosons on Frustrated

- Lattices", Dresden, January 11-13, 2007 (project 1, Group of Mila)
- C. MONNEY, *Electronic and atomic structure of  $\text{Na}_x\text{CoO}_2$  investigated by Angle-Resolved Photoemission*, Meeting of the Swiss Physical Society, Lausanne, February 14, 2006 (project 5, Group of Aebi)
  - E. MORENZONI, *Direct observation of non-local effects in superconductors*, Deutsche Physikalische Gesellschaft Tagung, Dresden, March 28, 2006 (project 2, Group Keller)
  - E. MORENZONI, *Depth dependent studies of magnetic and superconducting properties with polarized muons*, First Swiss-Japanese Workshop on the applications and new developments in muon spectroscopy on novel materials, Tsukuba, September 29, 2006 (project 2, Group Keller)
  - E. MORENZONI, *Advanced  $\mu\text{SR}$  techniques*, Workshop on Future Developments of European Muon Sources, Abingdon, November 2, 2006 (project 2, Group Keller)
  - H. R. OTT, *Open questions in relation to designing emergent matter*, ICAM meeting: Designing Emergent Matter, Snowmass, USA, June 21-26, 2006 (project 1, Group of Ott)
  - H. R. OTT, *Electronic and magnetic properties of low dimensional spin systems*, Miniworkshop on New States of stable and unstable Quantum Matters, Trieste, Italy, August 13-19, 2006 (project 1, Group of Ott)
  - H. R. OTT, *Introduction to the physics of low-D systems*, MaNEP Summer School on low-D systems, Saas Fee, Switzerland, September 11, 2006 (project 1, Group of Ott)
  - H. R. OTT, *Thermal properties of low-D systems*, MaNEP Summer School on low-D systems, Saas Fee, Switzerland, September 12, 2006 (project 1, Group of Ott)
  - P. PEDRAZZINI, D. JACCARD, T. JARLBORG, H. WILHELM, M. SCHMIDT, H. Q. YUAN, F. STEGLICH, *Unusual Metallic State in FeGe beyond its Quantum Critical Point*, Annual Meeting of the Swiss Physical Society, Lausanne, Switzerland, February 13-14, 2006 (projects 5 & 6, Group Triscone)
  - A. PIRIOU, *Doping-dependence of the Vortex Phase diagram in  $\text{Bi}_2\text{Sr}_2\text{Ca}_2\text{Cu}_3\text{O}_{10+\delta}$* , Swiss Physical Society, Zürich, Switzerland, February 21, 2007 (projects 2, 5 & 6, Group Fisher)
  - L. POLLET, *The fate of supersolidity in the ground state of Helium-4*, USA Aspen CO, Aspen summer programme on supersolidity, June 2006 (project 1, Group of Troyer)
  - L. POLLET, *The fate of supersolidity in the ground state of Helium-4*, Workshop on Numerical Methods in Strongly Correlated Electronic Systems, Taipei, Taiwan, August 29, 2006 (project 1, Group of Troyer)
  - L. POLLET, *the ALPS project*, Workshop on Numerical Methods in Strongly Correlated Electronic Systems, Taipei, Taiwan, August 30, 2006 (project 1, Group of Troyer)
  - V. POMJAKUSHIN, *Effect of oxygen isotope substitution on magnetic ordering and phase separation in  $(\text{La}_{1-y}\text{Pr}_y)_{0.7}\text{Ca}_{0.3}\text{MnO}_3$* , 8th SINQ Users Meeting, Paul Scherrer Institut, Villigen PSI, Switzerland, May 10, 2006 (projects 1, 3 & 6, Group of Mesot)
  - E. POMJAKUSHINA, K. CONDER, M. STINGACIU, V. POMJAKUSHIN, A. PODLESNYAK AND D.CHERNYSHOV, *metal-insulator transition in layered cobaltites  $\text{R}\text{BaCo}_2\text{O}_{5.5}$* , European Powder Diffraction Conference (EPDIC 2006), Geneva, Switzerland, August 31 - September 4, 2006 (projects 1, 3 & 6, Group of Mesot)
  - R. PUZNIAK, A. WISNIEWSKI, A. SZEWCZYK, K. KAPCIA, J. JUN, N.D. ZHIGADLO, S.M. KAZAKOV, J. KARPINSKI, *Anisotropic upper critical field of chemically substituted  $\text{MgB}_2$  single crystals studied by torque magnetometry*, 8th International Conference on Materials and Mechanism of Superconductivity and High Temperature Superconductors, M<sup>2</sup>S-HTSC VIII, Dresden, Germany, July 9-14, 2006 (projects 3 & 4, Group of Karpinski)
  - T.M. RICE, *High temperature superconductivity – phonon driven after all?* Workshop on superconductivity, Inst. Of Physics, Chinese Academy of Sciences, Beijing, China, November 9, 2008 (projects 1 & 2, Group of Sigris)
  - T.M. RICE, *Encounters with oxides – wins and losses*, Hong Kong Forum on Condensed Matter Physics, Hong Kong, December 18, 2006 (projects 1 & 2, Group of Sigris)
  - T.M. RICE, *A phenomenological theory for the pseudogap state*, Swiss Physical Society Meeting, Lausanne, Switzerland, February 14, 2006 (projects 1 & 2, Group of Sigris)
  - T.M. RICE, *A phenomenological theory for the pseudogap state*, Round table on microscopic theories for high-temperature superconductors, 2<sup>nd</sup> topical workshop of SCENET, Mallorca, Spain, March 15, 2006 (projects 1 & 2, Group of Sigris)
  - T.M. RICE, *A phenomenological theory for the pseudogap state*, International Conference on Materials and Mechanisms of Superconductivity, Dresden, Germany, July 12, 2006 (projects 1 & 2, Group of Sigris)

- T.M. RICE, *20 years of resonant valence bond theory*, International conference on magnetism, Kyoto, Japan, August 23, 2006 (projects 1 & 2, Group of Sigrist)
- K. ROGACKI, J. KARPINSKI, G. SCHUCK, N.D. ZHIGADLO, S.M. KAZAKOV, *Crystal growth, structural studies, and superconducting properties of  $\beta$ -pyrochlore  $KOs_2O_6$* , Swiss Physical Society-MaNEP Meeting, Lausanne, Switzerland, February 13-14, 2006 (projects 3 & 4, Group of Karpinski)
- K. ROGACKI, B. BATLOGG, J. KARPINSKI, N.D. ZHIGADLO, G. SCHUCK, S.M. KAZAKOV, R. PUZNAK, A. WISNIEWSKI, *MgB<sub>2</sub> single crystals substituted with magnetic ions: Strong suppression of superconductivity*, Swiss Physical Society-MaNEP Meeting, Lausanne, Switzerland, February 13-14, 2006 (projects 3 & 4, Group of Karpinski)
- H.M. RONNOW ET AL., *Exploring novel quantum magnets - advent of IN8c and prospects for multiplexing*, ILL millennium symposium, Grenoble, France, April 28, 2006 (projects 1, 3 & 6, Group of Mesot)
- H. M. RONNOW ET AL., *Exploring novel quantum magnets - a CuTe story and prospects for multiplexing*, American Conference on Neutron Scattering, Illinois, USA, June 21, 2006 (projects 1, 3 & 6, Group of Mesot)
- H.M. RONNOW ET AL., *The quasi-particle zoo ! - magnetic excitations in spin ladders*, Theoretical and Experimental Magnetism Meeting, Abbingdon, UK, August 4, 2006 (projects 1, 3 & 6, Group of Mesot)
- H.M. RONNOW ET AL., *Simulations for the new EIGER spectrometer at PSI*, MC-Workshop, PSI, Switzerland, October 4, 2006 (projects 1, 3 & 6, Group of Mesot)
- G. SCHUCK, J. KARPINSKI, N. ZHIGADLO, AND S. KAZAKOV, *Structural studies of  $\beta$ -pyrochlore  $RbOs_2O_6$ , 8th International Conference on Materials and Mechanism of Superconductivity and High Temperature Superconductors, M<sup>2</sup>S-HTSC VIII, July 9-14, 2006, Dresden, Germany* (projects 3 & 4, Group of Karpinski)
- G. SCHUCK, J. KARPINSKI, K. ROGACKI, N.D. ZHIGADLO, S.M. KAZAKOV, *Structural studies of beta-pyrochlore single crystals*, 14 Jahrestagung der Deutschen Gesellschaft für Kristallographie, Freiburg, Germany, April 3 - 6, 2006 (projects 3 & 4, Group of Karpinski)
- G. SCHUCK, J. KARPINSKI, N.D. ZHIGADLO, S.M. KAZAKOV, *Structural studies of  $\beta$ -pyrochlore  $RbOs_2O_6$* , Swiss Physical Society-MaNEP Meeting, Lausanne, Switzerland, February 13-14, 2006 (projects 3 & 4, Group of Karpinski)
- K. SCHMIDT, *Temperature in One-Dimensional Bosonic Mott Insulators*, German Physical Society, Dresden, March 28, 2006 (project 1, Group of Mila)
- B. SEEBER, A. FERREIRA, V. ABÄCHERLI, T. BOUTBOUL, L. OBERLI, R. FLÜKIGER, *Transport Properties up to 1000 A of Nb<sub>3</sub>Sn Wires Under Transverse Compressive Stress*, ASC06 Conference, Seattle, USA, August 27 - September 1, 2006 (project 6, Group of Flükiger)
- S. SEIRO, *Temperature Dependence of the Quasiparticle Excitation Spectrum in Manganites*, Swiss Physical Society, Zürich, Switzerland, February 21, 2007 (projects 2, 5 & 6, Group of Fischer)
- C. SENATORE, P. LEZZA, R. LORTZ, O. SHCHERBAKOVA, S.X. DOU, R. FLÜKIGER, *Specific heat and magnetic relaxation analysis of MgB<sub>2</sub> bulk samples with and without additives*, ASC06 Conference, Seattle, USA, August 27 - September 1, 2006 (project 6, Group of Flükiger)
- C. SENATORE, D. UGLIETTI, V. ABÄCHERLI, A. JUNOD, R. FLÜKIGER, *Specific heat, a method to determine the Tc distribution in various industrial Nb<sub>3</sub>Sn wires*, ASC06 Conference, Seattle, USA, August 27 - September 1, 2006 (project 6, Group of Flükiger)
- A. SHKABKO, I. MAROZAU, D. LOGVINOVICH, M. DÖBELI, T. LIPPERT, L. SCHLAPBACH, A. WOKAUN, A. WEIDENKAFF, *Microwave Synthesis of SrTiO<sub>3-x</sub>Ny oxynitrides and their properties*, SPS meeting 2007, Zürich, February 20-21, 2007 (projects 1, 3 & 4, Group of Schlapbach)
- M. SIGRIST, *Spin-orbit coupling and superconductivity in materials without inversion symmetry*, The fourth COE Symposium on Exploring New Science by Bridging Particle-Matter Hierachy, Sendai, Japan, June 28-30, 2006 (projects 1 & 2, Group of Sigrist)
- M. SIGRIST, *Intriguing properties of the chiral p-wave phase in Sr<sub>2</sub>RuO<sub>4</sub>*, Workshop on Strongly Correlated Electrons in Low Dimensions, Monte Verita, Ascona, Switzerland, July 3-7, 2006 2006 (projects 1 & 2, Group of Sigrist)
- M. SIGRIST, *Theory of superconductivity in non-centrosymmetric materials*, M<sub>2</sub>S-HTSC VIII, Dresden, Germany, July 9-14, 2006 (projects 1 & 2, Group of Sigrist)
- M. SIGRIST, *Superconductivity in non-centrosymmetric materials*, ICM 24, Kyoto, Japan, August 21-25, 2006 (projects 1 & 2, Group of Sigrist)
- M. SIGRIST, *Superconductivity in metals without inversion symmetry*, International Workshop on Strongly Correlated Transition Metal Compounds II, Köln, Germany, September 11-14, 2006 (projects 1 & 2, Group of Sigrist)
- M. SIGRIST, *Unconventional superconductivity - a prime target for muons*, First Swiss Japan Workshop on the applications and on new developments in



- muon spectroscopy on novel materials, KEK Tsukuba, Japan, September 28-29, 2006 (projects 1 & 2, Group of Sigrist)
- M. SIGRIST, *Theoretical aspects of non-centrosymmetric superconductivity*, Workshop on Superclean Systems, Awaji-Island Japan, December 13-16, 2006 (projects 1 & 2, Group of Sigrist)
  - M. SIGRIST, *Twisted Josephson junctions between spin triplet superconductors*, Workshop on spin-triplet superconductivity, Awaji-Island, Japan, December 17, 2006 (projects 1 & 2, Group of Sigrist)
  - M. SIGRIST, *Unconventional Superconductivity*, Ecole Nouveaux Etats Electroniques de la Matiere, Centre Paul Langevin, Aussois, France) May 27 - June 2, 2006 (projects 1 & 2, Group of Sigrist)
  - M. SIGRIST, *Sr<sub>2</sub>RuO<sub>4</sub>: An exemplary case of an unconventional superconductor*, Winterschool on Unconventional Superconductivity, International Center for Condensed Matter Physics, UnB, Brasilia, Brazil, July 24 - August 11, 2006 (projects 1 & 2, Group of Sigrist)
  - J. STAHN, *Elliptic beam guide - concept and first tests*, Workshop on neutron optics, ILL, Grenoble, France, April 26, 2006 (project # 1, 3 & 6, Group of Mesot)
  - J. STAHN, *A neutron polariser based on magnetically remanent Fe/Si supermirrors*, Workshop on neutron optics, ILL, Grenoble, France, April 26, 2006 (projects 1, 3 & 6, Group of Mesot)
  - J. STAHN, *NR in superconductivity - Antiphase magnetic proximity effect in superconductor / ferromagnet multilayers*, ADAM user meeting, Bochum, Germany, May 19, 2006 (projects 1, 3 & 6, Group of Mesot)
  - J. STAHN, *Antiphase magnetic proximity effect in perovskite superconductor / ferromagnet multilayers*, SNI 2006, Hamburg, Germany, October 4-6, 2006 (projects 1, 3 & 6, Group of Mesot)
  - S. STREULE, M. MEDARDE, A. PODLESNYAK, E. POMJAKUSHINA, K. CONDER, S. KAZAKOV, J. KARPINSKI AND J. MESOT, *Short-range charge ordering and ferromagnetism-antiferromagnetism competition in Ho<sub>0.7</sub>Sr<sub>0.9</sub>CoO<sub>3-x</sub> (0.15 ≤ x ≤ 0.49)*, 10th European Powder Diffraction Conference, EPDIC 10, Geneva, Switzerland, September 1-4, 2006 (projects 1, 3 & 6, Group of Mesot)
  - R. TEDIOSI, N. P. ARMITAGE, E. GIANNINI, D. VAN DER MAREL, *Evidence of Electron-Plasmon Coupling in Single Crystal Bismuth*, APS March Meeting, Denver, USA, March 8, 2007 (projects 2, 5 & 6, Group of Van der Marel)
  - J. TEYSSIER, A. KUZMENKO, D. VAN DER MAREL, F. MARSIGLIO, *Probing electronic structure and electron-phonon interaction in borides using optical spectroscopy*, APS March Meeting, Denver, USA, March 8, 2007 (projects 2, 5 & 6, Group of Van der Marel)
  - B. THIELEMANN, CH. RÜEGG, H.M. RØNNOW, J. STAHN, J. MESOT, D. F. MCMORROW, K.W. KRAEMER AND H.-U. GUEDEL, *Spin dynamics in the organic quantum magnet (C<sub>5</sub>H<sub>12</sub>N)<sub>2</sub>CuBr<sub>4</sub>*, Joint Swiss-Russian Workshop on Quantum Magnetism and Polarized Neutrons, Villigen PSI, Switzerland, April 01-03, 2006 (projects 1, 3 & 6, Group of Mesot)
  - B. THIELEMANN, CH. RÜEGG, H. M. RØNNOW, D. F. MCMORROW, J. MESOT, K. W. KRÄMER, D. BINER, H.-U. GÜDEL, J. STAHN, K. HABICHT, M. BOEHM, *Spin Dynamics in the Organic Quantum Magnet (H<sub>2</sub>q)<sub>2</sub>CuBr<sub>4</sub>*, SINQ User Meeting, Villigen PSI, Switzerland, May 10, 2006 (projects 1, 3 & 6, Group of Mesot)
  - J.-M. TRISCONE, *Nanoscope control of the polarization in ferroelectric thin films*, SPS meeting, Lausanne, Switzerland, February 12-13, 2006 (projects 5 & 6, Group of Triscone)
  - J.-M. TRISCONE, *Ferroelectricity in thin perovskite films and artificial ferroelectric materials with tailored properties*, Workshop "From solid state to biology", Dubrovnik, Yugoslavia, June 24-July 1, 2006 (projects 5 & 6, Group of Triscone)
  - J.-M. TRISCONE, *Electric field effect in superconducting oxide thin films*, Workshop on "Nanoscale superconductivity and magnetism" NSM 2006, Leuven, Belgium, July 6-8, 2006 (projects 5 & 6, Group of Triscone)
  - J.-M. TRISCONE, *Electric field effect in oxide thin films*, European School on "Nanosciences and Nanotechnologies" ESSON 2006, Grenoble, France, September 4-7, 2006 (projects 5 & 6, Group of Triscone)
  - J.-M. TRISCONE, *Nanoscope control of the polarization in ferroelectric thin films*, "Trends in nanotechnology" TNT2006, Grenoble, September 4-8, 2006 (projects 5 & 6, Group of Triscone)
  - J.-M. TRISCONE, *Electrostatic modulation of superconductivity in high T<sub>c</sub> and Nb-doped SrTiO<sub>3</sub> films*, 13 international workshop on "oxide electronics", Ischia, Italy, October 8-11, 2006 (projects 5 & 6, Group of Triscone)
  - J.-M. TRISCONE, *Ferroelectricity in thin perovskite films and artificial ferroelectric materials with tailored properties*, 1st international symposium on "transparent conductive oxides", Crete, October 23-25, 2006 (projects 5 & 6, Group of Triscone)
  - J.-M. TRISCONE, *Controlling ferroelectricity in PbTiO<sub>3</sub>/SrTiO<sub>3</sub> superlattices*, Journées couche minces ferroélectriques 2006 et 4<sup>ème</sup> rencontre Franco-Ukrainienne sur la ferroélectricité, Amiens, France, November 22-24, 2006 (projects 5 & 6, Group of Triscone)

- J.-M. TRISCONE, *Nanoscale ferroelectrics*, FAME Winterschool on "new architectures for passive electronics", La Clusaz, France, January 14-21, 2007 (projects 5 & 6, Group of Triscone)
- M. TROYER, *Stability of lattice supersolids*, Workshop on highly frustrated magnets, CECAM, Lyon, France, April 2006 (project 1, Group of Troyer)
- M. TROYER, *D-wave RVB states of ultracold atoms in optical lattices*, APS March Meeting, Baltimore, USA, March 2006 (project 1, Group of Troyer)
- M. TROYER, *The ALPS project*, Workshop on data formats and interoperability, CECAM, Lyon, France, April 2006 (project 1, Group of Troyer)
- M. TROYER, *The ALPS project*, CQCP workshop, Tokyo, Japan, August 2006 (project 1, Group of Troyer)
- M. TROYER, *The fate of vacancy-induced supersolidity in 4He*, CQCP symposium, Tokyo, Japan, August 2006 (project 1, Group of Troyer)
- M. TROYER, *Towards realistic simulation of quantum magnets in the ALPS project*, International Conference on Magnetism 2006, Kyoto, Japan, August 2006 (project 1, Group of Troyer)
- M. TROYER, *Computer simulations of strongly correlated quantum systems: past successes, current topics, and future challenges*, Hong Kong Forum on Condensed Matter Physics, Hong Kong, China, December 2006 (project 1, Group of Troyer)
- D. UGLIETTI, V. ABÄCHERLI, M. CANTONI, R. FLÜKIGER, *Grain growth, Morphology and Composition Profiles in Industrial Nb<sub>3</sub>Sn wires*, ASC06 Conference, Seattle, USA, August 27 - September 1, 2006 (project 6, Group of Flükiger)
- E. VAN HEUMEN, R. LORTZ, F. CARBONE, A.B. KUZMENKO, D. VAN DER MAREL, X. ZHAO, G. YU, Y. CHO, N. BARISIC, M. GREVEN, C.C. HOMES, S.V. DORDEVIC, *Optical and thermodynamic properties of Hg-1201*, APS March Meeting, Denver, USA, March 8, 2007 (projects 2, 5 & 6, Group of Van der Marel)
- D. VAN DER MAREL, *Magnetism, transport and optical properties of transition metal mono-silicides*, International Workshop on Strongly Correlated Transition Metal Compounds II Cologne, Germany, September 11-14, 2006 (projects 2, 5 & 6, Group of Van der Marel)
- D. VAN DER MAREL, *Optical properties of the cuprates in the normal and superconducting state*, M2S-HTSC, Dresden, July 9-14, 2006 (projects 2, 5 & 6, Group of Van der Marel)
- D. VAN DER MAREL, *XI Training Course in the Physics of Strongly Correlated Systems, lecture series*, Vietri sul Mare, Salerno, Italy, October 2-13, 2006 (projects 2, 5 & 6, Group of Van der Marel)
- D. VAN DER MAREL, *Optical properties of the cuprates in the normal and superconducting state*, *Low-Energy Excitations on High-Tc superconductors 2006*, MPI-Stuttgart, July 4-7, 2006 (projects 2, 5 & 6, Group of Van der Marel)
- D. VAN DER MAREL, *Suppressed reflectivity due to spin-controlled localization in a magnetic semiconductor*, International Conference on Low Energy Electrodynamics in Solids, Tallinn, Estonia, July 1-6, 2006 (projects 2, 5 & 6, Group of Van der Marel)
- D. VAN DER MAREL, *Optical properties of Cuprates in the Normal and superconducting state*, March Meeting of the American Physical Society, Baltimore, March 13-17, 2006 (projects 2, 5 & 6, Group of Van der Marel)
- D. VAN DER MAREL, *Magneto-optical properties of transition metal mono-silicides*, 21st Workshop on Novel Materials and superconductors, Plannersalm, Austria, February 11-18, 2006 (projects 2, 5 & 6, Group of Van der Marel)
- D. VAN MECHELEN, P. ARMITAGE, C. GRIMALDI, A. KUZMENKO, J. TEYSSIER, D. VAN DER MAREL, *Electron-phonon coupling in SrTi<sub>1-x</sub>NbxO<sub>3</sub>*, APS March Meeting, Denver, USA, March 8, 2007 (projects 2, 5 & 6, Group of Van der Marel)
- C. WEBER, MaNEP summer school, Saas-Fee, Switzerland, September 11-16, 2006 (projects 1 & 2, Group of Mila)
- C. WEBER, Swiss Physical Society Meeting, Lausanne, Switzerland, February 2006 (projects 1 & 2, Group of Mila)
- C. WEBER, Martin-Peter Colloquium, Geneva, Switzerland, October 2006 (projects 1 & 2, Group of Mila)
- C. WEBER, *Magnetism and superconductivity of strongly correlated electrons on the triangular lattice*, Martin-Peter Colloquium, Geneva, October 2006 (project 1, Group of Mila)
- WEIDENKAFF, *Anionensubstitutionen in Titanhaltigen Perowskitphasen*, ADUC, Hamburg, Germany, March 21, 2006 (projects 1, 3 & 4, Group of Schlapbach)
- A. WEIDENKAFF, *Materials for Energy Conversion and Storage*, International Conference on New Energy Materials, C-MRS, Beijing, China, June 8, 2006 (projects 1, 3 & 4, Group of Schlapbach)
- A. WEIDENKAFF, *The Development of Thermoelectric Oxides with Perovskite-type Structures for Alternative Energy Technologies*, International Conference on Advanced Ceramics & Composites, Daytona Beach, Florida, USA, January 21-

- 26, 2007 (projects 1, 3 & 4, Group of Schlapbach)
- M. WELLER, *NMR studies of BaVS<sub>3</sub>*, SPS/MaNEP meeting, Lausanne, Schweiz, February 14, 2006 (project 1, Group of Ott)
  - M. WELLER, *NMR study of CeTe at low temperatures*, SPS/MaNEP meeting, Lausanne, Schweiz, February 14, 2006 (project 1, Group of Ott)
  - A. WISNIEWSKI, R. PUZNIAK, A. BIENIAS, M. BARAN, J. JUN, N.D. ZHIGADLO, J. KARPINSKI, *Anisotropy of the lower and of the upper critical fields in Mg<sub>1-x</sub>Al<sub>x</sub>B<sub>2</sub> single crystals*, 8th International Conference on Materials and Mechanism of Superconductivity and High Temperature Superconductors, M<sup>2</sup>S-HTSC VIII, Dresden, Germany, July 9 -14, 2006 (projects 3 & 4, Group of Karpinski)
  - Y. YANASE, *Role of disorder in the multi-critical region of d-wave superconductivity and anti-ferromagnetism*, ICM 24. Kyoto, Japan, August 21-25, 2006 (projects 1 & 2, Group of Sigrist)
  - Y. YANASE, *Multi-orbital superconductivity and multi-component order parameter in Na<sub>x</sub>CoO<sub>2</sub>yH<sub>2</sub>O and Sr<sub>2</sub>RuO<sub>4</sub>*, First International workshop on the physical properties of lamellar cobaltates, Paris, France, July 5-7, 2006 (projects 1 & 2, Group of Sigrist)
  - N.D. ZHIGADLO, J. KARPINSKI, K. ROGACKI, B. BATLOGG, G. SCHUCK, S.M. KAZAKOV, R. PUZNIAK, A. WISNIEWSKI, *MgB<sub>2</sub> single crystals substituted with magnetic ions: Strong suppression of superconductivity*, 8th International Conference on Materials and Mechanism of Superconductivity and High Temperature Superconductors, M<sup>2</sup>S-HTSC VIII, 2006, Dresden, Germany, July 9 -14, 2006 (projects 3 & 4, Group of Karpinski)
  - N.D. ZHIGADLO, J. KARPINSKI, *High-pressure synthesis and superconductivity of Ca<sub>2-x</sub>Na<sub>x</sub>CuO<sub>2</sub>Cl<sub>2</sub>*, 8th International Conference on Materials and Mechanism of Superconductivity and High Temperature Superconductors, M<sup>2</sup>S-HTSC VIII, Dresden, Germany, July 9-14, 2006 (projects 3 & 4, Group of Karpinski)
  - N.D. ZHIGADLO, J. KARPINSKI, *Synthesis of Ca<sub>2-x</sub>Na<sub>x</sub>CuO<sub>2</sub>Cl<sub>2</sub> single crystals under high pressure*, Swiss Physical Society-MaNEP Meeting, Lausanne, Switzerland, February 13-14, 2006 (projects 3 & 4, Group of Karpinski)



## 8.6.2 Seminars and colloquia

- P. BARMETTLER, *A systematic method for constructing a spin-singlet basis*, Seminar in Theoretical Physics, Wroclaw, Poland, May 2006 (project 2, Group of Baeriswyl)
- D. BAERISWYL, *Superconductivity as a result of repulsive interactions*, Physics Colloquium, University of Graz, Austria, October 2006 (project 2, Group of Baeriswyl)
- D. BAERISWYL, *Superconductivity as a result of repulsive interactions*, Physics Colloquium, University of Neuchâtel, Switzerland, January 2007 (project 2, Group of Baeriswyl)
- D. BAERISWYL, *Superconductivity out of purely repulsive interactions*, Condensed Matter Theory Seminar, University of Basel, Switzerland, January 2007 (project 2, Group of Baeriswyl)
- D. BAERISWYL, *Superconductivity as a result of repulsive interactions*, Condensed Matter Seminar, University of Mainz, Germany, February 2007 (project 2, Group of Baeriswyl)
- C. BERNHARD, *Infrared Ellipsometry on cuprate high  $T_c$  superconductors – exploring the unusual c-axis response*, Colloquium at the Physics Department of Masaryk University in Brno, Czech Republic, October 10, 2006 (project 2, Group of Bernhard)
- G. BLATTER, *Superconducting Devices for Quantum Computing*, University of Tübingen, Germany, January, 2006 (projects 1 & 2 Group of Blatter)
- G. BLATTER, GIANNI, *The Physics of Superconducting Quantum Bits*, Würzburg, Germany, November 2006 (projects 1 & 2 Group of Blatter)
- G. BLATTER, *The Physics of Superconducting Quantum Bits*, University of Fribourg, Fribourg, Switzerland, January 29, 2007 (projects 1 & 2 Group of Blatter)
- G. BUCHS, *Local Modification and Characterization of the Electronic Structure of Carbon Nanotubes*, TU Delft, QT group, The Netherlands, April 28, 2006 (projects 1, 3 & 4 Group of Schlapbach)
- G. BUCHS, *STM/STS Investigations of SWNT Defects Induced by Low-Energy Ions*, Empa Ph. D Symposium 2006, Empa St-Gallen, Switzerland, October 19, 2006 (projects 1, 3 & 4 Group of Schlapbach)
- M. BÜTTIKER, *Quantum Shot Noise: From Schottky to Bell*, Colloquium, University of Michigan, East Lansing, USA, May 8, 2006 (projects 1 & 2 Group of Büttiker)
- M. BÜTTIKER, *Testing the quantum-ness of qubits*, Kvali Institute of NanoScience, Colloquium, Delft University of Technology, Delft, The Netherlands, October 11, 2006 (projects 1 & 2 Group of Büttiker)
- M. BÜTTIKER, *Quantum shot noise: From Schottky to Bell*, Colloquium, Technion, Haifa, Israel, January 11, 2007 (projects 1 & 2 Group of Büttiker)
- L. DEGIORGI, *Magneto-optical investigation of Ca-doped Europium Hexaborides*, Colloquium at the Physics Department of the Temple University, Philadelphia, U.S.A. March 20, 2006 (project 1, Group of Degiorgi)
- L. DEGIORGI, *Magneto-optical investigation of Ca-doped Europium Hexaborides*, Seminar at the Physics Department of the Boston University, Boston, U.S.A. March 22, 2006 (project 1, Group of Degiorgi)
- A. ENGEL, *Superconducting single-photon detectors – chances & challenges*, Istituto Nazionale di Ricerca Metrologica I.N.R.I.M., Torino, Italy, June 20, 2006 (projects 4 & 5 Group of Schilling)
- A. ENGEL, *Superconducting single-photon detectors*, Victoria University, Wellington, New Zealand, August 22, 2006 (projects 4 & 5 Group of Schilling)
- Ø. FISCHER, *Exploring superconductors with a Scanning Tunneling Microscope*, Colloquium, Konstanz, Germany, May 16, 2006 (projects 2,5 & 6, Group of Fischer)
- Ø. FISCHER, *Scanning Tunneling Spectroscopy on Superconductors and on Manganites*, Paul Scherrer Institute, Villigen, Switzerland, November 3, 2006 (projects 2,5 & 6, Group of Fischer)
- R. FLÜKIGER, *Actual state of industrial superconductors worldwide*, Status Seminar, Bundesamt für Forschung und Entwicklung (BFE), “Elektrizität” Bern, Switzerland, November 14, 2006 (project 6, Group of Flükiger)
- V. GESHKENBEIN, *Dissociation of vortex stacks into fractional-flux vortices*, Stanford University, California, USA, October 2006 (projects 1 & 2 Group of Blatter)
- T. GIAMARCHI, *Disordered Elastic Systems*, Minneapolis, USA, May 3, 2006 (projects 1 & 2 Group of Giamarchi)
- T. GIAMARCHI, *Disordered Elastic Systems*, SPS Colloquium, Grenoble, France, November 16, 2006 (projects 1 & 2 Group of Giamarchi)
- T. GIAMARCHI, *Organic superconductors, 20 years after*, Los Alamos National Lab, Los Alamos, USA, January 11, 2007 (projects 1 & 2 Group of Giamarchi)
- T. GIAMARCHI, *Disordered Elastic Systems*, PSI, Villigen Switzerland, February 5, 2007 (projects 1 & 2 Group of Giamarchi)
- M. GRIONI, *UV and x-ray photoelectron spectroscopy*, Hercules School on Neutrons and Synchrotron Radiation,

- Grenoble, France, March 2006 (projects 1 & 2 Group of Grioni)
- M. GRIONI, *High-resolution ARPES of two-dimensional modulated structures*, Workshop SPLDS "Statistical Physics and Low-dimensional Systems" 2006, Nancy, France, May 2006 (projects 1 & 2 Group of Grioni)
- M. GRIONI, *ARPES of broken-symmetry states in 2D*, Rencontres de St. Aubain LLB-SOLEIL, SOLEIL Synchrotron Laboratory, France, June 2006 (projects 1 & 2 Group of Grioni)
- M. GRIONI, *Broken symmetry and spin-split states at surfaces: the ARPES view*, Annual Meeting of the German Physical Society, Regensburg, March 2007 (projects 1 & 2 Group of Grioni)
- M. GRIONI, *Correlations and broken-symmetry states in 2D*, Workshop "Strong Correlations and Angle-resolved Photoemission Spectroscopy", Dresden, Germany, May 2007 (projects 1 & 2 Group of Grioni)
- E. GULL, *Performance analysis of continuous-time solvers for quantum impurity models*, SFB Seminar Sonderforschungsbereich 602, Universität Göttingen, Göttingen, Deutschland, December 8, 2006 (project 1, Group of Troyer)
- N. HAYASHI, *Superconductivity in systems without inversion symmetry*, Tokyo Institute of Technology, Tokyo, Japan, October 5, 2006 (projects 1 & 2 Group of Sigrist)
- J. HULLIGER, *Wie findet man die Stecknadel im Heuhafen? Kombinatorische Synthesen und magnetische Separation*, Ludwig-Maximilians-Universität München, Anorganische Chemie, München, Germany, June 29, 2006 (project 4, Group of Hulliger)
- J. HULLIGER, *How to find a pin in a haystack? Combinatorial chemistry and magnetic separation applied to the quest on new oxide superconductors*, EPFL, Institute of Physics and complex matter, Lausanne, Switzerland, November 14, 2006 (project 4, Group of Hulliger)
- J. HULLIGER, *How to find a pin in a haystack? Combinatorial chemistry and magnetic separation applied to the quest on new oxide superconductors*, University of Neuchâtel, Institute of Physics, Neuchâtel, Switzerland, December 11, 2006 (project 4, Group of Hulliger)
- D. JACCARD, *Valence fluctuation mediated superconductivity in Ce-based heavy-fermion systems*, ESPCI, Paris, France, February 16, 2006 (projects 5 & 6, Group of Triscone)
- D. JACCARD, *Bridgman anvil technique/steatite-pyrophyllite cell*, Osaka, Toyonaka, February 20, 2006 (projects 5 & 6, Group of Triscone)
- D. JACCARD, *Unusual metallic state in FeGe beyond its quantum critical point*, Osaka, Toyonaka, February 22, 2006 (projects 5 & 6, Group of Triscone)
- H. KELLER, *Unconventional isotope effects in cuprate high-temperature superconductors*, The Hong Kong University of Science and Technology, Hong Kong, China, October 4, 2006 (project 2, Group of Keller)
- C. KOLLATH, *Probing ultracold atoms*, Ecole Polytechnique, Paris, France, February 2007 (projects 1 & 2, Group of Giamarchi)
- C. KOLLATH, *Cold quantum gases: Non-equilibrium phenomena*, LPTMS, Paris France, February 2007 (projects 1 & 2, Group of Giamarchi)
- C. KOLLATH, *Probing strongly correlated quantum gases*, Seminar of condensed matter theory, EPF Lausanne, Switzerland, January 2007 (projects 1 & 2, Group of Giamarchi)
- C. KOLLATH, *Strong correlations in quantum gases*, Seminar of condensed matter theory, University of Frankfurt, Germany, July 2006 (projects 1 & 2, Group of Giamarchi)
- C. KOLLATH, *Strong correlations in quantum gases*, Seminar of theoretical physics, University of Stuttgart, Germany, February 2006 (projects 1 & 2, Group of Giamarchi)
- N. LAFLORENCIE, *Defect and spin impurities in quantum chains*, Laboratoire de Physique de l'ENS, Lyon, France, December 2006 (project 1, Group of Mila)
- N. LAFLORENCIE, *Defect and spin impurities in quantum chains*, Centre de Physique Théorique, Marseille, France, November 2006 (project 1, Group of Mila)
- N. LAFLORENCIE, *Defect and spin impurities in quantum chains*, Laboratoire Louis Neel, Grenoble, France, November 2006 (project 1, Group of Mila)
- A. LÄUCHLI, *Spin Nematic Phases in Frustrated Quantum Magnets*, School of Physics, University of New South Wales, Sydney, May 2006 (project 1, Group of Mila)
- A. LÄUCHLI, *Unconventional charge dynamics in doped frustrated magnets*, School of Physics, University of New South Wales, Sydney, Australia, May 2006 (project 1, Group of Mila)
- T. LIPPERT, *Interactions of photons with surfaces: structuring, modification, and applications*, Center for Applied Photonics (CAP), University of Konstanz, Germany, November 2006 (projects 1, 3 & 4 Group of Schlapbach)
- T. LIPPERT, *Laser Interaction with Materials: from thin film deposition to laser plasma thruster*, Institute of Electronic Structure and Laser, FORTH, Crete,

- Greece, May 2006 (projects 1, 3 & 4 Group of Schlapbach)
- T. LIPPERT, *Laser Interaction with Materials: from thin film deposition to laser plasma thruster*, Laboratory LP3, University of Marseille, France, March 2006 (projects 1, 3 & 4 Group of Schlapbach)
  - J. MESOT, *Testing Fermi Liquid Descriptions of Cuprates Superconductors by Means of Momentum Resolved Probes*, Séminaire du Département de la Matière Condensée (DPMC), University of Geneva, Geneva, Switzerland, June 16, 2006 (projects 1, 3 & 6 Group of Mesot)
  - F. MILA, *Frustrated Quantum Magnets: surprises on the way to polarization*, ESPCI, Paris, France, April 20, 2006 (project 1, Group of Mila)
  - F. MILA, *Looking for exotic ground states in quantum antiferromagnets*, University, Göttingen, Germany, June 7, 2006 (project 1, Group of Mila)
  - F. MILA, *Bosonic Models of Frustrated Quantum Magnets*, University, Cologne, Germany, December 6, 2006 (project 1, Group of Mila)
  - F. MILA, *Phase Transitions in Bosonic Models of Frustrated Quantum Magnets*, University of Geneva, Geneva, Switzerland, January 26, 2007 (project 1, Group of Mila)
  - E. MORENZONI, *Depth dependent studies of magnetic and superconducting properties with polarized muons*, Triumph, University of British Columbia, Vancouver, Canada, September 21, 2006 (project 2, Group of Keller)
  - L. POLLET, *What can vacancies tell us about supersolidity in Helium-4?*, weekly seminar, USA, University of Maryland MD, December 7, 2006 (project 1, Group of Troyer)
  - L. POLLET, *What can vacancies tell us about supersolidity in Helium-4?*, weekly seminar, University of Stuttgart, Germany, December 12, 2006 (project # 1, Group of Troyer)
  - T.M. RICE, *The high temperature superconductors – still fascinating after 20 years*, Physik Kolloquium, Uni Frankfurt, Frankfurt, Germany, May 31, 2006 (projects 1 & 2, Group of Sigrist)
  - T.M. RICE, *The high temperature superconductors – still fascinating after 20 years*, Tsinghua University, Beijing, China, November 7, 2006 (projects 1 & 2, Group of Sigrist)
  - T.M. RICE, *The high temperature superconductors – still fascinating after 20 years*, Nanjing University, Nanjing, China, November 30, 2006 (project 1 & 2 Group of Sigrist)
  - T.M. RICE, *High temperature superconductivity – phonon driven after all?* Hong Kong University, Hong Kong, November 1, 2006 (project 1 & 2 Group of Sigrist)
  - T.M. RICE, *A phenomenological theory for the pseudogap state*, Princeton University, Princeton, USA, April 27, 2006 (project 1 & 2 Group of Sigrist)
  - A. SACCHETTI, *Pressure-driven orbital reorientation and change in Mott Hubbard gap in YTiO<sub>3</sub>*, Journal Club LFKP ETHZ, Zürich, Schweiz, December 8, 2006 (project 1 Group of Ott)
  - K. SCHMIDT, *The Fate of Orbitons coupled to Phonons*, University of Dortmund, Germany, May 17, 2006 (project 1, Group of Mila)
  - M. SIGRIST, *Problems in strongly correlated electron systems*, University Augsburg, Augsburg, Germany, June 9, 2006 (project # 1 & 2 Group of Sigrist)
  - M. SIGRIST, *Superconductivity in metals without inversion symmetry*, Department for Applied Physics, University of Tokyo, Tokyo, Japan, December 19, 2006 (projects 1 & 2 Group of Sigrist)
  - M. SIGRIST, *Superconductivity in metals without inversion symmetry*, Institute for Solid State Physics, University of Tokyo, Tokyo, Japan, December 20, 2006 (projects 1 & 2 Group of Sigrist)
  - M. SIGRIST, *Superconductivity in metals without inversion symmetry*, Department of Physics, Kyoto University, Kyoto, Japan, January 9, 2007 (projects 1 & 2 Group of Sigrist)
  - M. SIGRIST, *Superconductivity in metals without inversion symmetry*, Department of Applied Physics, Osaka University, Osaka, Japan, January 26, 2007 (projects 1 & 2 Group of Sigrist)
  - M. SIGRIST, *Superconductivity in metals without inversion symmetry*, Department of Physics and Mathematics, Aoyama Gakuin University, Sagamihara, Japan, February 2, 2007 (projects 1 & 2 Group of Sigrist)
  - J. STAHN, *A neutron polariser based on magnetically remanent Fe/Si supermirrors*, Seminar at Institute Laue Langevin, Grenoble, France, January 18, 2006 (projects 1, 3 & 6 Group of Mesot)
  - J.-M. TRISCONE, *Ferroelectricity in thin perovskite films and artificial ferroelectric materials with tailored properties*, Cambridge, UK, August 31, 2007 (projects 5 & 6 Group of Triscone)
  - J.-M. TRISCONE, *Ferroélectricité à l'échelle nanoscopique*, Fribourg, Switzerland, November 16, 2006 (projects 5 & 6 Group of Triscone)
  - J.-M. TRISCONE, *Nanoscale ferroelectrics: artificial materials and novel devices*, Roma, Italy, September 25, 2007 (projects 5 & 6 Group of Triscone)
  - M. TROYER, *Breakdown of a topological phase*, Seminar, University of




- Massachusetts, Amherst, MA, USA, October 2006 (project 1, Group of Troyer)
- M. TROYER, *The ALPS project*, Colloquium, University of Marburg, Germany, January 2007 (project 1, Group of Troyer)
  - D. VAN DER MAREL, *Suppressed reflectivity due to spin-controlled localization in a magnetic semiconductor*, Instituut Lorentz, Universiteit Leiden, March, 2006 (projects 1, 2, 3 & 5 Group of Van der Marel)
  - D. VAN DER MAREL, *Optical properties of Cuprates in the Normal and Superconducting state*, Brescia, Italia, October 20, 2006 (projects 1, 2, 3 & 5 Group of Van der Marel)
  - D. VAN DER MAREL, *Suppressed reflectivity due to spin-controlled localization in a magnetic semiconductor*, Ecole Polytechnique Fédérale de Lausanne, Switzerland, January 9, 2006 (projects 1, 2, 3 & 5 Group of Van der Marel)
  - C. WEBER, *Magnetism and superconductivity of strongly correlated electrons on the triangular lattice*, Ecole Normale Supérieure, Paris, France, January 2007 (project 1, Group of Mila)
  - C. WEBER, *Bond-order wave-functions for the t-J model on the square lattice*, J.W.Goethe University, Frankfurt, Germany, February 2007 (project 1, Group of Mila)
  - A. WEIDENKAFF, *Tuning the properties of functional perovskite-type oxides and oxynitrides*, Institutskolloquium CRISMAT / University of Caen, France, November 10, 2006 (projects 1, 3 & 4 Group of Schlapbach)
  - A. WEIDENKAFF, *Synthesis and properties of perovskite-type oxides and oxynitrides*, Institutskolloquium Institute of Physics, Academy of Sciences of the Czech Republic, Prague, December 19, 2006 (projects 1, 3 & 4 Group of Schlapbach)
  - M. WELLER, *NMR/NQR studies of two unusual magnetic systems: BaVS<sub>3</sub> and CePd<sub>2</sub>In*, Institutseminar Hochfeldlabor Rossendorf, Rossendorf (Dresden), Deutschland, April 7, 2006 (project 1 Group of Ott)
  - M. WELLER, *Magnetic Field-Induces Superconductivity in the Ferromagnet U<sub>1-x</sub>Ge<sub>x</sub>*, F. LÉVY, I. SHEIKIN, B. GRENIER, ET AL. Science **309**, 1343 (2005), Journal Club LFKP ETHZ, Zürich, Schweiz, January, 27, 2006 (project 1, Group of Ott)
  - M. WELLER, *„Switching the electrical resistance of individual dislocations in single-crystalline SrTiO<sub>3</sub>“*, S. KRZYSZTOF ET AL. Nature Materials **5**, 312 (2006), Journal Club LFKP ETHZ, Zürich, Schweiz, July 7, 2006 (project 1, Group of Ott)
  - Y. YANASE, *Non-centrosymmetric superconductivity and antiferromagnetic order: microscopic discussion of CePt<sub>3</sub>Si*, Max-Planck Institute for Solid State Physics Stuttgart, Germany, January 30, 2007 (projects 1 & 2 Group of Sigrist)
  - O. ZAHARKO, *Coupled and isolated Cu<sup>2+</sup> S=1/2 spin tetrahedral systems studied by neutron scattering*, Seminar at Institut Jozef Stefan, Ljubljana, Slovenija, December 4, 2006 (projects 1, 3 & 6 Group of Mesot)



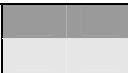




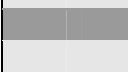

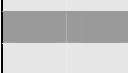
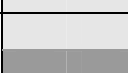
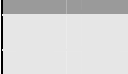






## Appendix– Milestones of the MaNEP projects

The tables of milestones (with colors) show the time evolution of each MaNEP's scientific activity. The tables below are the most recent version and serve as a tool to track the evolution of the activities.

Color codes:

Milestones unchanged since last year:	
Milestones added this year:	
Milestones suppressed this year:	

### A-1 Project 1 Strongly interacting electrons, low-dimensional and quantum fluctuation dominated systems

Milestones	Year 5	Year 6	Year 7	Year 8
<b>1. Systems with localized electronic degrees of freedom</b>				
Magneto optical spectroscopy TiOCl, TiOBr [Degiorgi]				
Magneto optical spectroscopy Cu <sub>2</sub> Te <sub>2</sub> O <sub>5</sub> Cl <sub>2</sub> [Degiorgi]				
Magneto optical spectroscopy Cu <sub>2</sub> Te <sub>2</sub> O <sub>5</sub> Br <sub>2</sub> [Degiorgi]				
Raman spectroscopy of TiOCl, TiOBr [Lemmens (outside MaNEP)]				
NMR and thermal properties of Na <sub>1-x</sub> CoO <sub>2</sub> [Ott]				
NMR and magnetic properties of MVT <sub>2</sub> O <sub>2</sub> (M=Li, Na; T= Si,Ge) [Ott]				
<b>Dimer systems</b>				
structure determination [Mesot]				
pressure dependence of magnetic structure [Degiorgi]				
inelastic neutron scattering: magnetic spectra [Mesot]				
theoretical discussion of phase diagram and excitation spectra [Sigrist, Mila, Giamarchi]				
<b>A<sub>3</sub>Cu<sub>2</sub>Ni(PO<sub>4</sub>)<sub>4</sub> (A=Ca, Sr, Pb)</b>				
synthesis, determination structure and				

intratrimer coupling [Mesot]				
single crystal growth, INS: magnetic spectra [Mesot]				
test of field-induced order [Mesot]				
characterization of pressure-induced order [Mesot]				
INS: finite-temperature effects [Mesot]				
<b>Cu<sub>2</sub>Te<sub>2</sub>O<sub>5</sub>X<sub>2</sub> (X= Cl, Br)</b>				
Magnetic structure determination [Mesot]				
INS: spectra, development of theoretical models [Mesot, Mila]				
Alloy Cu <sub>2</sub> Te <sub>2</sub> O <sub>5</sub> Cl <sub>2-x</sub> Br <sub>x</sub> : structure determination [Mesot]				
INS: spin spectra [Mesot]				
High-pressure/-field studies [Degiorgi]				
Theoretical investigation of microscopic models [Mila]				
LiCu <sub>2</sub> O <sub>2</sub> : on-campus ARPES [Grioni]				
Ab-initio calculations on LiCu <sub>2</sub> O: [Mila]				
BaVS <sub>3</sub> : temperature-dependent ARPES [Grioni]				
Sr-Ba- / S-Se-substitutions [Grioni]				
1 <sup>st</sup> high-resolution resonant x-ray emission spectroscopy at SLS [Grioni]				
Combined high-resolution x-ray ARPES-RIXS at SLS [Grioni]				
RIXS on heavy fermions [Grioni]				
Investigation of microscopic models for quantum phases with topological properties [Blatter, Mila, Troyer, Sigrist]				
Determination of phase diagrams of various dimer models [Blatter, Mila, Troyer, Sigrist]				
Investigation of effective models for quantum				

	liquids with defects <i>[Blatter, Mila, Troyer, Sigrist]</i>				
	Formulation of entanglement detection via excitations into a spectator level <i>[Büttiker]</i>				
	Analysis of cross-relation measurements and quantum limits <i>[Büttiker]</i>				
<b>2.</b>	<b>Itinerant electrons</b>				
	Synthesis of doped fullerene (DWNT) <i>[Forró]</i>				
	Synthesis of organic conductors <i>[Forró]</i>				
	Low-field ESR studies <i>[Forró]</i>				
	High-field ESR studies <i>[Forró]</i>				
	Study of the anisotropy effects <i>[Forró]</i>				
	High pressure study of superconducting intercalated graphite <i>[Forró]</i>				
	STM characterization of H-adsorption and vacancy defects on SWNT, modeling <i>[Schlapbach]</i>				
	Characterization of “quantum dot” states between two defects, barrier transparency dependence on topology of SWNT <i>[Schlapbach]</i>				
	Extension to DWNT, transport and optical properties <i>[Schlapbach]</i>				
	BaVS <sub>3</sub> : crystal growth <i>[Forró]</i>				
	Crystal growth: BaVS <sub>3</sub> , BaVSe <sub>3</sub> <i>[Forró]</i>				
	High-pressure NMR- and transport study of CePd <sub>2</sub> In, CeTe <i>[Ott]</i>				
	NMR- and transport study of BaVS <sub>3</sub> <i>[Ott]</i>				
	NMR-studies on BaVS <sub>3</sub> and BaVSe <sub>3</sub> <i>[Ott]</i>				
	NMR- and transport study of PrCu <sub>2</sub> <i>[Ott]</i>				
	High pressure NMR on CeAl <sub>3</sub> <i>[Ott]</i>				
	Optical study of CePt <sub>3</sub> Si and MnSi near QPT <i>[van der Marel]</i>				
	Optical study of UGe <sub>2</sub> , CeRhIn <sub>5</sub> near QPT				

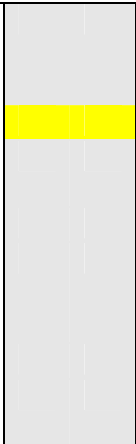

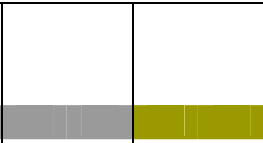
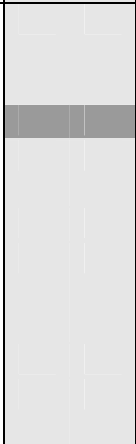

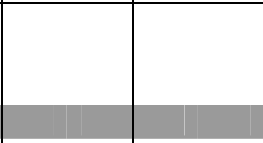
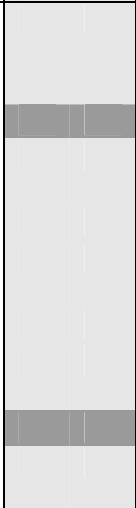

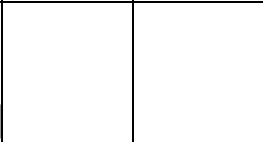
	<p><i>[van der Marel]</i></p> <p>Optical study of Lu<sub>5</sub>Ir<sub>4</sub>Si<sub>10</sub> near CDW transition <i>[van der Marel]</i></p>				
	<p>Investigation of spectral properties of Mott insulators and superfluid phases including behavior across phase transitions <i>[Blatter, Giamarchi, Troyer]</i></p> <p>Microscopic modeling of Bose-Hubbard systems with truncated Hilbert space <i>[Blatter, Giamarchi, Troyer]</i></p> <p>Construction and investigation of low-energy effective field theories <i>[Blatter, Giamarchi, Troyer]</i></p> <p>Thermometry of fermionic cold gases in optical lattices <i>[Blatter, Giamarchi, Troyer]</i></p> <p>Development of new impurity solvers for dynamical mean field theory and related methods for fermionic materials <i>[Troyer]</i></p> <p><b>Transport across correlated boundaries</b> <i>[Troyer]</i></p>				
<b>3.</b>	<b>Magnetism and the interface to spintronics</b>				
	<p><b>Fe<sub>1-x</sub>Co<sub>x</sub>Si:</b></p> <p>Synthesis <i>[van der Marel]</i></p> <p>Magneto-optical, x-ray absorption / dichroism measurement <i>[Degiorgi, van der Marel]</i></p>				
	<p><b>Magnetic nanoparticles:</b></p> <p>Synthesis and characterization <i>[Forró, Seo, Nesper]</i></p> <p>ESR measurements <i>[Forró, Seo, Nesper]</i></p> <p><b>Magnetic semiconductor: Mn-doped GaAs, InAs:</b></p> <p>Synthesis and characterization <i>[Forró, Seo, Nesper]</i></p> <p>ESR measurements <i>[Forró, Seo, Nesper]</i></p>				

A-2 Project 2

Superconductivity, unconventional mechanisms and novel materials




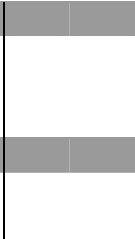
	Milestones	Year 5	Year 6	Year 7	Year 8
1.	<b>Superconducting and magnetic properties of novel and/or unconventional superconductors</b>				
1.1	<b>Cuprate superconductors</b>				
	Transport properties of $\text{Na}_x\text{Ca}_{2-x}\text{CuO}_2\text{Cl}_2$ <i>[Karpinski]</i>				
	Transport properties of $\text{SrCaCu}_2\text{O}_4\text{Cl}_2$ <i>[Karpinski]</i>				
	Spectroscopic properties of $\text{YBa}_2\text{Cu}_4\text{O}_8$ <i>[Fischer, van der Mare]</i>				
	Spectroscopic properties of $\text{Na}_x\text{Ca}_{2-x}\text{CuO}_2\text{Cl}_2$ <i>[Grioni, Fischer, van der Mare]</i>				
	Spectroscopic properties of $\text{SrCaCu}_2\text{O}_4\text{Cl}_2$ <i>[Grioni, Fischer, van der Mare]</i>				
1.2	<b>Other unconventional superconductivity</b>				
	Transport properties of $\text{T}_x\text{Mg}_{1-x}\text{B}_{2-y}\text{C}_y$ (T=Mn, Fe, Co, Ni) <i>[Karpinski]</i>				
	Spectroscopic properties of $\text{T}_x\text{Mg}_{1-x}\text{B}_{2-y}\text{C}_y$ <i>[van der Mare]</i>				
	Transport properties of $\text{K}_x\text{Rb}_{1-x}\text{Os}_2\text{O}_6$ <i>[Karpinski, Forró]</i>				
	Spectroscopic properties of $\text{K}_x\text{Rb}_{1-x}\text{Os}_2\text{O}_6$ <i>[Fischer, van der Mare]</i>				
2.	<b>Topological defects in superconductors, vortex matter</b>				
2.1	<b>Experimental study of the vortex liquid</b>				
	STM of vortex liquids <i>[Fischer]</i>				
	SANS of vortex lattice <i>[Mesot]</i>				
	STM of trapped vortices <i>[Fischer]</i>				
	STM of a vortex in double potential well <i>[Fischer]</i>				

<p>2.2</p>	<p><b>Theoretical study of the effects of the strong disorder on the vortex lattice</b></p> <p>Response of pulse fields [<i>Giamarchi</i>]</p> <p>Thermal smearing effects on strong pinning critical current density [<i>Blatter</i>]</p> <p>Thermal creep under strong pinning conditions [<i>Blatter</i>]</p> <p>Free energy distribution for the (1+1)-dimensional random directed polymer problem [<i>Blatter</i>]</p> <p>Crossover behavior of thermal depinning and creep in the weak-to-strong pinning crossover regime [<i>Blatter</i>]</p>				
<p>2.3</p>	<p><b>Theoretical study of unusual topological structures due to multi-component order parameters</b></p> <p>Phenomenological description and properties [<i>Sigrist</i>]</p> <p>Spectral features from microscopic modeling [<i>Giamarchi, Sigrist</i>]</p>				
<p>2.4</p>	<p><b>Local magnetic field profiles in multilayered superconductors</b></p> <p>Bulk <math>\mu</math>SR of SC multilayers [<i>Keller, Morenzoni</i>]</p> <p>Local magnetic field profiles near surfaces [<i>Keller, Morenzoni</i>]</p> <p><math>\mu</math>Sr experiments on Y123/Pr123 superlattices-study of the anomalous proximity effect coupling [<i>Keller, Morenzoni</i>]</p> <p><math>\mu</math>SR experiments on Y123/La<sub>2/3</sub>Ca<sub>1/3</sub>MnO<sub>3</sub> and SrRuO<sub>3</sub> superlattices – study of the competition between superconductivity and magnetism [<i>Bernhard, Morenzoni</i>]</p>				

3.	<b>Microscopic properties of high temperature superconductors</b>			
3.1	<b>Experimental and investigation of the pseudogap state</b>  STM of local order in pseudogap-state <i>[Fischer]</i>  Inelastic neutron scattering of LSCO in B-field <i>[Mesot]</i>  ARPES of $\text{Na}_x\text{Ca}_{2-x}\text{CuO}_2\text{Cl}_2$ <i>[Grioni]</i>			
3.2	<b>Microscopic theory of high temperature superconductors</b>  Theory of electronic structure of cuprates <i>[Sigrist, Baeriswyl, Giamarchi]</i>  Theory of random disorder in pseudogap state <i>[Büttiker]</i>  Comparison of latter with STM and ARPES in Bi-2223 <i>[Fischer, Grioni, Mesot]</i>			
3.3	<b>Search for the mechanisms which give rise to high-T<sub>c</sub> superconductivity</b>  Optics of spectral weight transfer Bi2223 <i>[van der Mare]</i>  Optics of spectral weight transfer in Y124 <i>[van der Mare]</i>  Optics of spectral weight transfer in Tl2201 <i>[van der Mare]</i>  Preparation of high T <sub>c</sub> thin films <i>[Fischer]</i>			

	Milestones	Year 5	Year 6	Year 7	Year 8
1	<b>Two-dimensional superconductors</b>				
	Exploring the miscibility limits of Pr in the preparation of $\text{Bi}_{2-x}\text{Pr}_x\text{Sr}_2\text{CaCu}_2\text{O}_{8-\delta}$ by the self-flux method. Optimizing the crystal homogeneity. <i>[Margaritondo, Berger]</i>				
	Synthesizing the above family with the traveling solvent floating zone method and compare the quality of the crystals <i>[van der Marel]</i>				
	Optimize the high pressure synthesis of $\text{YBa}_2\text{Cu}_4\text{O}_8$ single crystals of large size. <i>[Karpinski]</i>				
	Growing $\text{Ca}_{2-x}\text{Na}_x\text{CuO}_2\text{Cl}_2$ and $(\text{Sr,Ca})_3\text{Cu}_2\text{O}_{4+\delta}\text{Cl}_{2-y}$ single crystals of oxochlorates which mimic the underdoped cuprates. <i>[Karpinski]</i>				
	Crystal growth of hole-doped and Co-doped $\text{MgB}_2$ <i>[Karpinski]</i>				
2	<b>Geometrically frustrated systems</b>				
	Optimizing the growth conditions of $\text{BaVS}_3$ for NMR measurements <i>[Margaritondo, Berger]</i>				
	Synthesis of doped single crystals of $\text{BaVS}_3$ with Cr and Ti. <i>[Margaritondo, Berger]</i>				
	Exploring growth and synthesis of pyrochlores. <i>[Karpinski]</i>				
	Growth of large crystals of pyrochlore superconductors. <i>[Margaritondo, Berger]</i>				
3	<b>Magnetic materials</b>				
	Exploring the synthesis of the magnetic chain system $\text{Cu}_2\text{Te}_2\text{O}_5\text{Cl}_{2-x}\text{Br}_x$ <i>[Margaritondo, Berger]</i>				
	Preparation a wide range of metal oxide crystals. <i>[Mesot]</i>				



	<p>Optimizing the growth of magnetic shape memory materials, like the <math>RE_5(Si_xGe_{1-x})_4</math> [van der Marel]</p> <p>Improved quality of single crystals of perovskite-type <math>REMnO_3</math> manganites [Mesot]</p>				
--	---	--	---	---	---

	Milestones	Year 5	Year 6	Year 7	Year 8
1	<b>Synthesis of new bulk materials at ambient and high pressure</b>				
1.1	<b>Synthesis at high pressure</b> Crystal growth of borides, superconducting pyrochlor oxides, oxychloride cuprates, reaction of multicomponent oxide systems <i>[Karpinski]</i>				
1.2	<b>Synthesis of potentially superconducting Ni-oxides</b> (i) LnANiO <sub>4</sub> solid state chemistry (variation of Ln, A and incorporation of F) <i>[Schilling, Karpinski]</i> (ii) LnANiO <sub>2</sub> solid state chemistry (doping experiments) <i>[Schilling, Karpinski]</i> (iii) <b>characterization of physical properties</b> <i>[Schilling]</i>				
1.3	<b>A new method of combinatorial chemistry for finding ferromagnetic and superconducting oxides</b> (i) Theoretical studies on the exploration of phase systems by the SSC. Modeling of magnetic separation columns for superconductors. <i>[Hulliger]</i> (ii) SSC syntheses by using Cu, Ni and Co for a lead element. Study of reaction performance in SSC samples. <i>[Hulliger]</i> (iii) Characterization of SSC probes by various physical techniques. <i>[Hulliger]</i> (iv) Classical syntheses of potentially interesting compounds <i>[Hulliger]</i>				

2	<p><b>Preparation of thin films (2D)</b></p>
2.1	<p><b>Perovskite Oxynitrides by Pulsed Laser Deposition</b></p> <p>(i) Pulsed reactive crossed beam experiments using ammonia to obtain films of oxynitride titanates and <b>molybdates</b>. [Schlapbach]</p> <p>(ii) rf-plasma pulsed laser deposition of oxynitride titanates and <b>molybdates</b> [Schlapbach]</p> <p><b>(iii) microwave induced plasma ammonolysis of surfaces of large perovskite-type titanate single crystals.</b> [Schlapbach]</p> <p>(iv) Conductivity measurements and general physical and chemical characterization [Schlapbach]</p>
2.2	<p><b>Ferromagnetic oxides prepared by thin film techniques</b></p> <p>(i) Doped oxide semiconductors, thin film growth using titanates doped by transition metal ions [Seo]</p> <p>(ii) Study on the origin of ferromagnetism in low doped oxide systems [Seo]</p> <p>(iii) Structural, chemical and physical characterization of films [Seo]</p>
3	<p><b>Preparation and modification of 1D fiber-type materials</b></p>
	<p><u>(i) Optimized preparation of boride and oxide fibers</u> [Nesper]</p> <p><b>(ii) Superconducting <math>\text{Ca}_x\text{B}_y\text{C}</math> compounds and <math>\text{K}(\text{Al,Si})</math> compounds with <math>\text{MgB}_2</math> structure</b> [Nesper]</p> <p>(iii) Doped <math>\text{MgB}_2</math> coated metal wires and free-standing <math>\text{MgB}_2</math> forms [Nesper]</p> <p><b>(iv) Synthesis of nanoscopic boron with highest purity for enhancing critical currents in <math>\text{MgB}_2</math> ceramics</b> [Nesper, Flükiger]</p>



	<p>Realize infrared optical spectroscopy on Nb-STO thin films whose carrier density is modulated by field effect (determination of the induced carrier density, cyclotron mass changes, carrier life-time) [van der Marel, Triscone]</p>				
	<p>Probe the polaronic nature of the carriers in Nb-STO [van der Marel]</p>				
	<p>Probe the polaronic nature of the carriers in manganites (and in manganites whose carrier density is modified by field effect-coupling with project SNSF-divisionII) [van der Marel, Triscone]</p>				
	<p>Realization of large area Y123/Pr123 superlattices suitable for muons spin resonance studies [Fischer]</p>				
	<p>Realization of high quality 214 films with transfer under vacuum for ARPES-STM/STS studies [Fischer, Aebi]</p>				
	<p>Development of surface cleaning procedures [Aebi, Fischer]</p>				
	<p>Realization of (BaCuO<sub>x</sub>)(CaCuO<sub>2</sub>) multilayers for STM/STS studies [Fischer]</p>				
	<p>Spectroscopy on 124 films and on (BaCuO<sub>x</sub>)(CaCuO<sub>2</sub>) multilayers [Fischer]</p>				
	<p>Realize field effect devices using 214 superconducting channels and amorphous gate oxides [Martinoli]</p>				
	<p>Realize field effect devices using 214 superconducting channels and high-k SrTiO<sub>3</sub> gate oxides and probe the S-I transition in the underdoped regime of HTS using field effect [Martinoli, Triscone]</p>				
	<p>Determine the Cooper pair effective mass using the Bernouilli effect [Martinoli]</p>				
<b>3</b>	<p><b>Novel single photon detectors using low and high Tc superconducting nanostructures</b></p>				
	<p>Realization of superconducting films of NbN, TiN, or TaN [Schilling]</p>				

	Film nanostructuring and realization of superconducting meander photon detectors based on NbN, TiN, or TaN [Schilling]				
	Study and improvement of detector performance (detection efficiency, sensitivity, energy dispersion) [Schilling]				
	Study of thermal and quantum fluctuations in nanometer size superconductors [Schilling]				
	Realization of superconducting films of NbN, Ta, MoRe, HTS and superlattices [Schilling]				
	Film/superlattice nanostructuring and realization of superconducting meander photon detector [Fischer]				
	Study of the detector efficiency and relaxation time in S/I superlattices [Fischer]				
	Study of the detector response to voltage and current pulses [Fischer]				
<b>4</b>	<b>Giant electroresistive effect in correlated oxide thin films</b>				
	Realization of artificial ferroelectric materials with enhanced dielectric and piezoelectric properties [Triscone]				
	Giant electroresistive films production [Triscone]				
	Measure giant electroresistive switching at nanoscale [Triscone]				
	Measure resistance change relaxation [Triscone]				
	Theoretical investigations of the process [Blatter, Rice]				

**A-6 Project 6 Industrial applications and pre-application development**

	Milestones	Year 5	Year 6	Year 7	Year 8
1	<b>Applied superconductivity</b>				
	<p>New specific heat device for rapid determination of the Sn distribution in Nb<sub>3</sub>Sn multifilamentary wires up to 21 T [Flükiger]</p> <p>New device for studying the effect of transverse compressive stress on J<sub>c</sub> of multifilamentary Nb<sub>3</sub>Sn and MgB<sub>2</sub> wires up to 21 T [Flükiger]</p> <p>Improvement of Nb<sub>3</sub>Sn bronze wires at very high fields for NMR. Goal: J<sub>c</sub>(overall) ≥ 150 A/mm<sup>2</sup> at 4.2K and 21T (30% enhancement) [Flükiger]</p> <p>Improvement of Nb<sub>3</sub>Sn bronze wires at intermediate fields (for high field dipoles): J<sub>c</sub>(overall) ≥ 500 A/mm<sup>2</sup> at 4.2K, 15 T [Flükiger]</p> <p>Improvement of MgB<sub>2</sub> wires and tapes. New goal: J<sub>c</sub>(4.2K) ≥ 10<sup>2</sup> A/mm<sup>2</sup> at 12 T [Flükiger]</p> <p>Improvement of Nb<sub>3</sub>Sn bronze wires at very high fields for NMR. New goal: J<sub>c</sub>(overall) ≥ 180 A/mm<sup>2</sup> at 4.2K and 21T (criterion for 23.5 T magnets in persistent mode fulfilled) [Flükiger]</p> <p>Preparation of MgB<sub>2</sub> wires with full thermal stabilization. Optimization of the current carrying properties at 25 K for MRI applications: J<sub>c</sub>(4.2K) ≥ 10<sup>2</sup> A/mm<sup>2</sup> at 5 T [Flükiger]</p>				
	<p>Improving single wafer for homogeneous switching at low voltage [Fischer]</p> <p>Test of a 10 kVA FCL in a series and or parallel configuration [Fischer]</p> <p>Test of coated conductors on various substrates for FCL applications [Fischer]</p> <p>Completion of 50 kVA demonstrator to showing homogeneous switching of the wafers [Fischer]</p>				

	<p>Validation of electro-thermal FEM simulations with measurements [Hasler]</p> <p>FEM testing of new coated conductors geometries [Hasler, Fischer]</p> <p>Dynamic Hall probe field mapping development [Hasler]</p> <p>Dynamic Hall probe field mapping of current limiter [Hasler, Fischer]</p>				
<p>2</p>	<p><b>MaNEP sensors</b></p> <p>Synthesis and test of ESR materials for weak field measurements [Forró]</p> <p>Set-up of experimental tools for gas sensors. Identification of loss of sensitivity causes using local probe techniques. Fabrication of electrodes with selected thin film coatings [Fischer]</p> <p>Set-up of experimental tools and electronics (IDT structure and SAW resonators at 40MHz). Measure electrical conductivity of various sensing nano-materials in NH<sub>3</sub>, NO<sub>2</sub> and O<sub>3</sub>. Stability versus temperature [Fischer]</p> <p>First frequency-shift measurements at 40MHz with reference gas samples [Fischer]</p> <p>Best choice of thin film electrodes and surface morphology upon resistance to passivation, speed of response, sensitivity and selectivity [Fischer]</p> <p>Resistance and frequency-shift measurements of the response of sensing layers to NH<sub>3</sub>, NO<sub>2</sub> and O<sub>3</sub>. Develop SAW resonators and electronics working towards 100MHz frequencies [Fischer]</p> <p>Integration of the new cathodes in working sensors [Fischer]</p> <p>Identification of the best sensitive layer for each environment. Selectivity, speed of response and stability assessments. Measurement of the kinetics of adsorption/desorption [Fischer]</p>				



	<p>Field test of new cathodes at end-user site <i>[Fischer]</i></p> <p>Optimization, fine-tuning of the morphology / chemistry of the sensing layers <i>[Fischer]</i></p> <p>Implementation of SAW/resistive sensor on a commercial device for field testing <i>[Fischer]</i></p>				
<p><b>3</b></p>	<p><b><i>Thin film preparation and Applications</i></b></p> <p>Ni/Ti multilayers: Improved design of magnetic field and sputter targets <i>[Mesot]</i></p> <p>Neutron and x-ray diffraction and reflection investigation of substrates and coatings <i>[Mesot]</i></p> <p>Investigation of substrates and coatings by x-rays and local probes <i>[Mesot, Triscone]</i></p> <p>Investigation of multilayers prepared by simultaneous running of sputtering targets in pure Ar and Ar/N<sub>2</sub> gas <i>[Mesot]</i></p> <p>Determination of reflectivity by neutrons and x-rays <i>[Mesot]</i></p> <p>Scanning probe investigation of reactive sputtering <i>[Triscone]</i></p> <p>Fabrication of polarizing multilayers of type FeCo/Ti <i>[Mesot]</i></p> <p>Explore controlled interdiffusion on magnetization <i>[Mesot]</i></p> <p>Realization of epitaxial SrTiO<sub>3</sub> buffer layers on silicon <i>[Triscone]</i></p> <p>Realization of epitaxial piezoelectric layers on buffered silicon <i>[Triscone]</i></p> <p>Realization of a pyroelectric sensor using epitaxial PZT films on silicon <i>[Triscone]</i></p> <p>Realization of MEMS structures including functional AFM tips <i>[Triscone]</i></p>				

	<p>Realization of PIT-SAW devices on SrTiO<sub>3</sub>-doped SrTiO<sub>3</sub> / PZT structures [Triscone]</p> <p>Characterization of the structures (high frequency / elastic constants) [Triscone]</p> <p>Demonstration of the “frequency doubling” capability of the PIT-SAW technology [Triscone]</p> <p>Realization of a PIT-SAW device on silicon [Triscone]</p> <p>High frequency characterization of epitaxial PZT films [Triscone]</p>				
--	---	--	--	--	--